Journal of Mathematics and Physics

(Founded by C. L. E. Moore)

Volume XXIV - XXV

1945 - 1947

Feb. - Jan.

Editors

FREDERICK G. KEYES MANUEL S. VALLARTA
HENRY BAYARD PHILLIPS NORBERT WIENER
DIRK J. STRUIK FREDERICK S. WOODS

Managing Editor
PHILIP FRANKLIN

Published by the
MASSACHUSETTS INSTITUTE OF TECHNOLOGY

MATHEMATICS GRADUATE LIBRARY

OHIO STATE UNIVERSITY LIBRARY

QA 1
J87
v.24-25

CONTENTS

Table of Coefficients for Numerical Integration without Differences 1
By Arnold N. Lowan and Herbert E. Salzer

On the Problem of Heat Conduction in Thin Plates 22
By Arnold N. Lowan

Tables of Bessel Functions $J_n(x)$ for Large Arguments 30
By Murlan S. Corrington and William Miehle

The Parabolic Cylinder Functions 51
By C. P. Wells and R. D. Spence

Visual Dark Adaptation: A Mathematical Formulation 65
By Parry Moon and Domina Eberle Spencer

A Graphical Method for the Numerical Solution of Fredholm's Integral Equation of the Second Kind 109
By Peter L. Tea

Remarks on the Method of Stationary Phases 127
By Aurel Wintner

A Convergent Iterative Process 131
By Paul A. Samuelson

Table of Coefficients for Double Quadrature Without Differences, for Integrating Second Order Differential Equations 135
By Herbert E. Salzer

Formulas for Direct and Inverse Interpolation of a Complex Function Tabulated Along Equidistant Circular Arcs 141
By Herbert E. Salzer

Table of Bessel Functions $J_n(1000)$ 144
By Murlan S. Corrington

748335

TABLE OF COEFFICIENTS FOR NUMERICAL INTEGRATION WITHOUT DIFFERENCES

By Arnold N. Lowan and Herbert E. Salzer[1]

When a function $f(x)$ is known for n equally spaced arguments at interval h, the value of the integral between the limits $x_0 + rh$ and $x_0 + sh$ may be obtained (by the integration of the well-known Lagrangian Interpolation Formula) in the form

$$\int_{x_0+rh}^{x_0+sh} f(x)\,dx \sim h \sum_{i=-[(n-1)/2]}^{[n/2]} \{B_i^{(n)}(s) - B_i^{(n)}(r)\} f(x_0 + ih)$$

where $[x]$ denotes the largest integer in x and $B_i^{(n)}(p)$ are polynomials of the nth degree. The accompanying table gives the value of these polynomials $B_i^{(n)}(p)$ to ten decimals, for p ranging from $-[(n-1)/2]$ to $[n/2]$. For $n = 3$, 4 and 5 these polynomials are tabulated at intervals of 0.01; for $n = 6$ and 7, they are tabulated at intervals of 0.1.

[1] Mathematical Tables Project, National Bureau of Standards, New York City.

THREE-POINT COEFFICENTS

$$\int_{x_0+rh}^{x_0+sh} f(x)\,dx \sim h \sum_{i=-1}^{i=1} \{B_i^{(s)}(s) - B_i^{(s)}(r)\} f(x_0 + ih)$$

p	$B_{-1}^{(s)}(p)$	$B_0^{(s)}(p)$	$B_1^{(s)}(p)$	
−1.00	−0.41666 66667	−0.66666 66667	0.08333 33333	1.00
.99	.40674 15000	.66656 70000	.08330 85000	.99
.98	.39696 53333	.66626 93333	.08323 46667	.98
.97	.38733 71667	.66577 56667	.08311 28333	.97
.96	.37785 60000	.66508 80000	.08294 40000	.96
−.95	−0.36852 08333	−0.66420 83333	0.08272 91667	.95
.94	.35933 06667	.66313 86667	.08246 93333	.94
.93	.35028 45000	.66188 10000	.08216 55000	.93
.92	.34138 13333	.66043 73333	.08181 86667	.92
.91	.33262 01667	.65880 96667	.08142 98333	.91
−.90	−0.32400 00000	−0.65700 00000	0.08100 00000	.90
.89	.31551 98333	.65501 03333	.08053 01667	.89
.88	.30717 86667	.65284 26667	.08002 13333	.88
.87	.29897 55000	.65049 90000	.07947 45000	.87
.86	.29090 93333	.64798 13333	.07889 06667	.86
−.85	−0.28297 91667	−0.64529 16667	0.07827 08333	.85
.84	.27518 40000	.64243 20000	.07761 60000	.84
.83	.26752 28333	.63940 43333	.07692 71667	.83
.82	.25999 46667	.63621 06667	.07620 53333	.82
.81	.25259 85000	.63285 30000	.07545 15000	.81
−.80	−0.24533 33333	−0.62933 33333	0.07466 66667	.80
.79	.23819 81667	.62565 36667	.07385 18333	.79
.78	.23119 20000	.62181 60000	.07300 80000	.78
.77	.22431 38333	.61782 23333	.07213 61667	.77
.76	.21756 26667	.61367 46667	.07123 73333	.76
−.75	−0.21093 75000	−0.60937 50000	0.07031 25000	.75
.74	.20443 73333	.60492 53333	.06936 26667	.74
.73	.19806 11667	.60032 76667	.06838 88333	.73
.72	.19180 80000	.59558 40000	.06739 20000	.72
.71	.18567 68333	.59069 63333	.06637 31667	.71
−.70	−0.17966 66667	−0.58566 66667	0.06533 33333	.70
.69	.17377 65000	.58049 70000	.06427 35000	.69
.68	.16800 53333	.57518 93333	.06319 46667	.68
.67	.16235 21667	.56974 56667	.06209 78333	.67
.66	.15681 60000	.56416 80000	.06098 40000	.66
−.65	−0.15139 58333	−0.55845 83333	0.05985 41667	.65
.64	.14609 06667	.55261 86667	.05870 93333	.64
.63	.14089 95000	.54665 10000	.05755 05000	.63
.62	.13582 13333	.54055 73333	.05637 86667	.62
.61	.13085 51667	.53433 96667	.05519 48333	.61
−.60	−0.12600 00000	−0.52800 00000	0.05400 00000	.60
.59	.12125 48333	.52154 03333	.05279 51667	.59
.58	.11661 86667	.51496 26667	.05158 13333	.58
.57	.11209 05000	.50826 90000	.05035 95000	.57
.56	.10766 93333	.50146 13333	.04913 06667	.56
−.55	−0.10335 41667	−0.49454 16667	0.04789 58333	.55
.54	.09914 40000	.48751 20000	.04665 60000	.54
.53	.09503 78333	.48037 43333	.04541 21667	.53
.52	.09103 46667	.47313 06667	.04416 53333	.52
.51	.08713 35000	.46578 30000	.04291 65000	.51
−.50	−0.08333 33333	−0.45833 33333	0.04166 66667	.50
	$-B_1^{(s)}(p)$	$-B_0^{(s)}(p)$	$-B_{-1}^{(s)}(p)$	p

THREE-POINT COEFFICIENTS—*Continued*

$$\int_{x_0+rh}^{x_0+sh} f(x)\,dx \sim h \sum_{i=-1}^{i=1} \{B_i^{(3)}(s) - B_i^{(3)}(r)\} f(x_0 + ih)$$

p	$B_{-1}^{(3)}(p)$	$B_0^{(3)}(p)$	$B_1^{(3)}(p)$	
−.50	−0.08333 33333	−0.45833 33333	0.04166 66667	.50
.49	.07963 31667	.45078 36667	.04041 68333	.49
.48	.07603 20000	.44313 60000	.03916 80000	.48
.47	.07252 88333	.43539 23333	.03792 11667	.47
.46	.06912 26667	.42755 46667	.03667 73333	.46
−.45	−0.06581 25000	−0.41962 50000	0.03543 75000	.45
.44	.06259 73333	.41160 53333	.03420 26667	.44
.43	.05947 61667	.40349 76667	.03297 38333	.43
.42	.05644 80000	.39530 40000	.03175 20000	.42
.41	.05351 18333	.38702 63333	.03053 81667	.41
−.40	−0.05066 66667	−0.37866 66667	0.02933 33333	.40
.39	.04791 15000	.37022 70000	.02813 85000	.39
.38	.04524 53333	.36170 93333	.02695 46667	.38
.37	.04266 71667	.35311 56667	.02578 28333	.37
.36	.04017 60000	.34444 80000	.02462 40000	.36
−.35	−0.03777 08333	−0.33570 83333	0.02347 91667	.35
.34	.03545 06667	.32689 86667	.02234 93333	.34
.33	.03321 45000	.31802 10000	.02123 55000	.33
.32	.03106 13333	.30907 73333	.02013 86667	.32
.31	.02899 01667	.30006 96667	.01905 98333	.31
−.30	−0.02700 00000	−0.29100 00000	0.01800 00000	.30
.29	.02508 98333	.28187 03333	.01696 01667	.29
.28	.02325 86667	.27268 26667	.01594 13333	.28
.27	.02150 55000	.26343 90000	.01494 45000	.27
.26	.01982 93333	.25414 13333	.01397 06667	.26
−.25	−0.01822 91667	−0.24479 16667	0.01302 08333	.25
.24	.01670 40000	.23539 20000	.01209 60000	.24
.23	.01525 28333	.22594 43333	.01119 71667	.23
.22	.01387 46667	.21645 06667	.01032 53333	.22
.21	.01256 85000	.20691 30000	.00948 15000	.21
−.20	−0.01133 33333	−0.19733 33333	0.00866 66667	.20
.19	.01016 81667	.18771 36667	.00788 18333	.19
.18	.00907 20000	.17805 60000	.00712 80000	.18
.17	.00804 38333	.16836 23333	.00640 61667	.17
.16	.00708 26667	.15863 46667	.00571 73333	.16
−.15	−0.00618 75000	−0.14887 50000	0.00506 25000	.15
.14	.00535 73333	.13908 53333	.00444 26667	.14
.13	.00459 11667	.12926 76667	.00385 88333	.13
.12	.00388 80000	.11942 40000	.00331 20000	.12
.11	.00324 68333	.10955 63333	.00280 31667	.11
−.10	−0.00266 66667	−0.09966 66667	0.00233 33333	.10
.09	.00214 65000	.08975 70000	.00190 35000	.09
.08	.00168 53333	.07982 93333	.00151 46667	.08
.07	.00128 21667	.06988 56667	.00116 78333	.07
.06	.00093 60000	.05992 80000	.00086 40000	.06
−.05	−0.00064 58333	−0.04995 83333	0.00060 41667	.05
.04	.00041 06667	.03997 86667	.00038 93333	.04
.03	.00022 95000	.02999 10000	.00022 05000	.03
.02	.00010 13333	.01999 73333	.00009 86667	.02
.01	.00002 51667	.00999 96667	.00002 48333	.01
−.00	−0.00000 00000	−0.00000 00000	0.00000 00000	.00
	$-B_1^{(3)}(p)$	$-B_0^{(3)}(p)$	$-B_{-1}^{(3)}(p)$	p

FOUR-POINT COEFFICIENTS

$$\int_{x_0+rh}^{x_0+sh} f(x)\,dx \sim h \sum_{i=-1}^{i=2} \{B_i^{(4)}(s) - B_i^{(4)}(r)\} f(x_0 + ih)$$

p	$B_{-1}^{(4)}(p)$	$B_0^{(4)}(p)$	$B_1^{(4)}(p)$	$B_2^{(4)}(p)$
−1.00	−0.37500 00000	−0.79166 66667	0.20833 33333	−0.04166 66667
.99	.36509 13338	.79151 74988	.20825 89988	.04165 01663
.98	.35536 40067	.79107 33133	.20803 86467	.04160 13267
.97	.34581 60338	.79033 90654	.20767 62321	.04152 11329
.96	.33644 54400	.78931 96800	.20717 56800	.04141 05600
−.95	−0.32725 02604	−0.78802 00521	0.20654 08854	−0.04127 05729
.94	.31822 85400	.78644 50467	.20577 57133	.04110 21267
.93	.30937 83338	.78459 94988	.20488 39988	.04090 61663
.92	.30069 77067	.78248 82133	.20386 95467	.04068 36267
.91	.29218 47338	.78011 59654	.20273 61321	.04043 54329
−.90	−0.28383 75000	−0.77748 75000	0.20148 75000	−0.04016 25000
.89	.27565 41004	.77460 75321	.20012 73654	.03986 57329
.88	.26763 26400	.77148 07467	.19865 94133	.03954 60267
.87	.25977 12338	.76811 17988	.19708 72988	.03920 42663
.86	.25206 80067	.76450 53133	.19541 46467	.03884 13267
−.85	−0.24452 10938	−0.76066 58854	0.19364 50521	−0.03845 80729
.84	.23712 86400	.75659 80800	.19178 20800	.03805 53600
.83	.22988 88004	.75230 64321	.18982 92654	.03763 40329
.82	.22279 97400	.74779 54467	.18779 01133	.03719 49267
.81	.21585 96338	.74306 95988	.18566 80988	.03673 88663
−.80	−0.20906 66667	−0.73813 33333	0.18346 66667	−0.03626 66667
.79	.20241 90338	.73299 10654	.18118 92321	.03577 91329
.78	.19591 49400	.72764 71800	.17883 91800	.03527 70600
.77	.18955 26004	.72210 60321	.17641 98654	.03476 12329
.76	.18333 02400	.71637 19467	.17393 46133	.03423 24267
−.75	−0.17724 60938	−0.71044 92188	0.17138 67188	−0.03369 14063
.74	.17129 84067	.70434 21133	.16877 94467	.03313 89267
.73	.16548 54338	.69805 48654	.16611 60321	.03257 57329
.72	.15980 54400	.69159 16800	.16339 96800	.03200 25600
.71	.15425 67004	.68495 67321	.16063 35654	.03142 01329
−.70	−0.14883 75000	−0.67815 41667	0.15782 08333	−0.03082 91667
.69	.14354 61338	.67118 80988	.15496 45988	.03023 03663
.68	.13838 09067	.66406 26133	.15206 79467	.02962 44267
.67	.13334 01338	.65678 17654	.14913 39321	.02901 20329
.66	.12842 21400	.64934 95800	.14616 55800	.02839 38600
−.65	−0.12362 52604	−0.64177 00521	0.14316 58854	−0.02777 05729
.64	.11894 78400	.63404 71467	.14013 78133	.02714 28267
.63	.11438 82338	.62618 47988	.13708 42988	.02651 12663
.62	.10994 48067	.61818 69133	.13400 82467	.02587 65267
.61	.10561 59338	.61005 73654	.13091 25321	.02523 92329
−.60	−0.10140 00000	−0.60180 00000	0.12780 00000	−0.02460 00000
.59	.09729 54004	.59341 86321	.12467 34654	.02395 94329
.58	.09330 05400	.58491 70467	.12153 57133	.02331 81267
.57	.08941 38338	.57629 89988	.11838 94988	.02267 66663
.56	.08563 37067	.56756 82133	.11523 75467	.02203 56267
−.55	−0.08195 85938	−0.55872 83854	0.11208 25521	−0.02139 55729
.54	.07838 69400	.54978 31800	.10892 71800	.02075 70600
.53	.07491 72004	.54073 62321	.10577 40654	.02012 06329
.52	.07154 78400	.53159 11467	.10262 58133	.01948 68267
.51	.06827 73338	.52235 14988	.09948 49988	.01885 61663
−.50	−0.06510 41667	−0.51302 08333	0.09635 41667	−0.01822 91667

$$\int_{x_0+rh}^{x_0+sh} f(x)\,dx \sim h \sum_{i=-1}^{i=2} \{B_i^{(4)}(s) - B_i^{(4)}(r)\} f(x_0 + ih)$$

p	$B_{-1}^{(4)}(p)$	$B_0^{(4)}(p)$	$B_1^{(4)}(p)$	$B_2^{(4)}(p)$
−.50	−0.06510 41667	−0.51302 08333	0.09635 41667	−0.01822 91667
.49	.06202 68338	.50360 26654	.09323 58321	.01760 63329
.48	.05904 38400	.49410 04800	.09013 24800	.01698 81600
.47	.05615 37004	.48451 77321	.08704 65654	.01637 51329
.46	.05335 49400	.47485 78467	.08398 05133	.01576 77267
−.45	−0.05064 60938	−0.46512 42188	0.08093 67188	−0.01516 64063
.44	.04802 57067	.45532 02133	.07791 75467	.01457 16267
.43	.04549 23338	.44544 91654	.07492 53321	.01398 38329
.42	.04304 45400	.43551 43800	.07196 23800	.01340 34600
.41	.04068 09004	.42551 91321	.06903 09654	.01283 09329
−.40	−0.03840 00000	−0.41546 66667	0.06613 33333	−0.01226 66667
.39	.03620 04338	.40536 01988	.06327 16988	.01171 10663
.38	.03408 08067	.39520 29133	.06044 82467	.01116 45267
.37	.03203 97338	.38499 79654	.05766 51321	.01062 74329
.36	.03007 58400	.37474 84800	.05492 44800	.01010 01600
−.35	−0.02818 77604	−0.36445 75521	0.05222 83854	−0.00958 30729
.34	.02637 41400	.35412 82467	.04957 89133	.00907 65267
.33	.02463 36338	.34376 35988	.04697 80988	.00858 08663
.32	.02296 49067	.33336 66133	.04442 79467	.00809 64267
.31	.02136 66338	.32294 02654	.04193 04321	.00762 35329
−.30	−0.01983 75000	−0.31248 75000	0.03948 75000	−0.00716 25000
.29	.01837 62004	.30201 12321	.03710 10654	.00671 36329
.28	.01698 14400	.29151 43467	.03477 30133	.00627 72267
.27	.01565 19338	.28099 96988	.03250 51988	.00585 35663
.26	.01438 64067	.27047 01133	.03029 94467	.00544 29267
−.25	−0.01318 35938	−0.25992 83854	0.02815 75521	−0.00504 55729
.24	.01204 22400	.24937 72800	.02608 12800	.00466 17600
.23	.01096 11004	.23881 95321	.02407 23654	.00429 17329
.22	.00993 89400	.22825 78467	.02213 25133	.00393 57267
.21	.00897 45338	.21769 48988	.02026 33988	.00359 39663
−.20	−0.00806 66667	−0.20713 33333	0.01846 66667	−0.00326 66667
.19	.00721 41338	.19657 57654	.01674 39321	.00295 40329
.18	.00641 57400	.18602 47800	.01509 67800	.00265 62600
.17	.00567 03004	.17548 29321	.01352 67654	.00237 35329
.16	.00497 66400	.16495 27467	.01203 54133	.00210 60267
−.15	−0.00433 35938	−0.15443 67188	0.01062 42188	−0.00185 39063
.14	.00374 00067	.14393 73133	.00929 46467	.00161 73267
.13	.00319 47338	.13345 69654	.00804 81321	.00139 64329
.12	.00269 66400	.12299 80800	.00688 60800	.00119 13600
.11	.00224 46004	.11256 30321	.00580 98654	.00100 22329
−.10	−0.00183 75000	−0.10215 41667	0.00482 08333	−0.00082 91667
.09	.00147 42338	.09177 37988	.00392 02988	.00067 22663
.08	.00115 37067	.08142 42133	.00310 95467	.00053 16267
.07	.00087 48338	.07110 76654	.00238 98321	.00040 73329
.06	.00063 65400	.06082 63800	.00176 23800	.00029 94600
−.05	−0.00043 77604	−0.05058 25521	0.00122 83854	−0.00020 80729
.04	.00027 74400	.04037 83467	.00078 90133	.00013 32267
.03	.00015 45338	.03021 58988	.00044 53988	.00007 49663
.02	.00006 80067	.02009 73133	.00019 86467	.00003 33267
.01	.00001 68338	.01002 46654	.00004 98321	.00000 83329
−.00	−0.00000 00000	0.00000 00000	0.00000 00000	−0.00000 00000

FOUR-POINT COEFFICIENTS—*Continued*

$$\int_{x_0+rh}^{x_0+sh} f(x)\,dx \sim h \sum_{i=-1}^{i=2} [B_i^{(4)}(s) - B_i^{(4)}(r)]f(x_0 + ih)$$

p	$B_{-1}^{(4)}(p)$	$B_0^{(4)}(p)$	$B_1^{(4)}(p)$	$B_2^{(4)}(p)$
.00	−0.00000 00000	0.00000 00000	0.00000 00000	−0.00000 00000
.01	.00001 65004	.00997 46679	.00005 01654	.00000 83329
.02	.00006 53400	.01989 73533	.00020 13133	.00003 33267
.03	.00014 55338	.02976 61013	.00045 43988	.00007 49663
.04	.00025 61067	.03957 89867	.00081 03467	.00013 32267
.05	−0.00039 60938	0.04933 41146	0.00127 00521	−0.00020 80729
.06	.00056 45400	.05902 96200	.00183 43800	.00029 94600
.07	.00076 05004	.06866 36679	.00250 41654	.00040 73329
.08	.00098 30400	.07823 44533	.00328 02133	.00053 16267
.09	.00123 12338	.08774 02013	.00416 32988	.00067 22663
.10	−0.00150 41667	0.09717 91667	0.00515 41667	−0.00082 91667
.11	.00180 09338	.10654 96346	.00625 35321	.00100 22329
.12	.00212 06400	.11584 99200	.00746 20800	.00119 13600
.13	.00246 24004	.12507 83679	.00878 04654	.00139 64329
.14	.00282 53400	.13423 33533	.01020 93133	.00161 73267
.15	−0.00320 85938	0.14331 32813	0.01174 92188	−0.00185 39063
.16	.00361 13067	.15231 65867	.01340 07467	.00210 60267
.17	.00403 26338	.16124 17346	.01516 44321	.00237 35329
.18	.00447 17400	.17008 72200	.01704 07800	.00265 62600
.19	.00492 78004	.17885 15679	.01903 02654	.00295 40329
.20	−0.00540 00000	0.18753 33333	0.02113 33333	−0.00326 66667
.21	.00588 75338	.19613 11013	.02335 03988	.00359 39663
.22	.00638 96067	.20464 34867	.02568 18467	.00393 57267
.23	.00690 54338	.21306 91346	.02812 80321	.00429 17329
.24	.00743 42400	.22140 67200	.03068 92800	.00466 17600
.25	−0.00797 52604	0.22965 49479	0.03336 58854	−0.00504 55729
.26	.00852 77400	.23781 25533	.03615 81133	.00544 29267
.27	.00909 09338	.24587 83013	.03906 61988	.00585 35663
.28	.00966 41067	.25385 09867	.04209 03467	.00627 72267
.29	.01024 65338	.26172 94346	.04523 07321	.00671 36329
.30	−0.01083 75000	0.26951 25000	0.04848 75000	−0.00716 25000
.31	.01143 63004	.27719 90679	.05186 07654	.00762 35329
.32	.01204 22400	.28478 80533	.05535 06133	.00809 64267
.33	.01265 46338	.29227 84013	.05895 70988	.00858 08663
.34	.01327 28067	.29966 90867	.06268 02467	.00907 65267
.35	−0.01389 60938	0.30695 91146	0.06652 00521	−0.00958 30729
.36	.01452 38400	.31414 75200	.07047 64800	.01010 01600
.37	.01515 54004	.32123 33679	.07454 94654	.01062 74329
.38	.01579 01400	.32821 57533	.07873 89133	.01116 45267
.39	.01642 74338	.33509 38013	.08304 46988	.01171 10663
.40	−0.01706 66667	0.34186 66667	0.08746 66667	−0.01226 66667
.41	.01770 72338	.34853 35346	.09200 46321	.01283 09329
.42	.01834 85400	.35509 36200	.09665 83800	.01340 34600
.43	.01899 00004	.36154 61679	.10142 76654	.01398 38329
.44	.01963 10400	.36789 04533	.10631 22133	.01457 16267
.45	−0.02027 10938	0.37412 57813	0.11131 17188	−0.01516 64063
.46	.02090 96067	.38025 14867	.11642 58467	.01576 77267
.47	.02154 60338	.38626 69346	.12165 42321	.01637 51329
.48	.02217 98400	.39217 15200	.12699 64800	.01698 81600
.49	.02281 05004	.39796 46679	.13245 21654	.01760 63329
.50	−0.02343 75000	0.40364 58333	0.13802 08333	−0.01822 91667

FOUR-POINT COEFFICIENTS—*Continued*

$$\int_{x_0+rh}^{x_0+sh} f(x)\,dx \sim h \sum_{i=-1}^{i=2} [B_i^{(4)}(s) - B_i^{(4)}(r)] f(x_0 + ih)$$

p	$B_{-1}^{(4)}(p)$	$B_0^{(4)}(p)$	$B_1^{(4)}(p)$	$B_2^{(4)}(p)$
.50	−0.02343 75000	0.40364 58333	0.13802 08333	−0.01822 91667
.51	.02406 03338	.40921 45013	.14370 19988	.01885 61663
.52	.02467 85067	.41467 01867	.14949 51467	.01948 68267
.53	.02529 15338	.42001 24346	.15539 97321	.02012 06329
.54	.02589 89400	.42524 08200	.16141 51800	.02075 70600
.55	−0.02650 02604	0.43035 49479	0.16754 08854	−0.02139 55729
.56	.02709 50400	.43535 44533	.17377 62133	.02203 56267
.57	.02768 28338	.44023 90013	.18012 04988	.02267 66663
.58	.02826 32067	.44500 82867	.18657 30467	.02331 81267
.59	.02883 57338	.44966 20346	.19313 31321	.02395 94329
.60	−0.02940 00000	0.45420 00000	0.19980 00000	−0.02460 00000
.61	.02995 56004	.45862 19679	.20657 28654	.02523 92329
.62	.03050 21400	.46292 77533	.21345 09133	.02587 65267
.63	.03103 92338	.46711 72013	.22043 32988	.02651 12663
.64	.03156 65067	.47119 01867	.22751 91467	.02714 28267
.65	−0.03208 35938	0.47514 66146	0.23470 75521	−0.02777 05729
.66	.03259 01400	.47898 64200	.24199 75800	.02839 38600
.67	.03308 58004	.48270 95679	.24938 82654	.02901 20329
.68	.03357 02400	.48631 60533	.25687 86133	.02962 44267
.69	.03404 31338	.48980 59013	.26446 75988	.03023 03663
.70	−0.03450 41667	0.49317 91667	0.27215 41667	−0.03082 91667
.71	.03495 30338	.49643 59346	.27993 72321	.03142 01329
.72	.03538 94400	.49957 63200	.28781 56800	.03200 25600
.73	.03581 31004	.50260 04679	.29578 83654	.03257 57329
.74	.03622 37400	.50550 85533	.30385 41133	.03313 89267
.75	−0.03662 10938	0.50830 07813	0.31201 17188	−0.03369 14063
.76	.03700 49067	.51097 73867	.32025 99467	.03423 24267
.77	.03737 49338	.51353 86346	.32859 75321	.03476 12329
.78	.03773 09400	.51598 48200	.33702 31800	.03527 70600
.79	.03807 27004	.51831 62679	.34553 55654	.03577 91329
.80	−0.03840 00000	0.52053 33333	0.35413 33333	−0.03626 66667
.81	.03871 26338	.52263 64013	.36281 50988	.03673 88663
.82	.03901 04067	.52462 58867	.37157 94467	.03719 49267
.83	.03929 31338	.52650 22346	.38042 49321	.03763 40329
.84	.03956 06400	.52826 59200	.38935 00800	.03805 53600
.85	−0.03981 27604	0.52991 74479	0.39835 33854	−0.03845 80729
.86	.04004 93400	.53145 73533	.40743 33133	.03884 13267
.87	.04027 02338	.53288 62013	.41658 82988	.03920 42663
.88	.04047 53067	.53420 45867	.42581 67467	.03954 60267
.89	.04066 44338	.53541 31346	.43511 70321	.03986 57329
.90	−0.04083 75000	0.53651 25000	0.44448 75000	−0.04016 25000
.91	.04099 44004	.53750 33679	.45392 64654	.04043 54329
.92	.04113 50400	.53838 64533	.46343 22133	.04068 36267
.93	.04125 93338	.53916 25013	.47300 29988	.04090 61663
.94	.04136 72067	.53983 22867	.48263 70467	.04110 21267
.95	−0.04145 85938	0.54039 66146	0.49233 25521	−0.04127 05729
.96	.04153 34400	.54085 63200	.50208 76800	.04141 05600
.97	.04159 17004	.54121 22679	.51190 05654	.04152 11329
.98	.04163 33400	.54146 53533	.52176 93133	.04160 13267
.99	.04165 83338	.54161 65013	.53169 19988	.04165 01663
1.00	−0.04166 66667	0.54166 66667	0.54166 66667	−0.04166 66667

FOUR-POINT COEFFICIENTS—*Continued*

$$\int_{x_0+rh}^{x_0+sh} f(x)\,dx \sim h \sum_{i=-1}^{i=2} \{B_i^{(4)}(s) - B_i^{(4)}(r)\} f(x_0 + ih)$$

p	$B_{-1}^{(4)}(p)$	$B_0^{(4)}(p)$	$B_1^{(4)}(p)$	$B_2^{(4)}(p)$
1.00	−0.04166 66667	0.54166 66667	0.54166 66667	−0.04166 66667
1.01	.04165 83338	.54161 68346	.55169 13321	.04164 98329
1.02	.04163 33400	.54146 80200	.56176 39800	.04159 86600
1.03	.04159 17004	.54122 12679	.57188 25654	.04151 21329
1.04	.04153 34400	.54087 76533	.58204 50133	.04138 92267
1.05	−0.04145 85938	0.54043 82813	0.59224 92188	−0.04122 89063
1.06	.04136 72067	.53990 42867	.60249 30467	.04103 01267
1.07	.04125 93338	.53927 68346	.61277 43321	.04079 18329
1.08	.04113 50400	.53855 71200	.62309 08800	.04051 29600
1.09	.04099 44004	.53774 63679	.63344 04654	.04019 24329
1.10	−0.04083 75000	0.53684 58333	0.64382 08333	−0.03982 91667
1.11	.04066 44338	.53585 68013	.65422 96988	.03942 20663
1.12	.04047 53067	.53478 05867	.66466 47467	.03897 00267
1.13	.04027 02338	.53361 85346	.67512 36321	.03847 19329
1.14	.04004 93400	.53237 20200	.68560 39800	.03792 66600
1.15	−0.03981 27604	0.53104 24479	0.69610 33854	−0.03733 30729
1.16	.03956 06400	.52963 12533	.70661 94133	.03669 00267
1.17	.03929 31338	.52813 99013	.71714 95988	.03599 63663
1.18	.03901 04067	.52656 98867	.72769 14467	.03525 09267
1.19	.03871 26338	.52492 27346	.73824 24321	.03445 25329
1.20	−0.03840 00000	0.52320 00000	0.74880 00000	−0.03360 00000
1.21	.03807 27004	.52140 32679	.75936 15654	.03269 21329
1.22	.03773 09400	.51953 41533	.76992 45133	.03172 77267
1.23	.03737 49338	.51759 43013	.78048 61988	.03070 55663
1.24	.03700 49067	.51558 53867	.79104 39467	.02962 44267
1.25	−0.03662 10938	0.51350 91146	0.80159 50521	−0.02848 30729
1.26	.03622 37400	.51136 72200	.81213 67800	.02728 02600
1.27	.03581 31004	.50916 14679	.82266 63654	.02601 47329
1.28	.03538 94400	.50689 36533	.83318 10133	.02468 52267
1.29	.03495 30338	.50456 56013	.84367 78988	.02329 04663
1.30	−0.03450 41667	0.50217 91667	0.85415 41667	−0.02182 91667
1.31	.03404 31338	.49973 62346	.86460 69321	.02030 00329
1.32	.03357 02400	.49723 87200	.87503 32800	.01870 17600
1.33	.03308 58004	.49468 85679	.88543 02654	.01703 30329
1.34	.03259 01400	.49208 77533	.89579 49133	.01529 25267
1.35	−0.03208 35938	0.48943 82813	0.90612 42188	−0.01347 89063
1.36	.03156 65067	.48674 21867	.91641 51467	.01159 08267
1.37	.03103 92338	.48400 15346	.92666 46321	.00962 69329
1.38	.03050 21400	.48121 84200	.93686 95800	.00758 58600
1.39	.02995 56004	.47839 49679	.94702 68654	.00546 62329
1.40	−0.02940 00000	0.47553 33333	0.95713 33333	−0.00326 66667
1.41	.02883 57338	.47263 57013	.96718 57988	−0.00098 57663
1.42	.02826 32067	.46970 42867	.97718 10467	+0.00137 78733
1.43	.02768 28338	.46674 13346	.98711 58321	.00382 56671
1.44	.02709 50400	.46374 91200	0.99698 68800	.00635 90400
1.45	−0.02650 02604	0.46072 99479	1.00679 08854	+0.00897 94271
1.46	.02589 89400	.45768 61533	1.01652 45133	.01168 82733
1.47	.02529 15338	.45462 01013	1.02618 43988	.01448 70338
1.48	.02467 85067	.45153 41867	1.03576 71467	.01737 71733
1.49	.02406 03338	.44843 08346	1.04526 93321	.02036 01671
1.50	−0.02343 75000	0.44531 25000	1.05468 75000	+0.02343 75000

FOUR-POINT COEFFICIENTS—*Continued*

$$\int_{x_0+rh}^{x_0+sh} f(x)\,dx \sim h \sum_{i=-1}^{i=2} [B_i^{(4)}(s) - B_i^{(4)}(r)]f(x_0 + ih)$$

p	$B_{-1}^{(4)}(p)$	$B_0^{(4)}(p)$	$B_1^{(4)}(p)$	$B_2^{(4)}(p)$
1.50	−0.02343 75000	0.44531 25000	1.05468 75000	0.02343 75000
1.51	.02281 05004	.44218 16679	1.06401 81654	.02661 06671
1.52	.02217 98400	.43904 08533	1.07325 78133	.02988 11733
1.53	.02154 60338	.43589 26013	1.08240 28988	.03325 05338
1.54	.02090 96067	.43273 94867	1.09144 98467	.03672 02733
1.55	−0.02027 10938	0.42958 41146	1.10039 50521	0.04029 19271
1.56	.01963 10400	.42642 91200	1.10923 48800	.04396 70400
1.57	.01899 00004	.42327 71679	1.11796 56654	.04774 71671
1.58	.01834 85400	.42013 09533	1.12658 37133	.05163 38733
1.59	.01770 72338	.41699 32013	1.13508 52988	.05562 87338
1.60	−0.01706 66667	0.41386 66667	1.14346 66667	0.05973 33333
1.61	.01642 74338	.41075 41346	1.15172 40321	.06394 92671
1.62	.01579 01400	.40765 84200	1.15985 35800	.06827 81400
1.63	.01515 54004	.40458 23679	1.16785 14654	.07272 15671
1.64	.01452 38400	.40152 88533	1.17571 38133	.07728 11733
1.65	−0.01389 60938	0.39850 07813	1.18343 67188	0.08195 85938
1.66	.01327 28067	.39550 10867	1.19101 62467	.08675 54733
1.67	.01265 46338	.39253 27346	1.19844 84321	.09167 34671
1.68	.01204 22400	.38959 87200	1.20572 92800	.09671 42400
1.69	.01143 63004	.38670 20679	1.21285 47654	.10187 94671
1.70	−0.01083 75000	0.38384 58333	1.21982 08333	0.10717 08333
1.71	.01024 65338	.38103 31013	1.22662 33988	.11259 00338
1.72	.00966 41067	.37826 69867	1.23325 83467	.11813 87733
1.73	.00909 09338	.37555 06346	1.23972 15321	.12381 87671
1.74	.00852 77400	.37288 72200	1.24600 87800	.12963 17400
1.75	−0.00797 52604	0.37027 99479	1.25211 58854	0.13557 94271
1.76	.00743 42400	.36773 20533	1.25803 86133	.14166 35733
1.77	.00690 54338	.36524 68013	1.26377 26988	.14788 59338
1.78	.00638 96067	.36282 74867	1.26931 38467	.15424 82733
1.79	.00588 75338	.36047 74346	1.27465 77321	.16075 23671
1.80	−0.00540 00000	0.35820 00000	1.27980 00000	0.16740 00000
1.81	.00492 78004	.35599 85679	1.28473 62654	.17419 29671
1.82	.00447 17400	.35387 65533	1.28946 21133	.18113 30733
1.83	.00403 26338	.35183 74013	1.29397 30988	.18822 21338
1.84	.00361 13067	.34988 45867	1.29826 47467	.19546 19733
1.85	−0.00320 85938	0.34802 16146	1.30233 25521	0.20285 44271
1.86	.00282 53400	.34625 20200	1.30617 19800	.21040 13400
1.87	.00246 24004	.34457 93679	1.30977 84654	.21810 45671
1.88	.00212 06400	.34300 72533	1.31314 74133	.22596 59733
1.89	.00180 09338	.34153 93013	1.31627 41988	.23398 74338
1.90	−0.00150 41667	0.34017 91667	1.31915 41667	0.24217 08333
1.91	.00123 12338	.33893 05346	1.32178 26321	.25051 80671
1.92	.00098 30400	.33779 71200	1.32415 48800	.25903 10400
1.93	.00076 05004	.33678 26679	1.32626 61654	.26771 16671
1.94	.00056 45400	.33589 09533	1.32811 17133	.27656 18733
1.95	−0.00039 60938	0.33512 57813	1.32968 67188	0.28558 35938
1.96	.00025 61067	.33449 09867	1.33098 63467	.29477 87733
1.97	.00014 55338	.33399 04346	1.33200 57321	.30414 93671
1.98	.00006 53400	.33362 80200	1.33273 99800	.31369 73400
1.99	.00001 65004	.33340 76679	1.33318 41654	.32342 46671
2.00	−0.00000 00000	0.33333 33333	1.33333 33333	0.33333 33333

FIVE-POINT COEFFICIENTS

$$\int_{x_0+r\lambda}^{x_0+s\lambda} f(x)\,dx \sim h \sum_{i=-2}^{i=s} \{B_i^{(s)}(s) - B_i^{(s)}(r)\} f(x_0 + i\lambda)$$

p	$B_{-2}^{(s)}(p)$	$B_{-1}^{(s)}(p)$	$B_0^{(s)}(p)$	
−2.00	−0.32222 22222	−1.37777 77778	−0.26666 66667	2.00
1.99	.31232 59038	1.37757 92185	.26681 50883	1.99
1.98	.30263 50166	1.37698 92734	.26725 40798	1.98
1.97	.29314 66814	1.37601 64748	.26797 43205	1.97
1.96	.28385 80436	1.37466 92656	.26896 66082	1.96
−1.95	−0.27476 62734	−1.37295 60000	−0.27022 18594	1.95
1.94	.26586 85657	1.37088 49437	.27173 11078	1.94
1.93	.25716 21398	1.36846 42745	.27348 55043	1.93
1.92	.24864 42394	1.36570 20826	.27547 63162	1.92
1.91	.24031 21324	1.36260 63709	.27769 49264	1.91
−1.90	−0.23216 31111	−1.35918 50556	−0.28013 28333	1.90
1.89	.22419 44918	1.35544 59664	.28278 16497	1.89
1.88	.21640 36149	1.35139 68472	.28563 31025	1.88
1.87	.20878 78444	1.34704 53561	.28867 90319	1.87
1.86	.20134 45685	1.34239 90661	.29191 13909	1.86
−1.85	−0.19407 11988	−1.33746 54653	−0.29532 22448	1.85
1.84	.18696 51706	1.33225 19575	.29890 37705	1.84
1.83	.18002 39428	1.32676 58624	.30264 82557	1.83
1.82	.17324 49976	1.32101 44163	.30654 80988	1.82
1.81	.16662 58404	1.31500 47721	.31059 58078	1.81
−1.80	−0.16016 40000	−1.30874 40000	−0.31478 40000	1.80
1.79	.15385 70282	1.30223 90877	.31910 54012	1.79
1.78	.14770 24998	1.29549 69410	.32355 28452	1.78
1.77	.14169 80124	1.28852 43841	.32811 92733	1.77
1.76	.13584 11867	1.28132 81599	.33279 77335	1.76
−1.75	−0.13012 96658	−1.27391 49306	−0.33758 13802	1.75
1.74	.12456 11155	1.26629 12779	.34246 34731	1.74
1.73	.11913 32242	1.25846 37037	.34743 73771	1.73
1.72	.11384 37025	1.25043 86301	.35249 65615	1.72
1.71	.10869 02834	1.24222 24001	.35763 45993	1.71
−1.70	−0.10367 07222	−1.23382 12778	−0.36284 51667	1.70
1.69	.09878 27962	1.22524 14490	.36812 20426	1.69
1.68	.09402 43046	1.21648 90214	.37345 91078	1.68
1.67	.08939 30688	1.20757 00253	.37885 03447	1.67
1.66	.08488 69316	1.19849 04136	.38428 98362	1.66
−1.65	−0.08050 37578	−1.18925 60625	−0.38977 17656	1.65
1.64	.07624 14337	1.17987 27717	.39529 04158	1.64
1.63	.07209 78672	1.17034 62650	.40084 01683	1.63
1.62	.06807 09874	1.16068 21906	.40641 55042	1.62
1.61	.06415 87448	1.15088 61214	.41201 10007	1.61
−1.60	−0.06035 91111	−1.14096 35556	−0.41762 13333	1.60
1.59	.05667 00792	1.13091 99169	.42324 12740	1.59
1.58	.05308 96629	1.12076 05552	.42886 56905	1.58
1.57	.04961 58968	1.11049 07466	.43448 95461	1.57
1.56	.04624 68365	1.10011 56941	.44010 78989	1.56
−1.55	−0.04298 05582	−1.08964 05278	−0.44571 59010	1.55
1.54	.03981 51586	1.07907 03055	.45130 87985	1.54
1.53	.03674 87552	1.06841 00129	.45688 19300	1.53
1.52	.03377 94856	1.05766 45643	.46243 07268	1.52
1.51	.03090 55078	1.04683 88026	.46795 07121	1.51
−1.50	−0.02812 50000	−1.03593 75000	−0.47343 75000	1.50
	$-B_2^{(s)}(p)$	$-B_1^{(s)}(p)$	$-B_0^{(s)}(p)$	p

FIVE-POINT COEFFICIENTS—*Continued*

$$\int_{x_0+rh}^{x_0+sh} f(x)\,dx \sim h \sum_{i=-2}^{i=2} \{B_i^{(5)}(s) - B_i^{(5)}(r)\} f(x_0 + ih)$$

p	$B_1^{(5)}(p)$	$B_2^{(5)}(p)$	
−2.00	−0.04444 44444	0.01111 11111	2.00
1.99	.04437 85526	.01109 87633	1.99
1.98	.04418 39534	.01106 23234	1.98
1.97	.04386 52090	.01100 26857	1.97
1.96	.04342 68123	.01092 07297	1.96
−1.95	−0.04287 31875	0.01081 73203	1.95
1.94	.04220 86904	.01069 33076	1.94
1.93	.04143 76087	.01054 95273	1.93
1.92	.04056 41626	.01038 68006	1.92
1.91	.03959 25050	.01020 59347	1.91
−1.90	−0.03852 67222	0.01000 77222	1.90
1.89	.03737 08339	.00979 29419	1.89
1.88	.03612 87939	.00956 23585	1.88
1.87	.03480 44903	.00931 67227	1.87
1.86	.03340 17461	.00905 67715	1.86
−1.85	−0.03192 43194	0.00878 32283	1.85
1.84	.03037 59041	.00849 68027	1.84
1.83	.02876 01299	.00819 81909	1.83
1.82	.02708 05630	.00788 80758	1.82
1.81	.02534 07063	.00756 71267	1.81
−1.80	−0.02354 40000	0.00723 60000	1.80
1.79	.02169 38219	.00689 53389	1.79
1.78	.01979 34877	.00654 57736	1.78
1.77	.01784 62516	.00618 79213	1.77
1.76	.01585 53065	.00582 23866	1.76
−1.75	−0.01382 37847	0.00544 97613	1.75
1.74	.01175 47579	.00507 06245	1.74
1.73	.00965 12379	.00468 55429	1.73
1.72	.00751 61768	.00429 50709	1.72
1.71	.00535 24676	.00389 97503	1.71
−1.70	−0.00316 29444	0.00350 01111	1.70
1.69	−0.00095 03831	.00309 66709	1.69
1.68	+0.00128 24986	.00268 99354	1.68
1.67	.00353 30405	.00228 03983	1.67
1.66	.00579 86397	.00186 85417	1.66
−1.65	0.00807 67500	0.00145 48359	1.65
1.64	.01036 48816	.00103 97396	1.64
1.63	.01266 06008	.00062 36999	1.63
1.62	.01496 15294	+0.00020 71526	1.62
1.61	.01726 53445	−0.00020 94777	1.61
−1.60	0.01956 97778	−0.00062 57778	1.60
1.59	.02187 26156	.00104 13455	1.59
1.58	.02417 16981	.00145 57895	1.58
1.57	.02646 49192	.00186 87297	1.57
1.56	.02875 02259	.00227 97965	1.56
−1.55	0.03102 56181	−0.00268 86311	1.55
1.54	.03328 91479	.00309 48853	1.54
1.53	.03553 89196	.00349 82215	1.53
1.52	.03777 30890	.00389 83122	1.52
1.51	.03998 98632	.00429 48407	1.51
−1.50	0.04218 75000	−0.00468 75000	1.50
	$-B_{-1}^{(5)}(p)$	$-B_{-2}^{(5)}(p)$	p

FIVE-POINT COEFFICIENTS—*Continued*

$$\int_{x_0+rh}^{x_0+sh} f(x)\,dx \sim h \sum_{i=-2}^{i=2} \{B_i^{(s)}(s) - B_i^{(s)}(r)\} f(x_0 + ih)$$

p	$B_{-2}^{(s)}(p)$	$B_{-1}^{(s)}(p)$	$B_0^{(s)}(p)$	
−1.50	−0.02812 50000	−1.03593 75000	−0.47343 75000	1.50
1.49	.02543 61606	1.02496 53582	.47888 67954	1.49
1.48	.02283 72078	1.01392 70090	.48429 43932	1.48
1.47	.02032 63798	1.00282 70146	.48965 61775	1.47
1.46	.01790 19347	0.99166 98679	.49496 81215	1.46
−1.45	−0.01556 21502	−0.98045 99931	−0.50022 62865	1.45
1.44	.01330 53235	.96920 17459	.50542 68211	1.44
1.43	.01112 97715	.95789 94142	.51056 59614	1.43
1.42	.00903 38305	.94655 72181	.51564 00295	1.42
1.41	.00701 58558	.93517 93106	.52064 54335	1.41
−1.40	−0.00507 42222	−0.92376 97778	−0.52557 86667	1.40
1.39	.00320 73236	.91233 26395	.53043 63068	1.39
1.38	−0.00141 35726	.90087 18494	.53521 50158	1.38
1.37	+0.00030 85989	.88939 12958	.53991 15390	1.37
1.36	.00196 07404	.87789 48016	.54452 27042	1.36
−1.35	+0.00354 43828	−0.86638 61250	−0.54904 54219	1.35
1.34	.00506 10383	.85486 89597	.55347 66838	1.34
1.33	.00651 22004	.84334 69355	.55781 35628	1.33
1.32	.00789 93446	.83182 36186	.56205 32122	1.32
1.31	.00922 39279	.82030 25119	.56619 28649	1.31
−1.30	+0.01048 73889	−0.80878 70556	−0.57022 98333	1.30
1.29	.01169 11484	.79728 06274	.57416 15082	1.29
1.28	.01283 66091	.78578 65432	.57798 53585	1.28
1.27	.01392 51558	.77430 80571	.58169 89304	1.27
1.26	.01495 81555	.76284 83621	.58529 98469	1.26
−1.25	+0.01593 69575	−0.75141 05903	−0.58878 58073	1.25
1.24	.01686 28934	.73999 78135	.59215 45865	1.24
1.23	.01773 72774	.72861 30434	.59540 40342	1.23
1.22	.01856 14064	.71725 92323	.59853 20748	1.22
1.21	.01933 65598	.70593 92731	.60153 67064	1.21
−1.20	+0.02006 40000	−0.69465 60000	−0.60441 60000	1.20
1.19	.02074 49721	.68341 21887	.60716 80997	1.19
1.18	.02138 07042	.67221 05570	.60979 12212	1.18
1.17	.02197 24078	.66105 37651	.61228 36518	1.17
1.16	.02252 12773	.64994 44159	.61464 37495	1.16
−1.15	+0.02302 84905	−0.63888 50556	−0.61686 99427	1.15
1.14	.02349 52085	.62787 81739	.61896 07291	1.14
1.13	.02392 25761	.61692 62047	.62091 46756	1.13
1.12	.02431 17215	.60603 15261	.62273 04175	1.12
1.11	.02466 37568	.59519 64611	.62440 66578	1.11
−1.10	+0.02497 97778	−0.58442 32778	−0.62594 21667	1.10
1.09	.02526 08641	.57371 41900	.62733 57811	1.09
1.08	.02550 80794	.56307 13574	.62858 64038	1.08
1.07	.02572 24715	.55249 68863	.62969 30032	1.07
1.06	.02590 50724	.54199 28296	.63065 46122	1.06
−1.05	+0.02605 68984	−0.53156 11875	−0.63147 03281	1.05
1.04	.02617 89503	.52120 39077	.63213 93118	1.04
1.03	.02627 22131	.51092 28860	.63266 07870	1.03
1.02	.02633 76566	.50071 99666	.63303 40402	1.02
1.01	.02637 62355	.49059 69424	.63325 84192	1.01
−1.00	+0.02638 88889	−0.48055 55556	−0.63333 33333	1.00
	$-B_2^{(s)}(p)$	$-B_1^{(s)}(p)$	$-B_0^{(s)}(p)$	p

FIVE-POINT COEFFICIENTS—*Continued*

$$\int_{x_0+rh}^{x_0+sh} f(x)\,dx \sim h \sum_{i=-2}^{i=2} [B_i^{(5)}(s) - B_i^{(5)}(r)]f(x_0 + ih)$$

p	$B_1^{(5)}(p)$	$B_2^{(5)}(p)$	
−1.50	0.04218 75000	−0.00468 75000	1.50
1.49	.04436 43076	.00507 59935	1.49
1.48	.04651 86443	.00546 00344	1.48
1.47	.04864 89179	.00583 93460	1.47
1.46	.05075 35855	.00621 36614	1.46
−1.45	0.05283 11528	−0.00658 27231	1.45
1.44	.05488 01741	.00694 62835	1.44
1.43	.05689 92516	.00730 41045	1.43
1.42	.05888 70352	.00765 59571	1.42
1.41	.06084 22219	.00800 16220	1.41
−1.40	0.06276 35556	−0.00834 08889	1.40
1.39	.06464 98264	.00867 35565	1.39
1.38	.06649 98706	.00899 94326	1.38
1.37	.06831 25700	.00931 83341	1.37
1.36	.07008 68517	.00963 00863	1.36
−1.35	0.07182 16875	−0.00993 45234	1.35
1.34	.07351 60936	.01023 14884	1.34
1.33	.07516 91303	.01052 08325	1.33
1.32	.07677 99014	.01080 24154	1.32
1.31	.07834 75540	.01107 61051	1.31
−1.30	0.07987 12778	−0.01134 17778	1.30
1.29	.08135 03051	.01159 93178	1.29
1.28	.08278 39101	.01184 86175	1.28
1.27	.08417 14087	.01208 95771	1.27
1.26	.08551 21579	.01232 21045	1.26
−1.25	0.08680 55556	−0.01254 61155	1.25
1.24	.08805 10399	.01276 15333	1.24
1.23	.08924 80891	.01296 82888	1.23
1.22	.09039 62210	.01316 63202	1.22
1.21	.09149 49927	.01335 55731	1.21
−1.20	0.09254 40000	−0.01353 60000	1.20
1.19	.09354 28771	.01370 75608	1.19
1.18	.09449 12963	.01387 02224	1.18
1.17	.09538 89674	.01402 39584	1.17
1.16	.09623 56375	.01416 87494	1.16
−1.15	0.09703 10903	−0.01430 45825	1.15
1.14	.09777 51461	.01443 14515	1.14
1.13	.09846 76611	.01454 93568	1.13
1.12	.09910 85272	.01465 83051	1.12
1.11	.09969 76714	.01475 83094	1.11
−1.10	0.10023 50556	−0.01484 93889	1.10
1.09	.10072 06759	.01493 15689	1.09
1.08	.10115 45626	.01500 48806	1.08
1.07	.10153 67795	.01506 93614	1.07
1.06	.10186 74237	.01512 50543	1.06
−1.05	0.10214 66250	−0.01517 20078	1.05
1.04	.10237 45456	.01521 02764	1.04
1.03	.10255 13798	.01523 99199	1.03
1.02	.10267 73534	.01526 10034	1.02
1.01	.10275 27235	.01527 35974	1.01
−1.00	0.10277 77778	−0.01527 77778	1.00
	$-B_{-1}^{(5)}(p)$	$-B_{-2}^{(5)}(p)$	p

FIVE-POINT COEFFICIENTS—*Continued*

$$\int_{x_0+rh}^{x_0+sh} f(x)\,dx \sim h \sum_{i=-2}^{i=2} \{B_i^{(5)}(s) - B_i^{(5)}(r)\} f(x_0 + ih)$$

p	$B_{-2}^{(5)}(p)$	$B_{-1}^{(5)}(p)$	$B_0^{(5)}(p)$	
−1.00	0.02638 88889	−0.48055 55556	−0.63333 33333	1.00
.99	.02637 65410	.47059 74979	.63325 82525	.99
.98	.02634 01011	.46072 44112	.63303 27065	.98
.97	.02628 04635	.45093 78876	.63265 62846	.97
.96	.02619 85075	.44123 94701	.63212 86349	.96
−.95	0.02609 50981	−0.43163 06528	−0.63144 94635	.95
.94	.02597 10854	.42211 28815	.63061 85345	.94
.93	.02582 73050	.41268 75539	.62963 56685	.93
.92	.02566 45784	.40335 60203	.62850 07428	.92
.91	.02548 37125	.39411 95836	.62721 36906	.91
−.90	0.02528 55000	−0.38497 95000	−0.62577 45000	.90
.89	.02507 07197	.37593 69792	.62418 32139	.89
.88	.02484 01362	.36699 31850	.62243 99292	.88
.87	.02459 45005	.35814 92356	.62054 47960	.87
.86	.02433 45493	.34940 62039	.61849 80175	.86
−.85	0.02406 10061	−0.34076 51181	−0.61629 98490	.85
.84	.02377 45805	.33222 69619	.61395 05971	.84
.83	.02347 59687	.32379 26752	.61145 06199	.83
.82	.02316 58535	.31546 31541	.60880 03255	.82
.81	.02284 49045	.30723 92516	.60600 01720	.81
−.80	0.02251 37778	−0.29912 17778	−0.60305 06667	.80
.79	.02217 31167	.29111 15005	.59995 23653	.79
.78	.02182 35514	.28320 91454	.59670 58718	.78
.77	.02146 56991	.27541 53968	.59331 18375	.77
.76	.02110 01644	.26773 08976	.58977 09602	.76
−.75	0.02072 75391	−0.26015 62500	−0.58608 39844	.75
.74	.02034 84023	.25269 20157	.58225 16998	.74
.73	.01996 33207	.24533 87165	.57827 49413	.73
.72	.01957 28486	.23809 68346	.57415 45882	.72
.71	.01917 75281	.23096 68129	.56989 15634	.71
−.70	0.01877 78889	−0.22394 90556	−0.56548 68333	.70
.69	.01837 44487	.21704 39284	.56094 14067	.69
.68	.01796 77131	.21025 17592	.55625 63345	.68
.67	.01755 81761	.20357 28381	.55143 27089	.67
.66	.01714 63195	.19700 74181	.54647 16629	.66
−.65	0.01673 26137	−0.19055 57153	−0.54137 43608	.65
.64	.01631 75174	.18421 79095	.53614 20425	.64
.63	.01590 14777	.17799 41444	.53077 59327	.63
.62	.01548 49304	.17188 45283	.52527 73308	.62
.61	.01506 83001	.16588 91341	.51964 75648	.61
−.60	0.01465 20000	−0.16000 80000	−0.51388 80000	.60
.59	.01423 64323	.15424 11297	.50800 00382	.59
.58	.01382 19882	.14858 84930	.50198 51172	.58
.57	.01340 90481	.14305 00261	.49584 47103	.57
.56	.01299 79813	.13762 56319	.48958 03255	.56
−.55	0.01258 91467	−0.13231 51806	−0.48319 35052	.55
.54	.01218 28925	.12711 85099	.47668 58251	.54
.53	.01177 95563	.12203 54257	.47005 88941	.53
.52	.01137 94655	.11706 57021	.46331 43535	.52
.51	.01098 29371	.11220 90821	.45645 38763	.51
−.50	0.01059 02778	−0.10746 52778	−0.44947 91667	.50
	$-B_2^{(5)}(p)$	$-B_1^{(5)}(p)$	$-B_0^{(5)}(p)$	p

FIVE-POINT COEFFICIENTS—*Continued*

$$\int_{x_0+rh}^{x_0+sh} f(x)\,dx \sim h \sum_{i=-2}^{i=2} \{B_i^{(s)}(s) - B_i^{(s)}(r)\} f(x_0 + ih)$$

p	$B_1^{(s)}(p)$	$B_2^{(s)}(p)$	
−1.00	0.10277 77778	−0.01527 77778	1.00
.99	.10275 28346	.01527 36252	.99
.98	.10267 82421	.01526 12255	.98
.97	.10255 43782	.01524 06695	.97
.96	.10238 16499	.01521 20525	.96
−.95	0.10216 04931	−0.01517 54748	.95
.94	.10189 13719	.01513 10413	.94
.93	.10157 47786	.01507 88612	.93
.92	.10121 12330	.01501 90482	.92
.91	.10080 12822	.01495 17204	.91
−.90	0.10034 55000	−0.01487 70000	.90
.89	.09984 44866	.01479 50132	.89
.88	.09929 88683	.01470 58904	.88
.87	.09870 92969	.01460 97658	.87
.86	.09807 64495	.01450 67774	.86
−.85	0.09740 10278	−0.01439 70668	.85
.84	.09668 37581	.01428 07795	.84
.83	.09592 53906	.01415 80642	.83
.82	.09512 66992	.01402 90731	.82
.81	.09428 84809	.01389 39618	.81
−.80	0.09341 15556	−0.01375 28889	.80
.79	.09249 67654	.01360 60162	.79
.78	.09154 49746	.01345 35086	.78
.77	.09055 70690	.01329 55338	.77
.76	.08953 39557	.01313 22623	.76
−.75	0.08847 65625	−0.01296 38672	.75
.74	.08738 58376	.01279 05244	.74
.73	.08626 27493	.01261 24122	.73
.72	.08510 82854	.01242 97114	.72
.71	.08392 34530	.01224 26048	.71
−.70	0.08270 92778	−0.01205 12778	.70
.69	.08146 68041	.01185 59176	.69
.68	.08019 70941	.01165 67135	.68
.67	.07890 12277	.01145 38568	.67
.66	.07758 03019	.01124 75405	.66
−.65	0.07623 54306	−0.01103 79592	.65
.64	.07486 77439	.01082 53093	.64
.63	.07347 83881	.01060 97886	.63
.62	.07206 85250	.01039 15962	.62
.61	.07063 93317	.01017 09328	.61
−.60	0.06919 20000	−0.00994 80000	.60
.59	.06772 77361	.00972 30006	.59
.58	.06624 77603	.00949 61384	.58
.57	.06475 33064	.00926 76182	.57
.56	.06324 56215	.00903 76454	.56
−.55	0.06172 59653	−0.00880 64262	.55
.54	.06019 56101	.00857 41675	.54
.53	.05865 58401	.00834 10766	.53
.52	.05710 79512	.00810 73611	.52
.51	.05555 32504	.00787 32292	.51
−.50	0.05399 30556	−0.00763 88889	.50
	$-B_{-1}^{(s)}(p)$	$-B_{-2}^{(s)}(p)$	p

FIVE-POINT COEFFICIENTS—*Continued*

$$\int_{x_0+rh}^{x_0+sh} f(x)\,dx \sim h \sum_{i=-2}^{i=2} \{B_i^{(s)}(s) - B_i^{(s)}(r)\} f(x_0 + ih)$$

p	$B_{-2}^{(s)}(p)$	$B_{-1}^{(s)}(p)$	$B_0^{(s)}(p)$	
−.50	0.01059 02778	−0.10746 52778	−0.44947 91667	.50
.49	.01020 17843	.10283 39710	.44239 19596	.49
.48	.00981 77434	.09831 48134	.43519 40198	.48
.47	.00943 84317	.09390 74273	.42788 71417	.47
.46	.00906 41164	.08961 14056	.42047 31482	.46
−.45	0.00869 50547	−0.08542 63125	−0.41295 38906	.45
.44	.00833 14943	.08135 16837	.40533 12478	.44
.43	.00797 36733	.07738 70270	.39760 71255	.43
.42	.00762 18206	.07353 18226	.38978 34562	.42
.41	.00727 61557	.06978 55234	.38186 21977	.41
−.40	0.00693 68889	−0.06614 75556	−0.37384 53333	.40
.39	.00660 42213	.06261 73189	.36573 48710	.39
.38	.00627 83451	.05919 41872	.35753 28425	.38
.37	.00595 94437	.05587 75086	.34924 13031	.37
.36	.00564 76915	.05266 66061	.34086 23309	.36
−.35	0.00534 32543	−0.04956 07778	−0.33239 80260	.35
.34	.00504 62894	.04655 92975	.32385 05105	.34
.33	.00475 69453	.04366 14149	.31522 19270	.33
.32	.00447 53624	.04086 63563	.30651 44388	.32
.31	.00420 16727	.03817 33246	.29773 02291	.31
−.30	0.00393 60000	−0.03558 15000	−0.28887 15000	.30
.29	.00367 84599	.03309 00402	.27994 04724	.29
.28	.00342 91602	.03069 80810	.27093 93852	.28
.27	.00318 82007	.02840 47366	.26187 04945	.27
.26	.00295 56733	.02620 90999	.25273 60735	.26
−.25	0.00273 16623	−0.02411 02431	−0.24353 84115	.25
.24	.00251 62445	.02210 72179	.23427 98131	.24
.23	.00230 94890	.02019 90562	.22496 25984	.23
.22	.00211 14575	.01838 47701	.21558 91015	.22
.21	.00192 22047	.01666 33526	.20616 16705	.21
−.20	0.00174 17778	−0.01503 37778	−0.19668 26667	.20
.19	.00157 02169	.01349 50015	.18715 44638	.19
.18	.00140 75554	.01204 59614	.17757 94478	.18
.17	.00125 38194	.01068 55778	.16796 00160	.17
.16	.00110 90284	.00941 27536	.15829 85762	.16
−.15	0.00097 31953	−0.00822 63750	−0.14859 75469	.15
.14	.00084 63263	.00712 53117	.13885 93558	.14
.13	.00072 84209	.00610 84175	.12908 64398	.13
.12	.00061 94726	.00517 45306	.11928 12442	.12
.11	.00051 94684	.00432 24739	.10944 62219	.11
−.10	0.00042 83889	−0.00355 10556	−0.09958 38333	.10
.09	.00034 62089	.00285 90694	.08969 65452	.09
.08	.00027 28971	.00224 52952	.07978 68305	.08
.07	.00020 84163	.00170 84991	.06985 71674	.07
.06	.00015 27235	.00124 74341	.05991 00389	.06
−.05	0.00010 57700	−0.00086 08403	−0.04994 79323	.05
.04	.00006 75014	.00054 74455	.03997 33385	.04
.03	.00003 78579	.00030 59654	.02998 87512	.03
.02	.00001 67744	.00013 51043	.01999 66668	.02
.01	.00000 41803	.00003 35551	.00999 95833	.01
−.00	0.00000 00000	−0.00000 00000	−0.00000 00000	.00
	$-B_2^{(s)}(p)$	$-B_1^{(s)}(p)$	$-B_0^{(s)}(p)$	p

FIVE-POINT COEFFICIENTS—*Continued*

$$\int_{x_0+rh}^{x_0+sh} f(x)\,dx \sim h \sum_{i=-2}^{i=2} \{B_i^{(s)}(s) - B_i^{(s)}(r)\} f(x_0 + ih)$$

p	$B_1^{(s)}(p)$	$B_2^{(s)}(p)$	
−.50	0.05399 30556	−0.00763 88889	.50
.49	.05242 86949	.00740 45486	.49
.48	.05086 15066	.00717 04166	.48
.47	.04929 28385	.00693 67012	.47
.46	.04772 40477	.00670 36103	.46
−.45	0.04615 65000	−0.00647 13516	.45
.44	.04459 15696	.00624 01324	.44
.43	.04303 06388	.00601 01596	.43
.42	.04147 50974	.00578 16394	.42
.41	.03992 63425	.00555 47772	.41
−.40	0.03838 57778	−0.00532 97778	.40
.39	.03685 48136	.00510 68450	.39
.38	.03533 48661	.00488 61815	.38
.37	.03382 73572	.00466 79892	.37
.36	.03233 37139	.00445 24685	.36
−.35	0.03085 53681	−0.00423 98186	.35
.34	.02939 37559	.00403 02373	.34
.33	.02795 03176	.00382 39210	.33
.32	.02652 64970	.00362 10642	.32
.31	.02512 37412	.00342 18602	.31
−.30	0.02374 35000	−0.00322 65000	.30
.29	.02238 72256	.00303 51730	.29
.28	.02105 63723	.00284 80664	.28
.27	.01975 23959	.00266 53655	.27
.26	.01847 67535	.00248 72534	.26
−.25	0.01723 09028	−0.00231 39106	.25
.24	.01601 63021	.00214 55155	.24
.23	.01483 44096	.00198 22440	.23
.22	.01368 66832	.00182 42691	.22
.21	.01257 45799	.00167 17615	.21
−.20	0.01149 95556	−0.00152 48889	.20
.19	.01046 30644	.00138 38160	.19
.18	.00946 65586	.00124 87046	.18
.17	.00851 14880	.00111 97136	.17
.16	.00759 92997	.00099 69983	.16
−.15	0.00673 14375	−0.00088 07109	.15
.14	.00590 93416	.00077 10004	.14
.13	.00513 44483	.00066 80120	.13
.12	.00440 81894	.00057 18874	.12
.11	.00373 19920	.00048 27646	.11
−.10	0.00310 72778	−0.00040 07778	.10
.09	.00253 54631	.00032 60573	.09
.08	.00201 79581	.00025 87295	.08
.07	.00155 61667	.00019 89166	.07
.06	.00115 14859	.00014 67365	.06
−.05	0.00080 53056	−0.00010 23030	.05
.04	.00051 90079	.00006 57253	.04
.03	.00029 39671	.00003 71083	.03
.02	.00013 15490	.00001 65522	.02
.01	.00003 31107	.00000 41526	.01
−.00	0.00000 00000	−0.00000 00000	.00
	$-B_{-1}^{(s)}(p)$	$-B_{-2}^{(s)}(p)$	p

SIX-POINT COEFFICIENTS

$$\int_{x_0+rh}^{x_0+sh} f(x)\,dx \sim h \sum_{i=-2}^{i=3} \{B_i^{(6)}(s) - B_i^{(6)}(r)\} f(x_0 + ih)$$

p	$B_{-2}^{(6)}(p)$	$B_{-1}^{(6)}(p)$	$B_0^{(6)}(p)$
−2.0	−0.31111 11111	−1.43333 33333	−0.15555 55556
−1.9	.22192 02375	1.41039 94236	.17770 40972
−1.8	.15205 32000	1.34929 80000	.23367 60000
−1.7	.09836 07486	1.26037 11458	.30974 54306
−1.6	.05806 08000	1.15245 51111	.39463 82222
−1.5	−0.02871 09375	−1.03300 78125	−0.47929 68750
−1.4	−0.00818 19111	0.90823 13333	.55665 55556
−1.3	+0.00536 78625	.78318 94236	.62142 50972
−1.2	.01351 68000	.66192 00000	.66988 80000
−1.1	.01760 36514	.54754 26458	.69970 34306
−1.0	0.01875 00000	−0.44236 11111	−0.70972 22222
−0.9	.01788 17625	.34796 08125	.69981 18750
−0.8	.01574 96889	.26530 13333	.67069 15556
−0.7	.01294 88625	.19480 39236	.62377 70972
−0.6	.00993 72000	.13643 40000	.56103 60000
−0.5	0.00705 29514	−0.08977 86458	−0.48485 24306
−0.4	.00453 12000	.05411 91111	.39790 22222
−0.3	.00251 93625	.02849 83125	.30303 78750
−0.2	.00109 16889	.01178 33333	.20318 35556
−0.1	.00026 27625	.00272 29236	.10124 00972
0.0	0.00000 00000	−0.00000 00000	0.00000 00000
+0.1	.00023 51514	.00227 91458	+0.09792 75694
0.2	.00087 48000	.00824 91111	.19018 17778
0.3	.00180 98625	.01666 03125	.27470 51250
0.4	.00292 40889	.02635 73333	.34978 84444
0.5	0.00410 15625	−0.03630 64236	0.41410 59028
0.6	.00523 32000	.04561 80000	.46674 00000
0.7	.00622 22514	.05356 41458	.50719 65694
0.8	.00698 88000	.05959 11111	.53540 97778
0.9	.00747 32625	.06332 68125	.55173 71250
1.0	0.00763 88889	−0.06458 33333	0.55694 44444
1.1	.00747 32625	.06335 44236	.55218 09028
1.2	.00698 88000	.05980 80000	.53894 40000
1.3	.00622 22514	.05427 36458	.51903 45694
1.4	.00523 32000	.04722 51111	.49450 17778
1.5	0.00410 15625	−0.03925 78125	0.46757 81250
1.6	.00292 40889	.03106 13333	.44060 44444
1.7	.00180 98625	.02338 69236	.41594 49028
1.8	.00087 48000	.01701 00000	.39589 20000
1.9	.00023 51514	.01268 76458	.38256 15694
2.0	0.00000 00000	−0.01111 11111	0.37777 77778
2.1	.00026 27625	.01285 33125	.38294 81250
2.2	.00109 16889	.01831 13333	.39892 84444
2.3	.00251 93625	.02764 39236	.42587 79028
2.4	.00453 12000	.04070 40000	.46310 40000
2.5	0.00705 29514	−0.05696 61458	0.50889 75694
2.6	.00993 72000	.07544 91111	.56035 77778
2.7	.01294 88625	.09463 33125	.61320 71250
2.8	.01574 96889	.11237 33333	.66159 64444
2.9	.01788 17625	.12580 54236	.69789 99028
3.0	0.01875 00000	−0.13125 00000	0.71250 00000

SIX-POINT COEFFICIENTS—*Continued*

$$\int_{x_0+rh}^{x_0+sh} f(x)\,dx \sim h \sum_{i=-2}^{i=3} [B_i^{(6)}(s) - B_i^{(6)}(r)]f(x_0 + ih)$$

$B_1^{(6)}(p)$	$B_2^{(6)}(p)$	$B_3^{(6)}(p)$	p
−0.15555 55556	0.06666 66667	−0.01111 11111	−2.0
.14095 54583	.06122 20903	.01024 28736	−1.9
.10465 20000	.04779 00000	.00811 08000	−1.8
.05626 26806	.03004 99792	.00530 99736	−1.7
−0.00341 33333	+0.01086 57778	−0.00229 83111	−1.6
+0.04804 68750	−0.00761 71875	+0.00058 59375	−1.5
.09384 04444	.02387 93333	.00310 76889	−1.4
.13106 65417	.03693 94097	.00511 95264	−1.3
.15801 60000	.04627 20000	.00654 72000	−1.2
.17399 63194	.05173 00208	.00737 61264	−1.1
0.17916 66667	−0.05347 22222	0.00763 88889	−1.0
.17438 28750	.05189 56875	.00740 37375	−0.9
.16105 24444	.04757 33333	.00676 40889	−0.8
.14099 95417	.04119 64097	.00582 90264	−0.7
.11634 00000	.03352 20000	.00471 48000	−0.6
0.08936 63194	−0.02532 55208	0.00353 73264	−0.5
.06244 26667	.01735 82222	.00240 56889	−0.4
.03790 98750	.01030 96875	.00141 66375	−0.3
.01800 04444	.00477 53333	.00065 00889	−0.2
.00476 35417	.00122 89097	.00016 56264	−0.1
0.00000 00000	−0.00000 00000	0.00000 00000	0.0
.00520 73194	.00125 65208	.00016 56264	+0.1
.02153 46667	.00499 22222	.00065 00889	0.2
.04974 78750	.01101 91875	.00141 66375	0.3
.09020 44444	.01896 53333	.00240 56889	0.4
0.14283 85417	−0.02827 69097	0.00353 73264	0.5
.20715 60000	.03822 60000	.00471 48000	0.6
.28223 93194	.04792 30208	.00582 90264	0.7
.36676 26667	.05633 42222	.00676 40889	0.8
.45901 68750	.06230 41875	.00740 37375	0.9
0.55694 44444	−0.06458 33333	0.00763 88889	1.0
.65818 45417	.06186 04097	.00737 61264	1.1
.76012 80000	.05280 00000	.00654 72000	1.2
.85998 23194	.03608 50208	.00511 95264	1.3
0.95484 66667	−0.01046 42222	.00310 76889	1.4
1.04179 68750	+0.02519 53125	+0.00058 59375	1.5
1.11798 04444	.07185 06667	−0.00229 83111	1.6
1.18072 15417	.13022 05903	.00530 99736	1.7
1.22763 60000	.20071 80000	.00811 08000	1.8
1.25675 63194	.28337 74792	.01024 28736	1.9
1.26666 66667	0.37777 77778	−0.01111 11111	2.0
1.25664 78750	.48295 93125	.00996 47625	2.1
1.22683 24444	.59733 66667	−0.00587 79111	2.2
1.17836 95417	.71860 60903	+0.00227 10264	2.3
1.11360 00000	.84364 80000	.01582 08000	2.4
1.03624 13194	0.96842 44792	0.03634 98264	2.5
0.95158 26667	1.08787 17778	.06569 96889	2.6
.86668 98750	1.19578 78125	.10599 96375	2.7
.79062 04444	1.28471 46667	.15969 20889	2.8
.73464 85417	1.34581 60903	.22955 91264	2.9
0.71250 00000	1.36875 00000	0.31875 00000	3.0

SEVEN-POINT COEFFICIENTS

$$\int_{x_0+rh}^{x_0+sh} f(x)\,dx \sim h \sum_{i=-3}^{i=3} \{B_i^{(7)}(s) - B_i^{(7)}(r)\} f(x_0 + ih)$$

p	$B_{-3}^{(7)}(p)$	$B_{-2}^{(7)}(p)$	$B_{-1}^{(7)}(p)$	$B_0^{(7)}(p)$	
−3.0	−0.30580 35714	−1.44642 85714	−0.51830 35714	−0.97142 85714	3.0
−2.9	.21732 67591	1.41921 02938	.55116 30329	.94254 72478	2.9
−2.8	.14918 18430	1.34777 61422	.63296 67556	.87180 13630	2.8
−2.7	.09770 61343	1.24554 88318	.74228 73268	.77907 71893	2.7
−2.6	.05974 01945	1.12362 87441	.86219 02508	.67954 76656	2.6
−2.5	−0.03257 79183	−0.99105 59276	−0.97966 26984	−0.58433 57308	2.5
−2.4	.01391 98171	.85505 38971	1.08508 52571	.50112 36571	2.4
−2.3	−0.00182 94024	.72125 58345	1.17174 51812	.43471 03835	2.3
−2.2	+0.00530 74313	.59391 37879	1.23538 96413	.38751 88487	2.2
−2.1	.00882 01225	.47609 14725	1.27381 74750	.36005 53250	2.1
−2.0	0.00978 83598	−0.36984 12698	−1.28650 79365	−0.35132 27513	2.0
−1.9	.00907 42985	.27636 60283	1.27428 49466	.35919 00665	1.9
−1.8	.00735 21771	.19616 62629	1.23901 53429	.38071 95429	1.8
−1.7	.00513 54344	.12917 33552	1.18333 96294	.41245 41192	1.7
−1.6	.00280 14256	.07486 93537	1.11043 37270	.45066 67344	1.6
−1.5	+0.00061 38393	−0.03239 39732	−1.02380 02232	−0.49157 36607	1.5
−1.4	−0.00125 70859	−0.00063 93956	0.92708 76222	.53151 38370	1.4
−1.3	.00271 64447	+0.02166 65310	.82393 60948	.56709 62022	1.3
−1.2	.00372 85486	.03588 80914	.71784 82286	.59531 70286	1.2
−1.1	.00430 27088	.04341 99041	.61208 32776	.61364 92549	1.1
−1.0	−0.00448 08201	0.04563 49206	−0.50957 34127	−0.62010 58201	1.0
−0.9	.00432 66439	.04384 16261	.41286 04714	.61327 89964	0.9
−0.8	.00391 66916	.03924 98387	.32405 17079	.59235 77228	0.8
−0.7	.00333 29080	.03294 45103	.24479 30431	.55712 49380	0.7
−0.6	.00265 49543	.02586 69257	.17625 83143	.50793 69143	0.6
−0.5	−0.00195 82920	0.01880 27034	−0.11915 30258	−0.44568 65906	0.5
−0.4	.00130 74658	.01237 59949	.07373 10984	.37175 29058	0.4
−0.3	.00075 49871	.00704 92854	.03982 31196	.28793 81321	0.3
−0.2	.00033 94174	.00312 81930	.01687 45937	.19639 52085	0.2
−0.1	.00008 46512	.00077 06696	.00399 26913	.09954 70737	0.1
−0.0	−0.00000 00000	0.00000 00000	−0.00000 00000	0.00000 00000	0.0
+0.1	.00008 09752	.00072 10027	.00349 37740	+0.09954 70737	−0.1
0.2	.00031 06715	.00273 88292	.01290 91841	.19639 52085	−0.2
0.3	.00066 16504	.00577 97646	.02658 50679	.28793 81321	−0.3
0.4	.00109 82231	.00951 34273	.04283 06794	.37175 29058	−0.4
0.5	−0.00157 90344	0.01357 57688	−0.05999 19395	0.44568 65906	−0.5
0.6	.00205 98457	.01759 22743	.07651 56857	.50793 69143	−0.6
0.7	.00249 64184	.02120 07619	.09101 04222	.55712 49380	−0.7
0.8	.00284 73972	.02407 31835	.10230 20698	.59235 77228	−0.8
0.9	.00307 70936	.02593 58239	.10948 32161	.61327 89964	−0.9
1.0	−0.00315 80688	0.02658 73016	−0.11195 43651	0.62010 58201	−1.0
1.1	.00307 34176	.02591 37681	.10945 56877	.61364 92549	−1.1
1.2	.00281 86514	.02390 07086	.10208 77714	.59531 70286	−1.2
1.3	.00240 30816	.02064 07412	.09031 98704	.56709 62022	−1.3
1.4	.00185 06030	.01633 68178	.07498 41556	.53151 38370	−1.4
	$-B_3^{(7)}(p)$	$-B_2^{(7)}(p)$	$-B_1^{(7)}(p)$	$-B_0^{(7)}(p)$	p

SEVEN-POINT COEFFICIENTS—*Continued*

$$\int_{x_0+r\lambda}^{x_0+s\lambda} f(x)\,dx \sim h \sum_{i=-3}^{i=3} \{B_i^{(7)}(s) - B_i^{(7)}(r)\} f(x_0 + ih)$$

p	$B_{-3}^{(7)}(p)$	$B_{-2}^{(7)}(p)$	$B_{-1}^{(7)}(p)$	$B_0^{(7)}(p)$	
1.5	−0.00119 97768	0.01130 02232	−0.05725 44643	0.49157 36607	−1.5
1.6	−0.00050 31145	.00594 27759	.03860 80508	.45066 67344	−1.6
1.7	+0.00017 45392	+0.00076 26274	.02076 88359	.41245 41192	−1.7
1.8	.00075 86229	−0.00367 69371	−0.00563 06571	.38071 95429	−1.8
1.9	.00116 85751	.00677 62995	+0.00484 09813	.35919 00665	−1.9
2.0	0.00132 27513	−0.00793 65079	0.00873 01587	0.35132 27513	−2.0
2.1	.00114 46400	.00660 50775	+0.00431 62875	.36005 53250	−2.1
2.2	+0.00057 04798	−0.00233 11898	−0.00975 41365	.38751 88487	−2.2
2.3	−0.00044 16240	+0.00516 91067	.03426 82841	.43471 03835	−2.3
2.4	.00190 09829	.01593 70971	.06921 87429	.50112 36571	−2.4
2.5	−0.00377 19081	0.02968 43998	−0.11354 47669	0.58433 57308	−2.5
2.6	.00595 94944	.04569 41663	.16484 15270	.67954 76656	−2.6
2.7	.00829 35032	.06270 98818	.21903 58607	.77907 71893	−2.7
2.8	.01051 02459	.07881 11644	.27002 70222	.87180 13630	−2.8
2.9	.01223 23672	.09127 59660	.30929 09323	.94254 72478	−2.9
3.0	−0.01294 64286	0.09642 85714	−0.32544 64286	0.97142 85714	−3.0
	$-B_3^{(7)}(p)$	$-B_2^{(7)}(p)$	$-B_1^{(7)}(p)$	$-B_0^{(7)}(p)$	p

ON THE PROBLEM OF HEAT CONDUCTION IN THIN PLATES

By Arnold N. Lowan

Let d, ρ, c and k denote the thickness, density, specific heat and thermal diffusivity of a thin plate; let further H and T_0 denote the coefficient of heat transfer and the temperature of the surrounding medium. If we use the abbreviations $a = 2H/d\rho c$ and $b = aT_0$, it may be shown that the flow of heat in the plate is governed by the differential equation:

$$\text{(A)} \qquad \frac{\partial T}{\partial t} - k\Delta T = -aT + b$$

It is the object of this paper to derive solutions of (A) corresponding to various domains, initial and boundary conditions.

Section I. Circular plate of radius R. Initial temperature $f(r)$. Boundary temperature $\varphi(t)$.

In this case the temperature $T(r, t)$ must satisfy the following differential equation, initial and boundary conditions.

$$T\begin{cases} \text{(1-1)} & \left\{\dfrac{\partial}{\partial t} - k\left(\dfrac{\partial^2}{\partial r^2} + \dfrac{1}{r}\dfrac{\partial}{\partial r}\right)\right\} T(r, t) = -aT(r, t) + b \\ \text{(1-2)} & \lim_{t\to 0} T(r, t) = f(r) \\ \text{(1-3)} & T(R, t) = \varphi(t) \end{cases}$$

Let

$$\text{(1-4)} \qquad T(r, t) = e^{-at}u(r, t) + v(r, t)$$

where the functions $u(r, t)$ and $v(r, t)$ satisfy the systems

$$U\begin{cases} \text{(1-5)} & \left\{\dfrac{\partial}{\partial t} - k\left(\dfrac{\partial^2}{\partial r^2} + \dfrac{1}{r}\dfrac{\partial}{\partial r}\right)\right\} u(r, t) = 0 \\ \text{(1-6)} & \lim_{t\to 0} u(r, t) = f(r) \\ \text{(1-7)} & u(R, t) = e^{at}\varphi(t) = \psi(t) \quad \text{(say)} \end{cases}$$

$$V\begin{cases} \text{(1-8)} & \left\{\dfrac{\partial}{\partial t} - k\left(\dfrac{\partial^2}{\partial r^2} + \dfrac{1}{r}\dfrac{\partial}{\partial r}\right)\right\} v(r, t) = -av(r, t) + b \\ \text{(1-9)} & \lim_{t\to 0} v(r, t) = 0 \\ \text{(1-10)} & v(R, t) = 0 \end{cases}$$

The function $u(r, t)$ is evidently the temperature in an infinite circular cylinder initially at temperature $f(r)$ whose surface $r = R$ is kept at the temperature $\psi(t)$.

In the special case when $\psi(t) = 0$, a solution $\bar{u}(r, t)$ of the system U is given by H. S. Carslaw[1] in the form

$$\bar{u}(r, t) = \frac{2}{R^2}\int_0^R \rho f(\rho)\left\{\sum_{n=1}^{\infty} \frac{e^{-k\alpha_n^2 t} J_0(\alpha_n r) J_0(\alpha_n \rho)}{(J_0'(\alpha_n R))^2}\right\} d\rho$$

where the summation extends over the roots of $J_0(\alpha R) = 0$. From the expression of $\bar{u}(r, t)$ and from the developments in Carslaw's Art. 80, it follows that the Green's function $G(r, \rho, t)$ appropriate to the differential equation (1–5) and vanishing at $r = R$, is

$$G(r, \rho, t) = \frac{1}{\pi R^2}\sum_{n=1}^{\infty} \frac{e^{-k\alpha_n^2 t} J_0(\alpha_n r) J_0(\alpha_n \rho)}{(J_0'(\alpha_n R))^2}$$

With the aid of the Green's function and Carslaw's formula (4), Art. 80, the solution of the system U may be written (after some obvious transformations) in the form

$$u(r, t) = 2\pi\int_0^R \rho f(\rho) G(r, \rho, t)\, d\rho - 2\pi k R\int_0^t \psi(t-\eta)\left\{\frac{\partial}{\partial \rho} G(r, \rho, \eta)\right\}_{\rho=R} d\eta$$

whence ultimately

$$u(r, t) = \frac{2}{R^2}\sum_{n=1}^{\infty} \frac{e^{-k\alpha_n^2 t} J_0(\alpha_n r)}{(J_0'(\alpha_n R))^2}\int_0^R \rho f(\rho) J_0(\alpha_n \rho)\, d\rho$$

(1–11)

$$-\frac{2k}{R} e^{\alpha t}\int_0^t e^{-\alpha\eta}\varphi(t-\eta)\left\{\sum_{n=1}^{\infty} \frac{\alpha_n e^{-k\alpha_n^2 \eta}(J_0(\alpha_n r))}{J_0'(\alpha_n R)}\right\} d\eta$$

where the summation extends over the roots of

(1–12) $$J_0(\alpha R) = 0$$

We proceed to the solution of the system V. The Laplace transform

$$v^*(r, p) = \int_0^{\infty} e^{-pt} v(r, t)\, dt = L\{v(r, t)\} \quad \text{(say)}$$

of the function $v(r, t)$ is readily seen to satisfy the following differential equation and boundary condition

$$V^*\left\{\begin{array}{ll} \text{(1–13)} & \left(\dfrac{\partial^2}{\partial r^2} + \dfrac{1}{r}\dfrac{\partial}{\partial r} - \dfrac{p+a}{k}\right) v^*(r, p) = -\dfrac{b}{pk} \\ \text{(1–14)} & v^*(R, p) = 0 \end{array}\right\}$$

The solution of the system V^* is

$$v^*(r, p) = \frac{b}{p(p+a)} - \frac{b}{p(p+a)}\frac{I_0(qr)}{I_0(qR)} \quad \text{where } q = \sqrt{(p+a)/k}$$

[1] Mathematical Theory of the Conduction of Heat in Solids. Art. 57.

or

$$v^*(r, p) = \frac{b}{a}\left(\frac{1}{p} - \frac{1}{p+a}\right) - b\,\frac{1}{p}\,w^*(r, p) \quad \text{(say)} \tag{1-15}$$

From (1-15) we get

$$v(r, t) = \frac{b}{a}\,L^{-1}\left\{\frac{1}{p} - \frac{1}{p+a}\right\} - bL^{-1}\left\{\frac{1}{p}\,w^*(r, p)\right\} \tag{1-16}$$

where L^{-1} denotes the inverse Laplace operator. Clearly

$$L^{-1}\left\{\frac{1}{p} - \frac{1}{p+a}\right\} = 1 - e^{-at} = a\int_0^t e^{-a\eta}\,d\eta$$

Moreover if

$$w(r, t) = L^{-1}\{w^*(r, p)\}$$

so that

$$\int_0^\infty e^{-pt}\,w(r, t)\,dt = w^*(r, p) = \frac{1}{p+a}\cdot\frac{I_0(r\sqrt{(p+a)/k})}{I_0(R\sqrt{(p+a)/k})} \tag{1-17}$$

then[2]

$$L^{-1}\left\{\frac{1}{p}\,w^*(r, p)\right\} = \int_0^t w(r, \eta)\,d\eta$$

Accordingly (1-16) yields

$$v(r, t) = b\int_0^t \{e^{-a\eta} - w(r, \eta)\}\,d\eta \tag{1-18}$$

With (1-17) let us associate the equation

$$\int_0^\infty e^{-pt}\,w_1(r, t)\,dt = \frac{1}{p}\,\frac{I_0(r\sqrt{p/k})}{I_0(R\sqrt{p/k})} = w_1^*(r, p) \tag{1-17'}$$

If in (1-17′) we replace p by $p + a$ and compare with (1-17), we get

$$w(r, t) = e^{-at}w_1(r, t) \tag{1-19}$$

In $w_1^*(r, p)$ we recognize the Laplace transform of the temperature $w_1(r, t)$ in a circular cylinder initially at 0° whose surface $r = R$ is kept at the temperature unity. The expression for $w_1(r, t)$ may be obtained from (1-11) and is also given by H. S. Carslaw and J. C. Jaeger[3] in the form

$$w_1(r, t) = 1 + \frac{2}{R}\sum_{n=1}^{\infty}\frac{e^{-k\alpha_n^2 t}\,J_0(\alpha_n r)}{\alpha_n J_0'(\alpha_n R)} \tag{1-20}$$

where the summation extends over the roots of (1-12).

[2] J. R. Carson "Electric Circuit Theory and Operational Calculus," Theorem II, p. 42 (1926).

[3] Operational Methods in Applied Mathematics, Art. 53, p. 123 (1941).

In view of (1–20), (1–18) becomes

$$v(r, t) = b \int_0^t \left\{ e^{-a\eta} - 1 - \frac{2}{R} \sum_{n=1}^{\infty} \frac{e^{-k\alpha_n^2 \eta} J_0(\alpha_n r)}{\alpha_n J_0'(\alpha_n R)} \right\} d\eta \tag{1–21}$$

In view of (1–4), (1–11) and (1–21), the solution of the system T becomes

$$\begin{aligned} T(r, t) = {} & \frac{2e^{-at}}{R^2} \sum_{n=1}^{\infty} \frac{e^{-k\alpha_n^2 t} J_0(\alpha_n r)}{(J_0'(\alpha_n R))^2} \int_0^R \rho f(\rho) J_0(\alpha_n \rho)\, d\rho \\ & - \frac{2k}{R} \int_0^t e^{-a\eta} \varphi(t - \eta) \left\{ \sum_{n=1}^{\infty} \frac{\alpha_n e^{-k\alpha_n^2 \eta} J_0(\alpha_n r)}{J_0'(\alpha_n R)} \right\} d\eta \\ & + b \int_0^t \left\{ e^{-a\eta} - 1 - \frac{2}{R} \sum_{n=1}^{\infty} \frac{e^{-k\alpha_n^2 \eta} J_0(\alpha_n r)}{\alpha_n J_0'(\alpha_n R)} \right\} d\eta \end{aligned} \tag{1–22}$$

where the summation extends over the roots of (1–12).

Section II. Circular plate initially at temperature $f(r)$; edge impervious to heat.

In this case we make the substitution

$$T(r, t) = e^{-at} u(r, t) + v(r, t) \tag{2–1}$$

where $u(r, t)$ satisfies the system U except that the boundary condition (1–7) is replaced by

$$\frac{\partial}{\partial r} u(r, t) = 0 \quad \text{for } r = R \tag{2–2}$$

and where $v(r, t)$ satisfies the system V except that the boundary condition (1–13) is replaced once more by (2–2), with $v(r, t)$ written for $u(r, t)$. The function $u(r, t)$ is clearly the temperature in an infinite circular cylinder whose lateral surface $r = R$ is impervious to heat. This is given by Carslaw in the form

$$u(r, t) = \frac{2}{R^2} \sum_{n=1}^{\infty} \frac{e^{-k\alpha_n^2 t} J_0(\alpha_n r)}{(J_0(\alpha_n R))^2} \int_0^R \rho f(\rho) J_0(\alpha_n \rho)\, d\rho \tag{2–3}$$

where the summation extends over the roots of

$$J_0'(\alpha R) = 0 \tag{2–4}$$

The Laplace transform $v^*(r, p)$ satisfies the differential equation (1–13) and the boundary condition (2–2) with $v(r, t)$ written for $u(r, t)$. We readily get

$$v^*(r, p) = \frac{b}{p(p + a)} = \frac{b}{a} \left(\frac{1}{p} - \frac{1}{p + a} \right)$$

whence

$$v(r, t) = \frac{b}{a} (1 - e^{-at}) \tag{2–5}$$

The solution of our problem is thus given by (2–1) in conjunction with (2–3) and (2–5).

Section III. Plate of infinite extent. Following the procedure of the preceding sections, we get

$$T(x, y, t) = e^{-at}u(x, y, t) + \frac{b}{a}(1 - e^{-at}) \tag{3-1}$$

where $u(x, y, t)$ is the temperature in a solid of infinite extent, initially at temperature $f(x, y)$.

Using Carslaw's expression[4] for $u(x, y, t)$ we get

$$T(x, y, t) = \frac{e^{-at}}{4\pi kt}\int_{-\infty}^{\infty}\int_{-\infty}^{\infty} f(\xi, \eta)e^{-((x-\xi)^2+(y-\eta)^2)/4kt}\,d\xi\,d\eta + \frac{b}{a}(1 - e^{-at}) \tag{3-2}$$

Section IV. Plate of semi-infinite extent; boundary $x = 0$ impervious to heat. In this case

$$T(x, y, t) = e^{-at}u(x, y, t) + \frac{b}{a}(1 - e^{-at}) \tag{4-1}$$

where $u(x, y, t)$ is the temperature in a semi-infinite solid whose boundary plane $x = 0$ is impervious to heat. This leads to the solution

$$T(x, y, t) = \frac{e^{-at}}{4\pi kt}\int_0^{\infty} d\xi \int_{-\infty}^{\infty} \{e^{-((x-\xi)^2+(y-\eta)^2)/4kt} + e^{-((x+\xi)^2+(y-\eta)^2)/4kt}\}\,d\eta + \frac{b}{a}(1 - e^{-at}) \tag{4-2}$$

Section V. Plate of semi-infinite extent; initial temperature $f(x, y)$; boundary $x = 0$ kept at temperature $\varphi(y, t)$.

In this case

$$T(x, y, t) = e^{-at}u(x, y, t) + v(x, y, t) \tag{5-1}$$

where $u(x, y, t)$ is the temperature in a semi-infinite solid initially at the temperature $f(x, y)$ whose boundary $x = 0$ is kept at temperature $e^{at}\varphi(y, t)$ and where $v(x, y, t)$ is the inverse Laplace transform of the function $v^*(x, y, p)$ satisfying the equations

$$\left(\frac{\partial^2}{\partial x^2} + \frac{\partial^2}{\partial y^2} - \frac{p + a}{k}\right)v^*(x, y, p) = -\frac{b}{kp} \tag{5-2}$$

$$v^*(0, y, p) = 0 \tag{5-3}$$

The value of $u(x, y, t)$ may be obtained by a slight change of notation from Carslaw's Art. 86 in the form

$$u(x, y, t) = \frac{1}{4\pi kt}\int_0^{\infty}\int_{-\infty}^{\infty} f(\xi, \eta)\{e^{-((x-\xi)^2+(y-\eta)^2)/4kt} - e^{-((x+\xi)^2+(y-\eta)^2)/4kt}\}\,d\xi\,d\eta + \frac{x}{4\pi k}\int_0^{\infty}\int_{-\infty}^{\infty}\frac{\varphi(\eta, \tau)}{(t-\tau)^2}e^{-(x^2+(y-\eta)^2)/4k(t-\tau)}\,d\eta\,d\tau \tag{5-4}$$

[4] Loc. cit. p. 103.

The solution of the equations (5–2) and (5–3) may be written in the form

$$v^*(x, y, p) = \frac{b}{p(p+a)} + v_1^*(x, y, p) \tag{5–5}$$

where $v_1^*(x, y, p)$ satisfies the equations

$$\left(\frac{\partial^2}{\partial x^2} + \frac{\partial^2}{\partial y^2} - \frac{p+a}{k}\right) v_1^*(x, y, p) \tag{5–6}$$

$$v_1^*(0, y, p) = -\frac{b}{p(p+a)} \tag{5–7}$$

If in the identity

$$F(y) = \frac{1}{\pi} \int_0^\infty d\xi \int_{-\infty}^\infty F(\eta) \cos \xi(y - \eta)\, d\eta$$

we put

$$F(y) = \begin{cases} 1 & y > 0 \\ -1 & y < 0 \end{cases}$$

we obtain

$$\frac{2}{\pi} \int_0^\infty d\xi \int_0^\infty \sin \xi y \sin \xi\eta\, d\eta = \begin{cases} 1 & \text{for } y > 0 \\ -1 & \text{for } y < 0 \end{cases} \tag{5–8}$$

The expression $e^{-az} \sin \xi y$ is a solution of (5–6) provided that $\xi^2 + a^2 = \frac{p+a}{k}$. It follows in view of (5–8) that the expression

$$v^*(x, y, p) = \frac{2}{\pi} \frac{b\delta}{p(p+a)} \int_0^\infty \int_0^\infty e^{-x\sqrt{(p+a-k\xi^2)/k}} \sin \xi y \sin \xi\eta\, d\xi\, d\eta + \frac{b}{p(p+a)} \quad \text{where } \delta = \begin{cases} -1 & \text{for } y > 0 \\ 1 & \text{for } y < 0 \end{cases} \tag{5–9}$$

is a solution of the differential equation (5–2) satisfying the boundary condition (5–3). From (5–9) we get

$$v(x, y, t) = \frac{2}{\pi} \frac{b\delta}{a} \int_0^\infty \int_0^\infty L^{-1}\left\{\left(\frac{1}{p} - \frac{1}{p+a}\right) e^{-x\sqrt{(p+a-k\xi^2)/k}}\right\} \sin \xi y \sin \xi\eta\, d\xi\, d\eta + \frac{b}{a} L^{-1}\left\{\frac{1}{p} - \frac{1}{p+a}\right\}$$

whence, making use of Borel's theorem,

$$v(x, y, t) = \frac{2}{\pi} \frac{b\delta}{a} \int_0^\infty \int_0^\infty \int_0^t \{1 - e^{-a(t-\tau)}\} w(x, \xi, \tau) \sin \xi y \sin \xi\eta\, d\xi\, d\eta\, d\tau + \frac{b}{a}(1 - e^{-at}) \tag{5–10}$$

where

$$w(x, \xi, t) = L^{-1}\{e^{-x\sqrt{(p+a-k\xi^2)/k}}\}$$

or

$$\int_0^\infty e^{-pt} w(x, \xi, t)\, dt = e^{-x\sqrt{(p+a-k\xi^2)/k}} \tag{5-11}$$

If in the known identity

$$\int_0^\infty e^{-pt} \sqrt{\frac{\lambda}{p}}\, e^{-\lambda/t} t^{-3/2}\, dt = e^{-2\sqrt{\lambda p}}$$

we put $\lambda = x^2/4k$ and replace p by $p + a - k\xi^2$, we get

$$\frac{x}{2\sqrt{\pi k}} \int_0^\infty e^{-pt} e^{-(a-k\xi^2)t} e^{-x^2/4kt} t^{-3/2}\, dt = e^{-x\sqrt{(p+a-k\xi^2)/k}}$$

whence

$$w(x, \xi, t) = \frac{x}{2\sqrt{\pi k}}\, e^{-(a-k\xi^2)t} e^{-x^2/4kt} t^{-3/2} \tag{5-12}$$

The complete solution of our problem is thus given by (5–1) in conjunction with (5–4), (5–10) and (5–12).

Section VI. Plate bounded by $x = 0$ and $y = 0$. Initial temperature $f(x, y)$; boundary $x = 0$ kept at temperature $\varphi_1(y, t)$; boundary $y = 0$ kept at temperature $\varphi_2(x, t)$.

In this case

$$T(x, y, t) = e^{-at} u(x, y, t) + v(x, y, t) \tag{6-1}$$

where $u(x, y, t)$ is the temperature in the two-dimensional domain $0 < x < \infty$, $0 < y < \infty$, satisfying the initial and boundary conditions prescribed for $T(x, y, t)$, except that $\varphi_1(y, t)$ and $\varphi_2(x, t)$ are replaced by $e^{at}\varphi_1(y, t)$ and $e^{at}\varphi_2(x, t)$ respectively, and where $v(x, y, t)$ is the inverse Laplace transform of the function $v^*(x, y, p)$ which satisfies the following differential equation and boundary conditions:

$$\left(\frac{\partial^2}{\partial x^2} + \frac{\partial^2}{\partial y^2} - q^2\right) v^*(x, y, p) = -\frac{b}{kp}; \quad q = \sqrt{(p + a)/k} \tag{6-2}$$

$$v^*(0, y, p) = v^*(x, 0, p) = 0 \tag{6-3}$$

Let $G(x, y, \xi, \eta; t)$ denote the Green's function appropriate to the differential equation satisfied by $u(x, y, t)$ and vanishing at $x = 0$ and $y = 0$; then the solution $u(x, y, t)$ may be written in the form[5]

$$\begin{aligned} u(x, y, t) = {} & \int_0^\infty \int_0^\infty f(\xi, \eta) G(x, y, \xi, \eta; t)\, d\xi\, d\eta \\ & + k \int_0^t d\tau \int_0^\infty e^{a\tau} \varphi_1(y, \tau) \left\{\frac{\partial}{\partial \xi} G(x, y, \xi, \eta; t)\right\}_{\xi=0} d\eta \\ & + k \int_0^t d\tau \int_0^\infty e^{a\tau} \varphi_2(x, \tau) \left\{\frac{\partial}{\partial \eta} G(x, y, \xi, \eta; t)\right\}_{\eta=0} d\xi \end{aligned} \tag{6-4}$$

[5] Carslaw, loc. cit. chapter X.

The Green's function may be written in the two alternative forms[6]

$$(6\text{–}5)\quad \begin{cases} G(x, y, \xi, \eta; t) = \dfrac{1}{4\pi kt}\{e^{-((x-\xi)^2+(y+\eta)^2)/4kt} \\ \qquad -e^{-((x+\xi)^2+(y-\eta)^2)/4kt} + e^{-((x+\xi)^2+(y+\eta)^2)/4kt} - e^{-((x-\xi)^2+(y+\eta)^2)/4kt}\} \end{cases}$$

$$(6\text{–}5')\quad \left\{ G(x, y, \xi, \eta; t) = \frac{4}{\pi^2}\int_0^\infty\int_0^\infty e^{-k(\alpha^2+\beta^2)t}\cdot \sin \alpha x \sin \beta y \sin \alpha\xi \sin \beta\eta \, d\alpha \, d\beta \right.$$

The solution of (6–2) and (6–3) may be written in the form

$$(6\text{–}6)\quad \begin{aligned} v^*(x, y, p) = {} & \frac{-2b}{\pi p(p+a)}\int_0^\infty\int_0^\infty e^{-x\sqrt{(p+a-k\xi^2)/k}} \sin \xi y \sin \xi\eta \, d\xi \, d\eta \\ & - \frac{2b}{\pi p(p+a)}\int_0^\infty\int_0^\infty e^{-y\sqrt{(p+a-k\xi^2)/k}} \sin \xi x \sin \xi\eta \, d\xi \, d\eta + \frac{b}{p(p+a)} \end{aligned}$$

or

$$\begin{aligned} v^*(x, y, p) = {} & -\frac{2b}{\pi a}\int_0^\infty\int_0^\infty \left(\frac{1}{p} - \frac{1}{p+a}\right) w_1^*(x, \xi, p) \sin \xi y \sin \xi\eta \, d\xi \, d\eta \\ & - \frac{2b}{\pi a}\int_0^\infty\int_0^\infty \left(\frac{1}{p} - \frac{1}{p+a}\right) w_2^*(y, \xi, p) \sin \xi x \sin \xi\eta \, d\xi \, d\eta \\ & + \frac{b}{a}\left(\frac{1}{p} - \frac{1}{p+a}\right) \end{aligned}$$

whence

$$\begin{aligned} v(x, y, t) = {} & \frac{2b}{\pi a}\int_0^t \{-1 + e^{-a(t-\tau)}\}\, d\tau \cdot \int_0^\infty\int_0^\infty w_1(x, \xi, \tau) \sin \xi y \sin \xi\eta \, d\xi \, d\eta \\ & + \frac{2b}{\pi a}\int_0^t \{-1 + e^{-a(t-\tau)}\}\, d\tau \cdot \int_0^\infty\int_0^\infty w_2(y, \xi, \tau) \sin \xi x \sin \xi\eta \, d\xi \, d\eta \\ & + \frac{b}{a}(1 - e^{-at}) \end{aligned}$$

It is clear that $w_1(x, \xi, t)$ is identical with $w(x, \xi, t)$ given in (5–12); also $w_2(y, \xi, t)$ may be obtained from (5–12) by replacing x by y.
Thus

$$(6\text{–}8)\qquad w_1(x, \xi, t) = \frac{x}{2\sqrt{\pi k}}\, e^{-(a-k\xi^2)t} e^{-x^2/4kt} t^{-3/2}$$

$$(6\text{–}9)\qquad w_2(y, \xi, t) = \frac{y}{2\sqrt{\pi k}}\, e^{-(a-k\xi^2)t} e^{-y^2/4kt} t^{-3/2}$$

The final solution of our problem is given by (6–1) where $u(x, y, t)$ is given by (6–4) in conjunction with (6–5) or (6–5′) and where $v(x, y, t)$ is given by (6–7) in conjunction with (6–8) and (6–9).

NEW YORK CITY

[6] Note on Green's function in the Theory of Heat Conduction. Phil. Mag. Vol. 35 No. 246, July 1944.

TABLES OF BESSEL FUNCTIONS $J_n(x)$ FOR LARGE ARGUMENTS

By Murlan S. Corrington and William Miehle[1]

Summary

Tables of $J_n(ms)$ are given for $n = 0(1)10$, $s = 1(1)20$ and $m = 1(1)10$ to five decimal places. A second set of tables includes $n = 0(1)10$, $s = 1(1)20$ and $m = \pi, 2\pi, \cdots 5\pi$ also to five decimal places.

These computed values have been arranged in tables with increasing s for use in the summation of the Schlömilch series which occur in the theory of frequency modulation.

The computed values have been checked against existing tables wherever possible.

Introduction

The mathematical theory of frequency-modulated radio broadcasting shows that the sideband amplitudes of a carrier modulated with sinusoidal variations in frequency are proportional to the Bessel functions of the first kind $J_n(m)$, where n is the sideband number and m is the modulation index. Since m equals the maximum deviation in frequency, D, divided by the audio frequency μ, it is evident that at the lower audio frequencies the ratio D/μ can become quite large. This means that in order to determine the sideband amplitudes it is necessary to use tables of Bessel functions for large values of the argument m.

Need for the Tables

Nearly all calculations of the harmonic-distortion terms and of the combination-frequency amplitudes produced when an interfering signal is present in frequency-modulation transmission require the evaluation of a Schlömilch-type series. In this form of series the Bessel functions of the first kind are summed in the argument instead of in the order as in the customary series. Under conditions of multipath transmission or when an interfering carrier is present on the same channel as the frequency-modulated signal, the amplitudes of the harmonics produced in the output from the discriminator are proportional to the functions

$$C(m, n; x, \theta) = \sum_{s=1}^{\infty} \frac{(-x)^s}{s} J_n(ms) \cos s\theta$$

and

$$S(m, n; x, \theta) = \sum_{s=1}^{\infty} \frac{(-x)^s}{s} J_n(ms) \sin s\theta \qquad x^2 \leq 1$$

where x is the ratio of the amplitudes of the two voltages, n is the harmonic number, m is the modulation index, and θ is the phase angle between the two carriers when the modulation is removed. The numerical evaluation of this series requires tables of the Bessel functions $J_n(ms)$ and the tables in this paper are arranged especially to facilitate such a summation.

[1] Radio Engineers, Advanced Development Section of the RCA Victor Division, Radio Corporation of America, Camden, N. J.

Similar series occur in other modulation problems in radio broadcasting.[2,3] They usually arise when the signal is distorted and all components which lead to the same frequency are then added together.

Method of Computation

The usual power series for the Bessel function of the first kind $J_n(x)$ converges for all positive values of x and n but as x becomes large the convergence is very slow. It is not suitable for numerical computation when either x or n is large. For this reason an asymptotic series was derived by Jacobi which converges rapidly for large values of x.

This series is of the form[4]

$$J_n(z) = \sqrt{\frac{2}{\pi z}}\left\{1 - \frac{(4n^2-1^2)(4n^2-3^2)}{2!\,(8z)^2} + \frac{(4n^2-1^2)(4n^2-3^2)(4n^2-5^2)(4n^2-7^2)}{4!\,(8z)^4} - \cdots\right\}\cos\left(z - \frac{\pi}{4} - \frac{n\pi}{2}\right)$$
$$- \sqrt{\frac{2}{\pi z}}\left\{\frac{(4n^2-1^2)}{1!\,8z} - \frac{(4n^2-1^2)(4n^2-3^2)(4n^2-5^2)}{3!\,(8z)^3} + \cdots\right\}\sin\left(z - \frac{\pi}{4} - \frac{n\pi}{2}\right)$$

where $-\pi/2 < \text{amp } z < \pi/2$.

It converges very rapidly when z becomes large. The expressions for $J_0(x)$ and $J_1(x)$ become

$$J_0(x) = \sqrt{\frac{2}{\pi x}}\left\{P_0(x)\cos\left(x - \frac{\pi}{4}\right) - Q_0(x)\sin\left(x - \frac{\pi}{4}\right)\right\}$$

$$J_1(x) = \sqrt{\frac{2}{\pi x}}\left\{P_1(x)\cos\left(x - \frac{3\pi}{4}\right) - Q_1(x)\sin\left(x - \frac{3\pi}{4}\right)\right\}$$

where

$$P_0(x) \backsim 1 - \frac{1^2 3^2}{2!\,(8x)^2} + \frac{1^2 3^2 5^2 7^2}{4!\,(8x)^4} - \frac{1^2 3^2 5^2 7^2 9^2 11^2}{6!\,(8x)^6} + \cdots$$

$$Q_0(x) \backsim -\frac{1^2}{1!\,8x} + \frac{1^2 3^2 5^2}{3!\,(8x)^3} - \frac{1^2 3^2 5^2 7^2 9^2}{5!\,(8x)^5} + \cdots$$

$$P_1(x) \backsim 1 + \frac{1^2(3)(5)}{2!\,(8x)^2} - \frac{1^2 3^2 5^2(7)(9)}{4!\,(8x)^4} + \frac{1^2 3^2 5^2 7^2 9^2(11)(13)}{6!\,(8x)^6} - \cdots$$

$$Q_1(x) \backsim \frac{1(3)}{1!\,8x} - \frac{1^2 3^2 5(7)}{3!\,(8x)^3} + \frac{1^2 3^2 5^2 7^2(9)(11)}{5!\,(8x)^5} - \cdots$$

In P_1 the signs alternate after the first.

[2] Eugene Peterson and Clyde R. Keith, "Grid current modulation," Bell Sys. Tech. Journ., vol. 7, No. 1, January, 1928, pp. 106–139.

[3] W. R. Bennett, "New results in the calculation of modulation products," Bell Sys. Tech. Journ., vol. 12, 1933, pp. 228–243.

[4] Gray, Mathews and MacRobert, "A treatise on Bessel functions and their applications to physics," Macmillan and Co., Ltd., London 1931, p. 57.

TABLE I—$J_n(ns)$
BESSEL FUNCTIONS WITH INCREASING ARGUMENT

s	$J_0(s)$	$J_1(s)$	$J_2(s)$	$J_3(s)$	$J_4(s)$	$J_5(s)$
1	+0.76520	+0.44005	+0.11490	+0.01956	+0.00248	+0.00025
2	+0.22389	+0.57672	+0.35283	+0.12894	+0.03400	+0.00704
3	−0.26005	+0.33906	+0.48609	+0.30906	+0.13203	+0.04303
4	−0.39715	−0.06604	+0.36413	+0.43017	+0.28113	+0.13209
5	−0.17760	−0.32758	+0.04657	+0.36483	+0.39123	+0.26114
6	+0.15065	−0.27668	−0.24287	+0.11477	+0.35764	+0.36209
7	+0.30008	−0.00468	−0.30142	−0.16756	+0.15780	+0.34790
8	+0.17165	+0.23464	−0.11299	−0.29113	−0.10536	+0.18577
9	−0.09033	+0.24531	+0.14485	−0.18094	−0.26547	−0.05504
10	−0.24594	+0.04347	+0.25463	+0.05838	−0.21960	−0.23406
11	−0.17119	−0.17679	+0.13905	+0.22735	−0.01504	−0.23829
12	+0.04769	−0.22345	−0.08493	+0.19514	+0.18250	−0.07347
13	+0.20693	−0.07032	−0.21774	+0.00332	+0.21928	+0.13162
14	+0.17107	+0.13338	−0.15202	−0.17681	+0.07624	+0.22038
15	−0.01422	+0.20510	+0.04157	−0.19402	−0.11918	+0.13046
16	−0.17490	+0.09040	+0.18620	−0.04385	−0.20264	−0.05747
17	−0.16985	−0.09767	+0.15836	+0.13493	−0.11074	−0.18704
18	−0.01336	−0.18799	−0.00753	+0.18632	+0.06964	−0.15537
19	+0.14663	−0.10570	−0.15776	+0.07249	+0.18065	+0.00357
20	+0.16702	+0.06683	−0.16034	−0.09890	+0.13067	+0.15117
21	+0.03658	+0.17112	−0.02028	−0.17498	−0.02971	+0.16366
22	−0.12065	+0.11718	+0.13130	−0.09330	−0.15675	+0.03630
23	−0.16241	−0.03952	+0.15898	+0.06717	−0.14145	−0.11637
24	−0.05623	−0.15404	+0.04339	+0.16127	−0.00308	−0.16230
25	+0.09627	−0.12535	−0.10629	+0.10834	+0.13230	−0.06601
26	+0.15600	+0.01505	−0.15484	−0.03887	+0.14587	+0.08375
27	+0.07274	+0.13658	−0.06262	−0.14586	+0.03021	+0.15481
28	−0.07316	+0.13055	+0.08248	−0.11877	−0.10793	+0.08793
29	−0.14785	+0.00693	+0.14833	+0.01352	−0.14553	−0.05367
30	−0.08637	−0.11875	+0.07845	+0.12921	−0.05261	−0.14324
31	+0.05121	−0.13302	−0.05979	+0.12531	+0.08404	−0.10362
32	+0.13808	−0.02659	−0.13974	+0.00912	+0.14145	+0.02624
33	+0.09727	+0.10062	−0.09117	−0.11167	+0.07087	+0.12885
34	−0.03042	+0.13297	+0.03824	−0.12847	−0.06091	+0.11414
35	−0.12685	+0.04399	+0.12936	−0.02921	−0.13437	−0.00151
36	−0.10557	−0.08233	+0.10099	+0.09355	−0.08540	−0.11253
37	+0.01086	−0.13058	−0.01792	+0.12864	+0.03878	−0.12026
38	+0.11433	−0.05916	−0.11745	+0.04680	+0.12484	−0.02052
39	+0.11136	+0.06406	−0.10807	−0.07514	+0.09651	+0.09494
40	+0.00737	+0.12604	−0.00106	−0.12614	−0.01786	+0.12257

BESSEL FUNCTIONS WITH INCREASING ARGUMENT—*Continued*

x	$J_6(x)$	$J_7(x)$	$J_8(x)$	$J_9(x)$	$J_{10}(x)$
1	+0.00002	+0.00000	+0.00000	+0.00000	+0.00000
2	+0.00120	+0.00017	+0.00002	+0.00000	+0.00000
3	+0.01139	+0.00255	+0.00049	+0.00008	+0.00001
4	+0.04909	+0.01518	+0.00403	+0.00094	+0.00020
5	+0.13105	+0.05338	+0.01841	+0.00552	+0.00147
6	+0.24584	+0.12959	+0.05653	+0.02117	+0.00696
7	+0.33920	+0.23358	+0.12797	+0.05892	+0.02354
8	+0.33758	+0.32059	+0.22345	+0.12632	+0.06077
9	+0.20432	+0.32746	+0.30507	+0.21488	+0.12469
10	−0.01446	+0.21671	+0.31785	+0.29186	+0.20749
11	−0.20158	+0.01838	+0.22497	+0.30886	+0.28043
12	−0.24372	−0.17025	+0.04510	+0.23038	+0.30048
13	−0.11803	−0.24057	−0.14105	+0.06698	+0.23378
14	+0.08117	−0.15080	−0.23197	−0.11431	+0.08501
15	+0.20615	+0.03446	−0.17398	−0.22005	−0.09007
16	+0.16672	+0.18251	−0.00702	−0.18953	−0.20621
17	+0.00072	+0.18755	+0.15374	−0.04286	−0.19911
18	−0.15596	+0.05140	+0.19593	+0.12276	−0.07317
19	−0.17877	−0.11648	+0.09294	+0.19474	+0.09155
20	−0.05509	−0.18422	−0.07387	+0.12513	+0.18648
21	+0.10765	−0.10215	−0.17575	−0.03175	+0.14853
22	+0.17325	+0.05820	−0.13622	−0.15726	+0.00755
23	+0.09086	+0.16377	+0.00883	−0.15763	−0.13219
24	−0.06455	+0.13002	+0.14039	−0.03643	−0.16771
25	−0.15870	−0.01017	+0.15301	+0.10809	−0.07518
26	−0.11366	−0.13621	+0.04032	+0.16102	+0.07116
27	+0.02713	−0.14276	−0.10115	+0.08282	+0.15636
28	+0.13934	−0.02821	−0.15344	−0.05947	+0.11521
29	+0.12702	+0.10623	−0.07574	−0.14802	−0.01614
30	+0.00486	+0.14519	+0.06289	−0.11164	−0.12988
31	−0.11747	+0.05815	+0.14373	+0.01603	−0.13442
32	−0.13325	−0.07621	+0.09991	+0.12616	−0.02894
33	−0.03182	−0.14042	−0.02775	+0.12697	+0.09701
34	+0.09448	−0.08079	−0.12775	+0.02067	+0.13870
35	+0.13394	+0.04743	−0.11497	−0.09998	+0.06355
36	+0.05414	+0.13058	−0.00336	−0.13207	−0.06267
37	−0.07128	+0.09714	+0.10804	−0.05042	−0.13257
38	−0.13024	−0.02061	+0.12264	+0.07225	−0.08842
39	−0.07217	−0.11714	+0.03012	+0.12950	+0.02965
40	+0.04850	−0.10802	−0.08631	+0.07350	+0.11938

BESSEL FUNCTIONS WITH INCREASING ARGUMENT—*Continued*

s	$J_0(2s)$	$J_1(2s)$	$J_2(2s)$	$J_3(2s)$	$J_4(2s)$	$J_5(2s)$
1	+0.22389	+0.57672	+0.35283	+0.12894	+0.03400	+0.00704
2	−0.39715	−0.06604	+0.36413	+0.43017	+0.28113	+0.13209
3	+0.15065	−0.27668	−0.24287	+0.11477	+0.35764	+0.36209
4	+0.17165	+0.23464	−0.11299	−0.29113	−0.10536	+0.18577
5	−0.24594	+0.04347	+0.25463	+0.05838	−0.21960	−0.23406
6	+0.04769	−0.22345	−0.08493	+0.19514	+0.18250	−0.07347
7	+0.17107	+0.13338	−0.15202	−0.17681	+0.07624	+0.22038
8	−0.17490	+0.09040	+0.18620	−0.04385	−0.20264	−0.05747
9	−0.01336	−0.18799	−0.00753	+0.18632	+0.06964	−0.15537
10	+0.16702	+0.06683	−0.16034	−0.09890	+0.13067	+0.15117
11	−0.12065	+0.11718	+0.13130	−0.09330	−0.15675	+0.03630
12	−0.05623	−0.15404	+0.04339	+0.16127	−0.00308	−0.16230
13	+0.15600	+0.01505	−0.15484	−0.03887	+0.14587	+0.08375
14	−0.07316	+0.13055	+0.08248	−0.11877	−0.10793	+0.08793
15	−0.08637	−0.11875	+0.07845	+0.12921	−0.05261	−0.14324
16	+0.13808	−0.02659	−0.13974	+0.00912	+0.14145	+0.02624
17	−0.03042	+0.13297	+0.03824	−0.12847	−0.06091	+0.11414
18	−0.10557	−0.08233	+0.10099	+0.09355	−0.08540	−0.11253
19	+0.11433	−0.05916	−0.11745	+0.04680	+0.12484	−0.02052
20	+0.00737	+0.12604	−0.00106	−0.12614	−0.01786	+0.12257

s	$J_6(2s)$	$J_7(2s)$	$J_8(2s)$	$J_9(2s)$	$J_{10}(2s)$
1	+0.00120	+0.00017	+0.00002	+0.00000	+0.00000
2	+0.04909	+0.01518	+0.00403	+0.00094	+0.00020
3	+0.24584	+0.12959	+0.05653	+0.02117	+0.00696
4	+0.33758	+0.32059	+0.22345	+0.12632	+0.06077
5	−0.01446	+0.21671	+0.31785	+0.29186	+0.20749
6	−0.24372	−0.17025	+0.04510	+0.23038	+0.30048
7	+0.08117	−0.15080	−0.23197	−0.11431	+0.08501
8	+0.16672	+0.18251	−0.00702	−0.18953	−0.20621
9	−0.15596	+0.05140	+0.19593	+0.12276	−0.07317
10	−0.05509	−0.18422	−0.07387	+0.12513	+0.18648
11	+0.17325	+0.05820	−0.13622	−0.15726	+0.00755
12	−0.06455	+0.13002	+0.14039	−0.03643	−0.16771
13	−0.11366	−0.13621	+0.04032	+0.16102	+0.07116
14	+0.13934	−0.02821	−0.15344	−0.05947	+0.11521
15	+0.00486	+0.14519	+0.06289	−0.11164	−0.12988
16	−0.13325	−0.07621	+0.09991	+0.12616	−0.02894
17	+0.09448	−0.08079	−0.12775	+0.02067	+0.13870
18	+0.05414	+0.13058	−0.00336	−0.13207	−0.06267
19	−0.13024	−0.02061	+0.12264	+0.07225	−0.08842
20	+0.04850	−0.10802	−0.08631	+0.07350	+0.11938

BESSEL FUNCTIONS WITH INCREASING ARGUMENT—*Continued*

s	$J_0(3s)$	$J_1(3s)$	$J_2(3s)$	$J_3(3s)$	$J_4(3s)$	$J_5(3s)$
1	−0.26005	+0.33906	+0.48609	+0.30906	+0.13203	+0.04303
2	+0.15065	−0.27668	−0.24287	+0.11477	+0.35764	+0.36209
3	−0.09033	+0.24531	+0.14485	−0.18094	−0.26547	−0.05504
4	+0.04769	−0.22345	−0.08493	+0.19514	+0.18250	−0.07347
5	−0.01422	+0.20510	+0.04157	−0.19402	−0.11918	+0.13046
6	−0.01336	−0.18799	−0.00753	+0.18632	+0.06964	−0.15537
7	+0.03658	+0.17112	−0.02028	−0.17498	−0.02971	+0.16366
8	−0.05623	−0.15404	+0.04339	+0.16127	−0.00308	−0.16230
9	+0.07274	+0.13658	−0.06262	−0.14586	+0.03021	+0.15481
10	−0.08637	−0.11875	+0.07845	+0.12921	−0.05261	−0.14324
11	+0.09727	+0.10062	−0.09117	−0.11167	+0.07087	+0.12885
12	−0.10557	−0.08233	+0.10099	+0.09355	−0.08540	−0.11253
13	+0.11136	+0.06406	−0.10807	−0.07514	+0.09651	+0.09494
14	−0.11474	−0.04599	+0.11255	+0.05671	−0.10445	−0.07661
15	+0.11582	+0.02835	−0.11456	−0.03853	+0.10942	+0.05798
16	−0.11471	−0.01133	+0.11424	+0.02085	−0.11164	−0.03946
17	+0.11156	−0.00486	−0.11176	−0.00390	+0.11130	+0.02136
18	−0.10652	+0.02003	+0.10726	−0.01208	−0.10861	−0.00401
19	+0.09976	−0.03400	−0.10095	+0.02691	+0.10379	−0.01235
20	−0.09147	+0.04660	+0.09303	−0.04040	−0.09706	+0.02745

s	$J_6(3s)$	$J_7(3s)$	$J_8(3s)$	$J_9(3s)$	$J_{10}(3s)$
1	+0.01139	+0.00255	+0.00049	+0.00008	+0.00001
2	+0.24584	+0.12959	+0.05653	+0.02117	+0.00696
3	+0.20432	+0.32746	+0.30507	+0.21488	+0.12469
4	−0.24372	−0.17025	+0.04510	+0.23038	+0.30048
5	+0.20615	+0.03446	−0.17398	−0.22005	−0.09007
6	−0.15506	+0.05140	+0.19593	+0.12276	−0.07317
7	+0.10765	−0.10215	−0.17575	−0.03175	+0.14853
8	−0.06455	+0.13002	+0.14039	−0.03643	−0.16771
9	+0.02713	−0.14276	−0.10115	+0.08282	+0.15636
10	+0.00486	+0.14519	+0.06289	−0.11164	−0.12988
11	−0.03182	−0.14042	−0.02775	+0.12697	+0.09701
12	+0.05414	+0.13058	−0.00336	−0.13207	−0.06267
13	−0.07217	−0.11714	+0.03012	+0.12950	+0.02965
14	+0.08621	+0.10124	−0.05246	−0.12122	+0.00051
15	−0.09654	−0.08373	+0.07049	+0.10879	−0.02697
16	+0.10342	+0.06531	−0.08437	−0.09343	+0.04933
17	−0.10711	−0.04656	+0.09433	+0.07616	−0.06745
18	+0.10787	+0.02798	−0.10061	−0.05779	+0.08135
19	−0.10595	−0.00996	+0.10351	+0.03902	−0.09119
20	+0.10164	−0.00713	−0.10330	−0.02042	+0.09718

BESSEL FUNCTIONS WITH INCREASING ARGUMENT—*Continued*

s	$J_0(4s)$	$J_1(4s)$	$J_2(4s)$	$J_3(4s)$	$J_4(4s)$	$J_5(4s)$
1	−0.39715	−0.06604	+0.36413	+0.43017	+0.28113	+0.13209
2	+0.17165	+0.23464	−0.11299	−0.29113	−0.10536	+0.18577
3	+0.04769	−0.22345	−0.08493	+0.19514	+0.18250	−0.07347
4	−0.17490	+0.09040	+0.18620	−0.04385	−0.20264	−0.05747
5	+0.16702	+0.06683	−0.16034	−0.09890	+0.13067	+0.15117
6	−0.05623	−0.15404	+0.04339	+0.16127	−0.00308	−0.16230
7	−0.07316	+0.13055	+0.08248	−0.11877	−0.10793	+0.08793
8	+0.13808	−0.02659	−0.13974	+0.00912	+0.14145	+0.02624
9	−0.10557	−0.08233	+0.10099	+0.09355	−0.08540	−0.11253
10	+0.00737	+0.12604	−0.00106	−0.12614	−0.01786	+0.12257
11	+0.08631	−0.08280	−0.09007	+0.07462	+0.10025	−0.05639
12	−0.11471	−0.01133	+0.11424	+0.02085	−0.11164	−0.03946
13	+0.06466	+0.09041	−0.06118	−0.09512	+0.05020	+0.10284
14	+0.02477	−0.10348	−0.02847	+0.10145	+0.03934	−0.09583
15	−0.09147	+0.04660	+0.09303	−0.04040	−0.09706	+0.02745
16	+0.09259	+0.03779	−0.09141	−0.04350	+0.08733	+0.05442
17	−0.03149	−0.09172	+0.02879	+0.09342	−0.02055	−0.09583
18	−0.04729	+0.08094	+0.04954	−0.07819	−0.05606	+0.07196
19	+0.08996	−0.01627	−0.09038	+0.01151	+0.09129	−0.00190
20	−0.06974	−0.05606	+0.06834	+0.05947	−0.06388	−0.06586

s	$J_6(4s)$	$J_7(4s)$	$J_8(4s)$	$J_9(4s)$	$J_{10}(4s)$
1	+0.04909	+0.01518	+0.00403	+0.00094	+0.00020
2	+0.33758	+0.32059	+0.22345	+0.12632	+0.06077
3	−0.24372	−0.17025	+0.04510	+0.23038	+0.30048
4	+0.16672	+0.18251	−0.00702	−0.18953	−0.20621
5	−0.05509	−0.18422	−0.07387	+0.12513	+0.18648
6	−0.06455	+0.13002	+0.14039	−0.03643	−0.16771
7	+0.13934	−0.02821	−0.15344	−0.05947	+0.11521
8	−0.13325	−0.07621	+0.09991	+0.12616	−0.02894
9	+0.05414	+0.13058	−0.00336	−0.13207	−0.06267
10	+0.04850	−0.10802	−0.08631	+0.07350	+0.11938
11	−0.11306	+0.02555	+0.12119	+0.01852	−0.11362
12	+0.10342	+0.06531	−0.08437	−0.09343	+0.04933
13	−0.03042	−0.10986	+0.00085	+0.11012	+0.03727
14	−0.05645	+0.08373	+0.07739	−0.06162	−0.09719
15	+0.10164	−0.00713	−0.10330	−0.02042	+0.09718
16	−0.07883	−0.06920	+0.06369	+0.08512	−0.03975
17	+0.00645	+0.09697	+0.01351	−0.09379	−0.03834
18	+0.06605	−0.06095	−0.07791	+0.04364	+0.08882
19	−0.09154	−0.01255	+0.08923	+0.03134	−0.08181
20	+0.05565	+0.07421	−0.04266	−0.08274	+0.02404

BESSEL FUNCTIONS WITH INCREASING ARGUMENT—*Continued*

s	$J_0(5s)$	$J_1(5s)$	$J_2(5s)$	$J_3(5s)$	$J_4(5s)$	$J_5(5s)$
1	−0.17760	−0.32758	+0.04657	+0.36483	+0.39123	+0.26114
2	−0.24594	+0.04347	+0.25463	+0.05838	−0.21960	−0.23406
3	−0.01422	+0.20510	+0.04157	−0.19402	−0.11918	+0.13046
4	+0.16702	+0.06683	−0.16034	−0.09890	+0.13067	+0.15117
5	+0.09627	−0.12535	−0.10629	+0.10834	+0.13230	−0.06601
6	−0.08637	−0.11875	+0.07845	+0.12921	−0.05261	−0.14324
7	−0.12685	+0.04399	+0.12936	−0.02921	−0.13437	−0.00151
8	+0.00737	+0.12604	−0.00106	−0.12614	−0.01786	+0.12257
9	+0.11582	+0.02835	−0.11456	−0.03853	+0.10942	+0.05798
10	+0.05581	−0.09751	−0.05971	+0.09273	+0.07084	−0.08140
11	−0.07455	−0.07825	+0.07170	+0.08346	−0.06260	−0.09257
12	−0.09147	+0.04660	+0.09303	−0.04040	−0.09706	+0.02745
13	+0.01869	+0.09733	−0.01569	−0.09830	+0.00662	+0.09911
14	+0.09491	+0.00999	−0.09462	−0.01539	+0.09330	+0.02806
15	+0.03464	−0.08514	−0.03691	+0.08317	+0.04357	−0.07852
16	−0.06974	−0.05606	+0.06834	+0.05947	−0.06388	−0.06586
17	−0.07094	+0.04915	+0.07210	−0.04576	−0.07533	+0.03867
18	+0.02663	+0.07993	−0.02485	−0.08103	+0.01945	+0.08276
19	+0.08181	−0.00239	−0.08186	−0.00105	+0.08180	+0.00794
20	+0.01999	−0.07715	−0.02153	+0.07628	+0.02611	−0.07420

s	$J_6(5s)$	$J_7(5s)$	$J_8(5s)$	$J_9(5s)$	$J_{10}(5s)$
1	+0.13105	+0.05338	+0.01841	+0.00552	+0.00147
2	−0.01446	+0.21671	+0.31785	+0.29186	+0.20749
3	+0.20615	+0.03446	−0.17398	−0.22005	−0.09007
4	−0.05509	−0.18422	−0.07387	+0.12513	+0.18648
5	−0.15870	−0.01017	+0.15301	+0.10809	−0.07518
6	+0.00486	+0.14519	+0.06289	−0.11164	−0.12988
7	+0.13394	+0.04743	−0.11497	−0.09998	+0.06355
8	+0.04850	−0.10802	−0.08631	+0.07350	+0.11938
9	−0.09654	−0.08373	+0.07049	+0.10879	−0.02697
10	−0.08712	+0.06049	+0.10406	−0.02719	−0.11385
11	+0.04577	+0.10256	−0.01966	−0.10828	−0.01577
12	+0.10164	−0.00713	−0.10330	−0.02042	+0.09718
13	+0.00863	−0.09752	−0.02963	+0.09022	+0.05462
14	−0.08958	−0.04141	+0.08130	+0.06000	−0.06587
15	−0.05404	+0.06988	+0.06708	−0.05557	−0.08042
16	+0.05565	+0.07421	−0.04266	−0.08274	+0.02404
17	+0.07988	−0.02739	−0.08439	+0.01151	+0.08682
18	−0.01026	−0.08413	−0.00283	+0.08362	+0.01955
19	−0.08096	−0.01817	+0.07828	+0.03135	−0.07234
20	−0.03353	+0.07017	+0.04335	−0.06324	−0.05473

BESSEL FUNCTIONS WITH INCREASING ARGUMENT—*Continued*

s	$J_0(6s)$	$J_1(6s)$	$J_2(6s)$	$J_3(6s)$	$J_4(6s)$	$J_5(6s)$
1	+0.15065	−0.27668	−0.24287	+0.11477	+0.35764	+0.36209
2	+0.04769	−0.22345	−0.08493	+0.19514	+0.18250	−0.07347
3	−0.01336	−0.18799	−0.00753	+0.18682	+0.06964	−0.15537
4	−0.05623	−0.15404	+0.04339	+0.16127	−0.00308	−0.16230
5	−0.08637	−0.11875	+0.07845	+0.12921	−0.05261	−0.14324
6	−0.10557	−0.08233	+0.10099	+0.09355	−0.08540	−0.11253
7	−0.11474	−0.04599	+0.11255	+0.05671	−0.10445	−0.07661
8	−0.11471	−0.01133	+0.11424	+0.02085	−0.11164	−0.03946
9	−0.10652	+0.02003	+0.10726	−0.01208	−0.10861	−0.00401
10	−0.09147	+0.04660	+0.09303	−0.04040	−0.09706	+0.02745
11	−0.07114	+0.06718	+0.07317	−0.06274	−0.07888	+0.05318
12	−0.04729	+0.08094	+0.04954	−0.07819	−0.05606	+0.07196
13	−0.02182	+0.08753	+0.02407	−0.08629	−0.03071	+0.08314
14	+0.00340	+0.08701	−0.00133	−0.08707	−0.00489	+0.08661
15	+0.02663	+0.07993	−0.02485	−0.08103	+0.01945	+0.08276
16	+0.04633	+0.06721	−0.04493	−0.06908	+0.04062	+0.07247
17	+0.06131	+0.05012	−0.06033	−0.05249	+0.05724	+0.05698
18	+0.07074	+0.03018	−0.07018	−0.03278	+0.06836	+0.03784
19	+0.07422	+0.00899	−0.07407	−0.01159	+0.07346	+0.01674
20	+0.07182	−0.01181	−0.07202	+0.00940	+0.07249	−0.00457

s	$J_6(6s)$	$J_7(6s)$	$J_8(6s)$	$J_9(6s)$	$J_{10}(6s)$
1	+0.24584	+0.12959	+0.05653	+0.02117	+0.00696
2	−0.24372	−0.17025	+0.04510	+0.23038	+0.30048
3	−0.15596	+0.05140	+0.19593	+0.12276	−0.07317
4	−0.06455	+0.13002	+0.14039	−0.03643	−0.16771
5	+0.00486	+0.14519	+0.06289	−0.11164	−0.12988
6	+0.05414	+0.13058	−0.00336	−0.13207	−0.06267
7	+0.08621	+0.10124	−0.05246	−0.12122	+0.00051
8	+0.10342	+0.06531	−0.08437	−0.09343	+0.04933
9	+0.10787	+0.02798	−0.10061	−0.05779	+0.08135
10	+0.10164	−0.00713	−0.10330	−0.02042	+0.09718
11	+0.08603	−0.03737	−0.09486	+0.01438	+0.09878
12	+0.06605	−0.06095	−0.07791	+0.04364	+0.08882
13	+0.04137	−0.07678	−0.05515	+0.06547	+0.07025
14	+0.01520	−0.08444	−0.02927	+0.07886	+0.04617
15	−0.01026	−0.08413	−0.00283	+0.08362	+0.01955
16	−0.03307	−0.07660	+0.02190	+0.08025	−0.00685
17	−0.05165	−0.06306	+0.04300	+0.06980	−0.03068
18	−0.06485	−0.04504	+0.05901	+0.05379	−0.05005
19	−0.07199	−0.02432	+0.06900	+0.03400	−0.06363
20	−0.07287	−0.00272	+0.07255	+0.01239	−0.07070

BESSEL FUNCTIONS WITH INCREASING ARGUMENT—*Continued*

x	$J_0(7x)$	$J_1(7x)$	$J_2(7x)$	$J_3(7x)$	$J_4(7x)$	$J_5(7x)$
1	+0.30008	−0.00468	−0.30142	−0.16756	+0.15780	+0.34790
2	+0.17107	+0.13338	−0.15202	−0.17681	+0.07624	+0.22038
3	+0.03658	+0.17112	−0.02028	−0.17498	−0.02971	+0.16366
4	−0.07316	+0.13055	+0.08248	−0.11877	−0.10793	+0.08793
5	−0.12685	+0.04399	+0.12936	−0.02921	−0.13437	−0.00151
6	−0.11474	−0.04599	+0.11255	+0.05671	−0.10445	−0.07661
7	−0.05290	−0.10151	+0.04876	+0.10549	−0.03584	−0.11134
8	+0.02477	−0.10348	−0.02847	+0.10145	+0.03934	−0.09583
9	+0.08186	−0.05770	−0.08369	+0.05238	+0.08868	−0.04112
10	+0.09491	+0.00999	−0.09462	−0.01539	+0.09330	+0.02606
11	+0.06238	+0.06656	−0.06065	−0.06971	+0.05522	+0.07545
12	+0.00340	+0.08701	−0.00133	−0.08707	−0.00489	+0.08661
13	−0.05245	+0.06486	+0.05388	−0.06249	−0.05800	+0.05740
14	−0.07935	+0.01371	+0.07963	−0.01046	−0.08027	+0.00391
15	−0.06675	−0.04041	+0.06598	+0.04292	−0.06353	−0.04776
16	−0.02322	−0.07183	+0.02194	+0.07262	−0.01805	−0.07391
17	+0.02874	−0.06714	−0.02987	+0.06613	+0.03320	−0.06390
18	+0.06400	−0.03067	−0.06449	+0.02862	+0.06585	−0.02444
19	+0.06674	+0.01849	−0.06646	−0.02049	+0.06554	+0.02443
20	+0.03736	+0.05627	−0.03655	−0.05732	+0.03410	+0.05927

x	$J_6(7x)$	$J_7(7x)$	$J_8(7x)$	$J_9(7x)$	$J_{10}(7x)$
1	+0.33920	+0.23358	+0.12797	+0.05892	+0.02354
2	+0.08117	−0.15080	−0.23197	−0.11431	+0.08501
3	+0.10765	−0.10215	−0.17575	−0.03175	+0.14853
4	+0.13934	−0.02821	−0.15344	−0.05947	+0.11521
5	+0.13394	+0.04743	−0.11497	−0.09998	+0.06355
6	+0.08621	+0.10124	−0.05246	−0.12122	+0.00051
7	+0.01312	+0.11455	+0.01961	−0.10815	−0.05934
8	−0.05645	+0.08373	+0.07739	−0.06162	−0.09719
9	−0.09521	+0.02299	+0.10031	+0.00249	−0.09960
10	−0.08958	−0.04141	+0.08130	+0.06000	−0.06587
11	−0.04542	−0.08253	+0.03042	+0.08885	−0.00965
12	+0.01520	−0.08444	−0.02927	+0.07886	+0.04617
13	+0.06431	−0.04892	−0.07183	+0.03629	+0.07901
14	+0.08067	+0.00597	−0.07982	−0.01900	+0.07633
15	+0.05898	+0.05450	−0.05171	−0.06238	+0.04102
16	+0.01145	+0.07513	−0.00206	−0.07543	−0.01007
17	−0.03857	+0.06001	+0.04563	−0.05388	−0.05378
18	−0.06779	+0.01799	+0.06979	−0.00912	−0.07109
19	−0.06370	−0.03018	+0.06052	+0.03746	−0.05545
20	−0.02986	−0.06183	+0.02368	+0.06453	−0.01539

BESSEL FUNCTIONS WITH INCREASING ARGUMENT—*Continued*

s	$J_0(8s)$	$J_1(8s)$	$J_2(8s)$	$J_3(8s)$	$J_4(8s)$	$J_5(8s)$
1	+0.17165	+0.23464	−0.11299	−0.29113	−0.10536	+0.18577
2	−0.17490	+0.09040	+0.18620	−0.04385	−0.20264	−0.05747
3	−0.05623	−0.15404	+0.04339	+0.16127	−0.00308	−0.16230
4	+0.13808	−0.02659	−0.13974	+0.00912	+0.14145	+0.02624
5	+0.00737	+0.12604	−0.00106	−0.12614	−0.01786	+0.12257
6	−0.11471	−0.01133	+0.11424	+0.02085	−0.11164	−0.03946
7	+0.02477	−0.10348	−0.02847	+0.10145	+0.03934	−0.09583
8	+0.09259	+0.03779	−0.09141	−0.04350	+0.08733	+0.05442
9	−0.04729	+0.08094	+0.04954	−0.07819	−0.05606	+0.07196
10	−0.06974	−0.05606	+0.06834	+0.05947	−0.06388	−0.06586
11	+0.06215	−0.05771	−0.06346	+0.05483	+0.06720	−0.04872
12	+0.04633	+0.06721	−0.04493	−0.06908	+0.04062	+0.07247
13	−0.07014	+0.03434	+0.07080	−0.03162	−0.07262	+0.02603
14	−0.02322	−0.07183	+0.02194	+0.07262	−0.01805	−0.07391
15	+0.07182	−0.01181	−0.07202	+0.00940	+0.07249	−0.00457
16	+0.00147	+0.07051	−0.00037	−0.07053	−0.00294	+0.07034
17	−0.06788	−0.00879	+0.06775	+0.01079	−0.06728	−0.01474
18	+0.01782	−0.06400	−0.01871	+0.06348	+0.02135	−0.06229
19	+0.05916	+0.02643	−0.05881	−0.02797	+0.05771	+0.03101
20	−0.03369	+0.05322	+0.03435	−0.05237	−0.03632	+0.05055

s	$J_6(8s)$	$J_7(8s)$	$J_8(8s)$	$J_9(8s)$	$J_{10}(8s)$
1	+0.33758	+0.32050	+0.22345	+0.12632	+0.06077
2	+0.16672	+0.18251	−0.00702	−0.18953	−0.20621
3	−0.06455	+0.13002	+0.14039	−0.03643	−0.16771
4	−0.13325	−0.07621	+0.09991	+0.12616	−0.02894
5	+0.04850	−0.10802	−0.08631	+0.07350	+0.11938
6	+0.10342	+0.06531	−0.08437	−0.09343	+0.04933
7	−0.05645	+0.08373	+0.07739	−0.06162	−0.09719
8	−0.07883	−0.06920	+0.06369	+0.08512	−0.03975
9	+0.06605	−0.06095	−0.07791	+0.04364	+0.08882
10	+0.05565	+0.07421	−0.04266	−0.08274	+0.02404
11	−0.07274	+0.03880	+0.07891	−0.02445	−0.08391
12	−0.03307	−0.07660	+0.02190	+0.08025	−0.00685
13	+0.07512	−0.01736	−0.07746	+0.00544	+0.07840
14	+0.01145	+0.07513	−0.00206	−0.07543	−0.01007
15	−0.07287	−0.00272	+0.07255	+0.01239	−0.07070
16	+0.00843	−0.06955	−0.01604	+0.06755	+0.02554
17	+0.06619	+0.02058	−0.06407	−0.02812	+0.06035
18	−0.02568	+0.06015	+0.03152	−0.05665	−0.03861
19	−0.05567	−0.03541	+0.05241	+0.04092	−0.04756
20	+0.03948	−0.04750	−0.04364	+0.04323	+0.04850

BESSEL FUNCTIONS WITH INCREASING ARGUMENT—*Continued*

s	$J_0(9s)$	$J_1(9s)$	$J_2(9s)$	$J_3(9s)$	$J_4(9s)$	$J_5(9s)$
1	−0.09033	+0.24531	+0.14485	−0.18094	−0.26547	−0.05504
2	−0.01336	−0.18799	−0.00753	+0.18632	+0.06964	−0.15537
3	+0.07274	+0.13658	−0.06262	−0.14586	+0.03021	+0.15481
4	−0.10557	−0.08233	+0.10099	+0.09355	−0.08540	−0.11253
5	+0.11582	+0.02835	−0.11456	−0.03853	+0.10942	+0.05798
6	−0.10652	+0.02003	+0.10726	−0.01208	−0.10861	−0.00401
7	+0.08186	−0.05770	−0.08369	+0.05238	+0.08868	−0.04112
8	−0.04729	+0.08094	+0.04954	−0.07819	−0.05606	+0.07196
9	+0.00907	−0.08813	−0.01124	+0.08758	+0.01773	−0.08583
10	+0.02663	+0.07993	−0.02485	−0.08103	+0.01945	+0.08276
11	−0.05447	−0.05912	+0.05328	+0.06128	−0.04957	−0.06528
12	+0.07074	+0.03018	−0.07018	−0.03278	+0.06836	+0.03784
13	−0.07374	+0.00156	+0.07377	+0.00006	−0.07372	−0.00600
14	+0.06400	−0.03067	−0.06449	+0.02862	+0.06585	−0.02444
15	−0.04403	+0.05254	+0.04481	−0.05121	−0.04708	+0.04842
16	+0.01782	−0.06400	−0.01871	+0.06348	+0.02135	−0.06229
17	+0.00986	+0.06378	−0.00903	−0.06402	+0.00652	+0.06436
18	−0.03426	−0.05260	+0.03361	+0.05343	−0.03163	−0.05500
19	+0.05144	+0.03297	−0.05105	−0.03416	+0.04985	+0.03649
20	−0.05886	−0.00865	+0.05877	+0.00995	−0.05843	−0.01255

s	$J_6(9s)$	$J_7(9s)$	$J_8(9s)$	$J_9(9s)$	$J_{10}(9s)$
1	+0.20432	+0.32746	+0.30507	+0.21488	+0.12469
2	−0.15596	+0.05140	+0.19593	+0.12276	−0.07317
3	+0.02713	−0.14276	−0.10115	+0.08282	+0.15636
4	+0.05414	+0.13058	−0.00336	−0.13207	−0.06267
5	−0.09654	−0.08373	+0.07049	+0.10879	−0.02697
6	+0.10787	+0.02798	−0.10061	−0.05779	+0.08135
7	−0.09521	+0.02299	+0.10031	+0.00249	−0.09960
8	+0.06605	−0.06095	−0.07791	+0.04364	+0.08882
9	−0.02833	+0.08163	+0.04243	−0.07325	−0.05871
10	−0.01026	−0.08413	−0.00283	+0.08362	+0.01955
11	+0.04297	+0.07049	−0.03300	−0.07582	+0.01922
12	−0.06485	−0.04504	+0.05901	+0.05379	−0.05005
13	+0.07320	+0.01351	−0.07159	−0.02330	+0.06800
14	−0.06779	+0.01799	+0.06979	−0.00912	−0.07109
15	+0.05067	−0.04392	−0.05522	+0.03737	+0.06021
16	−0.02568	+0.06015	+0.03152	−0.05665	−0.03961
17	−0.00231	−0.06454	−0.00360	+0.06416	+0.01114
18	+0.02824	+0.05709	−0.02330	−0.05939	+0.01670
19	−0.04772	−0.03984	+0.04446	+0.04400	−0.03983
20	+0.05774	+0.01640	−0.05646	−0.02142	+0.05432

BESSEL FUNCTIONS WITH INCREASING ARGUMENT—*Continued*

s	$J_0(10s)$	$J_1(10s)$	$J_2(10s)$	$J_3(10s)$	$J_4(10s)$	$J_5(10s)$
1	−0.24594	+0.04347	+0.25463	+0.05838	−0.21960	−0.23406
2	+0.16702	+0.06683	−0.16034	−0.09890	+0.13067	+0.15117
3	−0.08637	−0.11875	+0.07845	+0.12921	−0.05261	−0.14324
4	+0.00737	+0.12604	−0.00106	−0.12614	−0.01786	+0.12257
5	+0.05581	−0.09751	−0.05971	+0.09273	+0.07084	−0.08140
6	−0.09147	+0.04660	+0.09303	−0.04040	−0.09706	+0.02745
7	+0.09491	+0.00999	−0.09462	−0.01539	+0.09330	+0.02606
8	−0.06974	−0.05606	+0.06834	+0.05947	−0.06388	−0.06586
9	+0.02663	+0.07993	−0.02485	−0.08103	+0.01945	+0.08276
10	+0.01999	−0.07715	−0.02153	+0.07628	+0.02611	−0.07420
11	−0.05606	+0.05117	+0.05699	−0.04910	−0.05967	+0.04476
12	+0.07182	−0.01181	−0.07202	+0.00940	+0.07249	−0.00457
13	−0.06423	−0.02803	+0.06379	+0.03000	−0.06241	−0.03384
14	+0.03736	+0.05627	−0.03655	−0.05732	+0.03410	+0.05927
15	−0.00077	−0.06515	−0.00009	+0.06514	+0.00270	−0.06500
16	−0.03369	+0.05322	+0.03435	−0.05237	−0.03632	+0.05055
17	+0.05557	−0.02547	−0.05587	+0.02415	+0.05672	−0.02148
18	−0.05886	−0.00865	+0.05877	+0.00995	−0.05843	−0.01255
19	+0.04358	+0.03821	−0.04318	−0.03912	+0.04194	+0.04089
20	−0.01544	−0.05430	+0.01489	+0.05460	−0.01326	−0.05513

s	$J_6(10s)$	$J_7(10s)$	$J_8(10s)$	$J_9(10s)$	$J_{10}(10s)$
1	−0.01446	+0.21671	+0.31785	+0.29186	+0.20749
2	−0.05509	−0.18422	−0.07387	+0.12513	+0.18648
3	+0.00486	+0.14519	+0.06289	−0.11164	−0.12988
4	+0.04850	−0.10802	−0.08631	+0.07350	+0.11938
5	−0.08712	+0.06049	+0.10406	−0.02719	−0.11385
6	+0.10164	−0.00713	−0.10330	−0.02042	+0.09718
7	−0.08958	−0.04141	+0.08130	+0.06000	−0.06587
8	+0.05565	+0.07421	−0.04266	−0.08274	+0.02404
9	−0.01026	−0.08413	−0.00283	+0.08362	+0.01955
10	−0.03353	+0.07017	+0.04335	−0.06324	−0.05473
11	+0.06374	−0.03780	−0.06855	+0.02783	+0.07311
12	−0.07287	−0.00272	+0.07255	+0.01239	−0.07070
13	+0.05981	+0.03936	−0.05557	−0.04620	+0.04917
14	−0.02986	−0.06183	+0.02368	+0.06453	−0.01539
15	−0.00703	+0.06444	+0.01305	−0.06304	−0.02061
16	+0.03948	−0.04759	−0.04364	+0.04323	+0.04850
17	−0.05799	+0.01739	+0.05942	−0.01180	−0.06067
18	+0.05774	+0.01640	−0.05646	−0.02142	+0.05432
19	−0.03979	−0.04340	+0.03659	+0.04648	−0.03219
20	+0.01050	+0.05576	−0.00660	−0.05629	+0.00153

Auxiliary Functions

When x is large the sine and cosine functions can be expanded and the formulas arranged in the form

$$J_0(x) = A_0(x) \sin x + B_0(x) \cos x$$
$$J_1(x) = B_1(x) \sin x - A_1(x) \cos x$$

where

$$A_0(x) = \frac{P_0(x) - Q_0(x)}{(\pi x)^{1/2}} \qquad B_0(x) = \frac{P_0(x) + Q_0(x)}{(\pi x)^{1/2}}$$
$$A_1(x) = \frac{P_1(x) - Q_1(x)}{(\pi x)^{1/2}} \qquad B_1(x) = \frac{P_1(x) + Q_1(x)}{(\pi x)^{1/2}}$$

The functions $A_0(x)$, $A_1(x)$, $B_0(x)$, $B_1(x)$ have been tabulated[5] for

$x = 25(0.1)50(1)150(10)1150$ and
$1000(100)6000$ to 8 decimal places,

where 25(0.1)50 means that x goes from 25 to 50 at intervals of 0.1, etc. These tables were used wherever possible to compute the tables in this article. The values of the trigonometric functions for x are tabulated,[6] $x = 0(1)100$; 8 decimals. For values larger than this, whole multiples of π were subtracted from x to bring the angle into the first or fourth quadrants and the angle interpolated from tables for sines and cosines.[7] By using the usual recurrence formula for the Bessel functions,[8]

$$J_{n-1}(x) + J_{n+1}(x) = \frac{2n}{x} J_n(x)$$

the values of $J_3(x)$ can be computed from $J_0(x)$ and $J_1(x)$. Similarly $J_3(x)$ can be obtained from $J_2(x)$ and $J_1(x)$. By this process the tables were extended to $J_{10}(x)$.

Method of Checking

The values of $J_m(s)$, $m = 1(1)10$ and $s = 1(1)24$ were obtained by rounding off the eighteen-place tables given in Gray, Mathews and MacRobert.[9] The known errors in their tables[10] did not cause any discrepancies.

For higher values of the argument the values were all computed from the asymptotic formula. The auxiliary functions were used when possible.

[5] British Association for the Advancement of Science, "Mathematical Tables," Vol. VI, Bessel Functions, pp. 203–212.

[6] Arnold N. Lowan, "Tables of Sines and Cosines for Radian Arguments," Federal Works Agency, 1940, p. 251.

[7] Arnold N. Lowan, "Tables of Circular and Hyperbolic Sines and Cosines for Radian Arguments," Federal Works Agency, 1939, $x = 0(0.0001)2$; 9 decimal places.

[8] Gray, Mathews and MacRobert, op. cit., p. 16.

[9] Gray, Mathews and MacRobert, op. cit., Table II, p. 286–299.

[10] British Association Tables, op. cit., p. xii.

TABLE II—$J_n(m\pi s)$
BESSEL FUNCTIONS WITH INCREASING ARGUMENT

s	$J_0(\pi s)$	$J_1(\pi s)$	$J_2(\pi s)$	$J_3(\pi s)$	$J_4(\pi s)$	$J_5(\pi s)$
1	−0.30424	+0.28462	+0.48543	+0.33346	+0.15142	+0.05214
2	+0.22028	−0.21238	−0.28788	+0.02911	+0.31568	+0.37282
3	−0.18121	+0.17673	+0.21871	−0.08390	−0.27213	−0.14709
4	+0.15751	−0.15453	−0.18210	+0.09657	+0.22821	+0.04872
5	−0.14118	+0.13903	+0.15888	−0.09857	−0.19653	−0.00153
6	+0.12906	−0.12741	−0.14258	+0.09715	+0.17351	−0.02351
7	−0.11961	+0.11829	+0.13037	−0.09458	−0.15617	+0.03776
8	+0.11197	−0.11088	−0.12079	+0.09166	+0.14267	−0.04624
9	−0.10563	+0.10471	+0.11303	−0.08872	−0.13186	+0.05141
10	+0.10025	−0.09947	−0.10658	+0.08590	+0.12299	−0.05458
11	−0.09562	+0.09494	+0.10112	−0.08324	−0.11557	+0.05648
12	+0.09158	−0.09098	−0.09641	+0.08075	+0.10926	−0.05757
13	−0.08801	+0.08748	+0.09230	−0.07844	−0.10382	+0.05810
14	+0.08483	−0.08435	−0.08866	+0.07629	+0.09907	−0.05827
15	−0.08197	+0.08154	+0.08543	−0.07429	−0.09489	+0.05818
16	+0.07938	−0.07899	−0.08252	+0.07242	+0.09116	−0.05791
17	−0.07702	+0.07666	+0.07989	−0.07068	−0.08783	+0.05752
18	+0.07486	−0.07453	−0.07749	+0.06905	+0.08482	−0.05705
19	−0.07287	+0.07257	+0.07530	−0.06752	−0.08209	+0.05652
20	+0.07103	−0.07075	−0.07329	+0.06609	+0.07960	−0.05595
21	−0.06933	+0.06907	+0.07142	−0.06474	−0.07731	+0.05536
22	+0.06774	−0.06750	−0.06969	+0.06346	+0.07520	−0.05476
23	−0.06626	+0.06603	+0.06808	−0.06226	−0.07325	+0.05415
24	+0.06487	−0.06465	−0.06658	+0.06112	+0.07145	−0.05354
25	−0.06356	+0.06336	+0.06517	−0.06004	−0.06976	+0.05293
26	+0.06233	−0.06214	−0.06385	+0.05901	+0.06819	−0.05234
27	−0.06117	+0.06099	+0.06261	−0.05804	−0.06671	+0.05174
28	+0.06007	−0.05990	−0.06143	+0.05711	+0.06533	−0.05116
29	−0.05903	+0.05887	+0.06032	−0.05622	−0.06402	+0.05060
30	+0.05804	−0.05788	−0.05927	+0.05537	+0.06279	−0.05004
31	−0.05710	+0.05695	+0.05827	−0.05456	−0.06163	+0.04950
32	+0.05620	−0.05606	−0.05731	+0.05378	+0.06052	−0.04896
33	−0.05534	+0.05521	+0.05641	−0.05303	−0.05948	+0.04844
34	+0.05453	−0.05440	−0.05554	+0.05232	+0.05848	−0.04794
35	−0.05374	+0.05362	+0.05472	−0.05163	−0.05754	+0.04744
36	+0.05299	−0.05288	−0.05393	+0.05097	+0.05663	−0.04696
37	−0.05227	+0.05216	+0.05317	−0.05033	−0.05577	+0.04649
38	+0.05158	−0.05147	−0.05244	+0.04972	+0.05494	−0.04604
39	−0.05092	+0.05081	+0.05175	−0.04913	−0.05415	+0.04559
40	+0.05028	−0.05018	−0.05108	+0.04855	+0.05340	−0.04515

BESSEL FUNCTIONS WITH INCREASING ARGUMENT—*Continued*

s	$J_6(\pi s)$	$J_7(\pi s)$	$J_8(\pi s)$	$J_9(\pi s)$	$J_{10}(\pi s)$
1	+0.01455	+0.00342	+0.00070	+0.00013	+0.00002
2	+0.27769	+0.15752	+0.07330	+0.02912	+0.01014
3	+0.11606	+0.29486	+0.32194	+0.25168	+0.15873
4	−0.18944	−0.22962	−0.06637	+0.14511	+0.27423
5	+0.19556	+0.15092	−0.06105	−0.21311	−0.18315
6	−0.18598	−0.09489	+0.11551	+0.19293	+0.06873
7	+0.17334	+0.05683	−0.13717	−0.15662	+0.00897
8	−0.16107	−0.03066	+0.14399	+0.12233	−0.05638
9	+0.15004	+0.01227	−0.14397	−0.09374	+0.08429
10	−0.14036	+0.00097	+0.14079	+0.07074	−0.10026
11	+0.13191	−0.01068	−0.13624	−0.05240	+0.10895
12	−0.12453	+0.01793	+0.13119	+0.03775	−0.11316
13	+0.11805	−0.02342	−0.12607	−0.02597	+0.11463
14	−0.11232	+0.02762	+0.12111	+0.01643	−0.11439
15	+0.10723	−0.03087	−0.11640	−0.00865	+0.11310
16	−0.10269	+0.03340	+0.11199	+0.00225	−0.11118
17	+0.09860	−0.03537	−0.10787	+0.00305	+0.10890
18	−0.09491	+0.03691	+0.10405	−0.00747	−0.10643
19	+0.09156	−0.03811	−0.10050	+0.01118	+0.10387
20	−0.08850	+0.03905	+0.09720	−0.01430	−0.10130
21	+0.08570	−0.03977	−0.09414	+0.01694	+0.09876
22	−0.08313	+0.04033	+0.09129	−0.01919	−0.09629
23	+0.08075	−0.04074	−0.08864	+0.02111	+0.09390
24	−0.07855	+0.04104	+0.08617	−0.02275	−0.09160
25	+0.07650	−0.04125	−0.08385	+0.02416	+0.08939
26	−0.07459	+0.04138	+0.08169	−0.02538	−0.08728
27	+0.07281	−0.04144	−0.07965	+0.02642	+0.08526
28	−0.07114	+0.04146	+0.07774	−0.02732	−0.08333
29	+0.06958	−0.04143	−0.07594	+0.02810	+0.08149
30	−0.06810	+0.04137	+0.07425	−0.02876	−0.07974
31	+0.06671	−0.04128	−0.07264	+0.02934	+0.07807
32	−0.06539	+0.04116	+0.07113	−0.02984	−0.07647
33	+0.06415	−0.04102	−0.06969	+0.03026	+0.07494
34	−0.06297	+0.04086	+0.06833	−0.03063	−0.07349
35	+0.06185	−0.04069	−0.06703	+0.03094	+0.07210
36	−0.06078	+0.04051	+0.06580	−0.03120	−0.07077
37	+0.05977	−0.04032	−0.06463	+0.03143	+0.06949
38	−0.05880	+0.04013	+0.06351	−0.03161	−0.06827
39	+0.05787	−0.03992	−0.06244	+0.03177	+0.06710
40	−0.05699	+0.03971	+0.06141	−0.03189	−0.06598

BESSEL FUNCTIONS WITH INCREASING ARGUMENT—*Continued*

x	$J_0(2\pi x)$	$J_1(2\pi x)$	$J_2(2\pi x)$	$J_3(2\pi x)$	$J_4(2\pi x)$	$J_5(2\pi x)$
1	+0.22028	−0.21238	−0.28788	+0.02911	+0.31568	+0.37282
2	+0.15751	−0.15453	−0.18210	+0.09657	+0.22821	+0.04872
3	+0.12906	−0.12741	−0.14258	+0.09715	+0.17351	−0.02351
4	+0.11197	−0.11088	−0.12079	+0.09166	+0.14267	−0.04624
5	+0.10025	−0.09947	−0.10658	+0.08590	+0.12299	−0.05458
6	+0.09158	−0.09098	−0.09641	+0.08075	+0.10926	−0.05757
7	+0.08483	−0.08435	−0.08866	+0.07629	+0.09907	−0.05827
8	+0.07938	−0.07899	−0.08252	+0.07242	+0.09116	−0.05791
9	+0.07486	−0.07453	−0.07749	+0.06905	+0.08482	−0.05705
10	+0.07103	−0.07075	−0.07329	+0.06609	+0.07960	−0.05595
11	+0.06774	−0.06750	−0.06969	+0.06346	+0.07520	−0.05476
12	+0.06487	−0.06465	−0.06658	+0.06112	+0.07145	−0.05354
13	+0.06233	−0.06214	−0.06385	+0.05901	+0.06819	−0.05234
14	+0.06007	−0.05990	−0.06143	+0.05711	+0.06533	−0.05116
15	+0.05804	−0.05788	−0.05927	+0.05537	+0.06279	−0.05004
16	+0.05620	−0.05606	−0.05731	+0.05378	+0.06052	−0.04896
17	+0.05453	−0.05440	−0.05554	+0.05232	+0.05848	−0.04794
18	+0.05299	−0.05288	−0.05393	+0.05097	+0.05663	−0.04696
19	+0.05158	−0.05147	−0.05244	+0.04972	+0.05494	−0.04604
20	+0.05028	−0.05018	−0.05108	+0.04855	+0.05340	−0.04515

x	$J_6(2\pi x)$	$J_7(2\pi x)$	$J_8(2\pi x)$	$J_9(2\pi x)$	$J_{10}(2\pi x)$
1	+0.27769	+0.15752	+0.07330	+0.02912	+0.01014
2	−0.18944	−0.22962	−0.06637	+0.14511	+0.27423
3	−0.18598	−0.09489	+0.11551	+0.19293	+0.06873
4	−0.16107	−0.03066	+0.14399	+0.12233	−0.05638
5	−0.14036	+0.00097	+0.14079	+0.07074	−0.10026
6	−0.12453	+0.01793	+0.13119	+0.03775	−0.11316
7	−0.11232	+0.02762	+0.12111	+0.01643	−0.11439
8	−0.10269	+0.03340	+0.11199	+0.00225	−0.11118
9	−0.09491	+0.03691	+0.10405	−0.00747	−0.10643
10	−0.08850	+0.03905	+0.09720	−0.01430	−0.10130
11	−0.08313	+0.04033	+0.09129	−0.01919	−0.09629
12	−0.07855	+0.04104	+0.08617	−0.02275	−0.09160
13	−0.07459	+0.04138	+0.08169	−0.02538	−0.08728
14	−0.07114	+0.04146	+0.07774	−0.02732	−0.08333
15	−0.06810	+0.04137	+0.07425	−0.02876	−0.07974
16	−0.06539	+0.04116	+0.07113	−0.02984	−0.07647
17	−0.06297	+0.04086	+0.06833	−0.03063	−0.07349
18	−0.06078	+0.04051	+0.06580	−0.03120	−0.07077
19	−0.05880	+0.04013	+0.06351	−0.03161	−0.06827
20	−0.05699	+0.03971	+0.06141	−0.03189	−0.06598

BESSEL FUNCTIONS WITH INCREASING ARGUMENT—*Continued*

s	$J_0(3\pi s)$	$J_1(3\pi s)$	$J_2(3\pi s)$	$J_3(3\pi s)$	$J_4(3\pi s)$	$J_5(3\pi s)$
1	−0.18121	+0.17673	+0.21871	−0.08390	−0.27213	−0.14709
2	+0.12906	−0.12741	−0.14258	+0.09715	+0.17351	−0.02351
3	−0.10563	+0.10471	+0.11303	−0.08872	−0.13186	+0.05141
4	+0.09158	−0.09098	−0.09641	+0.08075	+0.10926	−0.05757
5	−0.08197	+0.08154	+0.08543	−0.07429	−0.09489	+0.05818
6	+0.07486	−0.07453	−0.07749	+0.06905	+0.08482	−0.05705
7	−0.06933	+0.06907	+0.07142	−0.06474	−0.07731	+0.05536
8	+0.06487	−0.06465	−0.06658	+0.06112	+0.07145	−0.05354
9	−0.06117	+0.06099	+0.06261	−0.05804	−0.06671	+0.05174
10	+0.05804	−0.05788	−0.05927	+0.05537	+0.06279	−0.05004
11	−0.05534	+0.05521	+0.05641	−0.05303	−0.05948	+0.04844
12	+0.05299	−0.05288	−0.05393	+0.05097	+0.05663	−0.04696
13	−0.05092	+0.05081	+0.05175	−0.04913	−0.05415	+0.04559
14	+0.04907	−0.04898	−0.04981	+0.04747	+0.05197	−0.04432
15	−0.04741	+0.04733	+0.04808	−0.04596	−0.05003	+0.04313
16	+0.04591	−0.04583	−0.04651	+0.04460	+0.04829	−0.04203
17	−0.04454	+0.04447	+0.04509	−0.04334	−0.04672	+0.04101
18	+0.04328	−0.04322	−0.04379	+0.04219	+0.04529	−0.04005
19	−0.04213	+0.04207	+0.04260	−0.04112	−0.04398	+0.03916
20	+0.04107	−0.04101	−0.04150	+0.04013	+0.04278	−0.03832

s	$J_6(3\pi s)$	$J_7(3\pi s)$	$J_8(3\pi s)$	$J_9(3\pi s)$	$J_{10}(3\pi s)$
1	+0.11606	+0.29486	+0.32194	+0.25168	+0.15873
2	−0.18598	−0.09489	+0.11551	+0.19293	+0.06873
3	+0.15004	+0.01227	−0.14397	−0.09374	+0.08429
4	−0.12453	+0.01793	+0.13119	+0.03775	−0.11316
5	+0.10723	−0.03087	−0.11640	−0.00865	+0.11310
6	−0.09491	+0.03691	+0.10405	−0.00747	−0.10643
7	+0.08570	−0.03977	−0.09414	+0.01694	+0.09876
8	−0.07855	+0.04104	+0.08617	−0.02275	−0.09160
9	+0.07281	−0.04144	−0.07965	+0.02642	+0.08526
10	−0.06810	+0.04137	+0.07425	−0.02876	−0.07974
11	+0.06415	−0.04102	−0.06969	+0.03026	+0.07494
12	−0.06078	+0.04051	+0.06580	−0.03120	−0.07077
13	+0.05787	−0.03992	−0.06244	+0.03177	+0.06710
14	−0.05533	+0.03928	+0.05950	−0.03207	−0.06387
15	+0.05308	−0.03863	−0.05691	+0.03219	+0.06100
16	−0.05108	+0.03797	+0.05460	−0.03218	−0.05844
17	+0.04928	−0.03732	−0.05254	+0.03207	+0.05614
18	−0.04765	+0.03668	+0.05067	−0.03190	−0.05406
19	+0.04617	−0.03606	−0.04899	+0.03169	+0.05217
20	−0.04481	+0.03546	+0.04745	−0.03144	−0.05045

BESSEL FUNCTIONS WITH INCREASING ARGUMENT—*Continued*

s	$J_0(4\pi s)$	$J_1(4\pi s)$	$J_2(4\pi s)$	$J_3(4\pi s)$	$J_4(4\pi s)$	$J_5(4\pi s)$
1	+0.15751	−0.15453	−0.18210	+0.09657	+0.22812	+0.04872
2	+0.11197	−0.11088	−0.12079	+0.09166	+0.14267	−0.04624
3	+0.09158	−0.09098	−0.09641	+0.08075	+0.10926	−0.05757
4	+0.07938	−0.07899	−0.08252	+0.07242	+0.09116	−0.05791
5	+0.07103	−0.07075	−0.07329	+0.06609	+0.07960	−0.05595
6	+0.06487	−0.06465	−0.06658	+0.06112	+0.07145	−0.05354
7	+0.06007	−0.05990	−0.06143	+0.05711	+0.06533	−0.05116
8	+0.05620	−0.05606	−0.05731	+0.05378	+0.06052	−0.04896
9	+0.05299	−0.05288	−0.05393	+0.05097	+0.05663	−0.04696
10	+0.05028	−0.05018	−0.05108	+0.04855	+0.05340	−0.04515
11	+0.04794	−0.04786	−0.04864	+0.04645	+0.05065	−0.04352
12	+0.04591	−0.04583	−0.04651	+0.04460	+0.04829	−0.04203
13	+0.04411	−0.04404	−0.04465	+0.04295	+0.04622	−0.04068
14	+0.04251	−0.04245	−0.04299	+0.04147	+0.04440	−0.03945
15	+0.04107	−0.04101	−0.04150	+0.04013	+0.04278	−0.03832
16	+0.03976	−0.03971	−0.04016	+0.03892	+0.04132	−0.03727
17	+0.03858	−0.03853	−0.03894	+0.03780	+0.04000	−0.03631
18	+0.03749	−0.03745	−0.03782	+0.03678	+0.03880	−0.03541
19	+0.03649	−0.03646	−0.03680	+0.03584	+0.03770	−0.03458
20	+0.03557	−0.03554	−0.03585	+0.03496	+0.03669	−0.03380

s	$J_6(4\pi s)$	$J_7(4\pi s)$	$J_8(4\pi s)$	$J_9(4\pi s)$	$J_{10}(4\pi s)$
1	−0.18944	−0.22962	−0.06637	+0.14511	+0.27423
2	−0.16107	−0.03066	+0.14399	+0.12233	−0.05638
3	−0.12453	+0.01793	+0.13119	+0.03775	−0.11316
4	−0.10269	+0.03340	+0.11199	+0.00225	−0.11118
5	−0.08850	+0.03905	+0.09720	−0.01430	−0.10130
6	−0.07855	+0.04104	+0.08617	−0.02275	−0.09160
7	−0.07114	+0.04146	+0.07774	−0.02732	−0.08333
8	−0.06539	+0.04116	+0.07113	−0.02984	−0.07647
9	−0.06078	+0.04051	+0.06580	−0.03120	−0.07077
10	−0.05699	+0.03971	+0.06141	−0.03189	−0.06598
11	−0.05380	+0.03885	+0.05773	−0.03217	−0.06192
12	−0.05108	+0.03797	+0.05460	−0.03218	−0.05844
13	−0.04871	+0.03711	+0.05189	−0.03202	−0.05542
14	−0.04664	+0.03627	+0.04953	−0.03176	−0.05278
15	−0.04481	+0.03546	+0.04745	−0.03144	−0.05045
16	−0.04317	+0.03469	+0.04559	−0.03107	−0.04837
17	−0.04170	+0.03396	+0.04393	−0.03067	−0.04651
18	−0.04036	+0.03327	+0.04242	−0.03027	−0.04483
19	−0.03915	+0.03261	+0.04106	−0.02986	−0.04331
20	−0.03803	+0.03198	+0.03981	−0.02945	−0.04192

BESSEL FUNCTIONS WITH INCREASING ARGUMENT—*Continued*

s	$J_0(5\pi s)$	$J_1(5\pi s)$	$J_2(5\pi s)$	$J_3(5\pi s)$	$J_4(5\pi s)$	$J_5(5\pi s)$
1	−0.14118	+0.13903	+0.15888	−0.09857	−0.19653	−0.00153
2	+0.10025	−0.09947	−0.10658	+0.08590	+0.12299	−0.05458
3	−0.08197	+0.08154	+0.08543	−0.07429	−0.09489	+0.05818
4	+0.07103	−0.07075	−0.07329	+0.06609	+0.07960	−0.05595
5	−0.06356	+0.06336	+0.06517	−0.06004	−0.06976	+0.05293
6	+0.05804	−0.05788	−0.05927	+0.05537	+0.06279	−0.05004
7	−0.05374	+0.05362	+0.05472	−0.05163	−0.05754	+0.04744
8	+0.05028	−0.05018	−0.05108	+0.04855	+0.05340	−0.04515
9	−0.04741	+0.04733	+0.04808	−0.04596	−0.05003	+0.04313
10	+0.04498	−0.04491	−0.04555	+0.04375	+0.04722	−0.04134
11	−0.04289	+0.04283	+0.04339	−0.04182	−0.04484	+0.03975
12	+0.04107	−0.04101	−0.04150	+0.04013	+0.04278	−0.03832
13	−0.03946	+0.03941	+0.03984	−0.03863	−0.04098	+0.03702
14	+0.03802	−0.03798	−0.03837	+0.03728	+0.03939	−0.03585
15	−0.03674	+0.03670	+0.03705	−0.03607	−0.03797	+0.03478
16	+0.03557	−0.03554	−0.03585	+0.03496	+0.03669	−0.03380
17	−0.03451	+0.03448	+0.03477	−0.03396	−0.03553	+0.03289
18	+0.03354	−0.03351	−0.03377	+0.03303	+0.03448	−0.03206
19	−0.03264	+0.03262	+0.03286	−0.03218	−0.03351	+0.03128
20	+0.03182	−0.03179	−0.03202	+0.03139	+0.03262	−0.03055

s	$J_6(5\pi s)$	$J_7(5\pi s)$	$J_8(5\pi s)$	$J_9(5\pi s)$	$J_{10}(5\pi s)$
1	+0.19556	+0.15092	−0.06105	−0.21311	−0.18315
2	−0.14036	+0.00097	+0.14079	+0.07074	−0.10026
3	+0.10723	−0.03087	−0.11640	−0.00865	+0.11310
4	−0.08850	+0.03905	+0.09720	−0.01430	−0.10130
5	+0.07650	−0.04125	−0.08385	+0.02416	+0.08939
6	−0.06810	+0.04137	+0.07425	−0.02876	−0.07974
7	+0.06185	−0.04069	−0.06703	+0.03094	+0.07210
8	−0.05699	+0.03971	+0.06141	−0.03189	−0.06598
9	+0.05308	−0.03863	−0.05691	+0.03219	+0.06100
10	−0.04985	+0.03753	+0.05320	−0.03212	−0.05688
11	+0.04714	−0.03647	−0.05009	+0.03184	+0.05341
12	−0.04481	+0.03546	+0.04745	−0.03144	−0.05045
13	+0.04279	−0.03451	−0.04516	+0.03097	+0.04789
14	−0.04102	+0.03361	+0.04316	−0.03047	−0.04565
15	+0.03944	−0.03277	−0.04139	+0.02996	+0.04368
16	−0.03803	+0.03198	+0.03981	−0.02945	−0.04192
17	+0.03676	−0.03124	−0.03840	+0.02894	+0.04035
18	−0.03561	+0.03054	+0.03712	−0.02844	−0.03893
19	+0.03456	−0.02989	−0.03596	+0.02796	+0.03765
20	−0.03359	+0.02927	+0.03490	−0.02749	−0.03647

As an over-all check, the values of $J_{10}(x)$ were computed directly from the asymptotic formula. The functions $\begin{matrix}\sin\\ \cos\end{matrix}\left(x-\frac{\pi}{4}\right)$ were obtained by interpolation. This checked all the computations completely since the methods are entirely independent.

The tabular values were computed to seven or eight decimal places and later rounded off to five decimal places. Where there was any reasonable doubt as to whether to add or drop a half, the function was recalculated more accurately.

As a further check the values were compared with known tables. Nagaoka[11] has given values of $J_0(n\pi)$ for $n = 1(1)50$ and no errors were found in his tables. Hayashi[12] also gives tables of $J_n(20)$, $J_n(30)$, $J_n(40)$, $J_n(50)$ and $J_n(100)$; these results agree with ours.

Steiner[13] has given $J_1(x)$ for $x = [20.1(0.1)31.0(0.2)41.0;\ 6D]$ and his values for integral values of x were compared with our tables; no disagreement was found. It is therefore hoped that the tables are free from error.

[11] H. Nagaoka, "Diffraction phenomena produced by an aperture on a curved surface," The Journal of the College of Science, Imperial University, Japan, vol. 4, 1891, p. 315. This table is reprinted in Keiichi Hayashi, Fünfstellige Funktionentafeln, Julius Springer, Berlin, 1930, p. 99.

[12] Hayashi, ibid.

[13] Ludwig Steiner, "Intensitäts-verhältnisse der Beugungserscheinung durch eine kreisförmige Öffnung," Mathematische und Naturwissenschaftliche Berichte aus Ungarn, vol. 11, 1894, p. 372–373.

THE PARABOLIC CYLINDER FUNCTIONS

By C. P. Wells and R. D. Spence

1. **Introduction.** The purpose of this paper is to discuss the parabolic cylinder functions and their representation in a form suitable for the solution of problems involving standing waves. The propagation of electromagnetic waves in parabolic pipes[1] and the vibrations of a parabolic membrane[2] are examples of such problems. Other problems in radiation and diffraction are readily formulated in parabolic cylinder coordinates, and while both Whittaker[3] and Epstein[4] have studied parabolic cylinder functions for these cases, the forms which they evolved are not suitable for the representation of standing waves.

2. **The wave equation in parabolic coordinates.** The scalar wave equation in parabolic cylinder coordinates ξ, η, z is

$$\frac{1}{\xi^2+\eta^2}\left(\frac{\partial^2\varphi}{\partial\xi^2}+\frac{\partial^2\varphi}{\partial\eta^2}\right)+\frac{\partial^2\varphi}{\partial z^2}=\frac{1}{c^2}\frac{\partial^2\varphi}{\partial t^2}, \tag{1}$$

where ξ, η, and z are related to the rectangular coordinates x, y, z by

$$x=\tfrac{1}{2}(\eta^2-\xi^2), \tag{2a}$$

$$y=\xi\eta, \tag{2b}$$

$$z=z, \tag{2c}$$

and $-\infty<\eta<\infty$, $0<\xi<\infty$. The scalar function φ may be expressed as the following product,

$$\varphi(\xi,\eta,z,t)=U(\xi)V(\eta)Z(z)\begin{matrix}\sin\\ \cos\end{matrix}(\omega t). \tag{3}$$

The first three functions satisfy the ordinary differential equations

$$\frac{d^2Z}{dz^2}+\beta^2Z=0, \tag{4}$$

$$\frac{d^2U}{d\xi^2}+(\gamma^2\xi^2+b)U=0, \tag{5}$$

$$\frac{d^2V}{d\eta^2}+(\gamma^2\eta^2-b)V=0, \tag{6}$$

[1] R. D. Spence and C. P. Wells, *Propagation of Electromagnetic Waves in Parabolic Pipes*, Phys. Rev, 62, July 1 and 15, 1942.

[2] H. Weber, *Die partiellen Differentialgleichungen der Math. Physik*, (Braunschweig 1912) 5th ed., Vol. 2, p. 258.

[3] E. T. Whittaker and G. N. Watson, *Modern Analysis*, (Cambridge Univ. Press, 1915) 2nd ed. p. 341.

[4] P. S. Epstein, *Diss., Munich.*

where

$$\gamma^2 = k^2 - \beta^2, \qquad k = \frac{\omega}{c},$$

ω is the angular frequency, β is the propagation constant along the z axis and b is a separation parameter. The only general requirement[5] on b is that it be so chosen that at each point in space φ is single valued and finite. However, in this paper the solutions U and V of (5) and (6) are to be chosen to represent standing waves and must be real; therefore b is restricted to real values.

The values of γ considered here will be positive and different from zero. (The case for $\gamma = 0$ is of some practical importance since it represents the propagation of two dimensional waves along the z axis between two infinitely extending parabolic cylinders.)

Since Eqs. (5) and (6) are identical except for the sign of b it is necessary to consider solutions of Eq. (5) only. The latter equation may be reduced by the transformations

$$\zeta = \gamma^{1/2}\xi, \tag{7}$$

$$a = \frac{b}{\gamma}, \tag{8}$$

to the dimensionless form

$$\frac{d^2 U_a(\zeta)}{d\zeta^2} + (\zeta^2 + a)U_a(\zeta) = 0 \tag{9}$$

3. **Properties of solutions of Eq. (9).** Before considering explicit forms of solutions of (9) we shall state some useful and important properties of the solutions which arise from the form of the differential equation.

(a) Both even and odd solutions exist. We shall indicate these by ${}_eU_a(\zeta)$ and ${}_oU_a(\zeta)$ and consider them as a fundamental set of solutions.

(b) From the Sturmian oscillation theorems it follows that for $a > 0$, ${}_eU_a(\zeta)$ oscillates faster than $\cos\zeta$, ${}_oU_a(\zeta)$ oscillates faster than $\sin\zeta$, and hence both must have an infinite set of real roots. For $a < 0$ similar statements hold provided $\zeta^2 > |a|$. These results are important if real finite boundary conditions are to be satisfied.

(c) If γ_i, $i = 1, 2, 3, \cdots$ are the roots of the equation $U_a(\gamma^{1/2}c_1) = 0$ for a fixed a, then the functions $U_a(\gamma_1^{1/2}\xi)$, $U_a(\gamma_2^{1/2}\xi)$, $U_a(\gamma_3^{1/2}\xi)\cdots$ form an orthogonal set in the interval $(0, c_1)$ i.e.,

$$\int_0^{c_1} \xi^2 U_a(\gamma_i^{1/2}\xi)U_a(\gamma_j^{1/2}\xi)\,d\xi = 0, \; i \neq j. \tag{10}$$

4. **Power series solution.** Eq. (9) has a single irregular point at $\zeta = \infty$. Therefore solutions of (9) may be found from the power series

$$U_a(\zeta) = \sum_{n=0}^{\infty} A_n \zeta^n, \tag{11}$$

[5] The periodicity of the azimuthal coordinates of the circular and elliptical cylinder is absent in the case of the parabolic cylinder, and b is not limited in this fashion.

whose coefficients satisfy the recursion formula

$$A_n = \frac{-1}{n(n-1)}(A_{n-4} + aA_{n-2}). \tag{12}$$

The two independent, even and odd solutions of (9) are defined by

$$_eU_a(0) = 1, \quad _eU_a'(0) = 0, \tag{13}$$

$$_oU_a(0) = 0, \quad _oU_a'(0) = 1. \tag{14}$$

These definitions are quite arbitrary and are taken only for the sake of convenience since with exception of the special case when $a = 0$ we have not found simple expressions for the norms of $_eU_a(\zeta)$ and $_oU_a(\zeta)$.

Since the recursion formula (12) contains three successive coefficients, the coefficients for large values of n cannot be easily calculated. The first few terms are

$$_eU_a(\zeta) = 1 - \left(\frac{a}{2!}\right)\zeta^2 + \left(\frac{a^2-2}{4!}\right)\zeta^4 - \left(\frac{a^3-14a}{6!}\right)\zeta^6 + \left(\frac{a^4-44a^2+60}{8!}\right)\zeta^8 \cdots, \tag{15}$$

$$_oU_a(\zeta) = \zeta - \left(\frac{a}{3!}\right)\zeta^3 + \left(\frac{a^2-6}{5!}\right)\zeta^5 - \left(\frac{a^3-26a}{7!}\right)\zeta^7 + \left(\frac{a^4-68a^2+252}{9!}\right)\zeta^9 \cdots. \tag{16}$$

Examination of Eq. (9) when $a = 0$ shows that for this particular value of a the even and odd functions may be represented in terms of the quarter order Bessel functions. If the constants of these solutions be adjusted so that they satisfy the restrictions of (13) and (14) we find:

$$_eU_0(\zeta) = 2^{-1/2}\Gamma(3/4)\zeta^{1/2}J_{-1/4}(\zeta^2/2) \tag{17}$$

$$_oU_0(\zeta) = 2^{1/2}\Gamma(5/4)\zeta^{1/2}J_{1/4}(\zeta^2/2). \tag{18}$$

Since tables[6] of the quarter order Bessel functions are available, the zero order (i.e., $a = 0$) parabolic cylinder functions may be calculated without difficulty over a limited range on ζ.

5. Relation of $U_a(\zeta)$ functions to the confluent hypergeometric functions. As an alternative to the direct calculation of coefficients in the power series (15) and (16) we shall consider the representation of the parabolic cylinder functions in terms of the confluent hypergeometric functions. If we make the substitutions

$$U_a(\zeta) = e^{-i\zeta^2/2}f(\zeta), \tag{19}$$

$$t = i\zeta^2, \tag{20}$$

[6] E. Jahnke and F. Emde, *Tables of Functions* (G. E. Steckert 1938) 3rd ed., p. 164.

then $f(t)$ must satisfy

$$t\frac{d^2f}{dt^2}+\left(\frac{1}{2}-t\right)\frac{df}{dt}-\left(\frac{1+ia}{4}\right)f=0. \tag{21}$$

This is a special case of Kummer's[7] first form of the confluent hypergeometric equation. The solutions are given in Kummer's notation as:

$$f_1={}_1F_1(\alpha;c;t), \tag{22}$$

$$f_2=t^{1-c}{}_1F_1(\alpha-c+1;2-c;t), \tag{23}$$

where

$$\alpha=\frac{1+ia}{4},\qquad c=\frac{1}{2}.$$

In terms of these functions[8] the solutions of (9) are

$$U_a^1(\zeta)=e^{-i\zeta^2/2}f_1(i\zeta^2)=e^{-i\zeta^2/2}{}_1F_1\left(\frac{1+ia}{4};\frac{1}{2};i\zeta^2\right), \tag{24}$$

$$U_a^2(\zeta)=(B)e^{-i\zeta^2/2}f_2(i\zeta^2)=(B)(i\zeta^2)^{1/2}e^{-i\zeta^2/2}{}_1F_1\left(\frac{3+ia}{4};\frac{3}{2};i\zeta^2\right). \tag{25}$$

We shall write (24) and (25) as power series in $t=i\zeta^2$ and then making use of the product formula for the Gamma functions separate them into real and imaginary parts. From this we shall be able to deduce the result that the imaginary parts of (24) and (25) are identically zero if $B=i^{-1/2}$.

The power series representations of the confluent hypergeometric functions are given by

$${}_1F_1\left(\frac{1+ia}{4};\frac{1}{2};t\right)=\frac{\Gamma\left(\frac{1}{2}\right)}{\Gamma\left(\frac{1+ia}{4}\right)}\sum_{n=0}^{\infty}\frac{\Gamma\left(n+\frac{1+ia}{4}\right)}{\Gamma\left(n+\frac{1}{2}\right)\Gamma(n+1)}t^n, \tag{26}$$

$${}_1F_1\left(\frac{3+ia}{4};\frac{3}{2};t\right)=\frac{\Gamma\left(\frac{3}{2}\right)}{\Gamma\left(\frac{3+ia}{4}\right)}\sum_{n=0}^{\infty}\frac{\Gamma\left(n+\frac{3+ia}{4}\right)}{\Gamma\left(n+\frac{3}{2}\right)\Gamma(n+1)}t^n. \tag{27}$$

[7] E. G. C. Poole, *Introduction to the Theory of Linear Differential Equations* (Oxford, Clarendon Press, 1936) p. 139.

[8] Eqs. (24) and (25) may be written in terms of the $M_{k,m}(z)$ functions[9] of Whittaker and the $H(m,a,x)$ functions[10] defined by Lowan and Horenstein. Thus

$$U_a^1(\zeta)=(i\zeta)^{-1/2}M_{-ia/4,-1/4}(i\zeta^2)=H(-3/4,a/4,\zeta^2/2)$$

$$U_a^2(\zeta)=(B)(i\zeta)^{-1/2}M_{-ia/4,1/4}(i\zeta^2)=(B)H(-1/4,a/4,\zeta^2/2)$$

[9] Whittaker and Watson, p. 337–346.

[10] A. N. Lowan and W. Horenstein, *On the Function* $H(m,a,x)=\exp(-ix)F(m+1-ia;2m+2;2ix)$, Jour. of Math. and Physics, vol. 21, 1942.

These may be written as

$$ {}_1F_1\left(\frac{1+ia}{4};\frac{1}{2};t\right) = 1 + \sum_{n=1}^{\infty} \frac{\prod_{r=0}^{r=n-1}(1+4r+ia)}{\prod_{r=0}^{r=n-1}(1+2r)} \frac{t^n}{2^n n!}, \tag{28} $$

$$ {}_1F_1\left(\frac{3+ia}{4};\frac{3}{2};t\right) = 1 + \sum_{n=1}^{\infty} \frac{\prod_{r=0}^{r=n-1}(3+4r+ia)}{\prod_{r=0}^{r=n-1}(3+2r)} \frac{t^n}{2^n n!}. \tag{29} $$

If we make the substitutions

$$ B = i^{-1/2}, \qquad \theta_r = \tan^{-1}\left(\frac{a}{4r+1}\right), \qquad \theta'_r = \tan^{-1}\left(\frac{a}{4r+3}\right), \qquad t^n = \zeta^{2n} e^{in\pi/2} $$

$$ \varphi_n = \frac{n\pi}{2} + \sum_{r=0}^{r=n-1} \theta_r, \qquad \varphi'_n = \frac{n\pi}{2} + \sum_{r=0}^{r=n-1} \theta'_r, $$

$$ K_n = \frac{\prod_{r=0}^{r=n-1}[a^2+(4r+1)^2]^{1/2}}{\prod_{r=0}^{r=n-1}[1+2r]}, \qquad K'_n = \frac{\prod_{r=0}^{r=n-1}[a^2+(4r+3)^2]^{1/2}}{\prod_{r=0}^{r=n-1}[3+2r]} $$

we arrive at the following expressions

$$ \begin{aligned} U_a^1(\zeta) = {} & \cos\left(\frac{\zeta^2}{2}\right) + \sum_{n=1}^{\infty} K_n \cos\left(\frac{-\zeta^2}{2} + \varphi_n\right)\frac{\zeta^{2n}}{2^n n!} \\ & - i\left\{\sin\left(\frac{\zeta^2}{2}\right) - \sum_{n=1}^{\infty} K_n \sin\left(\frac{-\zeta^2}{2} + \varphi_n\right)\frac{\zeta^{2n}}{2^n n!}\right\}, \end{aligned} \tag{30} $$

$$ \begin{aligned} U_a^2(\zeta) = {} & \zeta\cos\left(\frac{\zeta^2}{2}\right) + \zeta\sum_{n=1}^{\infty} K'_n \cos\left(\frac{-\zeta^2}{2} + \varphi'_n\right)\frac{\zeta^{2n}}{2^n n!} \\ & - i\zeta\left\{\sin\left(\frac{\zeta^2}{2}\right) - \sum_{n=1}^{\infty} K'_n \cos\left(\frac{-\zeta^2}{2} + \varphi'_n\right)\frac{\zeta^{2n}}{2^n n!}\right\}. \end{aligned} \tag{31} $$

We can now show that the imaginary parts of (30) and (31) vanish identically. Let the imaginary part of $U_a^1(\zeta) = I_1[\zeta]$. From (30) and (31) we find $I_1[0] = 0$ and $I'_1[0] = 0$. Moreover since both the real and imaginary parts of $U_a^1(\zeta)$ must satisfy Eq. (9), it follows that $I''_1[0] = 0$, and hence all derivatives of all orders must vanish for $\zeta = 0$. Thus from the expansion of $I_1[\zeta]$ in a Taylor's series about the origin, it is seen that $I_1[\zeta] \equiv 0$. Similar statements apply to $I_2[\zeta]$, defined as the imaginary part of $U_a^2(\zeta)$. Thus we take as a set of solutions

$$ {}_aU_a(\zeta) = \text{Real}\,[U_a^1(\zeta)], \tag{32} $$

$$ {}_aU_a(\zeta) = \text{Real}\,[U_a^2(\zeta)], \tag{33} $$

or

$$ {}_eU_a(\zeta) = \cos\left(\frac{\zeta^2}{2}\right) + \sum_{n=1}^{\infty} K_n \cos\left(-\frac{\zeta^2}{2} + \varphi_n\right)\frac{\zeta^{2n}}{2^n n!}, \tag{34} $$

$$ {}_oU_a(\zeta) = \zeta \cos\left(\frac{\zeta^2}{2}\right) + \zeta \sum_{n=1}^{\infty} K'_n \cos\left(-\frac{\zeta^2}{2} + \varphi'_n\right)\frac{\zeta^{2n}}{2^n n!}. \tag{35} $$

Obviously these solutions satisfy the requirements (13) and (14) for $\zeta = 0$. When expanded they reduce to (15) and (16).

The fact that the imaginary parts of $U^1_a(\zeta)$ and $U^2_a(\zeta)$ vanish identically can be used to simplify (34) and (35). We have

$$ I_1[\zeta] = -\sin\left(\frac{\zeta^2}{2}\right) \mathrm{Re}\,\{{}_1F_1(\zeta)\} + \cos\left(\frac{\zeta^2}{2}\right) I\{{}_1F_1(\zeta)\} \equiv 0. \tag{36} $$

In this and that which follows ${}_1F_1(\zeta) \equiv {}_1F_1\left(\frac{1+ia}{4}; \frac{1}{2}; i\zeta^2\right)$. From (36)

$$ \tan\left(\frac{\zeta^2}{2}\right) = \frac{I\{{}_1F_1(\zeta)\}}{\mathrm{Re}\,\{{}_1F_1(\zeta)\}}, $$

and hence since

$$ {}_eU_a(\zeta) = \sin\left(\frac{\zeta^2}{2}\right) I\{{}_1F_1(\zeta)\} + \cos\left(\frac{\zeta^2}{2}\right) \mathrm{Re}\,\{{}_1F_1(\zeta)\} \tag{37} $$

we find

$$ {}_eU_a(\zeta) = \sec\left(\frac{\zeta^2}{2}\right) \mathrm{Re}\,\{{}_1F_1(\zeta)\} = \csc\left(\frac{\zeta^2}{2}\right) I\{{}_1F_1(\zeta)\}. \tag{38} $$

If we write

$$ \mathrm{Re}\,\{{}_1F_1(\zeta)\} = 1 + \sum_{n=1}^{\infty} K_n \cos(\varphi_n)\frac{\zeta^{2n}}{2^n n!}, \tag{39} $$

$$ I\{{}_1F_1(\zeta)\} = \sum_{n=1}^{\infty} K_n \sin(\varphi_n)\frac{\zeta^{2n}}{2^n n!}, \tag{40} $$

where K_n and φ_n are as previously defined, then Eq. (38) becomes

$$ \begin{aligned} {}_eU_a(\zeta) &= \sec\left(\frac{\zeta^2}{2}\right)\left(1 + \sum_{n=1}^{\infty} K_n \cos(\varphi_n)\frac{\zeta^{2n}}{2^n n!}\right) \\ &= \csc\left(\frac{\zeta^2}{2}\right)\left(\sum_{n=1}^{\infty} K_n \sin(\varphi_n)\frac{\zeta^{2n}}{2^n n!}\right). \end{aligned} \tag{41} $$

Similar considerations for ${}_oU_a(\zeta)$ lead to the result

$$ \begin{aligned} {}_oU_a(\zeta) &= \zeta \sec\left(\frac{\zeta^2}{2}\right)\left(1 + \sum_{n=1}^{\infty} K'_n \cos(\varphi'_n)\frac{\zeta^{2n}}{2^n n!}\right) \\ &= \zeta \csc\left(\frac{\zeta^2}{2}\right)\left(\sum_{n=1}^{\infty} K'_n \sin(\varphi'_n)\frac{\zeta^{2n}}{2^n n!}\right). \end{aligned} \tag{42} $$

These formulas for ${}_eU_a(\zeta)$ and ${}_oU_a(\zeta)$ lead to some results concerning the roots. For example, since the roots of ${}_eU_a(\zeta)$ are identical with the roots of ${}_1F_1(\zeta)$ these are simultaneous roots of Re $\{{}_1F_1(\zeta)\}$ and $I\{{}_1F_1(\zeta)\}$, and we see from (41) that all the roots of Re $\{{}_1F_1(\zeta)\}$ and $I\{{}_1F_1(\zeta)\}$ can be classified in two groups. First the roots of Re $\{{}_1F_1(\zeta)\}$ must contain the roots of ${}_1F_1(\zeta)$ and hence those of ${}_eU_a(\zeta)$, and second they must contain a set of roots which occur at points where $\sec\left(\frac{\zeta^2}{2}\right)$ becomes infinite and which are not roots of ${}_eU_a(\zeta)$. Similarly the roots of $I\{{}_1F_1(\zeta)\}$ contain the roots of ${}_eU_a(\zeta)$ and also a set of roots which occur where $\csc\left(\frac{\zeta^2}{2}\right)$ becomes infinite and which are not roots of ${}_eU_a(\zeta)$. Similar statements can be made for the roots of ${}_oU_a(\zeta)$ and the real and imaginary parts of ${}_1F_1\left(\frac{3+ia}{4}; \frac{3}{2}; i\zeta^2\right)$.

6. **Integral solutions.** Integral solutions of (9) were first obtained by Weber.[11] In our notation these are

$$ {}_eU_a(\zeta) = c_1 \int_0^1 s^{-3/4}(1-s)^{-3/4} \cos\left[\zeta^2\left(s-\frac{1}{2}\right) + \frac{a}{4}\log\frac{s}{1-s}\right] ds \quad (43) $$

$$ {}_oU_a(\zeta) = c_2 \int_0^1 s^{-1/4}(1-s)^{-1/4} \cos\left[\zeta^2\left(s-\frac{1}{2}\right) + \frac{a}{4}\log\frac{s}{1-s}\right] ds \quad (44) $$

where c_1 and c_2 are to be determined so that ${}_eU_a(0) = 1$ and ${}_oU_a'(0) = 1$. Making use of the transformations $s = \sin^2\left(\frac{\theta}{2}\right)$, and $\cos\theta = \tanh\varphi$, (43) and (44) may be written as

$$ {}_eU_a(\zeta) = 2^{1/2}c_1 \int_0^\infty (\operatorname{sech}\varphi)^{1/2} \cos\left[\frac{\zeta^2}{2}\tanh\varphi + \frac{a}{2}\varphi\right] d\varphi, \quad (45) $$

$$ {}_oU_a(\zeta) = 2^{-3/2}c_2 \int_0^\infty (\operatorname{sech}\varphi)^{3/2} \cos\left[\frac{\zeta^2}{2}\tanh\varphi + \frac{a}{2}\varphi\right] d\varphi. \quad (46) $$

These forms are analogous to the Parseval integrals for Bessel functions. The value of c_1 is given by

$$ 1 = 2^{1/2}c_1 \int_0^\infty (\operatorname{sech}\varphi)^{1/2} \cos\left(\frac{a}{2}\varphi\right) d\varphi, \quad (47) $$

and the value of c_2 by

$$ 1 = 2^{-3/2}c_2 \int_0^\infty (\operatorname{sech}\varphi)^{3/2} \cos\left(\frac{a}{2}\varphi\right) d\varphi. \quad (48) $$

The convergence of the integrals (45) and (46) can easily be established by well known methods.[12]

[11] H. Weber, *Die partiellen Differentialgleichungen der Math. Physik*, (Braunschweig 1912) 5th ed., Vol. 2, p. 258.

[12] See Townsend, Functions of Real Variables, (1928), p. 242.

Examination of Eq. (9) when $\zeta << a$ indicates that

$$ {}_eU_a(\zeta) \sim \cos(a^{1/2}\zeta), \tag{49} $$

$$ {}_oU_a(\zeta) \sim \frac{\sin(a^{1/2}\zeta)}{a^{1/2}}. \tag{50} $$

This leads to the considerations of solutions which are asymptotic in a and which are useful when ζ is not too much larger than a. Such solutions may be obtained by converting the differential equation (9) to an integral equation and then solving the integral equation by the method of successive substitutions.

Eq. (9) may be written

$$ \frac{d^2U_a(\zeta)}{d\zeta^2} + aU_a(\zeta) = f(\zeta) \tag{51} $$

where $f(\zeta) = \zeta^2 U_a(\zeta)$. The solution of the non-homogeneous Eq. (51) is the sum of the complementary function derived from the homogeneous equation plus a particular integral. Thus

$$ U_a(\zeta) = \frac{\sin(a^{1/2}\zeta)}{a^{1/2}} U_a'(0) + \cos(a^{1/2}\zeta) U_a(0) - \frac{1}{a^{1/2}} \int_0^\zeta \omega^2 \sin[a^{1/2}(\zeta - \omega)] U_a(\omega)\, d\omega. \tag{52} $$

One substitution yields

$$ {}_eU_a(\zeta) \sim \cos(a^{1/2}\zeta) - \frac{\zeta^3}{6a^{1/2}} \sin(a^{1/2}\zeta) - \frac{\zeta^2}{4a} \cos(a^{1/2}\zeta) + \frac{\zeta}{4a^{3/2}} \sin(a^{1/2}\zeta), \tag{53} $$

$$ {}_oU_a(\zeta) \sim \frac{\sin(a^{1/2}\zeta)}{a^{1/2}} + \frac{\zeta^3}{6a} \cos(a^{1/2}\zeta) - \frac{\zeta^2}{4a^{3/2}} \sin(a^{1/2}\zeta) - \frac{\zeta}{4a^2} \cos(a^{1/2}\zeta) + \frac{1}{4a^{5/2}} \sin(a^{1/2}\zeta). \tag{54} $$

7. Solutions asymptotic in ζ. For large values of ζ the labor involved in computing the functions by the power series (15) and (16) becomes excessive and the accuracy of the asymptotic series in a becomes poor. It therefore is desirable to obtain expansions asymptotic in ζ.

It has been shown previously that

$$ {}_eU_a(\zeta) = e^{-i\zeta^2/2} {}_1F_1\left(\frac{1+ia}{4}; \frac{1}{2}; i\zeta^2\right), \tag{55} $$

$$ {}_oU_a(\zeta) = i^{-1/2}(i\zeta^2)^{1/2} e^{-i\zeta^2/2} {}_1F_1\left(\frac{3+ia}{4}; \frac{1}{2}; i\zeta^2\right). \tag{56} $$

To obtain an asymptotic expression for ${}_oU_a(\zeta)$ and ${}_eU_a(\zeta)$ we insert the asymptotic expansion for the confluent hypergeometric function in (55) and (56). The asymptotic expansion of the confluent hypergeometric function[13] is

[13] Jahnke and Emde, p. 275.

$$ {}_1F_1(\alpha;\, c;\, t) \sim \Gamma(c)\left[\left\{\frac{(-t)^{-\alpha}}{\Gamma(c-\alpha)}\left(1+\sum_{n=1}^{\infty}\frac{\prod_{r=1}^{r=n}(\alpha+r-1)(\alpha+r-c)}{(-t)^n n!}\right)\right\}\right. $$

$$ \left.+\left\{\frac{e^t t^{\alpha-c}}{\Gamma(\alpha)}\left(1+\sum_{n=1}^{\infty}\frac{\prod_{r=1}^{r=n}(-\alpha+r)(-\alpha+r+c-1)}{(t)^n n!}\right)\right\}\right] \tag{57} $$

Inserting

$$ t = i\zeta^2, $$

$$ c = \frac{1}{2}, $$

$$ \alpha = \left(\frac{1+ia}{4}\right) $$

in (57) and making use of the relations

$$ \Gamma\left(\frac{1+ia}{4}\right) = \Gamma^*\left(\frac{1-ia}{4}\right), \tag{58} $$

$$ \Gamma\left(\frac{3+ia}{4}\right) = \Gamma^*\left(\frac{3-ia}{4}\right), \tag{59} $$

$$ \Gamma\left(\frac{1-ia}{4}\right) = \frac{2^{1/2}\pi}{\Gamma\left(\frac{3+ia}{4}\right)}\frac{1}{\cosh\frac{a\pi}{4} - i\sinh\frac{a\pi}{4}}, \tag{60} $$

we obtain from (56) and (57) after some simplification

$$ {}_1U_a(\zeta) \sim \frac{2\Gamma\left(\frac{1}{2}\right)e^{-\pi a/8}}{\left|\Gamma\left(\frac{1+ia}{4}\right)\right|}\left[\left\{\frac{\cos\left(\frac{\zeta^2}{2}+\frac{a}{2}\log\zeta-\left[\psi+\frac{\pi}{8}-\tan^{-1}\left(\tanh\frac{\pi a}{4}\right)\right]\right)}{\zeta^{1/2}}P(\zeta)\right\}\right. $$

$$ \left.+\left\{\frac{\sin\left(\frac{\zeta^2}{2}+\frac{a}{2}\log\zeta-\left[\psi+\frac{\pi}{8}-\tan^{-1}\left(\tanh\frac{\pi a}{4}\right)\right]\right)}{\zeta^{1/2}}Q(\zeta)\right\}\right], \tag{61} $$

$$ {}_1U_a(\zeta) \sim \frac{2\Gamma\left(\frac{3}{2}\right)e^{-\pi a/8}}{\left|\Gamma\left(\frac{3+ia}{4}\right)\right|}\left[\left\{\frac{\cos\left(\frac{\zeta^2}{2}+\frac{a}{2}\log\zeta-\left[\psi+\frac{3\pi}{8}\right]\right)}{\zeta^{1/2}}P(\zeta)\right\}\right. $$

$$ \left.+\left\{\frac{\sin\left(\frac{\zeta^2}{2}+\frac{a}{2}\log\zeta-\left[\psi+\frac{3\pi}{8}\right]\right)}{\zeta^{1/2}}Q(\zeta)\right\}\right] \tag{62} $$

TABLE I

Even Functions $_eU_a(\zeta)$

ζ	$a=1$	$a=2$	$a=3$	$a=-1$	$a=-2$	$a=-3$
0.00	1.0000	1.0000	1.0000	1.0000	1.0000	1.0000
0.10	.9950	.9901	.9850	1.0050	1.0100	1.0150
0.20	.9799	.9601	.9405	1.0199	1.0401	1.0605
0.30	.9547	.9107	.8674	1.0446	1.0907	1.1373
0.40	.9190	.8422	.7675	1.0789	1.1620	1.2474
0.50	.8727	.7556	.6435	1.1221	1.2548	1.3929
0.60	.8154	.6521	.4987	1.1738	1.3695	1.5767
0.70	.7471	.5331	.3371	1.2329	1.5066	1.8022
0.80	.6677	.4010	+.1639	1.2983	1.6665	2.0729
0.90	.5774	.2583	−.0153	1.3683	1.8489	2.3926
1.00	.4766	+.1084	−.1938	1.4409	2.0534	2.7646
1.10	.3663	−.0447	−.3645	1.5134	2.2782	3.1918
1.20	.2481	−.1963	−.5199	1.5827	2.5209	3.6760
1.30	+.1238	−.3411	−.6522	1.6450	2.7777	4.2173
1.40	−.0038	−.4733	−.7540	1.6959	3.0428	4.8136
1.50	−.1312	−.5867	−.8185	1.7305	3.3091	5.4597
1.60	−.2543	−.6752	−.8401	1.7434	3.5668	6.1463
1.70	−.3682	−.7330	−.8153	1.7292	3.8044	6.8595
1.80	−.4679	−.7551	−.7427	1.6823	4.0080	7.5797
1.90	−.5477	−.7378	−.6240	1.5978	4.1618	8.2812
2.00	−.6023	−.6793	−.4644	1.4717	4.2485	8.9316
2.10	−.6268	−.5802	−.2726	1.3017	4.2503	9.4923
2.20	−.6176	−.4443	−.0608	1.0875	4.1498	9.9187
2.30	−.5725	−.2782	+.1555	.8318	3.9318	10.1625
2.40	−.4917	−.0921	.3589	.5408	3.5849	10.1738
2.50	−.3778	+.1009	.5309	+.2244	3.1039	9.9048
2.60	−.2369	.2855	.6541	−.1035	2.4919	9.3150
2.70	−.0778	.4452	.7138	−.4252	1.7623	8.3765
2.80	+.0876	.5636	.7007	−.7200	.9405	7.0809
2.90	.2451	.6270	.6123	−.9656	+.0649	5.4451
3.00	.3796	.6256	.4548	−1.1398	−.8140	3.5178

where $\psi = arg\ \Gamma\left(\frac{3+ia}{4}\right)$, and

$$P(\zeta) = 1 - \frac{(4a)}{16\zeta^2} - \frac{(a^4 - 86a^2 + 105)}{16^2\zeta^4 2!} + \frac{(36a^5 - 3{,}480a^3 + 19{,}524a)}{16^3\zeta^6 3!} + \cdots \quad (63)$$

$$Q(\zeta) = -\frac{(a^2-3)}{16\zeta^2} + \frac{(16a^3 - 176a)}{16^2\zeta^4 2!} + \frac{(a^6 - 505a^4 + 12{,}139a^2 - 10{,}395)}{16^3\zeta^6 3!} + \cdots \quad (64)$$

TABLE II

Odd Functions ${}_0U_a(\zeta)$

ζ	$a=1$	$a=2$	$a=3$	$a=-1$	$a=-2$	$a=-3$
0.00	0.0000	0.0000	0.0000	0.0000	0.0000	0.0000
0.10	.0998	.0997	.0995	.1002	.1003	.1005
0.20	.1987	.1973	.1960	.2013	.2027	.2040
0.30	.2954	.2910	.2866	.3044	.3090	.3136
0.40	.3889	.3785	.3683	.4102	.4212	.4322
0.50	.4779	.4579	.4384	.5195	.5411	.5632
0.60	.5609	.5270	.4942	.6326	.6705	.7097
0.70	.6363	.5836	.5335	.7498	.8108	.8748
0.80	.7021	.6257	.5542	.8707	.9634	1.0620
0.90	.7565	.6513	.5548	.9947	1.1290	1.2742
1.00	.7971	.6587	.5343	1.1206	1.3080	1.5142
1.10	.8218	.6463	.4925	1.2463	1.5000	1.7845
1.20	.8283	.6132	.4301	1.3695	1.7038	2.0866
1.30	.8147	.5591	.3486	1.4865	1.9170	2.4211
1.40	.7792	.4844	.2509	1.5932	2.1360	2.7872
1.50	.7207	.3907	.1409	1.6845	2.3557	3.1821
1.60	.6389	.2805	+.0235	1.7547	2.5694	3.6006
1.70	.5344	.1575	−.0951	1.7976	2.7686	4.0347
1.80	.4092	+.0270	−.2081	1.8064	2.9430	4.4729
1.90	.2669	−.1049	−.3080	1.7749	3.0808	4.9001
2.00	+.1124	−.2308	−.3877	1.6971	3.1689	5.2970
2.10	−.0477	−.3428	−.4403	1.5686	3.1937	5.6406
2.20	−.2050	−.4330	−.4605	1.3869	3.1416	5.9045
2.30	−.3503	−.4936	−.4448	1.1521	3.0005	6.0597
2.40	−.4736	−.5184	−.3925	.8683	2.7611	6.0762
2.50	−.5649	−.5032	−.3061	.5436	2.4184	5.9254
2.60	−.6155	−.4469	−.1917	+.1907	1.9736	5.5826
2.70	−.6185	−.3517	−.0588	−.1728	1.4355	5.0308
2.80	−.5707	−.2242	+.0799	−.5252	.8224	4.2646
2.90	−.4729	−.0749	.2100	−.8415	+.1621	3.2935
3.00	−.3310	+.0819	.3161	−1.0956	−.5080	2.1460

TABLE III

Values of $\Gamma\left(\frac{3+ia}{4}\right) = \left|\Gamma\left(\frac{3+ia}{4}\right)\right| e^{i\psi}$

a	$\left\|\Gamma\left(\frac{3+ia}{4}\right)\right\|$	ψ
1	1.1353	−.2585
2	.8997	−.4528
3	.7110	−.6342
4	.5161	−.6474
5	.3728	−.6301

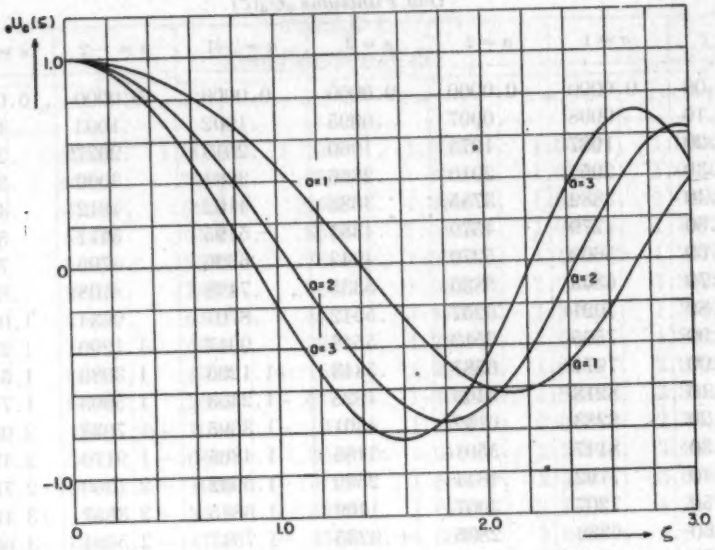
$U_0(\xi)$
1.0
0
-1.0
0
1.0
2.0
3.0
ξ
a=1
a=2
a=3
a=3
a=2
a=1

FIG. 1

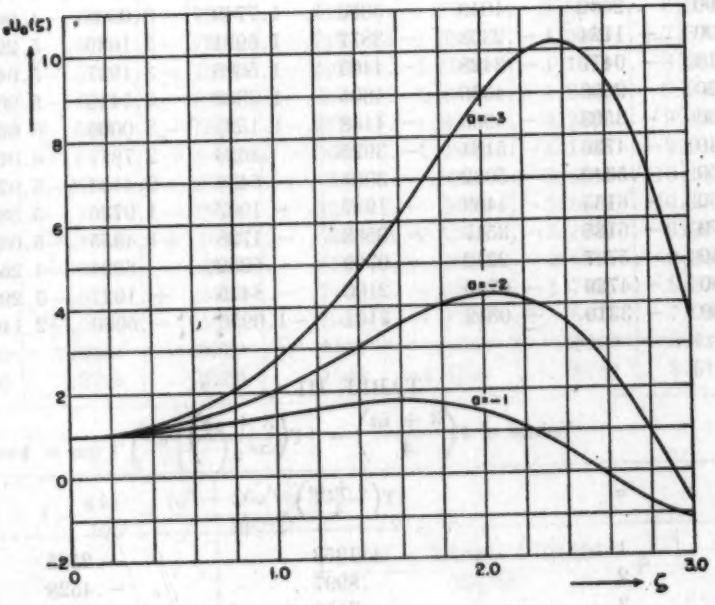
$U_0(\xi)$
10
8
6
4
2
0
-2
0
1.0
2.0
3.0
ξ
a=-3
a=-2
a=-1

FIG. 2

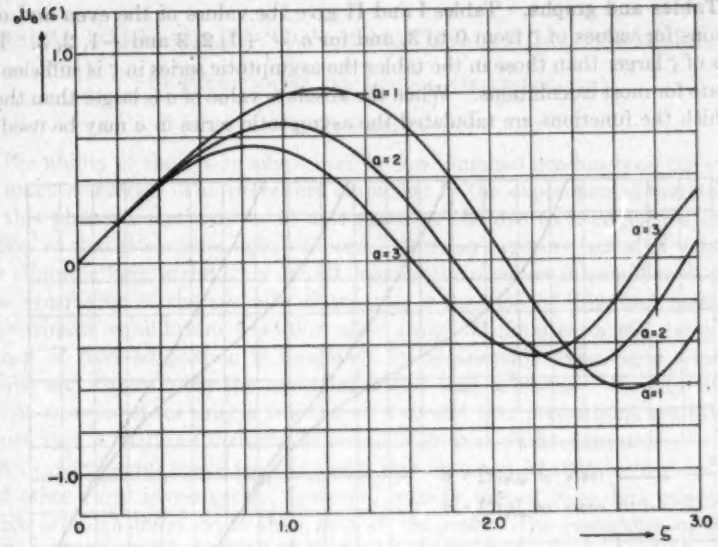
$_0U_0(\zeta)$
1.0
0
-1.0
a=1
a=2
a=3
a=3
a=2
a=1
0
1.0
2.0
3.0
ζ

FIG. 3

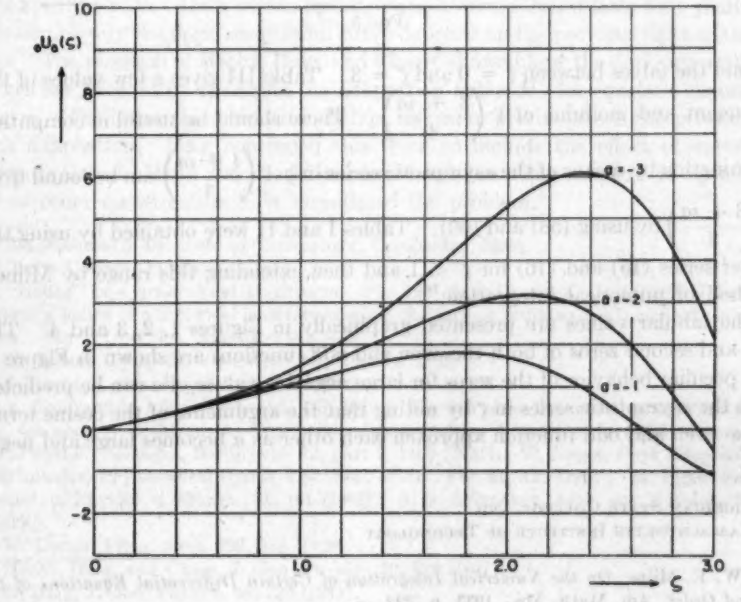
10
$_0U_0(\zeta)$
8
6
4
2
0
-2
a=-3
a=-2
a=-1
0
1.0
2.0
3.0
ζ

FIG. 4

8. **Tables and graphs.** Tables I and II give the values of the even and odd functions for values of ζ from 0 to 3, and for $a = +1, 2, 3$ and $-1, 2, 3$. For values of ζ larger than those in the tables the asymptotic series in ζ is sufficiently accurate for most calculations. When the absolute value of a is larger than those for which the functions are tabulated the asymptotic series in a may be used to

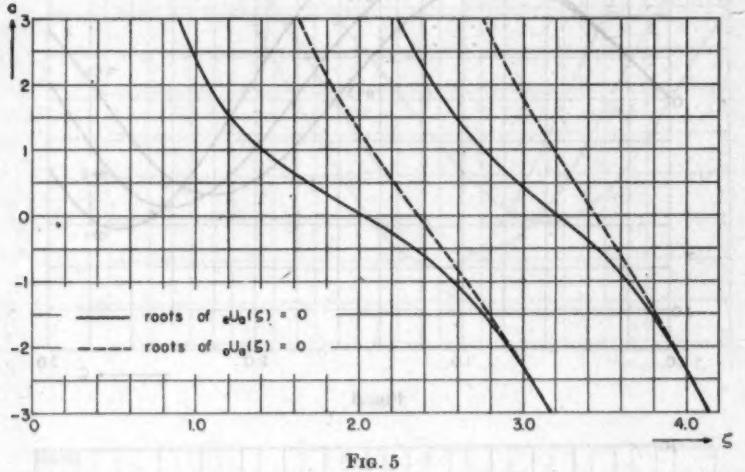

FIG. 5

extend the tables between $\zeta = 0$ and $\zeta = 3$. Table III gives a few values of the argument and modulus of $\Gamma\left(\frac{3+ia}{4}\right)$. These should be useful in computing the function by means of the asymptotic series in ζ. $\Gamma\left(\frac{1+ia}{4}\right)$ can be found from $\Gamma\left(\frac{3+ia}{4}\right)$ by using (58) and (60). Tables I and II were obtained by using the power series (15) and (16) for $\zeta < 1$ and then extending this range by Milne's method of numerical integration.[14]

The tabular values are presented graphically in Figures 1, 2, 3 and 4. The first and second zeros of both the even and odd functions are shown in Figure 5. The peculiar behavior of the zeros for large negative values of a can be predicted from the asymptotic series in ζ by noting that the arguments of the cosine terms of the even and odd function approach each other as a becomes large and negative.

MICHIGAN STATE COLLEGE AND
MASSACHUSETTS INSTITUTE OF TECHNOLOGY

[14] W. E. Milne, *On the Numerical Integration of Certain Differential Equations of the Second Order*, Am. Math. Mo., 1933, p. 322.

VISUAL DARK ADAPTATION: A MATHEMATICAL FORMULATION

By Parry Moon* and Domina Eberle Spencer†

1. Introduction

The ability of the eye to adapt itself to low illuminations has been the subject of much research. The procedure employed in the experimental investigation of this phenomenon consists in first exposing the eye to a large area of high helios[1] so that it becomes light-adapted. After an exposure period of τ seconds, the adapting light is suddenly cut off, leaving the observer in complete darkness. The sensitivity of the eye now changes as a function of time and reaches an approximate equilibrium condition after about 30 minutes in the dark. The course of dark-adaptation is measured by occasionally exposing a weak test source and determining the minimum helios that is visible. Usually the test source is exposed for only a fraction of a second and precautions are taken to insure that it shall not disturb the normal course of dark adaptation.

An experimental curve for rod vision was obtained in 1865 by Aubert[2]. He and other early investigators, however, entirely missed cone dark-adaptation, which is much more rapid than that of the rods. The researches of Hecht[3] (1921), Kohlrausch[4] (1922), and Dieter[5] (1929) have determined the dark-adaptation curve for the cones and have shown that its general shape is similar to that of the rods. Only within recent years, however, has it been fully realized how completely the dark-adaptation curve depends on the previous light adaptation. The research of Hecht, Haig, and Chase[6] showed how the dark-adaptation curves are affected by changing the adaptation helios H_A for constant exposure time τ. The lower the adaptation helios, the more precipitous is the process of dark adaptation. Haig continued this work to include the effect of variable exposure time.[7] Wald and Clark[8] employed an even wider range of τ. A number of other investigators have considered the problem.[9]

* Massachusetts Institute of Technology, Cambridge, Mass.

† Tufts College, Medford, Mass.

[1] "Helios" is a generalized brightness. For the special case of a perfectly diffusing surface, a helios of *one blondel* is obtained when the surface radiates one lumen per square meter. See J. Opt. Soc. Am. **32**, 348 (1942).

[2] H. Aubert, *Physiologie der Netzhaut*, Breslau, 1865.

[3] S. Hecht, J. Gen. Physiol., **4**, 113, (1921).

[4] A. Kohlrausch, Pflüg. Arch. 196, 113 (1922). For the older literature on dark adaptation, see also: A. Kohlrausch, *Tagessehen, Dämmersehen, Adaptation* in *Hdbk. d. nor. u. path. Physiol.*, Springer, Berlin, vol. 12, part 2, 1499 (1931). W. Nagel, *Dark Adaptation*, in Helmholtz, *Physiological Optics*, Opt. Soc. of Am. Vol. II, 320 (1924). H. Piper, Zs. f. Psychol. u. Physiol. d. Sinnes., **31**, 161 (1903). A. S. Achmatov, Arch. ges. Physiol., **215**, 10 (1926).

[5] W. Dieter, Pflüg. Arch. **222**, 381 (1929).

[6] Hecht, Haig, and Chase, J. Gen. Physiol. **20**, 831 (1937).

[7] C. Haig, J. Gen. Physiol. **24**, 735 (1941).

[8] G. Wald and A. B. Clark, J. Gen. Physiol. **21**, 93 (1937).

[9] Hecht, Haig, and Wald, J. Gen. Physiol. **19**, 321 (1935). H. K. Müller, Arch. Ophth. **125**, 624 (1931). D. E. Johannsen, J. Gen. Psychol. **10**, 4 (1934).

MATHEMATICS GRADUATE LIBRARY

Among the variables that affect the dark-adaptation curve may be mentioned the following:

1. The observer and his condition at the time of the test. Rather large variations are found from day to day in the same individual. Also the results are affected to a great extent by a deficiency in Vitamin A, as shown by recent investigations.[10]
2. Pupil size.
3. Size, helios, exposure time, and color of adapting field.
4. Size, flash time, color, and angle from the fovea of the test spot.

With so many independent variables, it becomes difficult, if not impossible, to adequately cover the entire range of all the variables by experimental means. And if such voluminous data were available, there would still remain the problem of so presenting them that they could be used in practice. Indeed, even the rather modest data now available require the use of several families of curves, with interpolation and extrapolation when numerical predictions are to be made regarding dark adaptation. For this reason, it seems fruitful to postulate a simplified behavior of the retina and to build a mathematical formulation on this basis. Such a formulation will allow the calculation of dark adaptation over a wide range of variables, by employing a mathematical equation instead of a multiplicity of curve sheets.

Developments of dark-adaptation theory on such a basis have been made by Pütter,[11] Lasareff,[12] and particularly by Hecht.[13] The initial phenomenon in vision is assumed to be photochemical, and a differential equation is written to express the behavior of the retina. Quite rightly, the unknown and highly complex phenomena of vision have been over-simplified, in accordance with the dictum of William of Occam (1300–1349): *Essentia non sunt multiplicanda praeter necessitatem.*

Crozier[14] objects to this method on the ground that the fortuitous agreement of an equation with an experimental curve does not mean that the true phenomena are identical with the postulated ones. Our attitude, however, is pragmatic: we look for equations that express the experimental results to within the limits of experimental error. In obtaining these equations, we find it convenient to postulate certain processes occurring in the retina. The postulates are justified if the resulting equations are useful in the quantitative prediction of dark-adaptation, regardless of whether they represent the "real" phenomena of vision.

Previous dark-adaptation theory, however, was so simplified that it was incapable of representing the more recent experimental findings. This weakness was pointed out, for example, by Winsor and Clark.[15] The purpose of the present paper is to so extend Hecht's equations that they become capable of handling all conditions of dark adaptation and light adaptation. In making

[10] Haig, Hecht, and Patek, Science **87**, 534 (1938).
[11] A. Pütter, Arch. ges. Physiol. **171**, 201 (1918).
[12] P. Lasareff, Pflüg. Arch. **213**, 256 (1926).
[13] S. Hecht, J. Gen. Physiol. **18**, 767 (1935).
[14] W. J. Crozier and A. H. Holway, J. Gen. Physiol. **23**, 101 (1939).
[15] C. P. Winsor and A. B. Clark, Proc. Nat. Acad. Sc., **22**, 400 (1936).

this extension, we find it necessary to introduce a number of quite arbitrary equations which have no theoretical basis. This is unfortunate, in as much as it leaves the century-old problem of visual theory still unsolved. But, as stated above, our aim has been to obtain equations that allow the calculation of adaptation curves for engineering purposes. This aim is realized in the following pages.

2. The Hecht Theory

The rods of the dark-adapted retinas of most vertebrates contain a rose-colored substance which is bleached by the action of light and which is called *rhodopsin*. It is a protein and is related to Vitamin A. Bleaching of rhodopsin yields a yellow substance called *retinene*. A similar photochemical reaction is supposed to occur in the cones of the retina, and the unbleached substance in this case has been named *iodopsin*.[16] Further details on the chemistry of the retina are not pertinent to the present investigation. In fact, the mathematics of dark adaptation can be stated without any reference to what substances are being considered. We have found it convenient, however, to talk about rhodopsin and retinene and we shall use these names in the development of the mathematical formulation, though the form of the equations will be the same for cone vision.

Consider a single rod containing a certain number of molecules of rhodopsin. If the rod is completely dark-adapted, the number of molecules of rhodopsin (expressed as a fraction of the maximum possible number) is 1.00, and the number of molecules of retinene is assumed to be zero. Under the action of light, the concentration of retinene rises to some value x while the concentration of rhodopsin changes to $(1 - x)$. As Wald and others have shown,[16] the reactions involve other materials and are really much more complex than the simplified two-substance formulation that will be developed in this paper.

Hecht[17] assumes two equations, the first representing the velocity of the photochemical reaction and the second representing the velocity of a chemical reaction that tends to renew the rhodopsin. The two reaction velocities are

$$\left(\frac{dx}{dt}\right)_1 = k_1 H(1 - x) \tag{1}$$

$$\left(\frac{dx}{dt}\right)_2 = -k_2 x^2 \tag{2}$$

where

x = number of molecules of retinene in one rod, expressed as a fraction of the maximum possible number associated with a rod;
H = helios (blondel) of the object which is imaged on the rod in question;
t = time (sec.);
k_1, k_2 = constants.

Equation (1) is the simplest possible expression for a photochemical reaction. Direct experimental evidence shows that the rate of bleaching of rhodopsin in solution is directly proportional to the amount of light.[16] This fact might be

[16] G. Wald, Biol. Symposia, 7, 43 (1942); *Medical Physics*, Otto Glasser, Editor, Chicago, 1658 (1944).

expected from the fact that, for a given spectral distribution and a given experimental set-up, the number of quanta is directly proportional to H. Thus Eq. (1) states that the reaction velocity is directly proportional to the number of quanta and directly proportional to the number of molecules of light-sensitive substance. Equation (2) represents a bimolecular reaction. The resulting velocity is the sum of Eqs. (1) and (2), or

$$\frac{dx}{dt} = k_1 H(1 - x) - k_2 x^2. \tag{3}$$

This is an ordinary differential equation of the first order, though unfortunately it is non-linear.

If light adaptation is accomplished by exposure to a field of helios H_A for such a long time that equilibrium is reached, $dx/dt = 0$ and the solution of Eq. (3) is

$$\frac{k_1}{k_2} H_A = \frac{x_0^2}{1 - x_0} \tag{4}$$

where x_0 is the value of x at the beginning of the dark-adaptation run. At $t = 0$, H is suddenly reduced to zero. The solution of Eq. (3) is then

$$x = \frac{1}{k_2 t + 1/x_0}. \tag{5}$$

How satisfactory it would be if the validity of Hecht's assumptions could be tested by comparing Eq. (5) with experimental results! The difficulty is that there are no experimental data on x: the state of the retina can be deduced only from indirect tests. Thus another assumption must be made; and if discrepancies are found between theory and experiment, one never knows whether the trouble lies in the additional assumption or in Eq. (3).

For his additional assumption applying to dark adaptation, Hecht takes

$$1 - x = \frac{k_3}{\log H_T}$$

or

$$\log (H_T/H_{T\infty}) = \frac{1}{1 - x} \tag{6}$$

where: H_T = helios threshold at time t after the adapting light is extinguished,
$H_{T\infty}$ = helios threshold for $t \to \infty$,
x = concentration of retinene at time t.

This equation states that the logarithm of the threshold helios H_T is inversely proportional to the concentration of rhodopsin. But in his study of minimum perceptible contrast,[17] Hecht discards Eq. (6) and assumes that the threshold is determined by the relation,

$$(dx/dt)_1 = c = \text{const.}$$

From Eq. (1) and the foregoing assumption,

[17] S. Hecht, *Handbook of General Experimental Psychology*, C. Murchison, Editor, Clark Univ. Press, Worcester, Mass. (1934), p. 704.

$$H_T/H_{T\infty} = \frac{1}{1-x} \tag{7}$$

where H_T is the difference in helios between the two half-fields and $H_{T\infty}$ is the value of H_T for $x = 0$. In the special case that one half-field is of zero helios, $H_T/H_{T\infty}$ has exactly the same significance as in Eq. (6). But the two equations are inconsistent. And neither one satisfies the more recent experimental results on dark adaptation.[15]

Thus it becomes desirable to search for modifications of Hecht's equations that will be in accord with dark-adaptation tests. The foregoing theory has the merit of utmost simplicity and it has been of unquestionable value, particularly in giving a qualitative picture of the visual process. Modified systems will almost inevitably become more complicated, the more closely they express the extremely complex phenomena of actual vision. But this is the price that one may expect to pay for numerical agreement of predicted and experimental thresholds.

3. Modified Equations

The first modification consists in the rejection of Eq. (6), which has been an important part of previous dark-adaptation theory. The problem is now to formulate a reasonable criterion for minimum perceptible helios H_T. Such a criterion can be based on the work of Hartline, Graham, and others,[16] who found that impulses traveling along a single optic nerve fiber are of constant amplitude but vary in frequency, depending on the state of adaptation and on the retinal illumination. As the helios of a test field is reduced, the frequency f of nerve impulses decreases until the observer is unable to distinguish between these impulses and those random physiological ones (the "*Eigenlicht*" of Helmholtz) not caused by light. This condition determines the threshold frequency f_T. *We assume that for a given number of excited rods, f_T is a constant.*

Next consider the production of these nerve impulses. Evidently, they are not caused by the mere *presence* of retinene (since the sensation ordinarily disappears when the light is cut off) but are closely related to the *rate of formation* of retinene, or $(dx/dt)_1$. Indeed we may think of the photochemical reaction as liberating electrons, each one of which initiates an impulse in the nerve fiber. On this basis, the oscillograms of Hartline and Graham[16] may be regarded as quantum counts. Each quantum that is absorbed by the receptor under test will dissociate one molecule of rhodopsin, liberate one electron, and produce one nerve impulse. This picture, is of course, pure hypothesis. It is offered as a mental "crutch" which may help in visualization but which is unessential to the acceptance of the equation. The postulated equation is

$$f = k_3(dx/dt)_1 \tag{8}$$

where f = frequency (pulses per sec.),
k_3 = constant.

[16] H. K. Hartline and C. H. Graham, J. Cell. and Comp. Physiol., **1**, 277 (1932). C. H. Graham, *Handbook of General Experimental Psychology*, C. Murchison, Editor, Clark Univ. Press, Worcester, Mass., (1934), p. 829.

The threshold helios is obtained by expressing $(dx/dt)_1$ in terms of H in the equation,

$$k_3(dx/dt)_1 = f_T = \text{const.} \tag{9}$$

Equation (8) will be used throughout this paper. The next step is to decide on the function $(dx/dt)_1$. It will now be shown that Eq. (1) does not give agreement with experimental data and that another equation must be employed.

Suppose that Eqs. (1) and (2) are accepted. Then the differential equation is

$$\frac{dx}{dt} = k_1 H(1 - x) - k_2 x^2 \tag{3}$$

and from Eq. (9),

$$f_T = k_1 k_3 H_T(1 - x) \tag{10}$$

or

$$H_T/H_{T\infty} = \frac{1}{1 - x} \tag{7}$$

where $H_{T\infty} = f_T/k_1k_3$.

The solution of Eq. (3) for dark adaptation is

$$x = \frac{1}{k_2 t + 1/x_0} \tag{5}$$

so Eq. (7) becomes

$$H_T/H_{T\infty} = \left[1 - \frac{1}{k_2 t + 1/x_0}\right]^{-1} = \frac{k_2 x_0 t + 1}{k_2 x_0 t + 1 - x_0}. \tag{11}$$

Equation (11) expresses the threshold helios as a function of time after the adapting light is extinguished. It can be compared directly with the results of dark-adaptation experiments.

Consider the slopes of experimental and theoretical curves. Probably the best way of plotting the data is with logarithmic scales along both axes, in which case it is convenient to write Eq. (11) in the form,

$$\log(H_T/H_{T\infty}) = \log (k_2 x_0 t + 1) - \log (k_2 x_0 t + 1 - x_0). \tag{11a}$$

Thus the slope of the curve of $\log (H_T/H_{T\infty})$ vs $\log t$ is

$$\frac{d[\log (H_T/H_{T\infty})]}{d[\log t]} = \frac{d[\log (H_T/H_{T\infty})]}{dt} \frac{dt}{d(\log t)} = -\frac{k_2 x_0 t}{(k_2 x_0 t + 1)(k_2 x_0 t + 1 - x_0)} \tag{12}$$

The maximum slope occurs when the second derivative is zero or when

$$k_2^2 x_0^2 t^2 - 1 + x_0 = 0.$$

Thus the time required to reach the point of maximum slope is

$$t = (1 - x_0)^{\frac{1}{2}}/k_2 x_0 \tag{13}$$

and the maximum slope is

$$\left[\frac{d(\log H_T)}{d(\log t)}\right]_{\max} = -\frac{x_0}{[(1-x_0)^{\frac{1}{2}}+1]^2}. \tag{14}$$

Evidently the maximum possible slope occurs when the eye is *completely* light adapted (a condition that is never obtained) and this slope is unity. Other calculated slopes are given in Table I. According to Eq. (14), the slope is independent of the constants f_∞, k_1 and k_2 and can never exceed 1.00. But *the experimentally determined slopes are between 2 and 7 as shown in Table II.* Thus we must conclude that the Hecht theory, as given in the preceding paragraphs, is untenable.

TABLE I

Calculated slopes of dark-adaptation curves according to the Hecht theory, eq. (16)

x_0	Max. slope
1.00	−1.000
0.50	−0.172
0.25	−0.072
0.10	−0.0262
0.01	−0.0083

TABLE II

Maximum slopes of a few typical dark-adaptation curves
($\log H_T$ vs. $\log t$)

Authority	Observer	Color of light	Max. slope
Kohlrausch[4]	1	Green	3.1
Kohlrausch[4]	1	Orange	2.7
Kohlrausch[4]	1	Red	2.4
Nagel	1	Inc.	4.0
Dieter[5]	Normal	Inc.	6.0
Piper	Englemann	Inc.	6.2
Piper	Schäfer	Inc.	3.7
Piper	Abelsdorff	Inc.	3.8
Piper	Demaria	Inc.	3.8
Piper	Nagel	Inc.	4.4
Piper	Piper	Inc.	4.4

Now consider the effect of changing to the more complicated differential equation suggested by Hecht:[13]

$$\frac{dx}{dt} = k_1 H(1-x)^p - k_2 x^q. \tag{15}$$

For dark adaptation, this equation reduces to

$$\frac{dx}{dt} = -k_2 x^q \tag{15a}$$

whose solution is

$$x = [x_0^{-(q-1)} + (q-1)k_2 t]^{-1/(q-1)}. \tag{16}$$

Equation (9) gives

$$H_T = \frac{f_T}{k_1 k_2 (1-x)^p}$$

or

$$\log (H_T/H_{T\infty}) = -p \log (1-x). \tag{17}$$

The slope of the curve of $\log (H_T/H_{T\infty})$ vs $\log t$ is obtained by differentiation:

$$\frac{d[\log (H_T/H_{T\infty})]}{d[\log t]} = -k_2 p t x^q/(1-x) \tag{18}$$

where $q = 1$ and where x is obtained from Eq. (16).

Conditions for maximum slope of the curve are obtained by differentiating Eq. (18) with respect to t and equating to zero. Then

$$\frac{d}{dt}\left(-k_2 pt \frac{x^q}{1-x}\right) = -k_2 p \left[\frac{x^q}{1-x} + t\frac{dx}{dt}\frac{d}{dx}\left(\frac{x^q}{1-x}\right)\right]$$

$$= -\frac{k_2 p x^q}{(1-x)^2}[(1-x) - k_2 tqx^{q-1} + k_2 t(q-1)x^q] = 0.$$

Thus the condition for maximum slope is

$$k_2 t(q-1)x^q - k_2 tqx^{q-1} + (1-x) = 0. \tag{19}$$

In the previous case ($p = 1$, $q = 2$) the maximum slope was obtained at $x_0 \to 1$ and $t \to 0$. We now prove that this same condition satisfies Eq. (19) in the general case. If $x_0 = 1$ and with small values of t,

$$x = [1 + (q-1)k_2 t]^{-(1/q-1)} \cong 1 - k_2 t. \tag{20}$$

Substitution in Eq. (19) gives

$$(q-1)(1 - qk_2 t) - q[1 - (q-1)k_2 t] + 1$$

which is identically zero. Thus a maximum slope is obtained as $t \to 0$ when the photochemical decomposition products approach saturation. There remains the problem of finding the value of this maximum slope. Substitution of Eq. (20) in Eq. (18) gives

$$\text{Slope} = -k_2 pt \frac{1 - k_2 qt}{k_2 t} \cong -p. \tag{21}$$

Thus the maximum slope of the dark-adaptation curves, according to the more complicated differential equation, is *independent of q and equal in magnitude to*

the exponent p. For the moderate concentrations x_0 obtained in practice, the slopes would be lower. Thus to obtain the slopes of 6 or more found experimentally, we would have to employ a very high value of p in Eq. (15).

A simpler and more satisfactory procedure is to use a different type of expression for $(dx/dt)_1$. Equation (1) represents the simplest possible photochemical reaction. Experiment shows, however, that even with simple compounds tested in the laboratory, this equation does not ordinarily hold, and it could hardly be expected to apply with the complex conditions that undoubtedly obtain in the retina. At very low values of x, a simple linear equation similar to Eq. (1) may be applicable:

$$\left(\frac{dx}{dt}\right)_1 = k_1 H(1 - ax). \tag{22}$$

If x becomes larger, an approximation can be obtained by adding higher-power terms. But Eq. (22) represents the first two terms of the power series representing an exponential, so suppose the function

$$1 - ax + \frac{(ax)^2}{2!} - \frac{(ax)^3}{3!} + \cdots = e^{-ax}$$

is used instead of $(1 - ax)$. A unique endpoint must be fixed; for when $x = 1$, $(dx/dt)_1 = 0$. Thus we take

$$\left(\frac{dx}{dt}\right)_1 = k_1 H(e^{-ax} - e^{-a}). \tag{23}$$

The justification for this expression must rest upon its ability to satisfy the experimental results. It is not an unreasonable form of equation, however. The helios H enters in the first power, in accordance with the Einstein photochemical equivalence principle. Apparently the initial photochemical reaction acts as a trigger which sets off other chemical reactions, one of the final products of which is instrumental in exciting the nerve endings. As Griffith and McKeown[19] state, "we must recognize that each photochemical reaction involves a primary process whose velocity is determined by the rate of energy absorption, and that *this is followed by two or more consecutive dark reactions involving activated molecules or atoms.*" In the specific case of rhodopsin, Wald says (Biol. Symposia, **7**, 47, 1942), "A study of bleaching in solution has shown that only the first step in even this process is photochemical. All the remainder of the cycle consists of ordinary thermal reactions."

Hecht found that the second power of x in Eq. (2) was slightly better than the first power. But this conclusion was obtained when using Eq. (1) and no longer holds when Eq. (23) is employed. It is simpler to replace Eq. (2) by

$$\left(\frac{dx}{dt}\right)_2 = -k_2 x. \tag{24}$$

[19] Griffith and McKeown, *Photo-processes in Gaseous and Liquid Systems.* Longmans, Green and Co., London, (1929), p. 406.

The differential equation then becomes

$$\frac{dx}{dt} = k_1 H(e^{-ax} - e^{-a}) - k_2 x. \tag{25}$$

Except for the unusual condition that $x > 0.90$, the second term is negligible and

$$\frac{dx}{dt} = k_1 H e^{-ax} - k_2 x. \tag{25a}$$

Equation (8) continues to apply so

$$f_T = k_3 \left(\frac{dx}{dt}\right)_1 \cong k_1 k_3 H_T e^{-ax}$$

or

$$H_T/H_{T\infty} = e^{ax}. \tag{26}$$

For dark adaptation, the differential equation yields the new and very simple solution,

$$x = x_0 e^{-k_2 t}. \tag{27}$$

The slope of the curve of log $(H_T/H_{T\infty})$ vs log t is

$$\frac{d[\log (H_T/H_{T\infty})]}{d[\log t]} = -0.4343\, ak_2 x_0 te^{-k_2 t}.$$

The maximum slope occurs at $t = 1/k_2$ and has the value,

$$\text{Max. slope} = -0.16\,(ax_0).$$

Thus by the use of a sufficiently large value of a, the new equations can fit all the data given in Table II.

4. Experimental Results

We now compare the theoretical predictions with the latest experimental results. Substitution of Eq. (27) in Eq. (26) gives

$$H_T/H_{T\infty} = e^{ax_0 e^{-k_2 t}} \tag{28}$$

or

$$ln\, ln(H_T/H_{T\infty}) = ln(ax_0) - k_2 t. \tag{28a}$$

This means that *a plot of ln ln $(H_T/H_{T\infty})$ against t should be a straight line.* Experimental data of Wald and Clark[8] are plotted in Fig. 1 and are seen to be in good agreement with the prediction of the new theory.

One of the most precise determinations of a dark-adaptation curve was obtained by Wolf and Zerrahn-Wolf[19] for the honey bee. Since the initial phenomenon in vision is photochemical in the bee as well as in human beings, the equations should apply also in this case. The 311 experimental points shown in Fig. 1 of the Wolf paper[20] are in excellent agreement. We have reproduced

[20] E. Wolf and G. Zerrahn-Wolf, J. Gen. Physiol. **19**, 229 (1935).

in Fig. 2 only a few points which represent the curve that Wolf drew to represent the data. The agreement with a straight line is close.[21] The black dots represent experimental data for a human observer, these data being again satisfied by a straight line in accordance with Eq. (28a). The surprising feature is that the two curves have exactly the same slope, which is nearly equal to the slope of the curve in Fig. 1.

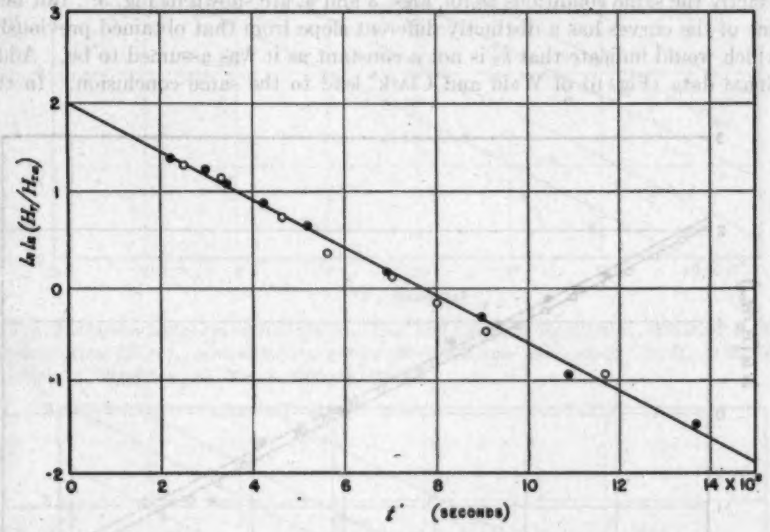

FIG. 1. Dark-adaptation data of Wald and Clark[2]. Rod vision. Natural pupil. Observer A-B. C., left eye, light adapted to $H_A = 3330$ blondels; ○, 600 sec. exposure time, ●, 1200 sec. exposure time.

In this and succeeding figures, the time scale runs to only 1500 sec., though experimental data are available somewhat beyond this limit. The use of $\ln \ln (H_T/H_{T_\infty})$ as ordinate exaggerates the experimental error as the threshold approaches its final value. Thus the data beyond 1500 sec. are of no value in determining the slope of the curve. It should be emphasized, however, that when the constants are determined in this way and the curves are plotted by use of Eq. (28), the graphs fit the experimental data within the limits of experimental error, *for all values of time*.

Figures 3 and 4 show similar results obtained by Hecht, Haig, and Chase.[6] The lines are all parallel and have the slope 2.54×10^{-3} as in Fig. 2. The different curves are for various values of adaptation helios H_A but are all for the same exposure time τ. Note that as the helios increases, the curve shifts upward. From Eq. (28), the value at $t = 0$ represents $\ln(ax_0)$, so an increase in

[21] In Reference 20, p. 236, the statement is made that the curve is "quite accurately rectilinear when log log (I_i/I_f) is plotted as a function of time in the dark." But no attempt seems to have been made to apply this method of plotting to other dark-adaptation data or to obtain a theoretical justification for it.

H_A increases the initial concentration, as would be expected. The slope of the curve, according to Eq. (28), evaluates[22] k_2, so

$$k_2 = 2.54 \times 10^{-3}.$$

It might seem that the phenomena of dark adaptation are adequately represented by Eqs. (23) and (24). An examination of further data, however, shows this belief to be too optimistic. Data for another observer,[6] working under exactly the same conditions as for Figs. 3 and 4, are shown in Fig. 5. But here one of the curves has a distinctly different slope from that obtained previously, which would indicate that k_2 is not a constant as it was assumed to be. Additional data (Fig. 6) of Wald and Clark[8] lead to the same conclusion. In the

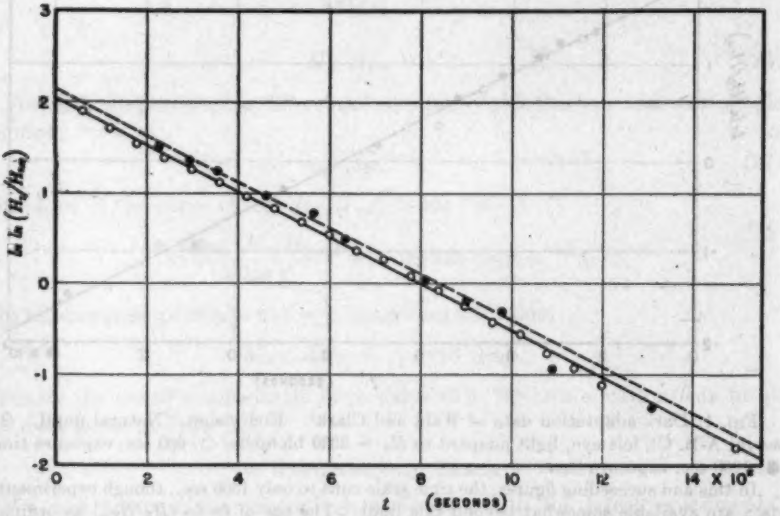

FIG. 2. Dark adaptation-curve for the honey bee. Data of Wolf and Zerrahn-Wolf. ○—○, honey bee[20] ●– –● human observer. Data of Hecht, Haig, and Chase,[6] S. H. with $H = 3800$, $\tau = 120$ sec,, rod vision.

upper curve, light adaptation was effected by exposure to a photoflash lamp (approximately $\frac{1}{25}$ sec. exposure) while the lower curve is obtained with 10 sec. exposure to a lower helios. The former has the slope of 2.58×10^{-3} but the latter has a slope of 3.70×10^{-3}.

Another investigation which shows a marked change of slope is that of Haig.[7] Fig. 7 indicates the results. Similar data of Wald and Clark[8] are presented in Fig. 8. In both cases, a decrease in helios causes an increase in slope. All the data indicate that with high helios and long exposures, the curve of $ln\ ln\ (H_T/$

[22] Further work shows that this value must be modified. See Section 7 and Table IX.

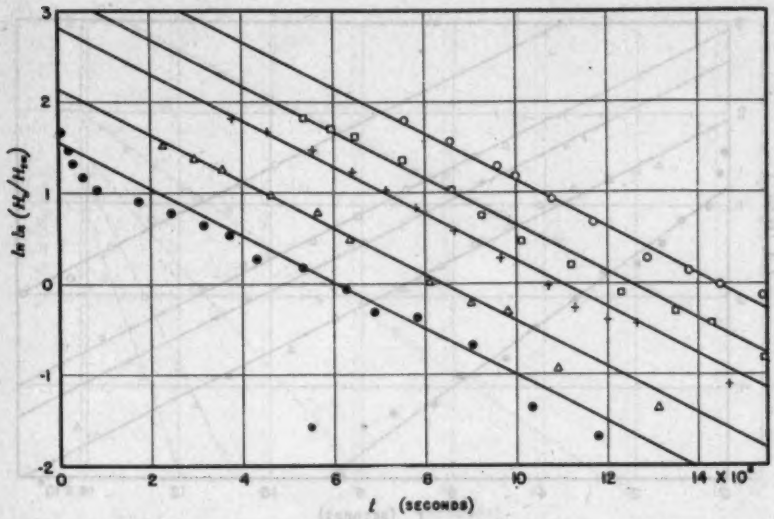

FIG. 3. Dark-adaptation data of Hecht, Haig, and Chase.[8] Rod vision, observer S. H., exposure time 120 sec., optical system giving effect of 2 mm. fixed pupil. ○, H_A = 400,000 blondel; □, 38,900; +, 19,500; △, 3800; ●, 263.

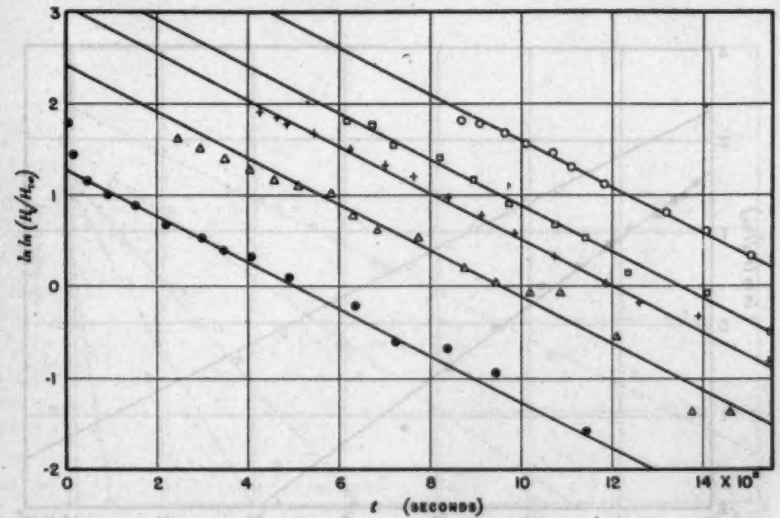

FIG. 4. Dark adaptation. Plotted from data of Hecht, Haig, and Chase.[8] Observer A. M. C., conditions same as in Fig. 3.

$H_{T\infty}$) vs t has a slope of approximately 2.54 × 10^{-3}; while at lower exposures, the slope becomes progressively greater as the exposure becomes less.

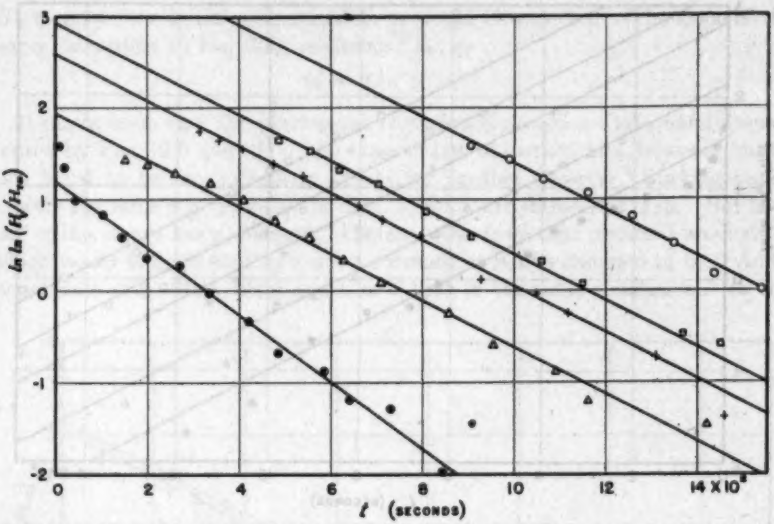

FIG. 5. Dark adaptation. Plotted from data of Hecht, Haig, and Chase.[4] Observer C. H. Conditions same as in Fig. 3.

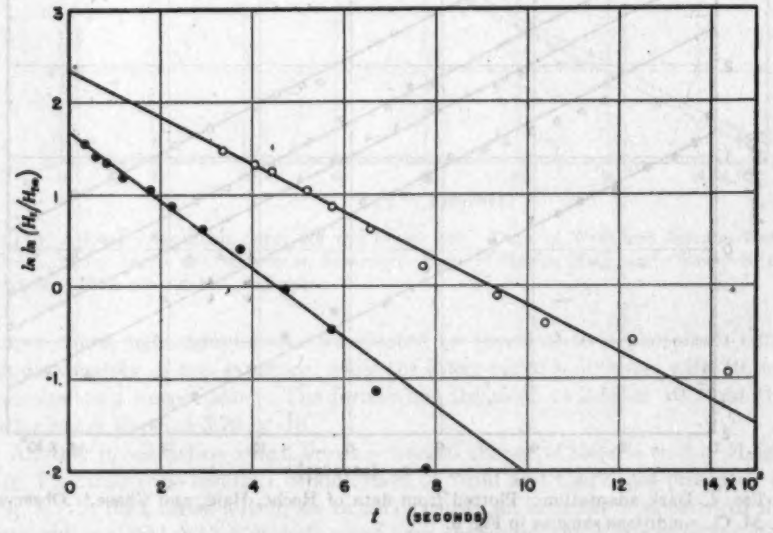

FIG. 6. Dark adaptation. Plotted from data of Wald and Clark.[6] Rod vision, observer A-B. C., natural pupil. ○, photoflash lamp, $\tau = 0.04$ sec.; ●, $H_A = 18{,}900$, $\tau = 10$ sec.

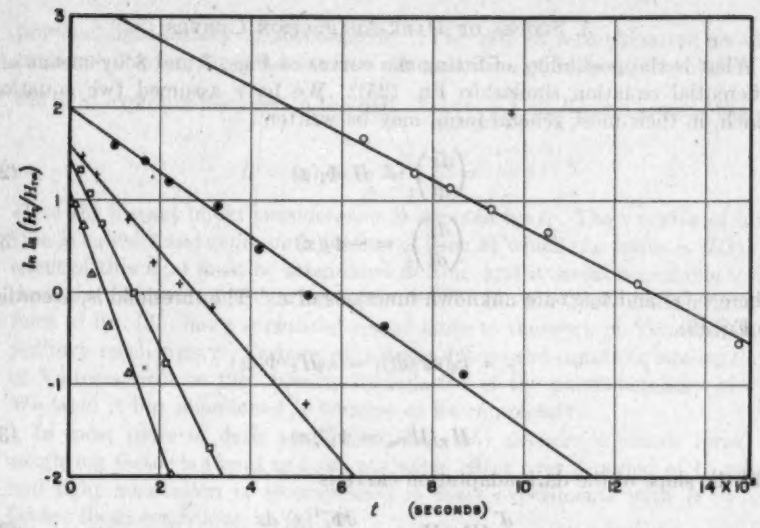

FIG. 7. Change of slope caused by altering the helios employed in light adaptation. Data of Haig.[7] Rod vision, observer E. M. H., exposure time 240 sec., 2 mm. fixed pupil. ○, H_A = 47,000 blondels; ●, 4470; +, 440; □, 200; △, 40.

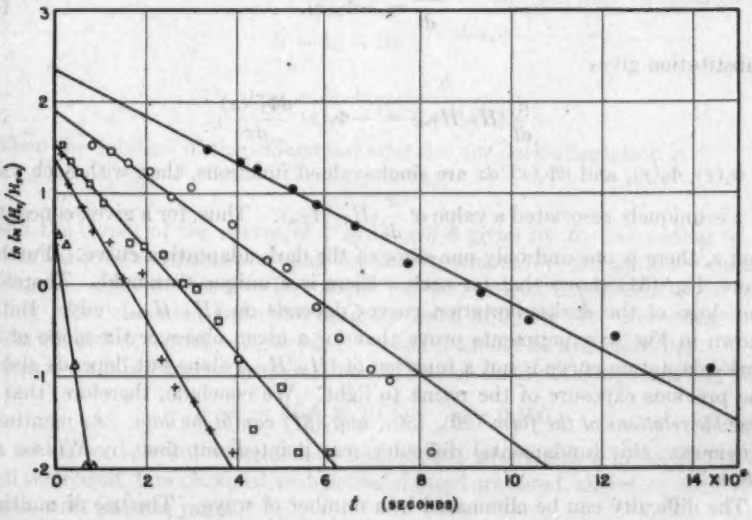

FIG. 8. Change of slope caused by change in light adaptation. Data of Wald and Clark.[8] Rod vision, observer A-B. C., natural pupil. ●, photoflash; ○, H = 18900, τ = 5 sec.; □, H = 7500, τ = 5; +, H = 2450, τ = 5; △, H = 36, τ = 5.

5. Slopes of Dark-Adaptation Curves

What is the possibility of fitting the curves of Figs. 7 and 8 by means of a differential equation similar to Eq. (25)? We have assumed two equations which, in their most general form, may be written

$$\left(\frac{dx}{dt}\right)_1 = H \cdot \Phi_1(x) \tag{29}$$

$$\left(\frac{dx}{dt}\right)_2 = -\Phi_2(x) \tag{30}$$

where $\Phi_1(x)$ and $\Phi_2(x)$ are unknown functions of x. The threshold is, according to Eq. (9),

$$f_T = k_3(dx/dt)_1 = k_3 H_T \cdot \Phi_1(x)$$

or

$$H_T/H_{T\infty} = \Phi_1^{-1}(x) \tag{31}$$

and the slope of the dark-adaptation curve is

$$\frac{d}{dt}(H_T/H_{T\infty}) = \frac{d\Phi_1^{-1}(x)}{dx}\frac{dx}{dt}. \tag{32}$$

But for dark adaptation, $H = 0$ and

$$\frac{dx}{dt} = -\Phi_2(x). \tag{33}$$

Substitution gives

$$\frac{d}{dt}(H_T/H_{T\infty}) = -\Phi_2(x)\frac{d\Phi_1^{-1}(x)}{dx}. \tag{34}$$

If $\Phi_1(x)$, $\Phi_2(x)$, and $d\Phi_1(x)/dx$ are single-valued functions, then with each value of x is uniquely associated a value of $\frac{d}{dt}(H_T/H_{T\infty})$. Thus, for a given concentration x, there is one and only one slope of the dark-adaptation curve. Furthermore, Eq. (31) shows that for each x there is a unique threshold. Therefore, the slope of the dark-adaptation curves depends on $(H_T/H_{T\infty})$ only. But as shown in Fig. 9, experiments prove that for a given observer the slope of the dark-adaptation curve is not a function of $(H_T/H_{T\infty})$ alone but depends also on the previous exposure of the retina to light. We conclude, therefore, that *no possible relations of the form (29), (30), and (31) can fit the data.* As mentioned previously, this fundamental difficulty was pointed out first by Winsor and Clark.[15]

The difficulty can be eliminated in a number of ways. The use of multiple-valued functions does not seem at all promising, which leaves the possibility of changing one or all of the fundamental equations (29), (30), and (31). Both (29) and (31) appear to be very satisfactory in their present form. A change is therefore made in the expression for $(dx/dt)_2$, which now takes into account the

previous light-history of the observer. The rate of recombination should depend not only on the instantaneous concentration of retinene but also on what the light exposure has been in the past. Let $\left(\frac{dx}{dt}\right)_2 = Bx$ and assume that

$$B = k_2 + Ae^{-c\int_{-\infty}^{t} \frac{ak_1 H(s)e^{-b(t-s)}}{1+ak_1 H(s)\cdot s}\,ds}. \tag{35}$$

Here the instant under consideration is denoted by t. The variable of integration is called s and represents a value of time at which the helios is $H(s)$. The effect of this $H(s)$ must be attenuated in time, and it seems reasonable to introduce the exponential weighting factor $e^{-b(t-s)}$ to effect this attenuation. The form of Eq. (35) has a superficial resemblance to the work of Volterra[23] in "hereditary mechanics." Perhaps an integro-differential equation, similar to those of Volterra, will be the ultimate formulation of the photochemistry of vision. We tried it but abandoned it because of its complexity.

In most cases of dark adaptation, Eq. (35) assumes a simple form. The weighting factor is found to have negligible effect over a period of 15 minutes, and light adaptation is accomplished in most experiments with H = const. Under these conditions,

$$\int_{-\infty}^{t} \frac{ak_1 H(s)e^{-b(t-s)}}{1 + ak_1 H(s)\cdot s}\,ds \cong \int_{-\infty}^{t} \frac{ak_1 H\,ds}{1 + ak_1 Hs} = \ell n(1 + ak_1 H\tau)$$

where τ = exposure time. Thus in most cases Eq. (35) may be replaced by

$$\begin{aligned} B &= k_2 + Ae^{-c\,\ell n\,(1+ak_1 H\tau)} \\ &= k_2 + \frac{A}{(1 + ak_1 H\tau)^c}. \end{aligned} \tag{35a}$$

Then the solution of the differential equation for dark-adaptation is

$$x = x_0 e^{-Bt} \tag{27a}$$

and the slopes of the curves of Figs. 7 and 8 given by B. According to Eqs. (35a), the slope B has a low value for large products $H\tau$; but for lower values of $H\tau$, the slope increases. The slopes of the various experimental curves of Haig[7] were measured and these data are given in Table IV. According to Eq. (35a), a plot of log $(B - k_2)$ vs log $(1 + k_1 H\tau)$ should be a straight line. Figure 10 shows a fairly good approximation. The constants obtained from Fig. 10 are

$$A = 55.6 \times 10^{-3}, \qquad c = 0.500.$$

A tabulation of results for modern tests on rod adaptation is given in Table V. All the recent data obtained with artificial pupil are listed, as well as some of the data with natural pupil.

The measured and calculated values of K are seen to be in fairly good agreement in the case of Haig's[7] data. The measured values were obtained by draw-

[23] V. Volterra, *Theory of Functionals*, Blackie & Son, London, 1930, p. 148.

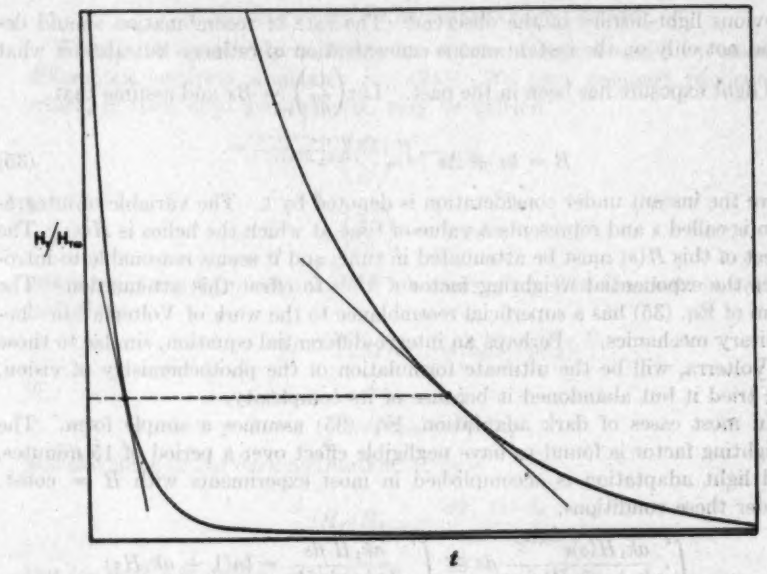

FIG. 9. Two typical dark-adaptation curves, showing that they cannot be superimposed by shifting them horizontally.

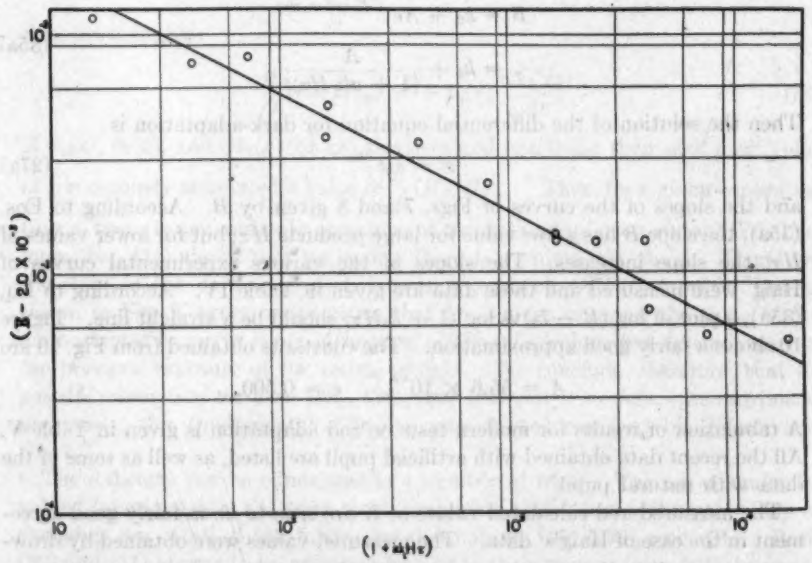

FIG. 10. Slopes of the Haig dark-adaptation curves. The data are from Table IV and determine the constants A and c in Eq. (35a).

TABLE III

Typical dark-adaptation data

Wald and Clark[8]. Rod vision, natural pupil, observer A-B. C., $H_A = 3330$ blondels

t	$\tau = 600$ sec., $\log H_{T\infty} = \bar{5}.05$			t	$\tau = 1200$ sec., $\log H_{T\infty} = \bar{5}.05$		
	$\log H_T$	$\log (H_T/H_{T\infty})$	$ln\, ln\, (H_T/H_{T\infty})$		$\log H_T$	$\log (H_T/H_{T\infty})$	$ln\, ln\, (H_T/H_{T\infty})$
sec.				sec.			
252	$\bar{4}.72$	1.67	+1.35	222	$\bar{4}.83$	1.78	+1.41
336	$\bar{4}.49$	1.44	1.20	300	$\bar{4}.62$	1.57	1.29
468	$\bar{5}.99$	0.94	0.772	348	$\bar{4}.41$	1.36	1.14
564	$\bar{5}.69$	0.64	0.388	426	$\bar{4}.14$	1.09	0.920
708	$\bar{5}.54$	0.49	+0.121	522	$\bar{5}.91$	0.86	0.683
804	$\bar{5}.42$	0.37	−0.160	696	$\bar{5}.57$	0.52	+0.180
912	$\bar{5}.32$	0.27	−0.475	900	$\bar{5}.37$	0.32	−0.305
1176	$\bar{5}.22$	0.17	−0.938	1092	$\bar{5}.22$	0.17	−0.938
1572	$\bar{5}.10$	0.05	−2.16	1374	$\bar{5}.15$	0.10	−1.47
1884	$\bar{5}.10$	0.05	−2.16	1812	$\bar{5}.10$	0.05	−2.16
2220	$\bar{5}.10$	0.05	−2.16	2112	$\bar{5}.07$	0.02	−3.08
2406	$\bar{5}.05$	0.00					

TABLE IV

Slopes of dark-adaptation curves

(Data plotted in Fig. 10)

Authority	H	τ	$(1+k_1H_T)$	B (measured)	$(B - 2.00)$
	blondel	*sec.*			
Haig[7], Table I	4470	600	4021	4.35×10^{-3}	2.35×10^{-3}
	4470	360	2421	4.35	2.35
	4470	240	1611	4.35	2.35
	4470	120	806	4.35	2.35
	4470	60	404	5.50	3.50
	4470	24	162	7.00	5.00
	4470	6	41.3	9.60	7.60
Haig[7], Table III	47,000	240	16,940	2.52	0.52
	20,900	240	7530	2.54	0.54
	11,500	240	4140	2.70	0.70
	4470	240	1611	3.44	1.44
	440	240	159	5.70	3.70
	200	240	73	10.1	8.1
	40	240	15.4	13.7	11.7

TABLE V

Analysis of dark-adaptation curves (rod vision)

Authority	H	τ	Measured			B	
			$\log (H\tau\omega)$	$ln (ax_0)$	ax_0	Measured	Calculated
	blondel	*sec.*					
Haig[7], Table I	4470	600	$\bar{4}.25$	2.45	11.6	4.35×10^{-3}	2.88×10^{-3}
	4470	360	$\bar{4}.25$	2.45	11.6	4.35	3.13
	4470	240	$\bar{4}.25$	2.45	11.6	4.35	3.39
	4470	120	$\bar{4}.25$	2.10	8.20	4.35	3.96
	4470	60	$\bar{4}.25$	1.80	6.05	5.50	4.77
	4470	24	$\bar{4}.25$	1.60	4.95	7.00	6.37
	4470	6	$\bar{4}.30$	1.30	3.67	9.60	10.7
Haig[7], Table III	47,000	240	$\bar{4}.00$	3.25	25.8	2.52	2.14
	20,900	240	$\bar{5}.95$	2.75	15.6	2.54	2.64
	11,500	240	$\bar{5}.95$	2.35	10.5	2.70	2.87
	4470	240	$\bar{5}.90$	2.00	7.40	3.44	3.39
	440	240	$\bar{4}.00$	1.60	4.95	5.70	6.41
	200	240	$\bar{4}.00$	1.45	4.25	10.1	8.52
	40	240	$\bar{4}.00$	1.10	3.00	13.7	16.2
Wald & Clark[8]	3330	600	$\bar{5}.05$	2.00	7.40	2.60	3.02
	3330	1200	$\bar{5}.05$	2.00	7.40	2.60	2.72
	Photo-flash	—	$\bar{6}.95$	2.35	10.5	2.58	—
	18,900	5	$\bar{6}.90$	1.90	6.70	3.60	6.66
	7500	5	$\bar{6}.93$	1.55	4.70	5.74	9.37
	2450	5	$\bar{6}.93$	1.40	4.06	8.76	8.35
	36	5	$\bar{6}.93$	0.45	1.57	32.0	30.4
Hecht, Haig & Chase[6]; Obs. S. H.	400,000	120	$\bar{4}.70$	3.70	40.5	2.54	2.21
	38,900	120	$\bar{4}.55$	3.20	24.5	2.54	2.67
	19,500	120	$\bar{4}.50$	2.83	17.0	2.54	2.94
	3800	120	$\bar{4}.45$	2.15	8.60	2.54	4.12
	263	120	$\bar{4}.50$	1.55	4.71	2.54	10.0
Obs. C. H.	400,000	120	$\bar{3}.03$	3.93	51.0	2.54	2.21
	38,900	120	$\bar{3}.03$	2.93	18.7	2.54	2.67
	19,500	120	$\bar{4}.94$	2.60	13.5	2.54	2.94
	3800	120	$\bar{4}.90$	1.94	6.95	2.54	4.12
	263	120	$\bar{4}.80$	1.20	3.32	3.64	10.0
Obs. A. M. C.	400,000	120	$\bar{4}.50$	4.14	62	2.54	2.21
	38,900	120	$\bar{4}.63$	3.42	30.5	2.54	2.67
	19,500	120	$\bar{4}.50$	3.07	21.5	2.54	2.94
	3800	120	$\bar{4}.34$	1.42	4.14	2.54	4.12
	263	120	$\bar{4}.20$	1.28	3.60	2.54	10.0

ing straight lines that appeared to fit the data and without any reference to calculations. An idea of the variation to be expected in the experimental data is shown by comparing Haig's run at $H = 4470$, $\tau = 240$ (in his Table I) and a second run under the same condition (in his Table III). In the first case, $ax_0 = 11.6$ while in the second case it is 7.40. The measured slopes are 4.35×10^{-3} and 3.44×10^{-3}. The calculated slope is of course the same in both cases and is 3.39×10^{-3} which appears to be within the experimental error.

Results are shown also for the research of Hecht, Haig, and Chase[6] with three observers. The experimental and calculated slopes are in fairly close agreement at the higher values of helios but there is considerable discrepancy at $H = 3800$ and $H = 263$. It is entirely possible that these discrepancies are caused by lack of complete dark adaptation before the beginning of light adaptation. The authors say that light adaptation is preceded by *10 min. in dim light*, which certainly is not equivalent to complete dark adaptation. Whatever may be the cause, it is evident from an examination of Table V that the data of Hecht, Haig, and Chase are not in agreement with those of Haig. The data of Wald and Clark,[8] on the other hand are in excellent agreement at the lower values of helios but show some discrepancies at the higher values.

6. Light Adaptation

A satisfactory mathematical representation of the dark-adaptation curves has now been obtained. The shape of the theoretical curves represents the data to within the limits of experimental variation, and the variation in slope obtained with a change in light adaptation is also in agreement with the available data. When the attempt is made to correlate the dark-adaptation curves with the known degree of light-adaptation, however, another discrepancy arises. The elimination of this discrepancy requires a slight modification of $(dx/dt)_2$.

It will be remembered that the intercept of the dark-adaptation curves (Figs. 1 to 7) at $t = 0$ is equal to $ln(ax_0)$. Thus the plot of dark-adaptation data in this form gives a convenient method for evaluating ax_0. But this quantity can be calculated also from the known helios and time of exposure for light adaptation. The differential equation is

$$\frac{dx}{dt} = k_1 H_e^{-ax} - \left[k_2 + \frac{A}{(1 + ak_1 Ht)^{\frac{1}{2}}}\right] x$$

for x less than about 0.90. It is found that if $x < 0.50$, the second term becomes negligible and the solution is

$$ax_0 = ln(1 + ak_1 H\tau) \tag{36}$$

where x_0 = concentration of retinene at the end of the light-adaptation period,

H = helios (const.) employed in light adaptation,

τ = duration of light adaptation.

Equation (36) may be used to calculate the initial value of ax_0, as has been done in Table VI. The fifth column gives the value of $ln\ ax_0$ calculated from

Eq. (36). The fourth column gives the value read from the intercepts of the dark-adaptation curves. It will be noted that the two are in good agreement except at the greater exposures. With $H = 4470$, agreement is obtained up to 120 sec., beyond which the calculated values are too low. Similarly, with a constant exposure time of 240 sec., agreement is found for $H = 4470$ but for higher values of helios the discrepancy becomes increasingly greater. Of course, the calculated values are obtained from the approximate formula, Eq. (36). But the correct solution of the differential equation for light adaptation gives even lower values of ax_0. Thus it is evident that a modification must be made in the dark-adaptation curves at high values of x, if agreement is to be obtained

TABLE VI

Light adaptation (rod vision)

Measured values of ax_o compared with values calculated by means of Eq. (36)

Authority	H	τ	$ln(ax_0)$	
			Measured	Calculated
	blondel	*sec.*		
Haig[7], Table I	4470	600	2.45	2.12
	4470	360	2.45	2.06
	4470	240	2.45	2.00
	4470	120	2.10	1.90
	4470	60	1.80	1.79
	4470	24	1.60	1.63
	4470	6	1.30	1.31
Haig[7], Table III	47,000	240	3.25	2.28
	20,900	240	2.75	2.19
	11,500	240	2.35	2.12
	4470	240	2.00	2.00
	440	240	1.60	1.62
	200	240	1.45	1.46
	40	240	1.10	0.955

between the initial concentration calculated from H and τ and that calculated by extrapolation from experimental dark-adaptation curves.

Perhaps the simplest way of obtaining this improvement is to introduce an additional term into the equation for $(dx/dt)_2$. This term must be negligible at low values of x so that it will not distort the previous agreement (Table VI) at low exposures; but at higher exposures, it must flatten the upper part of the dark-adaptation curves so that ax_0 is reduced. A satisfactory equation is

$$\left(\frac{dx}{dt}\right)_2 = -\left[k_2 - k_4 x^3 + \frac{A}{(1 + ak_1 Ht)^{\frac{1}{3}}}\right] x . \qquad (37)$$

In all the previous computations, ax is used as a variable and there has been no way of determining a itself. Equation (37) requires a knowledge of both x and ax and thus enables the determination of a.

A method of trial and error led to evaluation of the two constants:

$$k_4 = 1.98 \times 10^{-3},$$

$$a = 9.0.$$

7. Final Formulation, Rod Vision

In the foregoing sections, we have shown how a mathematical formulation of visual adaptation grew out of the original Hecht theory and how successive modifications were necessary to fit additional data. Many of the calculations of the preceding sections are still valid as special cases of the complete formulation, which will now be considered.

The final expressions for the reaction velocities are

$$\left(\frac{dx}{dt}\right)_1 = k_1 H(e^{-ax} - e^{-a}) \tag{38}$$

$$\left(\frac{dx}{dt}\right)_2 = -\left[k_2 - k_4 x^3 + Ae^{-c\int_{-\infty}^{t} \frac{ak_1 H(s) e^{-b(t-s)}}{1+ak_1 H(s)\cdot s}\, ds}\right] x \tag{39}$$

and the differential equation is

$$\frac{dx}{dt} = k_1 H(e^{-ax} - e^{-a}) - \left[k_2 - k_4 x^3 + Ae^{-c\int_{-\infty}^{t} \frac{ak_1 H(s) e^{-b(t-s)}}{1+ak_1 H(s)\cdot s}\, ds}\right] x. \tag{40}$$

Equation (40) may be solved numerically, for any constant or variable helios, by the ordinary graphical or mechanical methods. Usually, however, $H(s) =$ const. over an adaptation period τ. Also, the factor $e^{-b(t-s)}$ is essentially equal to unity unless times of an hour or more are being considered. If these two conditions are satisfied, Eq. (40) reduces to

$$\frac{dx}{dt} = k_1 H(e^{-ax} - e^{-a}) - [k_2 - k_4 x^3 + A(1 + ak_1 Ht)^{-1}]x. \tag{40a}$$

Light Adaptation

If the eye is completely dark-adapted at $t = 0$, the solution of Eq. (40a) may be written

$$t = \int_0^x \frac{dx}{k_1 H(e^{-ax} - e^{-a}) - [k_2 - k_4 x^3 + A(1 + ak_1 Ht)^{-1}]x} \tag{41}$$

which can be evaluated step by step to give a curve of x vs t for light adaptation. Such a curve is shown in Fig. 11 for $H = 4470$ blondels.

In attempting to lighten the labor associated with the numerical integration of Eq. (41), we devised the following method. It is based on the fact that $[k_2 - k_4 x^3 + A(1 - ak_1 Ht)^{-1}]x$ is almost a constant over a considerable range of x.

For example, at $H = 4470$ this quantity changes from 5.10 to 4.38 in the range $0.20 \leqq x \leqq 0.40$. If the assumption be made that for $x_1 \leqq x \leqq x_2$,

$$[k_2 - k_4x^3 + A(1 - ak_1Ht)^{-1}]x = D = \text{const},$$

then Eq. (41) becomes

$$\Delta t = \int_{x_1}^{x_2} \frac{dx}{k_1He^{-ax} - D} = \frac{1}{D}\left[\frac{1}{a}\ln\left(\frac{k_1He^{-ax_1} - D}{k_1He^{-ax_1} - D}\right) - (x_2 - x_1)\right]. \quad (41a)$$

The procedure is to divide the range of x into regions that are small enough so that D is essentially constant over each one. The total value of t for any x is then obtained by adding the Δt's obtained by means of Eq. (41a). This equation is sometimes convenient, though near equilibrium it appears to have no advantage over Eq. (41).

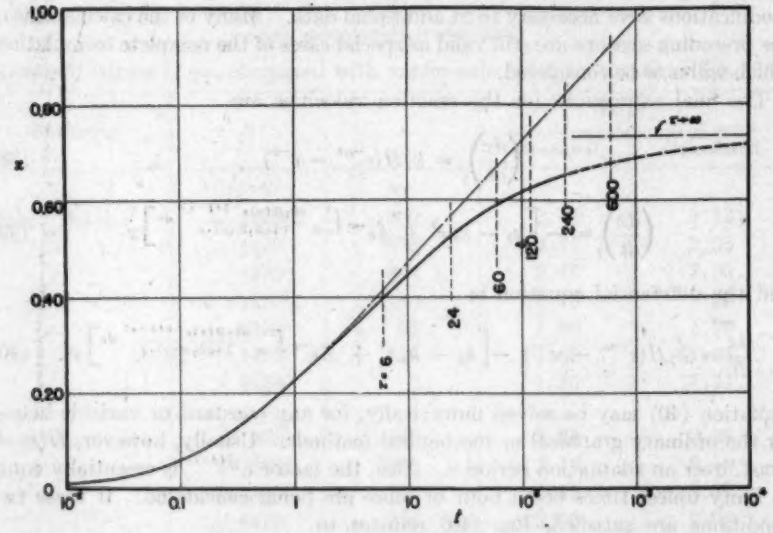

FIG. 11. Calculated light-adaptation curve, giving the concentration of retinene in a rod as a function of time. $H = 4470$. ——, eq. (41); — —, eq. (41c).

For the special case of $x << 1$, the second term in the denominator of Eq. (41) is ordinarily negligible in comparison with the first term. Then

$$t \cong \int_0^x \frac{dx}{k_1He^{-ax}} = \frac{1}{ak_1H}(e^{ax} - 1) \quad (41b)$$

or

$$ax = \ln(1 + ak_1Ht). \quad (41c)$$

These simple equations are useful in many cases.

For larger values of x, the foregoing approximation can still be applied to the second term of Eq. (41), giving

$$t \cong \int_0^x \frac{dx}{k_1 H e^{-ax} - [k_2 + A(1 + ak_1 Ht)^{-1}]x} = \int_0^x \frac{dx}{k_1 H e^{-ax} - [k_2 + Ae^{-ax/2}]x}. \tag{41d}$$

The validity of this approximation rests on the fact that for the high values of helios ordinarily employed in light adaptation, the second term in the denominator is small compared with the first term. Thus an approximation in the second term causes but little error in the calculation. This conclusion, however, does not apply near equilibrium, when the two terms approach equality and where an error in either is serious.

Equation (41d) is integrated by expanding in a series and integrating term by term:

$$t = \int_0^x \left\{ \frac{1}{k_1 H} e^{ax} + \frac{[k_2 + Ae^{-ax/2}]x}{(k_1 H)^2} e^{2ax} + \frac{[k_2 + Ae^{-ax/2}]^2 x^2}{(k_1 H)^3} e^{3ax} + \cdots \right\} dx$$

or

$$\begin{aligned} t = {} & \frac{1}{ak_1 H}(e^{ax} - 1) + \frac{1}{(ak_1 H)^2}\left\{ k_2 e^{2ax}\left(\frac{ax}{2} - \frac{1}{4}\right) + Ae^{3ax/2}\left(\frac{2ax}{3} - \frac{4}{9}\right) \right. \\ & \left. + \left(\frac{k_2}{4} + \frac{4A}{9}\right)\right\} + \frac{1}{(ak_1 H)^3}\left\{ k_2^2 e^{3ax}\left[\frac{(ax)^2}{3} - \frac{2ax}{9} + \frac{2}{27}\right] \right. \\ & + 2k_2 Ae^{5ax/2}\left[\frac{2(ax)^2}{5} - \frac{8ax}{25} + \frac{16}{125}\right] \\ & \left. + A^2 e^{2ax}\left[\frac{(ax)^2}{2} - \frac{ax}{2} + \frac{1}{4}\right] - \left[\frac{2}{27}k_2^2 + \frac{32}{125}k_2 A + \frac{A^2}{4}\right]\right\} + \cdots \end{aligned} \tag{41e}$$

Some calculated values of light adaptation for $H = 4470$ are given in Table VII and Fig. 11. One, two, and three terms of the series are calculated by means of Eq. (41e). These results are compared with the value of t obtained by numerical integration of Eq. (41). It will be noted that the one-term approximation is reasonably close to the true value if $x < 0.30$, the three-term approximation is fairly good up to $x = 0.60$, but at $x = 0.65$ the error caused by the approximation of the second term of Eq. (41) causes trouble.

The foregoing conclusions apply only to the particular case of $H = 4470$. For all values of helios, it is important that one be able to decide when the simple formula, Eq. (41b), applies and when more complicated methods are necessary. This question can be decided on the basis of Eq. (41e). Let R denote the ratio of the second term to the first term in Eq. (41e). Then

$$H = \frac{k_2 e^{2ax}\left(\frac{ax}{2} - \frac{1}{4}\right) + Ae^{3ax/2}\left(\frac{2ax}{3} - \frac{4}{9}\right)}{ak_1 R(e^{ax} - 1)}. \tag{42}$$

Some calculations based on $R = 0.10$ are given in Table VIII. Because of the occurrence of H in the denominator of the series, Eq. (41e) becomes progressively less useful as the helios is reduced. The third column of the table was calculated

from Eq. (41c) and gives the exposure time corresponding to the conditions of the first two columns. It is interesting to note that the exposure time is almost constant. We conclude, therefore, that *the approximate formula Eq.* (41c) *is always applicable for exposure times of less than approximately five seconds.*

TABLE VII

Calculated values of time (sec.)

H = 4470 blondels

x	Eq. (41e)			Numerical integration
	One Term	Two Terms	Three Terms	
0.30	2.070	2.17	2.18	2.19
0.40	5.309	5.98	6.07	6.08
0.50	13.28	16.7	17.8	18.2
0.60	32.87	51.1	63.8	73.5
0.65	51.63	244	287	225

TABLE VIII

Maximum concentrations at which the approximate formula, eq. (41b), *may be employed*

Calculated by means of Eq. (42) with R = 0.10

H	Max. concentration	Max. exposure time τ
blondel	x	*sec.*
258	0.10	3.8
880	0.20	3.8
2050	0.30	4.5
5260	0.40	4.5
11,400	0.50	5.2
25,000	0.60	5.8

Condition of Equilibrium

Suppose that conditions have remained fixed for a sufficient time so that equilibrium has been reached. Then $Ht \to \infty$, so $A(1 + k_1Ht) \to 0$ and $dx/dt = 0$. Thus Eq. (40) becomes

$$k_1H_A(e^{-ax_A} - e^{-a}) = (k_2 - k_4x_A^3)x_A$$

or

$$H_A = \frac{(k_2 - k_4x_A^3)ax_A}{ak_1(e^{-ax_A} - e^{-a})} \tag{43}$$

where x_A is the concentration corresponding to the constant helios H_A. For small values of x_A, Eq. (43) reduces to

$$H_A = \left(\frac{k_2}{ak_1}\right)(ax_A)e^{ax_A}. \tag{43a}$$

A calculated curve showing the relation between x_A and H_A is given in Fig. 12.

Figure 12 shows the equilibrium concentration of retinene as a function of H_A. When a dark-adaptation run is made and the exposure time has been sufficient, these values of x_A are equal to the initial concentrations x_0 for the

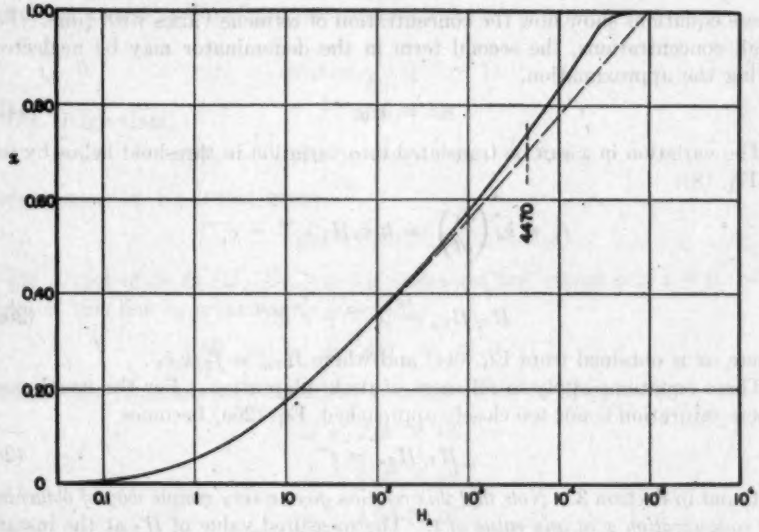

FIG. 12. Calculated concentration of retinene in a rod, equilibrium conditions. ——, eq. (43); — — eq. (43a).

dark-adaptation curve. With shorter exposure times, the initial concentration can be calculated by means of Eq. (41) or Eq. (41b).

Dark Adaptation

For dark adaptation, $H = 0$ and the differential equation becomes

$$\frac{dx}{dt} = -[k_2 - k_4x^3 + A(1 + ak_1H_A\tau)^{-1}]x \tag{40b}$$

with the initial condition that $x = x_0$ at $t = 0$. Therefore,

$$\int_{x_0}^{x} \frac{dx}{(B - k_4x^3)x} = -\int_0^t dt$$

or

$$t = \frac{1}{3B} \ln \left(\frac{x_0^3}{x^3} \frac{B - k_4 x^3}{B - k_4 x_0^3} \right) \tag{44}$$

where

$$B = k_2 + A(1 + ak_1 H_{AT})^{-\frac{1}{3}}. \tag{45}$$

Equation (44) may be written,

$$ax = ax_0 \left[\frac{B}{Be^{3Bt} - k_4 x_0^3 (e^{3Bt} - 1)} \right]^{\frac{1}{3}}. \tag{44a}$$

These equations show how the concentration of retinene varies with time. For small concentrations, the second term in the denominator may be neglected, giving the approximation,

$$ax = ax_0 e^{-Bt}. \tag{44b}$$

The variation in x can be translated into variation in threshold helios by use of Eq. (8):

$$f_T = k_3 \left(\frac{dx}{dt} \right)_1 = k_1 k_3 H_T (e^{-ax} - e^{-a})$$

or

$$H_T / H_{T\infty} = (e^{-ax} - e^{-a})^{-1} \tag{26a}$$

where ax is obtained from Eq. (44) and where $H_{T\infty} = f_T / k_1 k_3$.

These equations apply in all cases of dark adaptation. For the usual case, where saturation is not too closely approached, Eq. (26a) becomes

$$H_T / H_{T\infty} = e^{ax} \tag{26}$$

as found in Section 3. *Note that this relation gives a very simple way of obtaining the concentration x at any value of t.* The measured value of H_T at the instant t is divided by the final value $H_{T\infty}$, and

$$ax = \ln (H_T / H_{T\infty}). \tag{26b}$$

If the concentration is sufficiently low, Eq. (44b) may be employed instead of Eq. (44a), which gives the simple equation of Section 3,

$$\ln (H_T / H_{T\infty}) = ax = ax_0 e^{-Bt}$$

or

$$\ln \ln (H_T / H_{T\infty}) = \ln (ax_0) - Bt. \tag{28b}$$

Thus at the lower values of x, the dark-adaptation curves are straight lines at all values of t, as drawn in Figs. 1 to 6. Even at high values of x_0, the curves are straight except near $t = 0$. For in Eq. (44a) let t be large so that $e^{3Bt} >> 1$. Then

$$ax = ax_0 \left(1 - \frac{k_4 x_0^3}{B} \right)^{-\frac{1}{3}} e^{-Bt}$$

and

$$\ln \ln (H_T/H_{T\infty}) = I - Bt \tag{46}$$

where the intercept, obtained by extrapolating the straight line to $t = 0$, is

$$I = \ln \left[\frac{ax_0}{(1 - k_4 x_0^3/B)^{\frac{1}{3}}} \right]. \tag{47}$$

Constants

Some of the constants have been evaluated in previous sections. The steps were as follows:

(1) According to Eq. (36), the constant (ak_1) is

$$(ak_1) = \frac{1}{H_T} (e^{ax_0} - 1). \tag{36a}$$

From Haig's data,

$$H_T = 1.072 \times 10^6, \qquad ax_0 = 7.40.$$

Substitution in Eq. (36a) gives

$$ak_1 = 1.50 \times 10^{-3}.$$

(2) A plot of $\ln \ln (H_T/H_{T\infty})$ vs t is a straight line except near $t = 0$. The slope of this line is, according to Eq. (45),

$$B = k_2 + A(1 + ak_1 H_A T)^{-c}.$$

Satisfactory constants were found by comparison of the Haig data:

$$k_2 = 2.00 \times 10^{-3},$$

$$A = 55.6 \times 10^{-3},$$

$$ak_1 = 1.50 \times 10^{-3},$$

$$c = 0.500.$$

(3) At high helios and long exposure times, a further modification was necessary. Equation (37) was introduced, bringing in a new constant k_4 and requiring the evaluation of a. The Haig data were again employed, and a process of trial and error led to the values:

$$k_4 = 1.98 \times 10^{-3},$$

$$a = 9.0.$$

A list of the constants is given in Table IX.

The appearance of the dark-adaptation curves, taking into account the x^3 term of Eq. (44a), is shown in Fig. 13. The dark-adaptation curves for the lower values of helios are seen to have no curvature while the curvature becomes more and more marked as helios is increased above 4470 blondels. The experimental points at values of helios not exceeding 4470 are in almost as good agreement with these calculated curves as they were with the curves drawn to fit the

points, Fig. 7. The points for $H = 47{,}000$, however, are much higher than the calculated curve.

TABLE IX

Numerical constants

Quantity	Rods	Cones
ak_1	1.50×10^{-3}	3.0×10^{-5}
k_2	2.00×10^{-3}	0.0110
af_∞/k_2	8.25×10^{-8}	7.35×10^{-7}
A	55.6×10^{-3}	0.945
c	0.500	1.20
$H_{T\infty}$	3.6×10^{-6}	3×10^{-3}
a	9.0	30
k_1	1.67×10^{-4}	1.0×10^{-6}
k_4	1.98×10^{-3}	0

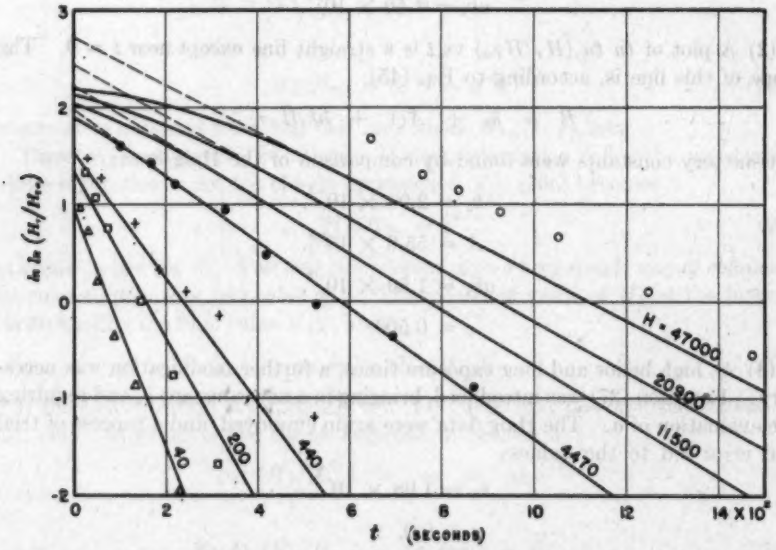

FIG. 13. Calculated dark-adaption curves with initial concentrations obtained from light-adaptation curve, Fig. 11. The experimental points are those of Haig. Rod vision, observer E. M. H., exposure time 240 sec., 2 mm. fixed pupil. ○, $H_A = 47{,}000$ blondels; ●, 4470; +, 440; □, 200; △, 40.

Table X shows the comparison of other experimental data. The fourth column gives the intercept of the straight lines drawn to fit the experimental data. The

fifth column gives the values calculated from the known helios and exposure time using the approximate formula, Eq. (41b). The final column gives values of I calculated by the more exact formula Eq. (41). It will be noted that, for lower values of H corresponding, for example, to ordinary conditions in rooms the agreement is very good. With very high degrees of light adaptation, Eq. (41) is an improvement over Eq. (41a) though there is still considerable discrepancy.

As seen from these tables the agreement between the calculations and the experimental values is far from perfect. Part of this trouble appears to be in the inconsistencies of the data. We believe that before the formulation can

TABLE X

Light adaptation (rod vision)

Authority	H	τ	I		
			Measured	Calc., eq. (41b)	Calc., eq. (41)
	blondel	*sec.*			
Haig[7], Table I (Values of ax_0 obtained from Fig. 11)	4470	600	2.45	1.81	1.89
	4470	360	2.45	1.79	1.86
	4470	240	2.45	1.77	1.83
	4470	120	2.10	1.73	1.77
	4470	60	1.80	1.67	1.70
	4470	24	1.60	1.55	1.57
	4470	6	1.30	1.28	1.29
Haig[7], Table III (Equilibrium assumed, values of ax_0 calculated from Eq. (43))	47,000	240	3.25	2.19	2.73
	20,900	240	2.75	2.13	2.44
	11,500	240	2.35	2.04	2.22
	4470	240	2.00	1.89	1.98
	440	240	1.60	1.51	1.52
	200	240	1.45	1.33	1.33
	40	240	1.10	0.924	0.925

be improved further it will be necessary to have additional experimental data. The older data make practically no reference to adaptation conditions. The newer investigations, which were used in this paper, give careful specification of light adaptation procedure. Yet we believe that further improvement in this direction is possible. We have been greatly handicapped by the lack of dark-adaptation data obtained after complete light adaptation. Many of the curves are obtained after an exposure time of 120 sec. or 240 sec. There is little guarantee that equilibrium has been reached under these conditions. On the other hand, with small degrees of light adaptation the conditions immediately prior to light adaptation are important and their importance does not seem to be recognized by experimentalists.

8. Cone Vision

In the preceding sections, attention has been confined exclusively to rod vision. But cone vision is also photochemical in its initial phenomena, and its mathematical formulation may be expected to be identical with that for the rods, except for the values of the constants. Indeed, some of the complexity of the rod formulation is unnecessary with the cones for *it is found that saturation is not approached in the cones.* Experimental data are available up to a helios of 400,000, or approximately 4 times the helios of a white surface in noon sunlight, yet no indication of cone saturation is exhibited. The fact allows the subject of cone vision to be worked out without any knowledge of the constant a; all equations can be expressed in terms of ax instead of x. To make the subject more specific, one may assume a value of a (such as $a = 30$) but such a step is not necessary and any other large value would be just as satisfactory.

For cone vision, the fundamental equations are

$$\left(\frac{dx}{dt}\right)_1 = k_1 H e^{-ax} \tag{38a}$$

$$\left(\frac{dx}{dt}\right)_2 = -\left[k_2 + Ae^{-c\int_{-\infty}^{t} \frac{ak_1 H(s) e^{-b(t-s)}}{1+ak_1 H(s)\cdot s}\, ds}\right] x. \tag{39a}$$

If $H(s) = \text{const.}$ and $e^{-b(t-s)} \cong 1$, the differential equation is

$$\frac{dx}{dt} = k_1 H e^{-ax} - [k_2 + A(1 + ak_1 Ht)^{-1}]x. \tag{40c}$$

The constants are given in Table IX.

For light adaptation,

$$ax = \ell n\,(1 + ak_1 Ht). \tag{41c}$$

For equilibrium,

$$H_A = \left(\frac{k_2}{ak_1}\right)(ax_A)e^{ax_A}, \tag{42a}$$

and the results are shown in Fig. 14. For dark adaptation,

$$ax = ax_0 e^{-Bt}. \tag{27b}$$

The helios threshold during the process of dark adaptation is given by the equation,

$$H_T/H_{T\infty} = e^{ax}$$

where $H_{T\infty} = f_T/k_1 k_3$. Thus,

$$\ell n\ \ell n\ (H_T/H_{T\infty}) = \ell n\ (ax_0) - Bt \tag{28b}$$

which gives the familiar linear relationship between $\ell n\ \ell n\ (H_T/H_{T\infty})$ and t.

Experimental data for cone vision are plotted in Figs. 15 and 16. Both are plotted from the data of Hecht, Haig, and Chase,[6] one set of curves being for red light and the other for violet. It will be noted that the cone data are

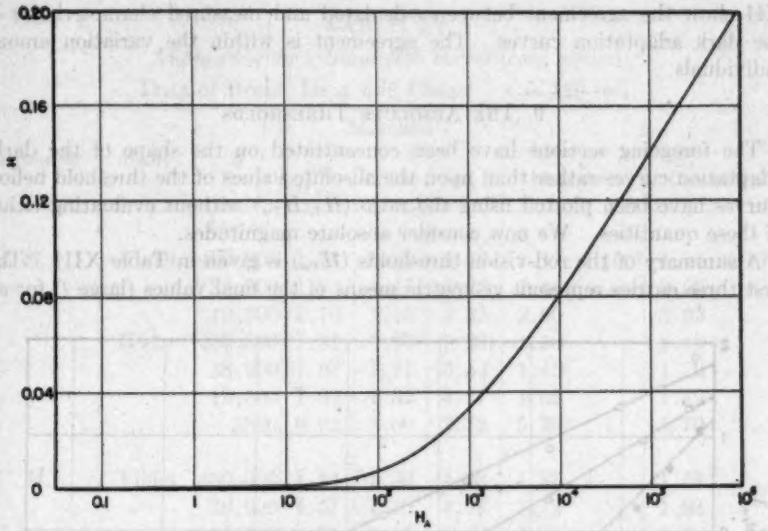

FIG. 14. Steady-state adaptation curve for cones

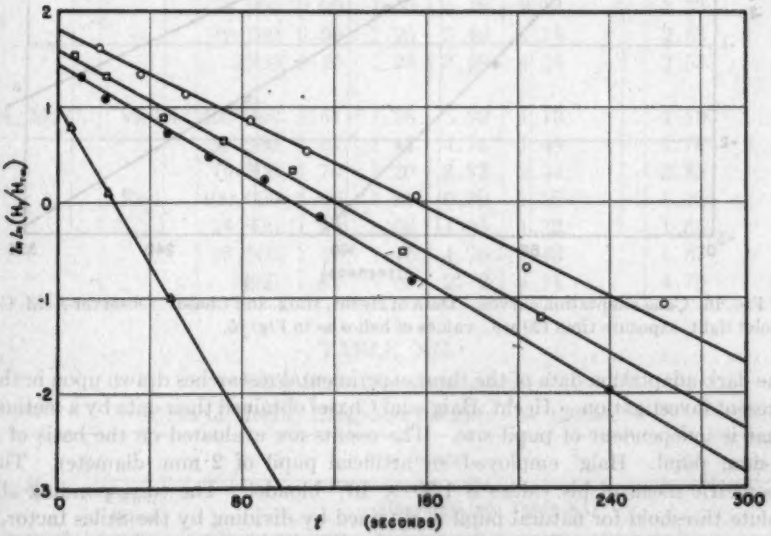

FIG. 15. Cone adaptation curves. Data of Hecht, Haig, and Chase. Observer A. M. C., red light, exposure time 120 sec. ○, H = 400,000 blondels; □, 38,900; ●, 19,500; △, 3800.

in agreement with the simple relation of Eq. (28b). A summary of experimental and calculated data for cone vision is given in Table XI. Table XI and Table

XII show the agreement between calculated and measured characteristics of the dark adaptation curves. The agreement is within the variation among individuals.

9. The Absolute Thresholds

The foregoing sections have been concentrated on the shape of the dark-adaptation curves rather than upon the absolute values of the threshold helios. Curves have been plotted using the ratio $(H_T/H_{T\infty})$ without evaluating either of these quantities. We now consider absolute magnitudes.

A summary of the rod-vision thresholds $(H_{T\infty})$ is given in Table XIII. The first three entries represent geometric means of the final values (large t) for all

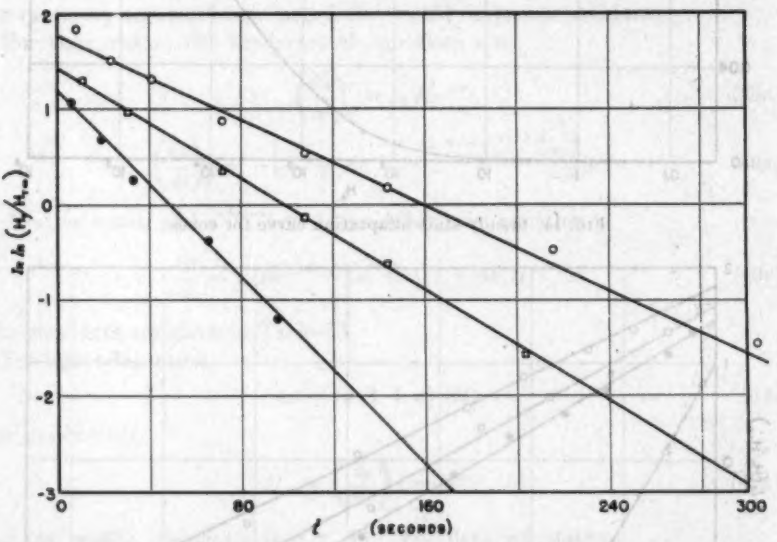

Fig. 16. Cone adaptation curves. Data of Hecht, Haig, and Chase. Observer A. M. C., violet light, exposure time 120 sec., values of helios as in Fig. 15.

the dark-adaptation data of the three experimental researches drawn upon in the present investigation. Hecht, Haig, and Chase[6] obtained their data by a method that is independent of pupil size. The results are evaluated on the basis of a 2 mm. pupil. Haig[7] employed an artificial pupil of 2 mm. diameter. The geometric mean of his values is 1.30×10^{-4} blondel. The corresponding absolute threshold for natural pupil is obtained by dividing by the Stiles factor,[24] $\zeta = 15.3$, which gives $H_{T\infty} = 8.5 \times 10^{-6}$. The Wald and Clark[8] data are for a natural pupil, the geometric mean of all their data giving $H_{T\infty} = 10.4 \times 10^{-6}$. The results of Hecht, Haig, and Chase[6] are not exactly comparable because they used as criterion the appearance of a black cross rather than the appearance of

[24] P. Moon and D. E. Spencer, J. Opt. Soc. Am. **34**, 319 (1944).

TABLE XI

Analysis of dark adaptation curves (cone vision)

Data of Hecht, Haig, and Chase[5]. $\tau = 120$ sec.

Observer	Light	H	Measured			B	
			$\log (H_{\tau\infty})$	$\ell_n(ax_0)$	ax_0	Measured	Calculated
		blondel					
S. H.	Violet	400,000	$\bar{1}.73$	1.85	6.36	1.11×10^{-3}	1.15×10^{-2}
		38,900	$\bar{1}.73$	1.17	3.22	1.46	3.09
		19,500	$\bar{1}.70$	1.18	3.25	2.00	3.02
	Red	400,000	$\bar{1}.82$	1.97	7.20	1.30	1.12
		38,900	$\bar{1}.97$	1.71	5.54	1.42	1.22
		19,500	$\bar{1}.92$	1.52	4.57	1.62	1.49
		3800	0.01	1.00	2.72	5.20	4.70
C. H.	Violet	400,000	$\bar{1}.54$	1.50	4.48	1.33	1.53
		38,900	$\bar{1}.57$	1.40	4.06	1.72	1.83
		19,500	$\bar{1}.54$	1.12	3.07	2.36	3.48
	Red	400,000	0.02	1.64	5.15	0.82	1.30
		38,900	0.00	1.50	4.48	2.14	1.53
		19,500	0.09	1.25	3.49	4.15	2.53
		3800	0.10	1.25	3.49	4.15	2.53
A. M. C.	Violet	400,000	$\bar{1}.51$	1.78	5.92	1.13	1.19
		38,900	$\bar{1}.61$	1.42	4.14	1.45	1.76
		19,500	$\bar{1}.70$	1.20	3.32	2.44	2.85
	Red	400,000	$\bar{1}.66$	1.81	6.10	1.16	1.16
		38,900	$\bar{1}.65$	1.60	4.95	1.32	1.35
		19,500	$\bar{1}.67$	1.45	4.26	1.43	1.67
		3800	$\bar{1}.62$	1.00	2.72	4.11	4.70

TABLE XII

Light adaptation (cone vision)

Data of Hecht, Haig, and Chase[5]; $\tau = 120$ sec.

H	$\ell n(ax_0)$	
	Calculated	Measured (see Table XI)
blondel		
400,000	1.98	1.85, 1.97, 1.50, 1.64, 1.78, 1.81
38,900	1.60	1.17, 1.71, 1.40, 1.50, 1.42, 1.60
19,500	1.45	1.18, 1.52, 1.12, 1.25, 1.20, 1.45
3800	0.985	1.00, 1.25, 1.00

the test field itself. They state that this difference in criterion introduces an additional factor of 3. When this factor as well as the value of $\zeta = 15.3$ are applied to the experimental results, a value of $H_{T\infty} = 9.5 \times 10^{-6}$ is obtained. The data of the other investigators (Table X) are seen to be in approximate agreement. In view of the differences between individuals, the variation of a given person from day to day, and the great effect of diet,[25] there appears to be

TABLE XIII

Absolute threshold (rod vision)

Authority	Obs.	Pupil	Fixation	$H_{T\infty}$ (blondel)	
				Art. pupil	Nat. pupil
Hecht, Haig & Chase[6]	3	2 mm.	30° from fovea	4.35×10^{-4}*	9.5×10^{-6}
Haig[7]	E. M. H.	2 mm.	7° from fovea	1.30×10^{-4}	8.5×10^{-6}
Wald[21]			15° and 25°		3.6×10^{-6}
Wald & Clark[8]	A. B. C.	Nat.	9.8° from fovea		10.4×10^{-6}
Nutting[26]	P. G. N.	Nat.	None		14.0×10^{-6}
Cobb[27]	15	Nat.	—		(3 to 30) 10^{-6}
Hecht & Mandelbaum[25] Fig. 5	—	Nat.	7° from fovea		6.3×10^{-6}
Fig. 6	J. M.	Nat.	7°		5.6×10^{-6}
Fig. 6	L. W.	Nat.	7°		5.6×10^{-6}
Hecht & Mandelbaum[25]	F. W.	Nat.	7°		14×10^{-6}
Bouma[28]	—	Nat.	None		10×10^{-6}

* Not a threshold. According to Hecht, Haig, and Chase, "the measurements represent not quite the threshold of vision but a brightness about 3 times as high, secured by using the appearance of a black cross as criterion." The calculated value for natural pupil includes this factor of 3 and thus represents the threshold.

no advantage in attempting to fix $H_{T\infty}$ with great precision. We shall take it as

$$H_{T\infty} = 10 \times 10^{-6} \text{ blondel}$$

with natural pupil.

[25] S. Hecht and J. Mandelbaum, J. Am. Med. Assn., **112**, 1910 (1939); Science, **88**, 219 (1938).

[26] P. G. Nutting, Trans. I. E. S., **11**, 1 (1916).

[27] P. W. Cobb, Psychol. Rev. **26**, 428 (1919). Arch. Ophth. **48**, 492 (1919).

[28] P. J. Bouma, Philips Tech. Rev. **5**, 296 (1940).

[21] G. Wald, J. Gen. Physiol. **21**, 269 (1938).

This value allows the calculation of H_T instead of $H_T/H_{T\infty}$ for all dark-adaptation curves. It also allows the evaluation of the constant (af_∞/k_3). According to Eq. (9),

$$af_\infty/k_3 = (ak_1)\zeta H_{T\infty} \tag{48}$$

where ζ is the *Stiles factor*. Substitution of the foregoing value of $H_{T\infty}$ in Eq. (47), with $\zeta = 15.3$ and $(ak_1) = 1.50 \times 10^{-3}$ gives the value of the final constant:

$$af_\infty/k_3 = 2.30 \times 10^{-7}.$$

This constant contains a factor (f_∞) which cannot be evaluated separately unless data are obtained on the actual frequencies of nerve impulses. The constant (af_∞/k_3) would look simpler if represented by a single symbol. But this change

TABLE XIV

Absolute threshold (cone vision)

Authority	Obs.	Pupil	Fixation	$H_{T\infty}$ (blondel)	
				2 mm. pupil	Nat. pupil
Hecht, Haig & Chase[6]	3	2 mm.	30° from fovea	0.590	72.3×10^{-3}
Hecht[39]	15	Nat.	Fovea		3×10^{-3}
Hecht & Mandelbaum[25] Fig. 5	1	Nat.	7° from fovea		2.1×10^{-3}
Hecht & Mandelbaum[25] Fig. 6	J. M.	Nat.	7° from fovea		3.2×10^{-3}
Hecht & Mandelbaum[25] Fig. 6	L. W.	Nat.	7° from fovea		1.8×10^{-3}
Hecht & Mandelbaum[25] Fig. 6	F. W.	Nat.	7° from fovea		3.2×10^{-3}

will not be made because of the advantage of visualization, even though the true values of f are not known.

Table XIV gives data on cone thresholds. A representative value appears to be

$$H_{T\infty} = 3.0 \times 10^{-3} \text{ blondels.}$$

Substitution in Eq. (47) with $\zeta = 8.17$ and $(ak_1) = 3 \times 10^{-5}$ gives for the cones,

$$af_\infty/k_3 = 7.35 \times 10^{-7}.$$

Values of the constants, for both rods and cones, are given in Table IX.

[39] S. Hecht, J. Gen. Physiol. 4, 113 (1921).

10. Applications and Predictions

The foregoing mathematical formulation can be used in making a great variety of quantitative predictions. Not only does it allow the calculation of dark-adaptation curves for any value of helios and any exposure time, but it also allows the calculation of light-adaptation curves. Such curves have not been obtained experimentally.

All previous researches have dealt with the special case of the dark-adapted eye suddenly exposed to light for a definite time, after which it is kept in darkness. But adaptation problems in practice are only remotely connected with the artificial condition studied in the laboratory. In everyday use, the eyes are constantly changing from one adaptation level to another, and none of these

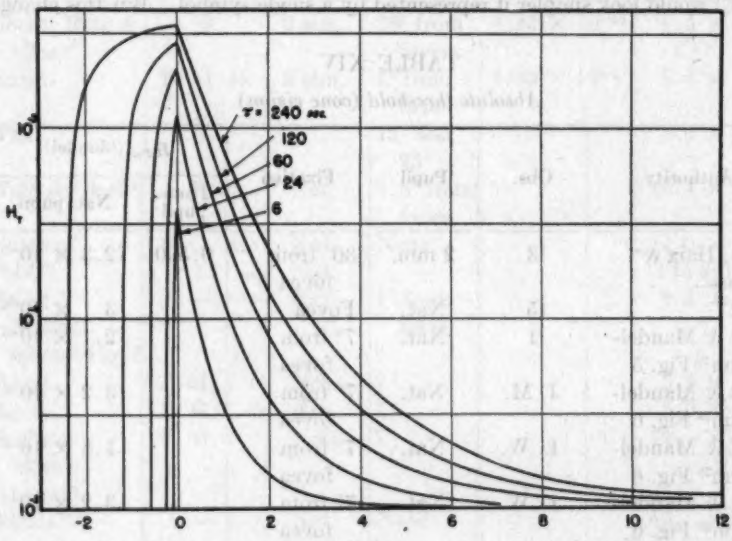

Fig. 17. Light adaptation and dark adaptation curves. Calculated curves for various exposure times and for $H = 4470$.

levels is absolute darkness. These more complicated cases can be calculated by the methods outlined in this paper.

An example of calculated light-adaptation curves is shown in Fig. 17. The conditions are those used by Haig, with rod vision, $H = 4470$, and various exposure times. The concentration of retinene can be calculated as a function of time for both light adaptation and the subsequent dark adaptation. The results can be plotted equally well in terms of the helios threshold, the transition to H_τ being made by means of Eq. (26b). Note how rapid is the process of light adaptation compared with the process of dark adaptation.

Another subject that can be treated theoretically is *reciprocity* of exposure time and helios. For rod vision and small concentrations of retinene, Eq. (41c)

applies. This equation contains H and τ only in the product $H\tau$, and thus states that x_0 (and therefore the initial point of the dark-adaptation curve) will be identical, no matter what H and τ are individually, provided their product is constant. Equation (45) shows that the slope of the dark-adaptation curve is likewise dependent on the product $H\tau$. Therefore, *at low concentrations of retinene, dark adaptation is identical if the product of helios and exposure time is constant.*

At higher concentrations, however, reciprocity no longer holds. According to Eq. (41e), the exposure time may be written,

$$\tau = \frac{M}{H} + \frac{N}{H^2} + \cdots$$

where M and N are constants for a given value of x_0. The second and higher terms of the series become important at the higher values of x_0 and destroy the simple reciprocity relation that applied when only the first term was significant. The conditions for departure from reciprocity are exactly the same as those for departure from the simplicity of Eq. (41c), which was discussed in Section 7. We can conclude, therefore, that *reciprocity holds to a good approximation for exposure times not exceeding 5 sec.*

A question that has aroused considerable discussion is this: Can dark-adaptation curves cross? Stated in a different way, if two dark-adaptation curves start at the same point, will they be identical throughout? Wald and Clark in 1937 found a case of intersecting curves. A curve resulting from short exposure at high helios had a greater slope than a curve obtained with long exposure at low helios. In 1941 Haig found, "In none of these trials (experiments of Haig) was the Wald-Clark effect observed. On the contrary, it was found that for equal degrees of light adaptation, as indicated by identical initial dark adaptation thresholds, the course of dark adaptation is the same whether pre-exposure is for a brief period to a light of high intensity or a prolonged period to a light of lower intensity." In 1944, Wald[30] replied as follows: "To meet this criticism directly, however, we have repeated our experiments with a new subject, with violet light as used by Haig, and with an artificial pupil 1.9 mm in diameter with results identical with those reported originally."

In the previous paragraphs of this section, we have considered a wide variety of conditions under which the dark adaptation curves are identical if their initial points are identical. This is in accordance with Haig's experiments. On the other hand, the theory predicts differences in slope if the initial concentration is rather high but obtained with wide differences of exposure time. For example, consider the two conditions:

(A) $H = 4470, \quad \tau = 120$ sec., $\quad x_0 = 0.626,$

$H\tau = 537{,}000.$

and

(B) $H = 100{,}000, \quad x_0 = 0.626.$

[30] G. Wald, Vision: Photochemistry, in *Medical Physics*, Chicago, 1944, p. 1663.

The exposure time in case B is adjusted to give the correct initial concentration. According to Eq. (41b)

$$\tau = \frac{1}{ak_1H}(e^{ax_0} - 1)$$

$$= \frac{1}{150}(e^{9(0.426)} - 1)$$

$$= 1.87 \text{ sec.}$$

and

$$H\tau = 187{,}000.$$

The slope of the dark-adaptation curve in (A) is, according to Eq. (45),

$$B_A = 2.0 + \frac{55.6}{\sqrt{1 + 1.5(537)}} = 3.96.$$

For (B)

$$B_B = 2.0 + \frac{55.6}{\sqrt{1 + 1.5(187)}} = 5.32.$$

Thus the two dark-adaptation curves start from the same point and have distinctly different slopes.

The foregoing conclusions apply to rod vision. For cones, all available data seem to indicate that x is always small, in practice. Equation (41c) holds and therefore reciprocity always applies to cone vision. For the same reason, we conclude that intersecting dark-adaptation curves do not occur with cone vision. All the calculations for cone vision are made as in the case of rods but are generally simpler. The complete dark-adaptation curves are composed of two parts with a relatively sharp transition from cone to rod vision.[6] These complete curves are obtained by calculating both the rod and the cone curves and retaining whichever is the lower.

11. Summary

A mathematical formulation of dark adaptation is developed. It stems from the photochemical theory of Hecht but introduces modified equations whose justification rests on their agreement with experimental data. The new theory predicts the following:

(1) A dark-adaptation curve, plotted in a specified way, is a *straight line* (except at high concentrations and very small values of time). Good agreement with modern experimental data is shown in Figs. 1 to 8.

(2) The *slope* of the straight-line dark-adaptation curve depends on the degree of light adaptation previous to the dark-adaptation run. With strong light adaptation, the dark-adaptation process is slow and the slope is small. With weak light adaptation, the dark-adaptation process is fast and the slope is large. The theory is in fairly good quantitative agreement with the available data.

(3) *Reciprocity* between exposure time and helios exists at the lower degrees of light adaptation but begins to fail when the exposure time exceeds five seconds.

(4) In most cases, the slope of the straight-line dark-adaptation curve is simply related to the instantaneous threshold; that is, curves that start at high values have low slopes while lines that start at lower values have progressively greater slopes. But by suitable change in the light-adaptation conditions, *intersecting curves are possible*. This prediction has bearing on the dispute between Haig (whose data allows only non-intersecting curves) and Wald (whose data gives intersection).

The new formulation satisfies a wide range of data within the limits of experimental variation. It should be of practical value, therefore, in *representing* a great mass of data and curves in the compact form of an equation. This equation can be used to compute adaptation curves in ranges for which there are no data and to predict new results and suggest new avenues of experimental attack.

We frankly admit that the foregoing mathematical formulation does not fit all the experimental data. No formulation could fit all the data. Modern results on dark adaptation agree in their general features, as does the new theory; but if one considers numerical details, he finds inconsistencies that would take several pages to enumerate. We have tried to steer a middle course through these inconsistencies, hoping that the mathematical formulation will be found of practical value in its present form, and that it will serve as a framework for a final theory which may be possible when more complete data are available.

INVERSE INTERPOLATION FOR EIGHT-, NINE-, TEN-, AND ELEVEN-POINT DIRECT INTERPOLATION

By Herbert E. Salzer*

In the present article formulas are given for inverse interpolation for functions that are tabulated at a uniform interval h, and which require direct interpolation polynomials ranging from the seventh to the tenth degree. Here f_i denotes $f(x_0 + ih)$ and the problem is to find p when we are given $f(x_0 + ph)$.

In a previous paper†, the author obtained all the terms involving the first six powers of $(f_p - f_0)$ in the expansion for p in terms of f_p and the tabular values, corresponding to the cases where three- to seven-point direct interpolation was required. In the present paper that same formula for p is extended to include all the terms involving the first ten powers of $(f_p - f_0)$ and, as before, quantities are defined in terms of f_p and the tabular entries to provide for inverse interpolation when eight-, nine-, ten-, or eleven-point formulas are required for direct interpolation. Although the greater part of the expression for p will hardly ever be needed in most practical problems, due to the rapidity of convergence and smallness of many of its terms, its full use can provide unusual accuracy in solving equations (both real and complex) up to the tenth degree when the values of the polynomials are tabulated near the root at equal intervals.

Corresponding to the cases where eight-, nine-, ten-, or eleven-point direct interpolation is used we define quantities $r, s, t, u, v, w, x, y, z$ and $\bar{z}$ as follows:

8-point

$$r = 5040(f_p - f_0)/\Delta, \text{ where } \Delta = -48f_{-3} + 504f_{-2} - 3024f_{-1} - 1260f_0 + 5040f_1 - 1512f_2 + 336f_3 - 36f_4,$$
$$s = [28(f_{-3} + f_3) - 378(f_{-2} + f_2) + 3780(f_{-1} + f_1) - 6860f_0]/\Delta,$$
$$t = [56f_{-3} - 497f_{-2} + 336f_{-1} + 1715f_0 - 3080f_1 + 1869f_2 - 448f_3 + 49f_4]/\Delta,$$
$$u = [-35(f_{-3} + f_3) + 420(f_{-2} + f_2) - 1365(f_{-1} + f_1) + 1960f_0]/\Delta,$$
$$v = [-7f_{-3} - 14f_{-2} + 189f_{-1} - 490f_0 + 595f_1 - 378f_2 + 119f_3 - 14f_4]/\Delta,$$
$$w = [7(f_{-3} + f_3) - 42(f_{-2} + f_2) + 105(f_{-1} + f_1) - 140f_0]/\Delta,$$
$$x = [-(f_{-3} - f_4) + 7(f_{-2} - f_3) - 21(f_{-1} - f_2) + 35(f_0 - f_1)]/\Delta,$$
$$y = z = \bar{z} = 0.$$

9-point

$$r = 40320(f_p - f_0)/\Delta, \text{ where } \Delta = 144(f_{-4} - f_4) - 1536(f_{-3} - f_3) + 8064(f_{-2} - f_2) - 32256(f_{-1} - f_1),$$
$$s = [-36(f_{-4} + f_4) + 512(f_{-3} + f_3) - 4032(f_{-2} + f_2) + 32256(f_{-1} + f_1) - 57400f_0]/\Delta,$$
$$t = [-196(f_{-4} - f_4) + 2016(f_{-3} - f_3) - 9464(f_{-2} - f_2) + 13664(f_{-1} - f_1)]/\Delta,$$

* Mathematical Tables Project, National Bureau of Standards, New York City.

† "A New Formula for Inverse Interpolation," Bull. Amer. Math. Soc., Aug. 1944, pp. 513–516.

$u = [49(f_{-4} + f_4) - 672(f_{-3} + f_3) + 4732(f_{-2} + f_2) - 13664(f_{-1} + f_1) + 19110f_0]/\Delta,$

$v = [56(f_{-4} - f_4) - 504(f_{-3} - f_3) + 1456(f_{-2} - f_2) - 1624(f_{-1} - f_1)]/\Delta,$

$w = [-14(f_{-4} + f_4) + 168(f_{-3} + f_3) - 728(f_{-2} + f_2) + 1624(f_{-1} + f_1) - 2100f_0]/\Delta,$

$x = [-4(f_{-4} - f_4) + 24(f_{-3} - f_3) - 56(f_{-2} - f_2) + 56(f_{-1} - f_1)]/\Delta,$

$y = [(f_{-4} + f_4) - 8(f_{-3} + f_3) + 28(f_{-2} + f_2) - 56(f_{-1} + f_1) + 70f_0]/\Delta,$

$z = \bar{z} = 0.$

10-*point*

$r = 362880(f_p - f_0)/\Delta,$ where $\Delta = 720f_{-4} - 8640f_{-3} + 51840f_{-2} - 241920f_{-1} - 72576f_0 + 362880f_1 - 120960f_2 + 34560f_3 - 6480f_4 + 576f_5,$

$s = [-324(f_{-4} + f_4) + 4608(f_{-3} + f_3) - 36288(f_{-2} + f_2) + 290304(f_{-1} + f_1) - 516600f_0]/\Delta,$

$t = [-944f_{-4} + 10764f_{-3} - 55656f_{-2} + 54096f_{-1} + 103320f_0 - 226296f_1 + 154056f_2 - 47664f_3 + 9144f_4 - 820f_5]/\Delta,$

$u = [441(f_{-4} + f_4) - 6048(f_{-3} + f_3) + 42588(f_{-2} + f_2) - 122976(f_{-1} + f_1) + 171990f_0]/\Delta,$

$v = [231f_{-4} - 2079f_{-3} + 3276f_{-2} + 8316f_{-1} - 34398f_0 + 49014f_1 - 36036f_2 + 14364f_3 - 2961f_4 + 273f_5]/\Delta,$

$w = [-126(f_{-4} + f_4) + 1512(f_{-3} + f_3) - 6552(f_{-2} + f_2) + 14616(f_{-1} + f_1) - 18900f_0]/\Delta,$

$x = [-6f_{-4} - 54f_{-3} + 576f_{-2} - 2016f_{-1} + 3780f_0 - 4284f_1 + 3024f_2 - 1296f_3 + 306f_4 - 30f_5]/\Delta,$

$y = [9(f_{-4} + f_4) - 72(f_{-3} + f_3) + 252(f_{-2} + f_2) - 504(f_{-1} + f_1) + 630f_0]/\Delta,$

$z = [-(f_{-4} - f_5) + 9(f_{-3} - f_4) - 36(f_{-2} - f_3) + 84(f_{-1} - f_2) - 126(f_0 - f_1)]/\Delta,$

$\bar{z} = 0.$

11-*point*

$r = 3628800(f_p - f_0)/\Delta,$ where $\Delta = -2880(f_{-5} - f_5) + 36000(f_{-4} - f_4) - 216000(f_{-3} - f_3) + 864000(f_{-2} - f_2) - 3024000(f_{-1} - f_1),$

$s = [576(f_{-5} + f_5) - 9000(f_{-4} + f_4) + 72000(f_{-3} + f_3) - 432000(f_{-2} + f_2) + 3024000(f_{-1} + f_1) - 5311152f_0]/\Delta,$

$t = [4100(f_{-5} - f_5) - 50440(f_{-4} - f_4) + 292140(f_{-3} - f_3) - 1048560(f_{-2} - f_2) + 1401960(f_{-1} - f_1)]/\Delta,$

$u = [-820(f_{-5} + f_5) + 12610(f_{-4} + f_4) - 97380(f_{-3} + f_3) + 524280(f_{-2} + f_2) - 1401960(f_{-1} + f_1) + 1926540f_0]/\Delta,$

$v = [-1365(f_{-5} - f_5) + 15960(f_{-4} - f_4) - 82215(f_{-3} - f_3) + 196560(f_{-2} - f_2) - 203490(f_{-1} - f_1)]/\Delta,$

$w = [273(f_{-5} + f_5) - 3990(f_{-4} + f_4) + 27405(f_{-3} + f_3) - 98280(f_{-2} + f_2) + 203490(f_{-1} + f_1) - 257796f_0]/\Delta,$

$x = [150(f_{-5} - f_5) - 1560(f_{-4} - f_4) + 6210(f_{-3} - f_3) - 12240(f_{-2} - f_2) + 11340(f_{-1} - f_1)]/\Delta,$

$y = [-30(f_{-5} + f_5) + 390(f_{-4} + f_4) - 2070(f_{-3} + f_3) + 6120(f_{-2} + f_2) - 11340(f_{-1} + f_1) + 13860f_0]/\Delta,$

$$z = [-5(f_{-5} - f_5) + 40(f_{-4} - f_4) - 135(f_{-3} - f_3) + 240(f_{-2} - f_2) - 210(f_{-1} - f_1)]/\Delta,$$

$$\bar{z} = [(f_{-5} + f_5) - 10(f_{-4} + f_4) + 45(f_{-3} + f_3) - 120(f_{-2} + f_2) + 210(f_{-1} + f_1) - 252f_0]/\Delta.$$

Then the extended formula for p now reads:

$$\begin{aligned}
p = {} & r - r^2s + r^3(2s^2 - t) + r^4(-5s^3 + 5st - u) \\
& + r^5(14s^4 - 21s^2t + 3t^2 + 6su - v) \\
& + r^6(-42s^5 + 84s^3t - 28st^2 - 28s^2u + 7tu + 7sv - w) \\
& + r^7(132s^6 - 330s^4t + 180s^2t^2 + 120s^3u - 12t^3 - 72stu - 36s^2v + 4u^2 + 8tv + 8sw - x) \\
& + r^8(-429s^7 + 1287s^5t - 990s^3t^2 - 495s^4u + 495s^2tu + 165st^3 + 165s^3v \\
& \quad - 45t^2u - 45su^2 - 90stv - 45s^2w + 9uv + 9tw + 9sx - y) \\
& + r^9(1430s^8 - 5005s^6t + 5005s^4t^2 + 2002s^5u - 1430s^2t^3 - 2860s^3tu - \\
& \quad 715s^4v + 55t^4 + 660st^2u + 330s^2u^2 + 660s^2tv + 220s^3w - 55tu^2 - 55t^2v - \\
& \quad 110suv - 110stw - 55s^2x + 5v^2 + 10uw + 10tx + 10sy - z) \\
& + r^{10}(-4862s^9 + 19448s^7t - 24024s^5t^2 - 8008s^6u + 10010s^3t^3 + \\
& \quad 15015s^4tu + 3003s^5v - 1001st^4 - 6006s^2t^2u - 2002s^3u^2 - 4004s^3tv - \\
& \quad 1001s^4w + 286t^3u + 858stu^2 + 858s^2tw + 858st^2v + 858s^2uv + 286s^3x - \\
& \quad 22u^3 - 132tuw - 66t^2w - 66sv^2 - 132suw - 132stx - 66s^2y + 11vw + \\
& \quad 11ux + 11ty + 11sz - \bar{z}).
\end{aligned}$$

A GRAPHICAL METHOD FOR THE NUMERICAL SOLUTION OF FREDHOLM'S INTEGRAL EQUATION OF THE SECOND KIND

By Peter L. Tea*

I. The Integral of the Product of Two Functions of y

1. *The Riemann-Stieltjes Integral; the Functional Line; the Functional Scale*

The object of this paper is to develop a graphical method for converting the integral of the product of two functions of y, given in Riemann form

$$I = \int_a^b \phi(y)K(y)\,dy \qquad a \leqq y \leqq b \tag{1}$$

into its equivalent Stieltjes integral form (Ref. 3)

$$I = \int_A^B \phi(y)\,dY(y) \tag{2}$$

where

$$dY(y) = K(y)dy \qquad Y(y) = \int_0^y K(y)dy \tag{3}$$

$$B = Y(b) \qquad A = Y(a) \qquad Y(0) = 0$$

and to show how the numerical value of Eq. (2) or (1) may be obtained by means of a planimeter, for numerical values of a and b. The method will be applied to a problem involving Fredholm's integral equation of the 2nd kind, and to the calculation of the first two iterated functions forming the reciprocal kernel.

We will assume that the integrals, Eqs. (1) and (2) exist, and that the functions $\phi(y)$ and $K(y)$ of Eq. (1) and the product $\psi(y) = \phi(y)K(y)$ shown in Fig. 1a are continuous, real functions of the real variable y, for $a \leqq y \leqq b$. We will name the integral curve $Y(y)$ *the functional line of* $K(y)$, or simply *the functional line.*

Consider that the interval (a, b) is divided by the set of points: $y_0, y_1, \cdots y_k, \cdots, y_n$, where

$$a = y_0 < y_1 < \cdots y_k \cdots < y_n = b \tag{4}$$

and that the set of points, and the origin 0, are projected orthogonally to an axis $0_1y \parallel 0y$, thus defining a second set of points, identical to (4), Fig. 1b. Only two points, y_{k+1} and y_k are shown in Figs. 1a, b, to represent the set (4). The functional line $Y(y)$ of $K(y)$ is plotted to the new axis of abscissae 0_1y.

The projectors of the points y_0 to y_n on the 0 y axis will cut the set of points $Y(y_0)$ to $Y(y_n)$ on the functional line. If the set of points on the functional line, including the origin 0_1, are projected orthogonally to a third axis 0_1y, placed to

* Assistant Professor of Drafting in the School of Technology, The College of the City of New York, New York, N. Y.

the left of Fig. 1b and $\perp 0_1 y$, then the points of division on $0_2 y$, Fig. 1c, if marked with their original designation on the uniform scale $0y$, will form a functional scale of $K(y)$.

The distance between the points y_k and y_{k+1}, on the functional scale $0_2 y$ will be equal to

$$Y(y_{k+1}) - Y(y_k) = K(y)(y_{k+1} - y_k) \tag{5}$$

where the y values are shown in true length on the uniform scale $0y$ and $(y_{k+1} - y_k) \to 0$, as $n \to \infty$.

If $\phi(y)$ is plotted on the functional scale $0_2 y$, the area of the resultant curve, measured by a planimeter for numerical values of a and b, will be the numerical value of the integrals Eq. (1) and Eq. (2). Note that the location of the ordinates on the functional scale $0_2 y$ corresponding to selected ordinates on the

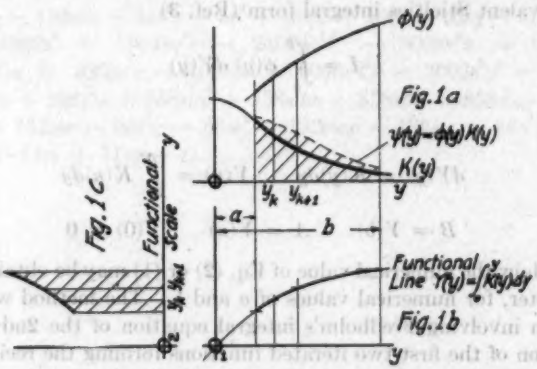

FIGS. 1a, b, c. Graphical method for converting the integral of the product of two functions of y from the Riemann form to the Stieltjes form.

uniform scale $0y$ will be geometrically exact. But the accuracy of the resultant curve will depend on the skill of the draftsman in drawing the curve through a suitable number of points. It is only when the functional scale is used repeatedly that it is of value to plot it. Should a single value of Eq. (1) be desired, then the product curve $\psi(y)$ is drawn and the planimeter used to get the area, Fig. 1a.

There is nothing better than the analytical solution of Eq. (1) in terms of a and b. If not obtainable, then the numerical values, by planimeter as explained, for a range of values of a and b, for easy interpolation, will be satisfactory in a practical problem.

2. *Properties of the Functional Line and Functional Scale*

Should there be any difficulty in integrating Eq. (3), the functional line can be obtained by means of an integraph on the plotted curve $K(y)$, or by obtaining points on $Y(y)$ by means of a planimeter.

(a) *If $K(y)$ is positive at all points within the interval (a, b), and single valued, then the functional line and scale will be non-decreasing with increasing y, hence will be single valued within the interval.*

This must be so since, for y positive $Y(y)$ increases with y, and $K(y)$ must cross the $0y$ axis to register a maximum in $Y(y)$, followed by a decrease. If $K(y)$ touches $0y$ in one of several possible ways, tangentially, or at a cusp or point of double tangency, or if $K(y)$ has finite stretches of zero values, but in no case crosses the axis $0y$, then $Y(y)$ will be non-decreasing as y increases, and hence must be single valued. Should the origin 0 be within the interval, in a similar manner $Y(y)$ will be non-increasing as y increases in the negative direction. Which proves statement (a).

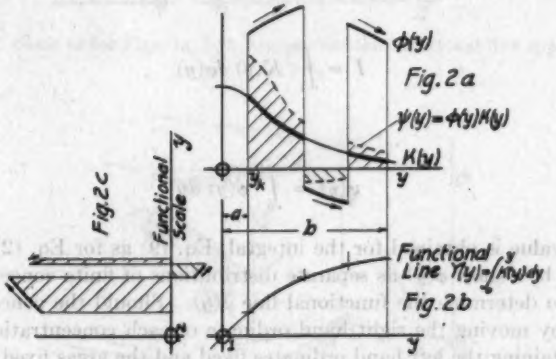

FIGS. 2a, b, c. Same as for Figs. 1a, b, c, except that one function is discontinuous

Should $K(y)$ have a negative segment or segments within the interval, of largest value $|C|$, by adding C to $K(y)$ the $Y(y)$ will be single valued, and

$$I = \left[\text{Area under } \phi(y) \text{ in Fig. 1c in sq. inches} - C\int_a^b \phi(y)\,dy\right] \Big/ mn \qquad (6)$$

where m and n are scales to which the drawing is made.

(b) *Scales of the drawing.*—A unit value of y, $K(y)$, and $Y(y)$ is represented by m inches, and a unit value of $\phi(y)$ by n inches. The values of the drawing scales m and n should be chosen with due regard to the accuracy desired, and to the capacity of the planimeter.

(c) *With the functional scale $Y(y)$ fixed to be single valued, $\phi(y)$ may be any single valued function, finite, continuous, or finitely discontinuous, having + and − regions, and zero value regions.* If an arrow, drawn on $\phi(y)$, Fig. 2c, in the direction of increasing y, is used as the direction of motion of the planimeter stylus, the correct net area will be obtained.

High density values of the function $\phi(y)$ may occur in narrow strips. The

contribution of such strips to $\phi(y)$ may be considered concentrated at such points as y_k, and have a value i_k

$$i_k = \phi(y_k)(y_{k+1} - y_k) \tag{7}$$

which, for n concentrations, will contribute the following value to the integral

$$\sum_1^n i_k K(y_k) \tag{8}$$

The graphical method applies for high concentrations, but their contribution to the value of the integral is more conveniently calculated by Eq. (8).

(d) *Step function for the functional line $Y(y)$.*

The function $\phi(y)$ may be used to form the functional line $\varphi(y)$. Eq. (1) becomes

$$I = \int_A^B K(y)\, d\varphi(y) \tag{9}$$

where

$$\varphi(\eta) = \int_0^y \phi(y)\, dy$$

The same value is obtained for the integral, Eq. (9) as for Eq. (2).

Figs. 3a, b, c show $\phi(y)$ as separate distributions of finite concentration, and $\phi(y)$ used to determine the functional line $\varphi(y)$. Should the concentrations be increased, by moving the right hand ordinate of each concentration to the left while maintaining the left hand ordinates fixed and the areas fixed and equal to i_k as in Eq. (7), the functional line $\varphi(y)$ will approach a step function, Fig. 3b, and $K(y)$ will approach a step function, shown dotted in Fig. 3c. In this case the integral approaches the value

$$\int_A^B K(y)\, d\varphi(y) = \sum_1^n i_K K(y_K) \tag{10}$$

as in Eq. (8).

For a single valued functional scale there is, in general, a point to point correspondance, in the same direction, between points on $0y$ and points on $0_\varphi y$, and a correspondance in integral values between any pair of points. For step functions for the functional line, all the points on a step have a single point on the $0_\varphi y$ scale, hence correspond to a zero area in the graph to the axis $0_\varphi y$, and they have zero area in the graph to the axis $0y$.

(e) *The conversion of the Riemann Integral, Eq. (1) into its Stieltjes form, Eq. (2), as the result of two successive projections of either function.*

In Fig. 3d, with $K(y)$ forming the functional cylinder $Y(y)$, if $\phi(y)$ in plane $\phi 0y$ is projected (orthogonally from $\phi 0y$) to the functional cylinder (or prism), followed by the projection of $\phi(y)$ from the cylinder orthogonally to the plane $\phi 0_\varphi y$, where $0_\varphi y$ is the functional scale, the area under the second projection of $\phi(y)$ will be equal to the value of the integral of Eqs. (2) or (1).

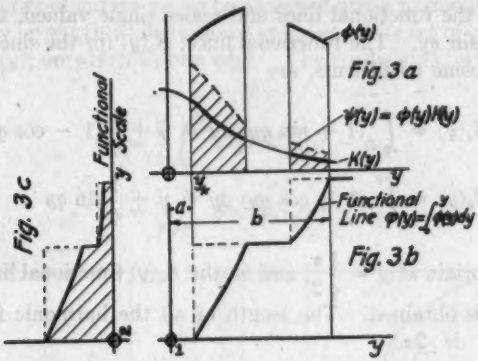

FIGS. 3a, b, c. Same as for Figs. 1a, b, c, except that the functional line approaches a step function

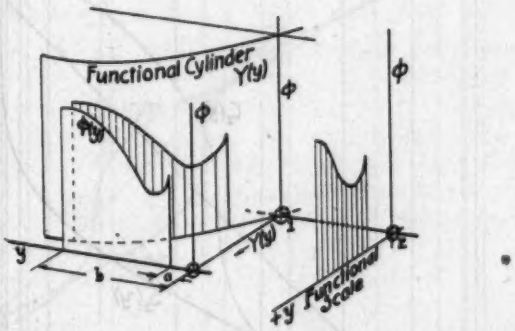

FIG. 3d. An integral of the product of two functions of y in Riemann form can be converted into the Stieltjes form by two projections.

3. *Application of the Functional Line and Scale to Harmonic Analysis*

With certain restrictions, a periodic function $\phi(y)$ of period 2π can be expanded into a Fourier series (ref. 2),

$$\phi(y) = a_0/2 + \sum_{q=1}^{q=\infty} (a_q \cos qy + b_q \sin qy) \qquad q = 1, 2, \cdots n \to \infty \tag{11}$$

where the coefficients for the full cycle are

$$b_q = \frac{1}{\pi}\int_0^{2\pi} \phi(y) \sin qy \, dy$$

$$a_q = \frac{1}{\pi}\int_0^{2\pi} \phi(y) \cos qy \, dy \tag{12}$$

$$a_0 = \frac{1}{\pi}\int_0^{2\pi} \phi(y) \, dy \quad \text{for} \quad q = 0$$

To maintain the functional lines and scales single valued, unity is added to cos qy, and to sin qy. The functional lines: $S_q(y)$ for the sine coefficients, and $C_q(y)$ for the cosine coefficients, are

$$S_q(y) = \int_0^y (1 + \sin qy)\, dy = y + \frac{1}{q}(1 - \cos qy)$$
$$C_q(y) = \int_0^y (1 + \cos qy)\, dy = y + \frac{1}{q}\sin qy \tag{13}$$

Place a new origin at $y = \frac{1}{q}\frac{\pi}{2}$, and *on* the $S_q(y)$ functional line, and the $C_q(y)$ functional line is obtained. The length of all the harmonic functional scales, for a full cycle, is 2π.

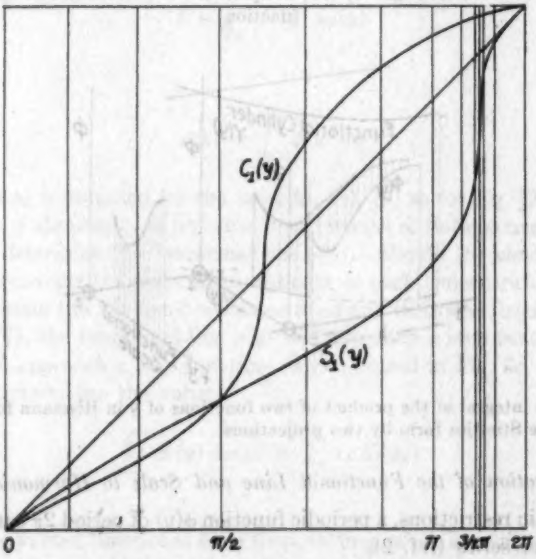

FIG. 4a. Functional lines $C_1(y)$ and $S_1(y)$, and Chart of ordinates for $S_1(y)$ for 30° intervals

Fig. 4a shows the $S_1(y)$ and the $C_1(y)$ harmonic functional lines, drawn to the functional scales as abscissae. A set of ordinate lines to the functional scale for $S_1(y)$ is shown for 30° intervals on the full cycle. A set of such ordinate lines will be called a *chart of ordinate lines*. Fig. 4b shows the $S_2(y)$ and the $C_2(y)$ harmonic functional lines, and a chart of ordinate lines for $S_2(y)$ for intervals of 30°.

(a) *Method of using the Charts of Ordinate Lines for the Harmonic Scales* $S_q(y)$ *and* $C_q(y)$.

If a large number of curves are to be analysed and a harmonic analyser is not available, it may be worth while to make up an accurate set of chart of ordinates of $S_q(y)$ and $C_q(y)$, on which to plot $\phi(y)$. The coefficients, in Stieltjes integral form, are

$$a_q = \frac{1}{\pi}\int_0^{2\pi} \phi(y)\, dC_q(y) - a_0$$
$$b_q = \frac{1}{\pi}\int_0^{2\pi} \phi(y)\, dS_q(y) - a_0 \qquad (14)$$

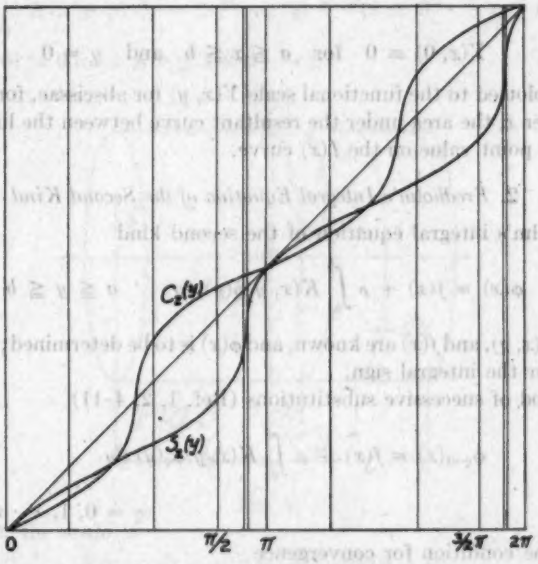

FIG. 4b. Functional lines $C_2(y)$ and $S_2(y)$, and Chart of ordinates for $S_2(y)$ for 30° intervals

Apply the factor $1/mn$ for the drawing scales, as in Eq. (6), to Eqs. (14). If the highest harmonic desired is q, divide the 2π cycle of the $\phi(y)$, the curve to be analysed, into $4q$ equal parts by $4q + 1$ ordinates. The charts of ordinate lines will have ordinates corresponding to these divisions. Line up the charts to a T square, and lay off each successive ordinate $\phi(y_k)$ on all the charts for $S(y_k)$ and $C(y_k)$. Draw the curves and measure the areas, applying Eqs. (14) and (6). Should $\phi(y)$ show sharp changes in direction in any locality, choose a suitable point on the curve and draw a new ordinate line through that point and new ordinate lines corresponding thereto on all the charts.

From Eqs. (13) and (14), as $q \to \infty$, the $S_q(y)$ and $C_q(y)$ functional lines approach the 45° line shown on Figs. 4a, b and the coefficients $\to 0$; but the latter result depends on the nature of $\phi(y)$.

II. The Integral of the Product of Two Functions of y, One Function Having a Parameter x

1. *The integral of the product of two functions, one having a parameter x, may be written as a Stieltjes integral*

$$I(x) = \int_a^b K(x, y)\phi(y)\,dy = \int_A^B \phi(y)\,dY \qquad a \leqq y \leqq b \tag{15}$$

$$dY = K(x, y)\,dy \qquad Y = Y(x, y) = \int_0^y K(x, y)\,dy \tag{16}$$

where

$$Y(x, 0) = 0 \quad \text{for} \quad a \leqq x \leqq b \quad \text{and} \quad y = 0$$

If $\phi(y)$ is plotted to the functional scale $Y(x, y)$ for abscissae, for any value of the parameter x, the area under the resultant curve between the limits A and B will be the x point value on the $I(x)$ curve.

2. *Fredholm's Integral Equation of the Second Kind*

In Fredholm's integral equation of the second kind

$$\phi(x) = f(x) + \rho \int_a^b K(x, y)\phi(y)\,dy \qquad a \leqq y \leqq b \tag{17}$$

the kernel $K(x, y)$, and $f(x)$ are known, and $\phi(x)$ is to be determined; but ϕ appears as $\phi(y)$ under the integral sign.

The method of successive substitutions (Ref. 1, 2, 4–11)

$$\phi_0(x) = f(x) \qquad \phi_{q+1}(x) = f(x) + \rho \int_a^b K(x, y)\phi_q(y)\,dy$$

$$q = 0, 1, \cdots n \to \infty \tag{18}$$

subject to the condition for convergence

$$|\rho M|\,(b - a) < 1 \tag{19}$$

is a suitable method for the application of the graphical procedure, based on functional lines and scales and charts of ordinate lines. In Eq. (19), M is the largest value assumed by $K(x, y)$ in the interval. In the method of successive substitutions the integrations can be performed graphically, in the order given in Eqs. (18); thus successive graphical approaches to the desired $\phi(x)$ may be obtained.

(a) *Preparation of the charts of ordinates.*

In an applied problem the approximate form of the unknown $\phi(x)$ may be estimated by physical reasoning. Divide the interval (a, b) into an adequate number of parts n, not necessarily equal, by the points of division $k = 1, 2, \cdots n + 1$. The division serves for both x and y in the interval. Make up a chart of ordinates for each x_k value, and an ordinate line on each chart for each y_k value. This is necessary because of the method of Eqs. (18), where $\phi_q(y)$ in the

integral yields the value of $\phi_{q+1}(x)$, which in turn is used in the integral as $\phi_{q+1}(y)$, etc. Should $\phi(x)$ develop a sudden change in direction during the graphical process, introduce a new chart for an x value in the neighborhood of the change, and add the ordinate line for the corresponding y value to all the charts. If the process is convergent, any errors will diminish as the process continues.

3. *Shifting Functions For the Kernel*

The graphical method is especially time saving if the kernel is of the form $K(x \pm y)$, in which case the functional lines and scales are, for any value of x

$$Y(x \pm y) = \int_0^y K(x \pm y)\, dy = \pm F(x \pm y) \mp F(x \pm 0) \qquad a \leqq y \leqq b \qquad (20)$$

where $Y(x \pm 0) \equiv 0$ for $a \leqq x \leqq b$ and $y = 0$.

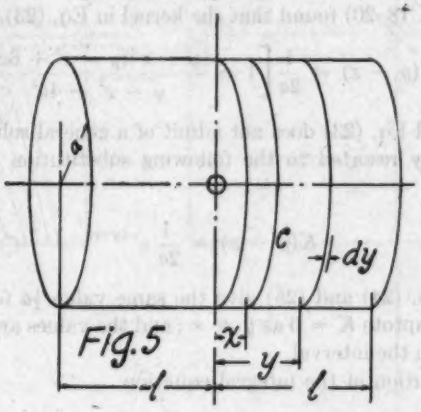

Fig. 5

FIG. 5

For $x = 0$, the scale is

$$Y(0 \pm y) = \pm F(0 \pm y) \mp F(0 \pm 0) \qquad (21)$$

Eqs. (20) and (21) represent the same curve except for the position of the origin. All the functional scales for x values are obtainable by shifting the origin on the functional line of Eq. (21) by a distance x and taking the origin on the intercept.

III. Application of the Graphical Method to a Problem in the Interreflection of Light on a Surface

In Fig. 5, that portion of the luminosity on the inside surface of the circular cylinder, at the circle C, distant x from the origin 0, due to the reflection from the area of the circular band, of width dy, and at the distance y from the origin, is

$$\rho K(y - x)dy \qquad (22)$$

where ρ (considered constant) is the reflection factor of the surface at any point, and $K(y - x)$ depends on the geometry of the surface in applying Lambert's

Law of reflection from mat surfaces (ref. 17–22). The luminosity at y is taken as of unit value in (22).

If $\phi_0(x)$ is the luminosity at the circle C with the interreflections suppressed, i.e. with the exciting luminosity only, hence $\rho = 0$, and $\phi(y)$ is the actual luminosity at y with interreflections, then

$$\phi(x) = \phi_0(x) + \rho \int_{-l}^{l} K(y - x)\phi(y)\, dy \tag{23}$$

will be the value of the luminosity at any value x of the cylinder, between the limits $\pm l$, under conditions of interreflections. The consideration of this problem will give a physical meaning to the successive approximations in Eqs. (18), and will explain how, for some values of $\rho > 1$, which are possible, (ref. 22) an expanding series is obtained.

H. Buckley (ref. 18–20) found that the kernel in Eq. (23) has the form

$$K(y - x) = \frac{1}{2a}\left[1 - \frac{|y - x|(y - x^2 + 6a^2)}{\sqrt{y - x^2 + 4a^2}}\right] \tag{24}$$

With this kernel Eq. (23) does not admit of a general solution by the known methods. Buckley resorted to the following substitution for the kernel (ref. 18, 19, 24)

$$K(y - x) \doteq \frac{1}{2a}\, e^{-|y-x|} \tag{25}$$

For $x = 0$, Eqs. (24) and (25) give the same value $\frac{1}{2}a$ for $y = 0$, and both approach the asymptote $K = 0$ as $y \doteq \infty$; and the values are fairly close for the same values of y in the interval.

The general solution of the integral equation

$$\phi(x) = \phi_0(x) + \frac{\rho}{2a} \int_{-l}^{l} e^{-|y-x|}\phi(y)\, dy \tag{26}$$

for $\rho = 1$, $l = 1$, $a = 1$, is

$$\phi(x) = \tfrac{1}{3}\phi_0(x)[5 - x^2] \tag{27}$$

W. R. Hedeman, Jr. (ref. 17) solved this problem using the kernel of Eq. (24) in the Cinema Integraph at the Massachusetts Institute of Technology as part of a thesis for the degree of Doctor of Science in Electrical Engineering. He found values for $\phi(x)$ as much as 4% higher than given by Eq. (27).

We will apply the graphical method to Eq. (26), for the same boundary conditions, and for $\phi_0(x) = 1$, using the method of successive substitutions. Hedeman adopted the method of Volterra of the reciprocal kernel. The graphical method will be used in section IV to obtain the first two iterated functions of the reciprocal kernel.

The kernel and the functional scale, Eqs. (25) and (28), both for $x = 0$, are plotted in Figs. 6a and 6b respectively.

$$Y(y - 0) = \pm \tfrac{1}{2}[1 - e^{-|y|}] \tag{28}$$

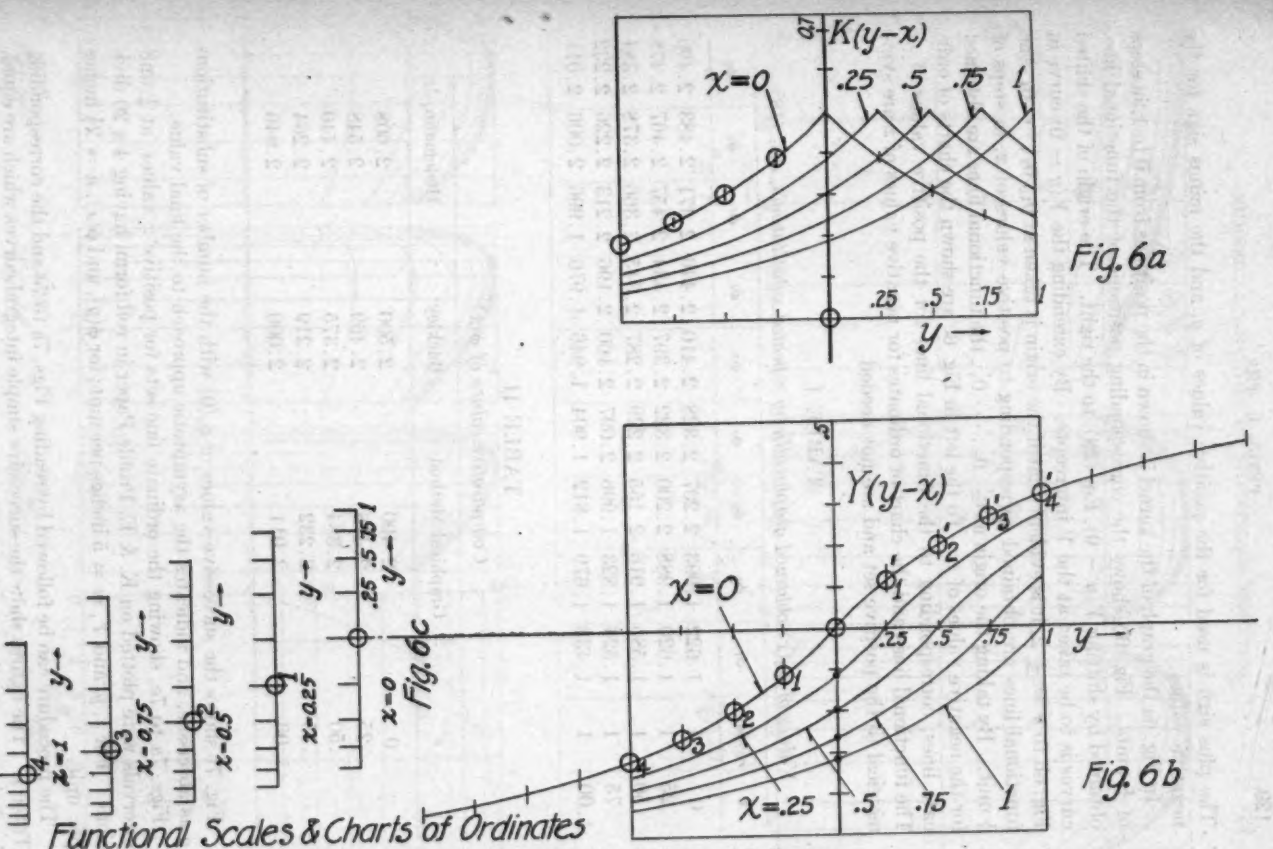

FIG. 6. Functional Scales, & Charts of Ordinates

The plus sign is used for the positive values of y, and the minus sign for the negative values.

In Fig. 6a the graph of the kernel is shown in the positions from 0 to 1, in steps of $\frac{1}{4}$ units. Fig. 6b shows the corresponding positions of the functional line, obtained by shifting $Y(y - 0)$, Eq. (28), to the right. The origin of the shifted curves is to be taken at the Y intercepts. By extending the $Y(y - 0)$ curve in Fig. 6b to $y = \pm 2$, it is evident that if the origin is taken at $0_1, 0_2, \cdots 0_4$, the functional lines are obtained corresponding to positive values of x, in steps of $\frac{1}{4}$ unit. By taking the origin at $0_1', 0_2', \cdots 0_4'$, the functional lines are obtained for the negative values of x. To the left in Fig. 6c are shown the charts of ordinate lines, corresponding to the functional lines for the positive values of x. The functional lines and the chart of ordinates for negative values of x are symmetrical to the positive set and are not needed.

TABLE I

Values of $\phi_q(x)$ obtained graphically by repeated substitutions, eqs. (18)

x	ϕ_0	ϕ_1	ϕ_2	ϕ_3	ϕ_4	ϕ_5	ϕ_6	ϕ_7	ϕ_8	ϕ_9
0	1	1.622	1.993	2.207	2.328	2.410	2.446	2.471	2.483	2.490
.25	1	1.620	1.988	2.200	2.322	2.397	2.434	2.457	2.467	2.478
.50	1	1.585	1.916	2.155	2.229	2.287	2.345	2.366	2.378	2.384
.75	1	1.524	1.823	1.996	2.097	2.160	2.196	2.213	2.226	2.232
1.00	1	1.438	1.679	1.812	1.904	1.946	1.976	1.996	2.006	2.011

TABLE II

Comparative values of $\phi(x)$

x	Graphical Method	Buckley	Hedemann, Jr.
0	2.490	2.500	2.608
.25	2.478	2.469	2.548
.50	2.384	2.375	2.440
.75	2.232	2.219	2.264
1.00	2.011	2.000	2.046

Fig. 7f shows the successive values of $\phi_q(0)$ with the number of substitutions q as abscissae, and indicates the asymptotic approach to the final value.

Figs. 7a to 7e, showing the ordinate line sets for positive x values, at $\frac{1}{4}$ unit intervals were plotted on K. & E. Profile Paper in roll form, having 4 x 20 divisions. For x, y, and Y, $m = 5$ inches per unit; for $\phi(y)$, and $\phi(x)$, $n = 2\frac{1}{2}$ inches per unit.

The procedure can be followed by reading Figs. 7a to 7e and the corresponding Table I. The figures show the successive simple integral curves which are equal, in their areas, to the integrals in Eqs. (18), after applying Eq. (6), with $C = 0$. These numbers were increased by the value of $\phi_0(x) = 1$, and entered into Table I, and also used in plotting the curves on the charts of ordinates, Figs. 7 to 7e, to

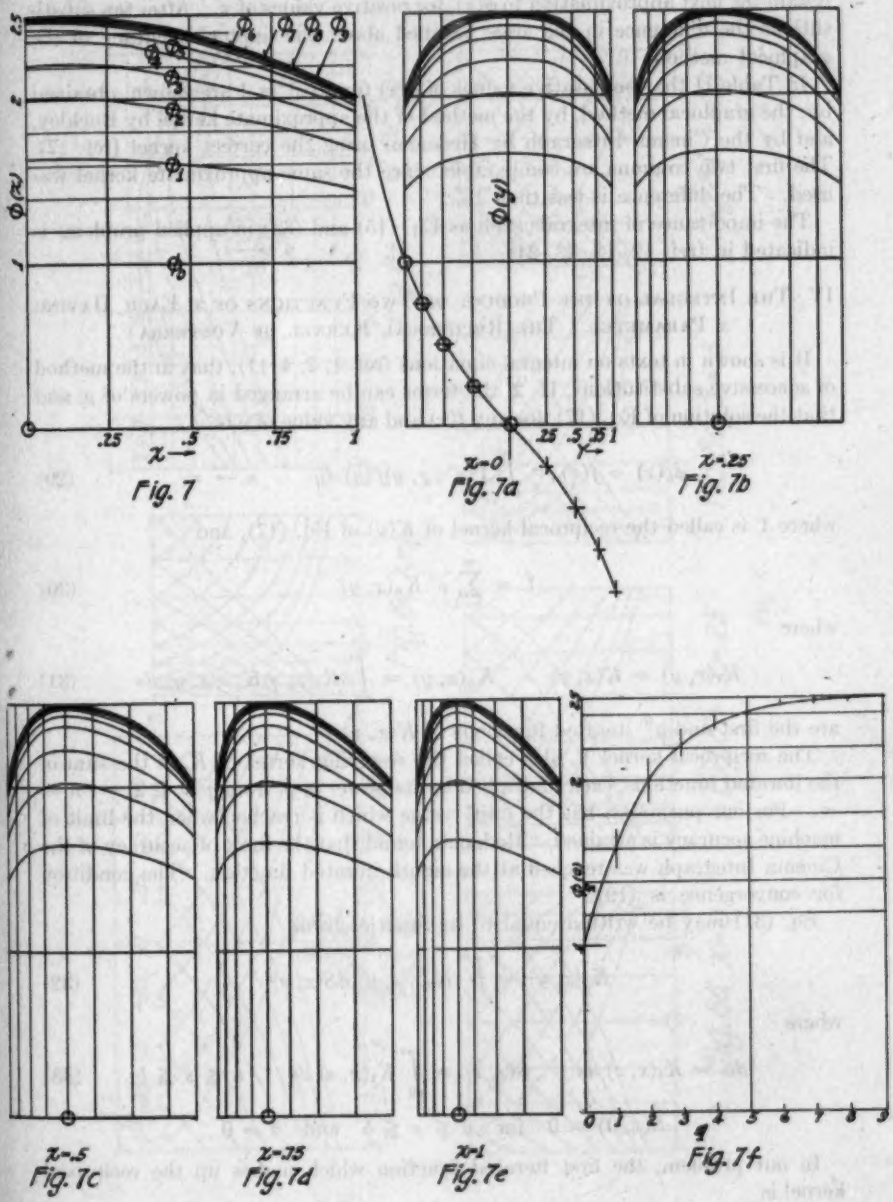

FIG. 7

obtain the next approximation to $\phi(x)$, for positive values of x. After ten substitutions the difference in the areas reached about the limit of accuracy of the graphical method.

In Table II the comparative values of $\phi(x)$ for $\phi_0(x) = 1$ are shown, obtained by: the graphical method, by the method of the approximate kernel by Buckley, and by the Cinema Integraph by Hedeman using the correct kernel (ref. 17). The first two columns are comparable, since the same approximate kernel was used. The difference is less than 1%.

The importance of integrals such as Eq. (15) and (33) in applied problems is indicated in (ref. 12, 13, 23, 24).

IV. The Integral of the Product of Two Functions of s, Each Having a Parameter. The Reciprocal Kernel of Volterra

It is shown in texts on integral equations (ref. 1, 2, 4–11), that in the method of successive substitutions, II, 2, the terms can be arranged in powers of ρ, and that the solution of Eq. (17), for any $f(x)$ and any value of ρ is

$$\phi_n(x) = f(x) + \int_a^b \Gamma(\rho^n; x, y) f(y)\, dy \qquad n \to \infty \tag{29}$$

where Γ is called the reciprocal kernel of $K(y)$ of Eq. (17), and

$$\Gamma = \sum_{n=1}^{\infty} \rho^n K_n(x, y) \tag{30}$$

where

$$K_1(x, y) = K(x, y) \qquad K_q(x, y) = \int_a^b K_1(x, s) K_{q-1}(s, y)\, ds \tag{31}$$

are the first and q^{th} iterated functions of $K(x, y)$.

The reciprocal kernel Γ, also called the resolving kernel of K, is the sum of the iterated functions, each multiplied by its power of ρ, from $q = 1, 2, \cdots n \to \infty$. For our purpose n has the finite value which is reached when the limit of machine accuracy is attained. Hedeman found that the limit of accuracy of the Cinema Integraph was reached at the eighth iterated function. The condition for convergence is (19).

Eq. (31) may be written equal to its Stieltjes form

$$K_q(x, y) = \int_A^B K_{q-1}(s, y)\, dS(x, s) \tag{32}$$

where

$$dS = K_1(x, s)\, ds \qquad S(x, s) = \int_0^s K_1(x, s)\, ds \qquad a \leqq s \leqq b \tag{33}$$

$$S(x, 0) \equiv 0 \quad \text{for} \quad a \leqq x \leqq b \quad \text{and} \quad s = 0$$

In our problem, the first iterated function which makes up the reciprocal kernel is

$$K_1(x, y) = \tfrac{1}{2} e^{-|y-x|} \tag{34}$$

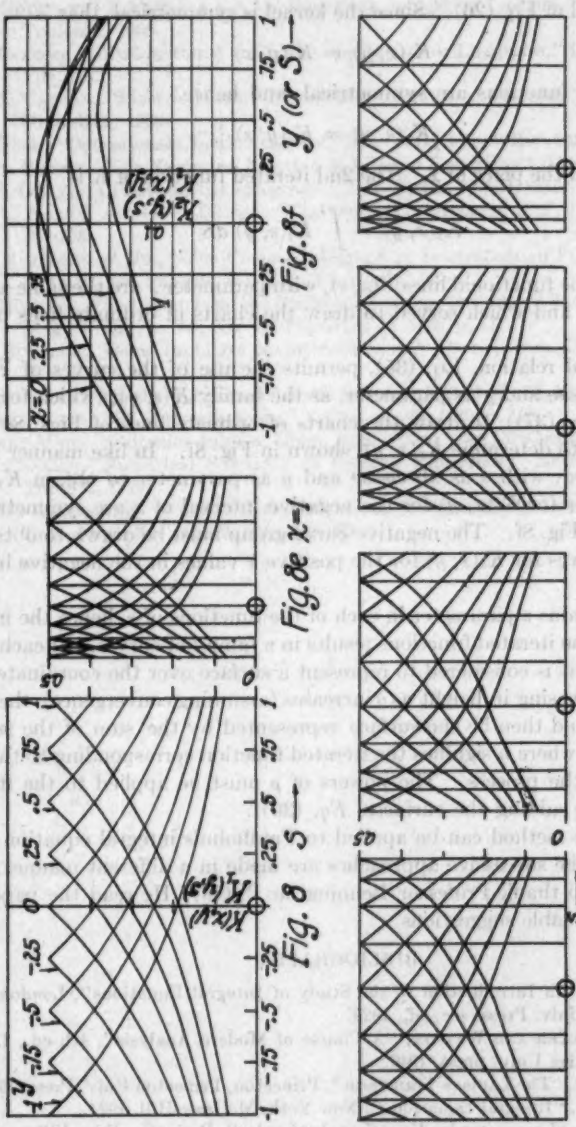

Fig. 8a x=0 Fig. 8b x=.25 Fig. 8c x=.5 Fig. 8d x=.75

Fig. 8 s —

Fig. 8e x=1 Fig. 8f y (or s) —

This family of curves is shown in Fig. 6a for positive values of x, and is identical to the kernel of Eq. (26). Since the kernel is symmetrical, that is

$$K_1(x, y) = K_1(y, x) \tag{35}$$

all the iterated functions are symmetrical, and hence

$$K_q(s, y) = K_q(y, s) \tag{36}$$

written with s in the place of x. The 2nd iterated function of K is

$$K_2(x, y) = \int_{-1}^{1} K_1(s, y)\, dS \tag{37}$$

Notice that the functional lines $S(x, s)$, with parameter x are the same as those used in Fig. 6b and which served to draw the charts of ordinate lines of Figs. 7a to e.

The reciprocal relation, Eq. (35), permits the use of the curves of Fig. 6a, with s as abscissae and y as parameter, as the family $K(s, y)$, (which forms the integrand of Eq. (37)), to draw the charts of ordinate lines of Figs. 8a to 8e, which are used to determine $K_2(x, y)$, shown in Fig. 8f. In like manner Fig. 8f can be relabelled, with s as abscissae and y as parameter to obtain $K_3(x, y)$, etc. The curves for $K_2(x, y)$ for the negative interval of x are symmetrical to those shown in Fig. 8f. The negative curve group must be drawn to obtain the parts of the curves for $K_3(x, y)$ for the positive x values in the negative interval of y.

Eq. (32) contains a parameter in each of the functions of s, hence the integration to obtain the iterated functions results in a family of curves. If each of the iterated functions is considered to represent a surface over the coordinate plane of x and y, decreasing in height as q increases (assuming convergence), the reciprocal kernel would then be the surface represented by the sum of the surfaces from K_1 to K_n, where n signifies the iterated function corresponding to the limit of accuracy of the process. The powers of ρ must be applied to the iterated functions before adding the surfaces, *Eq.* (30).

The graphical method can be applied to Fredholm's integral equation of the first kind; but the successive approaches are made in a different manner. The author wishes to thank Professor Bennington P. Gil. He read the paper and offered some valuable suggestions.

BIBLIOGRAPHY

[1] M. Bôcher, "An Introduction to the Study of Integral Equations", London, Cambridge Univ. Press, sec. ed., 1926.
[2] E. T. Whittaker and Watson, "A Course of Modern Analysis", 4th ed., London, Cambridge Univ. press, 1940.
[3] D. V. Widder, "The Laplace Transform", Princeton, Princeton Univ. Press, 1941.
[4] W. V. Lovitt, "Integral Equations", New York, McGraw-Hill, 1924.
[5] V. Volterra, "Leçons sur les Equations Intégrales", Paris, Gauthier-Villars, 1913.
[6] Courant, Hilbert, "Methoden der Math. Physik", Berlin, J. Springer, 2nd ed., 1931.
[7] G. Vivanti, "Equazioni Integrali Lineari", Milano, Hoepli, 1916.
[8] D. Hilbert, "Grundzüge Einer Allgemeinen Theorie der Linearen Integralgleichungen", Leipzig u. Berlin, Teubner, 1912.

[9] E. Goursat, "Cours d'Analyse Math.", Paris, Gauthier-Villars, Vol. III, 3rd ed., 1922.
[10] E. Goursat, "Recherches sur les Equations Intégrales Linéaires", Ann. Fac. Sc., Toulouse, 1908.
[11] T. Lalesco, "Introduction à la Théorie des Equations Intégrales," Paris, Hermann & Fils, 1912.
[12] J. R. Carson, "Electric Circuit Theory and Operational Calculus", New York, McGraw-Hill, 1926.
[13] V. Bush, "Operational Circuit Analysis", New York, John Wiley, 1937.
[14] G. S. Brown, "The Numerical Solution of Integral Equations", Thesis, M. I. T.
[15] T. S. Gray, "A Photoelectric Integraph", J. F. I., 212, 77–102, 1931.
[16] H. L. Hazen, and G. S. Brown, "The Cinema Integraph," J. F. I., 220, 21–44, and 185–205.
[17] W. R. Hedeman, Jr., "The Cinema Integraph in Interreflection Problems," Journal of Math. and Physics, vol. XX, No. 4, 1941, 402–417.
[18] H. Buckley, "Radiation from the Inside of a Circular Cylinder," Part I, Philosophical Mag., 4, 1927, p. 753; Part II, Phil. Mag., 6, 1928, p. 447.
[19] H. Buckley, "Some Problems on Interreflection," Proc. Intern. Cong. on Illumin., 1928, p. 888.
[20] H. Buckley, "On the Blackness of Black Bodies," J. O. S. A., 18, 1929, p. 216.
[21] Parry Moon, "On Interreflections," J. O. S. A., 30, 1940, p. 195.
[22] Parry Moon, "Scientific Basis of Illum. Eng.", New York, McGraw-Hill, 19.
[23] G. Prasad, "Numerical Solutions of Integral Equations," Intern. Math. Cong., Toronto, 1924.
[24] E. T. Whittaker, "Numerical Computations of Solutions of Integral Equations", Proc. Royal Soc., SCIV, 1918, 367–383.

REMARKS ON THE METHOD OF STATIONARY PHASES

By Aurel Wintner

The principle of stationary phases (Kelvin) states that, if $F(x)$ and $\phi(x)$ are sufficiently smooth, then

(i) the asymptotic behavior of

$$\int_a^b F(x)e^{it\phi(x)}\,dx$$

as $t \to \infty$ depends only on the contribution of the immediate vicinity of those points $x = x_0$ at which $\phi(x)$ becomes stationary, $\phi'(x_0) = 0$, (provided that there exist such points), and

(ii) the asymptotic contribution of the vicinities of these points x_0 can simply be obtained by replacing the functions $F(x)$ and $\phi(x)$ by their respective approximations, $F(x_0)$ and $\phi(x_0) + \frac{1}{2}(x - x_0)^2\phi''(x_0)$, near x_0.

The principle underlying the usual explanation offered by the physicists for this rule (cf. [2]) is quite sound, since it can be legalized as follows:

(i) On a closed x-interval not containing a zero of the (continuous) derivative $\phi'(x)$, the function $\phi(x)$ is strictly monotone. Hence, $\phi(x)$ can be introduced as an integration variable on every such an x-interval. The contribution of the latter then appears in the form

$$\int_0^c f(x)e^{itz}\,dx, \tag{1}$$

where ϕ (plus a constant) is denoted simply by x, and $f(x)$ is a function of class C' if $\phi(x)$ and $F(x)$ were of class C'' and class C' respectively. But, if $f(x)$ is of class C', a partial integration shows that the last integral is $O(1/t)$ as $t \to \infty$. Hence, (i) is correct if the contribution of the immediate vicinities of the points x_0, considered under (ii), proves to be of a lower order than $O(1/t)$.

(ii) What concerns the contributions of the immediate vicinities of the stationary points, x_0, of $\phi(x)$, Taylor's formula

$$\phi(x) = \phi(x_0) + \tfrac{1}{2}(x - x_0)^2\phi''(x_0) + o(x - x_0)^2,$$

where $\phi'(x_0) = 0$, makes possible the introduction of exactly one of the two "uniformizing" integration variables

$$y = \{\pm\, 2[\phi(x) - \phi(x_0)]/\phi''(x_0)\}^{\frac{1}{2}}$$

on a sufficiently small x-interval to the right, and on such an interval to the left, of x_0, *provided that* $\phi''(x_0) \neq 0$. If x_0 is either of the end points, a or b, of the full x-range, then only one of these two contributions exists. At any rate, the normal form corresponding to (1) in case of a one-sided immediate vicinity of a stationary point x_0 is seen to be an integral of the form

$$\int_0^c f(x)e^{\pm itx^2}\,dx, \qquad (c > 0). \tag{2}$$

Accordingly, what the principle really states is that, under reasonable restrictions of the behavior of $f(x)$ as $x \to +0$, the asymptotic behavior of either of the functions (2) of t, as $t \to \infty$, is the same as that of the corresponding function

$$\int_0^c f(+0)e^{\pm itx^2}\,dx, \qquad (c > 0).$$

Since the latter is identical with

$$f(+0)\left\{\int_0^\infty e^{\pm itx^2}\,dx - \int_{(ct)^{\frac{1}{2}}}^\infty e^{\pm itx^2}\,dx\right\}\Big/ t^{\frac{1}{2}} = f(+0)\{(\tfrac{1}{2}\pi)^{\frac{1}{2}}(\tfrac{1}{2} \pm \tfrac{1}{2}i) + o(1)\}/t^{\frac{1}{2}},$$

(and since $1/t^{\frac{1}{2}}$ *is* of a lower order than the $O(1/t)$ omitted above), it follows that everything depends on the truth or falsehood of the asymptotic relation

$$\int_0^c f(x)e^{itx^2}\,dx \sim \tfrac{1}{2}(1+i)(\tfrac{1}{2}\pi)^{\frac{1}{2}}f(+0)/t^{\frac{1}{2}}, \qquad (c > 0,\ t \to \infty). \tag{3}$$

Needless to say, (3) is understood to mean

$$\int_0^c f(x)e^{itx^2}\,dx = o(1/t^{\frac{1}{2}}), \qquad (c > 0,\ t \to \infty), \tag{4}$$

if $f(+0) = 0$. Conversely, if (4) is true under the assumption $f(+0) = 0$, then the replacement of $f(x)$ by $f(x) - f(+0)$ supplies (3) for any value of $f(+0) =$ const.

It was proved by Perron [5] that the crucial relation (3) is true whenever $f(x)$ is of class C'''.

The writer pointed out a few years ago that Perron's C'''-assumption is bound to be too severe; the more so as it supplies (just as the classical example of the asymptotic formula for Bessel's functions) the estimate $O(1/t)$ of the error term of (3), while (3) concerns itself merely with an error of the form $o(1/t^{\frac{1}{2}})$.

In this direction, Hartman [1] has shown that the relation (3) is true whenever $f(x)$ is of bounded variation (near $x = 0$). For an application, cf. Haviland [3].

The following proof will consist of a suitable adaptation of the deduction of "convergence criteria of the second kind" in the theory of Fourier series (cf. [4]). This raises the question as to a condition corresponding to "convergence criteria of the first kind," (Lipschitz-Dini), which involve the behavior of $f(x)$ only *at* $x = 0$, rather than *near* $x = 0$. However, it turns out that such a criterion cannot exist.

In view of the italicized proviso preceding (2), the usual treatment (and, as a matter of fact, even the wording) of Kelvin's rule (cf. [2]) tacitly assumes that $\phi''(x)$ does not vanish at the critical points, $x = x_0$, at which $\phi'(x)$ vanishes. Correspondingly, if $\phi(x)$ is of class $C^{(\lambda)}$, where $\lambda > 1$, and if $\phi'(x_0) = 0, \cdots,$ $\phi^{(\lambda-1)}(x_0) = 0$ but $\phi^{(\lambda)}(x_0) \neq 0$, then what corresponds to the normal form (2) results when x^2 is replaced by x^λ. As verified in [6], the corresponding generalization of (3) is

$$\int_0^c f(x)e^{itx^\lambda}\,dx \sim e^{\frac{1}{2}\pi i/\lambda}\Gamma(1 + 1/\lambda)f(+0)/t^{1/\lambda}, \qquad (c > 0,\ t \to \infty), \tag{3*}$$

(to be interpreted as

$$(4^*) \qquad \int_0^c f(x)e^{it x^\lambda}\,dx = o(1/t^{1/\lambda}), \qquad (c > 0,\ t \to \infty),$$

if $f(+0) = 0$), where λ need not be an integer (but must be greater than 1). However, what follows under Perron's C'''-assumption is again more than what is wanted, since what results is that the error term of (3*), instead of being just $o(1/t^{1/\lambda})$, is $O(1/t^{2/\lambda})$ if $\lambda > 2$; cf. [6].

In this regard, Hartman [1] has shown that (3*), where $\lambda > 1$, holds whenever $f(x)$ is of bounded variation. The proof of (3), indicated above, applies to this, more general, case also.

First, it is clear from the remark made after (4), that it is sufficient to prove (3*) under the assumption that $f(x)$ is of bounded variation and $f(+0)$ vanishes. But, whether $f(x)$ is or is not of bounded variation, the mere assumption $f(+0) = 0$ implies that a partial integration (in the Lebesgue-Stieltjes sense) transforms the integral (4*) into

$$0 - 0 - \int_0^c \left(-\int_x^c e^{iu^\lambda}\,du \right) df(x)$$

whenever $f(x)$ is L-integrable; in fact, the other factor is continuous. (Correspondingly, if $f(x)$ is R-integrable, Riemann-Stieltjes integration is sufficient). But, if $S_\lambda(x)$ is an abbreviation for the function defined by

$$(5) \qquad S_\lambda(x^\lambda) = \int_0^x e^{iu^\lambda}\,du,$$

then

$$\int_x^c e^{iu^\lambda}\,du = t^{-1/\lambda} S_\lambda(ct) - t^{-1/\lambda} S_\lambda(xt).$$

Consequently, the integral (4*) is identical with $t^{-1/\lambda}$ times

$$(6) \qquad \int_0^c \{S_\lambda(ct) - S_\lambda(xt)\}\,df(x).$$

In particular, (4*) is true if and only if the function (6) of t tends to 0 as $t \to \infty$.

This condition is satisfied if $f(x)$ is of bounded variation. In fact, since the assumption $\lambda > 1$ implies for (5) the existence of a constant C_λ satisfying $|S_\lambda(x)| < C_\lambda$, the contribution of the range $0 \leqq x \leqq \epsilon$ to the integral (6) is majorized by

$$2C_\lambda \int_0^\epsilon |\,df(x)\,|$$

and tends, therefore, to 0 as $\epsilon \to 0$. On the other hand, if ϵ is fixed (> 0), the contribution of the range $\epsilon \leqq x \leqq c$ to (6) is majorized by a constant multiple of

$$\operatorname*{Max}_{\epsilon \leqq x \leqq c} |\,S_\lambda(ct) - S_\lambda(xt)\,|,$$

the constant factor being the total variation of $f(x)$ over the interval $0 \leqq x \leqq c$. Consequently, it is sufficient to ascertain that, if a positive ϵ (less than c) is arbi-

trarily fixed, then the above Max, which is a function of t alone, tends to 0 as $t \to \infty$. But this is clear from the fact that, since $\lambda > 1$, the improper integral $S_\lambda(\infty)$ defined by (5), is convergent.

This proves (3*), where $f(x)$ is of bounded variation and $\lambda > 1$. If $\lambda = 1$, then the integral (3*) becomes an ordinary Fourier transform, and so nothing like an asymptotic formula (3*) can be true (not even if $f(x)$ is regular-analytic).

In order to see that no "criterion of the first kind" is possible for (4*) when $\lambda > 1$, it will be sufficient to consider the case of the particular assumptions $c = 1$, $\lambda = 2$, $f(+0) = 0$. In this case, the integral (4*) can be written in the form

$$\int_0^1 g(x)e^{itx}\,dx,$$

where $g(x) = \frac{1}{2}f(x^{\frac{1}{2}})/x^{\frac{1}{2}}$. Hence, even if $f(x)$ is continuous and it has a derivative at $x = 0$, all that follows from $f(+0) = 0$ and from the definition of $g(x)$ is that $g(x)$ is continuous for $0 \leqq x \leqq 1$ and vanishes at $x = 0$. Conversely, any such $g(x)$ leads to an $f(x)$ having the properties just mentioned. Hence, if these properties were sufficient for (4*), where $\lambda = 2$, it would follow that the integral of the last formula line is $o(1/t^{\frac{1}{2}})$ whenever $g(x)$ is a continuous function. But this is not true, since, as pointed out by Lebesgue, the $o(1)$ of the Riemann-Lebesgue lemma is incapable of improvement in the case of an unspecified continuous function.

REFERENCES

[1] P. Hartman, An asymptotic formula for exponential integrals, American Journal of Mathematics, vol. 62 (1940), pp. 115–121.

[2] T. H. Havelock, The propagation of disturbances in dispersive media, Cambridge Tracts, No. 17 (1914), pp. 26–27.

[3] E. K. Haviland, On an asymptotic formula for the Fourier transforms of distributions on certain curves, American Journal of Mathematics, vol. 62 (1940), pp. 655–665.

[4] H. Lebesgue, Leçons sur les séries trigonométriques, Paris, 1906, pp. 62–74.

[5] O. Perron, Ueber das infinitäre Verhalten der Koeffizienten einer gewissen Potenzreihe, Archiv der Mathematik und Physik, ser. 3, vol. 22 (1914), pp. 329–340.

[6] A. Wintner, On the asymptotic formulae of Riemann and of Laplace, Proceedings of the National Academy of Sciences (Washington), vol. 20 (1934), pp. 57–62.

A CONVERGENT ITERATIVE PROCESS

By Paul A. Samuelson

In applied mathematics it is often necessary to solve an implicit equation

$$G(X) - X = 0 \tag{1}$$

by an iteration of the form

$$X_{t+1} = G(X_t). \tag{2}$$

Let us suppose that

$$G(a) - a = 0;$$

then the above iteration will converge to a for all initial values, X_0, sufficiently close to a provided that $| G'(a) | < 1$.

Similarly, if $| G'(a) | > 1$, the iteration will diverge for initial values close to, but distinct from, a. This may be annoying in practice. Moreover, even if the process is convergent, an inordinately large number of whirls may be necessary to achieve a solution of given accuracy when $| G'(a) |$ is near to unity.

The following iteration is proposed to speed up convergence where convergence is slow and to guarantee convergence even in the unstable case.

$$Y_{t+1} = \frac{\{G[G(Y_t)]\}^2 - G(Y_t)G\{G[G(Y_t)]\}}{2G[G(Y_t)] - G(Y_t) - G\{G[G(Y_t)]\}} = F(Y_t) \tag{3}$$

By the application of L'Hospital's rule it can be shown that

$$F(a) - a = 0$$

$$F'(a) = 0$$

if $G'(a) \neq 1$.

By classical reasoning it follows that the proposed iteration converges to a for all sufficiently close initial values Y_0. Moreover, the convergence is faster than that of any linear process.

The present method may be used with profit at the last stage of the usual iterative sequence. Because the solution is given as the ratio of two small differences, care must be taken in dropping digits. This, of course, is a property of many methods which attempt to squeeze the maximum of information out of a few iterations. The present method bears a close relationship to the Aitken* device for accelerating convergence of the Bernoulli approximation to the root of a polynomial; however, the analytical problems which are to be solved are not identical.

The motivation for the sequence (3) proceeds from recognition of the fact that in a close neighborhood of a the iteration is "almost linear" and can be approximated by the following function of time

$$X_t = a + Km^t \tag{4}$$

* A. C. Aitken, "On Bernoulli's Numerical Solution of Algebraic Equations", *Proceedings of the Royal Society of Edinburgh*, 1926, Vol. 46, p. 289–305.

where $m = G'(a)$. Of course, a, m, and K are unknowns, but they may be determined from a knowledge of three values, X_t, X_{t+1}, X_{t+2} by substituting into (4) and solving the resulting three equations for a as in (3).

Our analysis admits of generalization in three different directions. First, we may consider iterations in many variables, interpreting the symbols in (1) as many variable vectors. Then in the neighborhood of a (vector) solution a, the vectors $(X_t - a)$ "almost" satisfy a linear difference equation in many variables

$$(X_{t+1} - a) = m(X_t - a) \tag{5}$$

where the matrix m is the Jacobian of the system at a. The sequence can be approximated by a sum of exponentials. From $(n + 2)$ observed vectors, the matrix of the system can be deduced, the exponential components, and finally an estimate of a. There is little of theoretical interest in this generalization, and its numerical application would be so tedious as to make its use impractical in most cases.

In our second generalization, we return to a one variable system and seek to accelerate convergence by taking account of the non-linear parts of the iteration process. If $G(X)$ admits of a formal power series development of the form $\sum_0^\infty b_i X^i$, then in a neighborhood of a there exists a formal solution of the non-linear difference equation system of the form

$$(X_t - a) = K_1 m^t + K_2 m^{2t} + K_3 m^{3t} + \cdots \tag{6}$$

where $m = G'(a)$ and the K's depend on the b's and the initial condition.

Our first method retained only the first term of (6). We now retain two terms and determine from four observed values $(X_t, X_{t+1}, X_{t+2}, X_{t+3})$ an estimate of a. These must almost satisfy a difference equation of the form

$$\begin{aligned} 0 &= X_{t+3} + C_1 X_{t+2} + C_2 X_{t+1} + C_3 X_t = P(E)X_t \\ &= (E - 1)(E - m)(E - m^2)X_t \\ &= X_{t+3} - (1 + m + m^2)X_{t+2} + (m + m^2 + m^3)X_{t+1} - m^3 X_t \end{aligned} \tag{7}$$

where $EX_t = X_{t+1}$, etc.

With the X's known, we have a cubic equation in m. Once this has been solved, three values of X_t substituted into (6), give us enough equations to solve for a.

As an alternative method we can determine the coefficients by expanding the *perisymmetric* determinant,

$$\begin{vmatrix} \Delta X_t & \Delta X_{t+1} & 1 \\ \Delta X_{t+1} & \Delta X_{t+2} & E \\ \Delta X_{t+2} & \Delta X_{t+3} & E^2 \end{vmatrix} = 0,$$

then finding the roots of this polynomial (one of which will be almost the square of the other); and finally substituting in (6) as before to get a.

The conditions under which this method can be profitably used remain to be investigated.

The third generalization concerns itself with speeding up the acceleration of iterative sequences which are already of great power—namely, those for which the linear term $G'(a)$ already vanishes. We have seen that $F(X_t)$ is such a process; the Newton-Raphson and many other common methods belong to this class.

For these processes, we may write our G in the form

$$G(X) = 0 + K(X - a)^2 + L(X - a)^3 + M(X - a)^4 + \cdots.$$

For initial values of X_0 close to a, the sequence X_t almost satisfies the quadratic difference equation

$$(X_{t+1} - a) = K(X_t - a)^2$$

where $K = G''(a)/2$ and a are unknowns. From three values, X_t, X_{t+1}, X_{t+2}, we can solve for a as follows

$$(X_{t+2} - a) = K(X_{t+1} - a)^2 = K^3(X_t - a)^4 = \frac{(X_{t+1} - a)^3(X_t - a)^4}{(X_t - a)^6}$$

or

$$(X_{t+2} - a)(X_t - a)^2 - (X_t - a)^3 = 0.$$

This gives us a quadratic equation in a. The correct root can be easily selected. Thus, we have in effect defined a new iteration

$$Y_{t+1} = F_1(Y_t).$$

Intuitively, it is clear that F_1 is powerful in the sense that $F_1'(a) = 0$; tortuous investigation would be necessary to reveal whether a number of further derivatives do not necessarily vanish as well.

In conclusion, a few general remarks about the "power" of convergent methods may be in order. Linear sequences, for which $G'(a) \neq 0$, converge exponentially; i.e., if we drop no digits at each stage, our number of *correct digits* will asymptotically increase as a linear function of the number of iterations.

Quadratic iterations or second order iterations, those for which $G'(a) = 0$, $G''(a) \neq 0$, yield "correct digits" which increase in geometric progression with number of iterations N; i.e., asymptotically as 2^N. An iteration of the rth order (whose first non-vanishing derivative is the rth) has correct digits which increase with number of iterations as r^N.

If sufficiently many correct digits are wished, it will always save effort to replace a first order method by a higher order one, even if the latter involves more labor at each stage—provided that both methods involve a finite amount of work. A similar comparison between say a second order system and *any* higher order system is not possible. For a repeated 2nd order iteration equals

a 4th order iteration; therefore, another 4th order iteration which involves more than twice the work of the given 2nd order iteration would not be profitable even when we wish great accuracy.

If enough correct digits are required, it would seem intuitively that an optimal choice between two methods (of which at least one is of order greater than one) would be to select that which maximizes $W(r) \log r$, where $W(r)$ is the amount of work required for each rth order iteration. However, in some cases, an optimal process might involve no "repeated" iterations of any order, but consist of a different set of rules at each stage.

MASSACHUSETTS INSTITUTE OF TECHNOLOGY.

TABLE OF COEFFICIENTS FOR DOUBLE QUADRATURE WITHOUT DIFFERENCES, FOR INTEGRATING SECOND ORDER DIFFERENTIAL EQUATIONS

By Herbert E. Salzer*

The accompanying table of coefficients can be used to calculate a function whenever its second derivative is known at equally spaced points. The coefficients were obtained by a double quadrature of the well-known Lagrangian interpolation formula. They cover the cases where the second derivative of the desired function is approximated by polynomials ranging from the second to the tenth degree, (i.e. for three-point through eleven-point formulas). They enable the user to determine the function itself at any one of the points x_p where its second derivative is given, to within an arbitrary $Ax_p + B$.

Employing the notation f_i for $f(x_0 + ih)$ (or f_i'' for $f''(x_0 + ih)$), where h is the tabular interval and given f_i'' at n points where i ranges from $-\left(\frac{n-1}{2}\right)$ to $\left(\frac{n-1}{2}\right)$ for n odd and from $-\left(\frac{n}{2} - 1\right)$ to $\left(\frac{n}{2}\right)$ for n even, for $x_p = x_0 + ph$ we have

$$f_p = h^2 \sum C_i(p) f_i'' + Ax_p + B \tag{1}$$

where for convenience $C_i(p)$ is given in the exact fractional form $D_i(p)/D(p)$, $D(p)$ being chosen as the smallest integral denominator for that particular p which will make every $D_i(p)$ an integer. Thus the user need only multiply each f_i'' by the corresponding $D_i(p)$, (denoted in the table simply as D_i), and then divide h^2 times the sum of the products by the denominator $D(p)$, (or simply, D). For repeated use it is sometimes worthwhile to divide all the D_i's for some particular p by a common factor, making them all smaller at the sole expense of changing the denominator into a number that is not an integer. A typical instance would be in the eleven-point coefficients for $p = -5$, where all the numerators D_i would be divided by 25 and the new denominator would be 1532805.12.

To determine A and B, the function must be known at any two of the n points, and after the evaluation of $\frac{h^2}{D} \sum D_i f_i''$ at those points, one can solve for A and B. Naturally, if one progresses beyond the original n points, there will be a different A and B for which to solve, say A' and B'; but we can make use of the knowledge of the function which has already been obtained at the original n points to solve for A' and B'. Since in all cases when $p = 0$, $D_i = 0$, it is not necessary to tabulate $D_i(0) = 0$, but the point $x_0 + 0 \cdot h$, where $f_0 = Ax_0 + B$, should be used as freely as any other $x_0 + ph$.

The advantage of this table in an ordinary double quadrature of a tabulated

* Mathematical Tables Project, National Bureau of Standards.

function without differences appears to be in the saving of labor (amounting to nearly 50%). Without these coefficients it would be necessary either to repeat the operation of a single quadrature or to multiply the integrand denoted by $f(t)$ by $(x - t)$ and then to perform a single quadrature.

The chief use of this table will be to facilitate the numerical integration of second order differential equations. Since every second order differential equation of the form

$$y'' + p(x)y' + g(x)y = h(x) \tag{2}$$

can be transformed into

$$u'' + r(x)u = h(x)e^{\frac{1}{2}\int_a^x p(t)\,dt} \tag{3}$$

where

$$r(x) = g(x) - \tfrac{1}{2}p'(x) - \tfrac{1}{4}[p(x)]^2$$

by the transformation

$$y = u \exp\left[-\frac{1}{2}\int_a^x p(t)\,dt\right]$$

and since many important functions (such as Bessel, Legendre and hypergeometric) are defined by an equation like (2) with $h(x) = 0$ while others, such as Mathieu functions, are defined directly by an equation like (3) with $h(x) = 0$, it is of special importance to integrate an equation of the form (4) $y'' + g(x)y = 0$ in the most efficient manner. Instead of (4) we may consider the generalization

$$y'' + \phi(x, y) = 0. \tag{5}$$

The methods advocated in the literature are based upon the expression of (5) as a simultaneous system of two equations of the first order with the result that almost twice as many multiplications are needed than by a direct double quadrature.

To illustrate this method for (5), suppose that we are given a set of values of y (and y'') at five points and it is desired to find y at the next point. From an extrapolated value of y we obtain y'' (or, alternatively, extrapolate directly for y'') and integrate using the five-point coefficients for $p = 2$, leaving out the first y'' but including the last new y'', to obtain a new y. This value of y will be determined save for the expression $Ax + B$, which can be evaluated from any of the known values of y other than the first. Then the entire process can be repeated to obtain a still better value for y'' and then y at the new point. The process can be continued and instead of refining the very next value of y, one can obtain several successive values of y and then refine them by using the coefficients for p equal to -2, -1, 0, or 1, as well as 2.* The convergence of

* In many cases, where the interval is suitable, the process can be started with a number of extrapolated values of y'' (obtained from a number of extrapolated values of y) instead of merely one new value of y''. Thus we can obtain more than one new y in each step.

this process is assured by the theory given in H. Levy and E. A. Baggott, "Numerical Studies in Differential Equations", pp. 54–61. The few values of y needed to start this process must be obtained as usual from the differential equation and initial conditions either by the usual numerical methods or by Taylor's theorem. The advantage of these coefficients will become greater as the number of desired values in the solution increases.

Since the use of this process necessitates particular use of the coefficients for the last value of p preceded by extrapolation for a first approximation to the next value of y'', for the sake of convenience we repeat here the well-known binomial coefficients that are needed to obtain f_{n+1} from the preceding f_n, f_{n-1}, etc., without taking differences.

Coefficients for Extrapolation

3-point	$f_{n+1} = 3f_n - 3f_{n-1} + f_{n-2}$
4-point	$f_{n+1} = 4f_n - 6f_{n-1} + 4f_{n-2} - f_{n-3}$
5-point	$f_{n+1} = 5f_n - 10f_{n-1} + 10f_{n-2} - 5f_{n-3} + f_{n-4}$
6-point	$f_{n+1} = 6f_n - 15f_{n-1} + 20f_{n-2} - 15f_{n-3} + 6f_{n-4} - f_{n-5}$
7-point	$f_{n+1} = 7f_n - 21f_{n-1} + 35f_{n-2} - 35f_{n-3} + 21f_{n-4} - 7f_{n-5} + f_{n-6}$
8-point	$f_{n+1} = 8f_n - 28f_{n-1} + 56f_{n-2} - 70f_{n-3} + 56f_{n-4} - 28f_{n-5} + 8f_{n-6} - f_{n-7}$
9-point	$f_{n+1} = 9f_n - 36f_{n-1} + 84f_{n-2} - 126f_{n-3} + 126f_{n-4} - 84f_{n-5} + 36f_{n-6} - 9f_{n-7} + f_{n-8}$
10-point	$f_{n+1} = 10f_n - 45f_{n-1} + 120f_{n-2} - 210f_{n-3} + 252f_{n-4} - 210f_{n-5} + 120f_{n-6} - 45f_{n-7} + 10f_{n-8} - f_{n-9}$
11-point	$f_{n+1} = 11f_n - 55f_{n-1} + 165f_{n-2} - 330f_{n-3} + 462f_{n-4} - 462f_{n-5} + 330f_{n-6} - 165f_{n-7} + 55f_{n-8} - 11f_{n-9} + f_{n-10}$

Three-Point Coefficients

p	D_{-1}	D_0	D_1	Denominator
−1	3	10	−1	24
1	−1	10	3	24

Four-Point Coefficients

p	D_{-1}	D_0	D_1	D_2	Denominator
−1	38	171	−36	7	360
1	−8	129	66	−7	360
2	−2	36	54	2	45

Five-Point Coefficients

p	D_{-2}	D_{-1}	D_0	D_1	D_2	Denominator
−2	5	104	78	−8	1	90
−1	−17	220	582	−76	11	1440
1	11	−76	582	220	−17	1440
2	1	−8	78	104	5	90

Six-Point Coefficients

p	D_{-2}	D_{-1}	D_0	D_1	D_2	D_3	Denominator
−2	37	718	566	−76	17	−2	630
−1	−82	1355	4444	−902	262	−37	10080
1	40	−347	3704	1910	−304	37	10080
2	5	−46	526	748	25	2	630
3	18	−153	1524	2466	1098	87	1120

Seven-Point Coefficients

p	D_{-3}	D_{-2}	D_{-1}	D_0	D_1	D_2	D_3	Denominator
−3	315	4590	9369	6756	−1107	270	−33	4480
−2	1	105	2169	1678	−213	45	−5	1890
−1	253	−2502	20055	48268	−7029	1626	−191	120960
1	−191	1626	−7029	48268	20055	−2502	253	120960
2	−5	45	−213	1678	2169	105	1	1890
3	−33	270	−1107	6756	9369	4590	315	4480

Eight-Point Coefficients

p	D_{-3}	D_{-2}	D_{-1}	D_0	D_1	D_2	D_3	D_4	Denominator
−3	1476	23643	44766	37245	−9000	3429	−858	99	22400
−2	−14	1778	31926	26185	−4210	1284	−278	29	28350
−1	2402	−27779	271572	772775	−154190	53643	−12616	1393	1814400
1	−1472	14639	−76182	675285	349580	−66783	13546	−1393	1814400
2	−46	472	−2586	24155	33550	966	218	−29	28350
3	−66	657	−3456	30315	50310	20871	2268	−99	22400
4	−16	232	−1776	23600	50320	24456	15728	856	14175

Nine-Point Coefficients

p	D_{-4}	D_{-3}	D_{-2}	D_{-1}	D_0	D_1	D_2	D_3	D_4	Denominator
−4	846	15808	24176	50880	22900	−1216	−48	64	−10	14175
−3	−279	8136	86760	194688	129450	−20376	5904	−1200	117	89600
−2	−47	320	5796	130336	101450	−14208	3820	−736	69	113400
−1	−3075	34208	−197216	1258488	2875850	−444560	128472	−25864	2497	7257600
1	2497	−25864	128472	−444560	2875850	1258488	−197216	34208	−3075	7257600
2	69	−736	3820	−14208	101450	130336	5796	320	−47	113400
3	117	−1200	5904	−20376	129450	194688	86760	8136	−279	89600
4	−10	64	−48	−1216	22900	50880	24176	15808	846	14175

Ten-Point Coefficients

p	D_{-4}	D_{-3}	D_{-2}	D_{-1}	D_0	D_1	D_2	D_3	D_4	D_5	Denominator
−4	27350	526776	777360	1726752	684132	31440	−49296	22560	−5442	568	467775
−3	−2380	83295	979164	2063692	1510764	−310950	122820	−38004	7488	−689	985600
−2	−589	1902	225900	4220280	3469062	−500076	206868	−58920	10935	−962	3742200
−1	−61154	765975	−5056572	38143140	99983496	−19750926	7626540	−2305068	445290	−40321	239500800
1	42080	−490623	2788020	−11283516	89822604	46610550	−9895092	2580420	−464364	40321	239500800
2	1315	−15630	91428	−388056	3226638	4422300	110460	45192	−10209	962	3742200
3	598	−6999	40140	−166260	1337136	2228382	896484	114300	−9270	689	985600
4	238	−3000	18864	−87840	827268	1607472	845520	501216	33030	−568	467775
5	26500	−283875	1432500	−4849500	26066100	37704750	31579500	16882500	10617000	574925	9580032

Eleven-Point Coefficients

p	D_{-5}	D_{-4}	D_{-3}	D_{-2}	D_{-1}	D_0	D_1	D_2	D_3	D_4	D_5	Denominator
−5	2222275	43242250	64045875	135609000	134559750	123775500	−35657250	15021000	−4619625	880250	−77425	38320128
−4	−620	33550	498876	851760	1596552	840372	−98760	25104	−5340	758	−52	467775
−3	1693	−26450	409365	3713496	8690298	5616420	−888270	288120	−75831	13022	−1063	3942400
−2	436	−4949	21522	173580	4311840	3359190	−498516	154548	−39300	6575	−526	3742200
−1	87299	−1117606	6992355	−30702168	170905350	377934636	−60670914	20030280	−5291817	908170	−73985	958003200
1	−73985	908170	−5291817	20030280	−60670914	377934636	170905350	−30702168	6992355	−1117606	87299	958003200
2	−526	6575	−39300	154548	−498516	3359190	4311840	173580	21522	−4949	436	3742200
3	−1063	13022	−75831	288120	−888270	5616420	8690298	3713496	409365	−26450	1693	3942400
4	−52	758	−5340	25104	−98760	840372	1596552	851760	498876	33550	−620	467775
5	−77425	880250	−4619625	15021000	−35657250	123775500	134559750	135609000	64045875	43242250	2222275	38320128

The utility of these coefficients extends, in all likelihood, to the numerical solution of partial differential equations of the second order. Suppose there is an equation of the type

$$u_{xx} = u_t + \psi(u, x, t), \tag{6}$$

and the solution satisfying specified boundary conditions is known along a rectangular array of points in the x, t plane, as well as for two points on the next row (by "row", we mean for the same t) after the last which is completely known. To obtain all the values corresponding to the next row of points, one might obtain u_t by an extrapolation in the t direction for u followed by numerical differentiation and then, after obtaining a row of values for u_{xx} from (6), apply these coefficients for some particular n for each value of p, to reach a new set of values for u on the next row. It is to be expected that these new u's will be more accurate than those obtained by extrapolation. Then this process could be iterated to refine the new row of u's. The "justification" for this procedure is that as a rule accuracy is lost in numerical differentiation and extrapolation but gained in numerical integration in conjunction with an iteration scheme (such as in the well-known Adams-Bashforth process for ordinary differential equations). It is expected in the above suggestion that the loss in accuracy engendered by the extrapolation for u, the formation of a first approximation to u_t, and a first approximation to $\psi(u, x, t)$ based upon the extrapolated value for u, will be more than offset by the double quadrature in the x direction. However, the actual conditions for convergence are still an open question.

In this table one may notice that for n – point coefficients, n odd, there is a duplication of values due to the relation $D_i(p) = D_{-i}(-p)$. This could have been avoided by top and bottom headings, the latter reading from right to left. But for the sake of maximum facility and uniformity in use, all coefficients are given with headings reading from left to right.

Grateful acknowledgment is due to Dr. Arnold N. Lowan, Director of the Mathematical Tables Project, for his cooperation and encouragement in the preparation of this table. Also, thanks are extended to Mrs. J. Cirminiello and Miss H. Larrier for assistance in checking the values, and to Miss S. Pyle for preparation of the final manuscript.

FORMULAS FOR DIRECT AND INVERSE INTERPOLATION OF A COMPLEX FUNCTION TABULATED ALONG EQUIDISTANT CIRCULAR ARCS

By Herbert E. Salzer*

A. Direct Interpolation

When an analytic function of z may be approximated by a complex polynomial of degree $n - 1$ passing through the values of the function at n points, according to the Lagrange-Hermite interpolation formula, it often occurs that those n points are equally spaced on the arc of a circle in the z plane, and it is desired to obtain the function corresponding to a value of z off the circle but near the arguments. Thus an important special case would be the problem of interpolation between rays for complex functions tabulated in polar form (i.e. argument $z = \rho e^{i\phi}$ and interpolating for an arbitrary z from values with the same value of ρ). Another application would be to functions tabulated along the vertices of any regular polygon.

Let θ denote the angle between successive chords joining the points z_{i-1} to z_i, z_i to z_{i+1}, etc. (measured counterclockwise). In every case we first orientate the circle so that the point z_0 is in the lower left-hand corner, by a rotation in the positive sense about the origin of angle $\pi - \alpha$, where α is the angle that the ray through z_0 makes with the imaginary axis, measuring counterclockwise from the imaginary axis. (If the center of the circle is not the origin, make it so by an obvious translation). This rotation $z' = ze^{i(\pi-\alpha)}$ introduces no complication; although not strictly necessary, it simplifies the calculation of $P \equiv (z - z_0)/h = p + iq$, where h now becomes merely the distance between successive points z_i. Otherwise h(or $z_1 - z_0$) would be a complex number depending upon the orientation. Thus the points of reference are situated according to the following diagram:

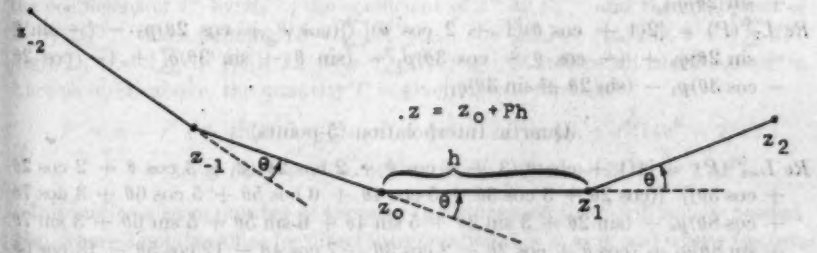

In the interpolation formula (1) $f(z) = \sum L_k^{(n)}(P) f(z_k)$, where k ranges from $-$ the nearest integer in $(n - 1)/2$ to the nearest integer in $n/2$, the polynomials

* Mathematical Tables Project, National Bureau of Standards.

$L_k^{(n)}(P)$ have coefficients that are functions of θ, as well as p and q. The following formulas enable the user to obtain the real and imaginary parts of $L_k^{(n)}(P)$ for the 3-, 4- and 5-point cases (complex quadratic, cubic and quartic interpolation). For extensive use for some fixed θ, these coefficients should first be obtained as functions of p and q only. For the sake of conciseness in presentation we let $P^n = p_n + iq_n$, so that $p_1 = p$, $q_1 = q$, $p_2 = p^2 - q^2$, $q_2 = 2pq$, $p_3 = p(p^2 - 3q^2)$, $q_3 = q(3p^2 - q^2)$, $p_4 = p^4 - 6p^2q^2 + q^4$, $q_4 = 4pq(p^2 - q^2)$. Also, to save space, only $Re\ L_k^{(4)}(P)$ and $Re\ L_k^{(5)}(P)$ are given, but in such form that $Im\ L_k^{(4)}(P)$ and $Im\ L_k^{(5)}(P)$ are immediately obvious by interchanging p_m with q_m and taking all signs before parentheses as + instead of alternately + and −. (However note that the term 1 appears only in $Re\ L_0^{(4)}(P)$ and $Re\ L_0^{(5)}(P)$).

Quadratic Interpolation (3-points)

$$Re\ L_{-1}^{(3)}(P) = [2(1 + \cos\theta)]^{-1}[(\cos\theta + \cos 2\theta)(p_2 - p_1) - (\sin\theta + \sin 2\theta)(q_2 - q_1)]$$

$$Im\ L_{-1}^{(3)}(P) = [2(1 + \cos\theta)]^{-1}[(\cos\theta + \cos 2\theta)(q_2 - q_1) + (\sin\theta + \sin 2\theta)(p_2 - p_1)]$$

$$Re\ L_0^{(3)}(P) = -\cos\theta\,(p_2 - p_1) + \sin\theta(q_2 - q_1) - p_1 + 1$$

$$Im\ L_0^{(3)}(P) = -\cos\theta\,(q_2 - q_1) - \sin\theta(p_2 - p_1) - q_1$$

$$Re\ L_1^{(3)}(P) = \tfrac{1}{2}(p_2 + p_1) - \sin\theta[2(1 + \cos\theta)]^{-1}(q_2 - q_1)$$

$$Im L_1^{(3)}(P) = \tfrac{1}{2}(q_2 + q_1) + \sin\theta[2(1 + \cos\theta)]^{-1}(p_2 - p_1)$$

Cubic Interpolation (4-points)

$$Re\ L_{-1}^{(4)}(P) = -[2(1 + \cos\theta)(1 + 2\cos\theta)]^{-1}[(\cos\theta + \cos 2\theta)p_3 - (\sin\theta + \sin 2\theta)q_3 + (-2\cos\theta - 3\cos 2\theta - \cos 3\theta)p_2 - (-2\sin\theta - 3\sin 2\theta - \sin 3\theta)q_2 + (\cos\theta + 2\cos 2\theta + \cos 3\theta)p_1 - (\sin\theta + 2\sin 2\theta + \sin 3\theta)q_1]$$

$$Re\ L_0^{(4)}(P) = 1 + [2(1 + \cos\theta)]^{-1}[(1 + \cos\theta)p_3 - \sin\theta q_3 + (-1 - 2\cos\theta - \cos 2\theta)p_2 - (-4\sin\theta - \sin 2\theta)q_2 + (-2 - \cos\theta + \cos 2\theta)p_1 - (3\sin\theta + \sin 2\theta)q_1]$$

$$Re L_1^{(4)}(P) = -[2(1 + \cos\theta)]^{-1}[(1 + \cos\theta)p_3 - (-\sin\theta)q_3 + (-2 - \cos\theta + \cos 2\theta)p_2 - (-\sin\theta - \sin 2\theta)q_2 + (-1 - 2\cos\theta - \cos 2\theta)p_1 - (2\sin\theta + \sin 2\theta)q_1]$$

$$Re\ L_2^{(4)}(P) = [2(1 + \cos\theta)(1 + 2\cos\theta)]^{-1}[(\cos\theta + \cos 2\theta)p_3 - (-\sin\theta - \sin 2\theta)q_3 + (-\cos\theta + \cos 3\theta)p_2 - (\sin\theta - \sin 3\theta)q_2 + (-\cos 2\theta - \cos 3\theta)p_1 - (\sin 2\theta + \sin 3\theta)q_1]$$

Quartic Interpolation (5-points)

$$Re\ L_{-2}^{(5)}(P) = [4(1 + \cos\theta)(3 + 4\cos\theta + 2\cos 2\theta)(2 + 3\cos\theta + 2\cos 2\theta + \cos 3\theta)]^{-1}[(\cos 2\theta + 3\cos 3\theta + 5\cos 4\theta + 6\cos 5\theta + 5\cos 6\theta + 3\cos 7\theta + \cos 8\theta)p_4 - (\sin 2\theta + 3\sin 3\theta + 5\sin 4\theta + 6\sin 5\theta + 5\sin 6\theta + 3\sin 7\theta + \sin 8\theta)q_4 + (\cos\theta + \cos 2\theta - 2\cos 3\theta - 7\cos 4\theta - 12\cos 5\theta - 13\cos 6\theta - 10\cos 7\theta - 5\cos 8\theta - \cos 9\theta)p_3 - (\sin\theta + \sin 2\theta - 2\sin 3\theta - 7\sin 4\theta - 12\sin 5\theta - 13\sin 6\theta - 10\sin 7\theta - 5\sin 8\theta - \sin 9\theta)q_3 + (-2\cos\theta - 6\cos 2\theta - 9\cos 3\theta - 9\cos 4\theta - 5\cos 5\theta + 3\cos 7\theta + 3\cos 8\theta + \cos 9\theta)p_2 - (-2\sin\theta - 6\sin 2\theta - 9\sin 3\theta - 9\sin 4\theta - 5\sin 5\theta + 3\sin 7\theta + 3\sin 8\theta$$

$+ \sin 9\theta)q_2 + (\cos\theta + 4\cos 2\theta + 8\cos 3\theta + 11\cos 4\theta + 11\cos 5\theta + 8\cos 6\theta + 4\cos 7\theta + \cos 8\theta)p_1 - (\sin\theta + 4\sin 2\theta + 8\sin 3\theta + 11\sin 4\theta + 11\sin 5\theta + 8\sin 6\theta + 4\sin 7\theta + \sin 8\theta)q_1]$

$Re\ L_{-1}^{(5)}(P) = -[2(1+\cos\theta)(1+2\cos\theta)]^{-1}[(\cos 3\theta + \cos 4\theta)p_4 - (\sin 3\theta + \sin 4\theta)q_4 + (\cos\theta + 2\cos 2\theta - \cos 3\theta - 3\cos 4\theta - \cos 5\theta)p_3 - (\sin\theta + 2\sin 2\theta - \sin 3\theta - 3\sin 4\theta - \sin 5\theta)q_3 + (-2\cos\theta - 5\cos 2\theta - 3\cos 3\theta + \cos 4\theta + \cos 5\theta)p_2 - (-2\sin\theta - 5\sin 2\theta - 3\sin 3\theta + \sin 4\theta + \sin 5\theta)q_2 + (\cos\theta + 3\cos 2\theta + 3\cos 3\theta + \cos 4\theta)p_1 - (\sin\theta + 3\sin 2\theta + 3\sin 3\theta + \sin 4\theta)q_1]$

$Re\ L_0^{(5)}(P) = 1 + [2(1+\cos\theta)]^{-2}[(\cos\theta + 2\cos 2\theta + \cos 3\theta)p_4 - (\sin\theta + 2\sin 2\theta + \sin 3\theta)q_4 + (4 + 4\cos\theta - 3\cos 2\theta - 4\cos 3\theta - \cos 4\theta)p_3 - (2\sin\theta - 3\sin 2\theta - 4\sin 3\theta - \sin 4\theta)q_3 + (-6 - 11\cos\theta - 5\cos 2\theta + \cos 3\theta + \cos 4\theta)p_2 - (-13\sin\theta - 7\sin 2\theta + \sin 3\theta + \sin 4\theta)q_2 + (-4 - 2\cos\theta + 4\cos 2\theta + 2\cos 3\theta)p_1 - (10\sin\theta + 8\sin 2\theta + 2\sin 3\theta)q_1]$

$Re\ L_1^{(5)}(P) = -[2(1+\cos\theta)(3+4\cos\theta+2\cos 2\theta)]^{-1}[(2 + 3\cos\theta + \cos 2\theta)p_4 - (\sin\theta + \sin 2\theta)q_4 + (2 + 3\cos\theta + \cos 2\theta)p_3 - (-7\sin\theta - 7\sin 2\theta - 2\sin 3\theta)q_3 + (-10 - 14\cos\theta - 3\cos 2\theta + 2\cos 3\theta + \cos 4\theta)p_2 - (-\sin 2\theta - 2\sin 3\theta - \sin 4\theta)q_2 + (-4 - 8\cos\theta - 7\cos 2\theta - 4\cos 3\theta - \cos 4\theta)p_1 - (6\sin\theta + 7\sin 2\theta + 4\sin 3\theta + \sin 4\theta)q_1]$

$Re\ L_2^{(5)}(P) = [4(1+2\cos\theta)(1+\cos\theta)(2+3\cos\theta+2\cos 2\theta+\cos 3\theta)]^{-1}[(2 + 3\cos\theta + 2\cos 2\theta + \cos 3\theta)p_4 - (-\sin\theta - 2\sin 2\theta - \sin 3\theta)q_4 + (2\cos\theta + 4\cos 2\theta + 5\cos 3\theta + 4\cos 4\theta + \cos 5\theta)p_3 - (-4\sin\theta - 4\sin 2\theta - 5\sin 3\theta - 4\sin 4\theta - \sin 5\theta)q_3 + (-2 - 4\cos\theta - 3\cos 2\theta - 2\cos 3\theta + 2\cos 5\theta + \cos 6\theta)p_2 - (4\sin\theta + 3\sin 2\theta + 2\sin 3\theta - 2\sin 5\theta - \sin 6\theta)q_2 + (-\cos\theta - 3\cos 2\theta - 4\cos 3\theta - 4\cos 4\theta - 3\cos 5\theta - \cos 6\theta)p_1 - (\sin\theta + 3\sin 2\theta + 4\sin 3\theta + 4\sin 4\theta + 3\sin 5\theta + \sin 6\theta)q_1]$

B. Inverse Interpolation

For inverse interpolation when n-point direct interpolation suffices, note from the above formulas for $L_k^{(n)}(P) = Re + i\,Im$, the value of the complex coefficient of P^m or $(p+iq)^m$. Then in $L_k^{(n)}(P)$ denote the coefficient of P by $A_k^{(n)}$, the coefficient of P^2 by $B_k^{(n)}$, the coefficient of P^3 by $C_k^{(n)}$, and the coefficient of P^4 by $D_k^{(n)}$. Then defining $D = \sum A_k^{(n)} f(z_k)$, $r = [f(z) - f(z_0)]/D$, $s = [\sum B_k^{(n)} f(z_k)]/D$, $t = [\sum C_k^{(n)} f(z_k)]/D$, $u = [\sum D_k^{(n)} f(z_k)]/D$, where all summations in k are as in (1) above, the quantity P is given by the formula*

$$P = r - r^2 s + r^3(2s^2 - t) + r^4(-5s^3 + 5st - u) + r^5(14s^4 - 21s^2 t + 3t^2 + 6su) + r^6(-42s^5 + 84s^3 t - 28st^2 - 28s^2 u + 7tu) + \cdots \tag{2}$$

In practice a large number of terms in the expression for P will not be needed. Also, where 3 points suffice for direct interpolation, $t = u = 0$, and where 4 points suffice, $u = 0$.

* See the author's "A New Formula for Inverse Interpolation", Bull. Amer. Math. Soc., vol. 50, No. 8, Aug. 1944, pp. 513-516.

TABLE OF BESSEL FUNCTIONS $J_n(1000)$

By Murlan S. Corrington[1]

Summary

A table of Bessel functions for $J_n(1000)$ is given covering the range $n = 935(1)1035$; 8D.

Introduction

When a frequency-modulated radio wave is analyzed into a spectrum, the carrier and side-frequency amplitudes are proportional to Bessel functions of the first kind, with order equal to the number of the side frequency and argument equal to the modulation index, in accord with the following equation:

$$\sin\left(\omega_0 t + \frac{D}{\mu}\sin 2\pi\mu t\right) = \sum_{n=-\infty}^{\infty} J_n\left(\frac{D}{\mu}\right)\sin(\omega_0 + 2\pi n\mu)t$$

where ω_0 = carrier frequency, radians per second
t = time in seconds
D = deviation in cycles per second
μ = audio frequency in cycles per second

According to the present standards for commercial broadcasting, the deviation can be as much as 75,000 cycles per second and the audio frequency can be as low as 30 cycles per second, so the maximum value of the modulation index, $\frac{D}{\mu}$, is 2500. The table in this article was computed to determine the relative side frequency amplitudes near the edge of the band for a modulation index of 1000. Figure 1 shows that when the side frequency number, n, exceeds 1000, the amplitudes decrease very rapidly toward zero.

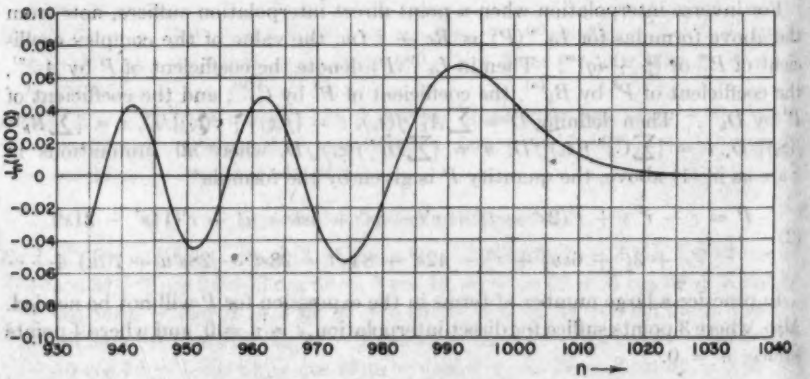

Fig. 1. Graph of $J_n(1000)$

[1] Radio Engineer, Advanced Development Section of the RCA Victor Division, Radio Corporation of America, Camden, N. J.

Method of Computation

The value of $J_{1000}(1000)$ was computed from Meissel's formula[2]

$$J_n(n) = \frac{0.44730\ 73184}{n^{1/3}}\left[1 - \frac{1}{225n^2} + \frac{0.0006938}{n^4} - \frac{0.000354}{n^6} + \cdots\right] - \frac{0.00586\ 92885}{n^{5/3}}\left[1 - \frac{1213}{14625n^2} + \frac{0.03070}{n^4} - \cdots\right]$$

to obtain

$$J_{1000}(1000) = 0.0447\ 3067\ 295$$

A second formula developed by Meissel[3] gives

$$J_{n-1}(n) - J_n(n) = J_n(n) - J_{n+1}(n) = \frac{0.41085\ 0195}{n^{2/3}}\left[1 + \frac{23}{3150n^2} \cdots\right] - \frac{0.08946\ 146368}{n^{4/3}}\left[1 - \frac{947}{69300n^2} + \cdots\right]$$

so

$$J_{999}(1000) = 0.0488\ 3022\ 878$$

From these two results, the rest of the values in the table were computed from the recurrence formula for the Bessel functions

$$J_{n-1}(1000) + J_{n+1}(1000) = \frac{n}{500} J_n(1000)$$

All computations were made to eleven decimal places and later rounded off to eight.

Method of Checking

Meissel[4] has given a table of $J_n(1000)$ for $n = 1000(1)981, 968, 967$; 8D. All of his results check exactly with these except for $n = 967, 968$; for these two values there is a discrepancy.

n	$J_n(1000)$	
	Meissel	Corrington
967	+0.0075 2995	+0.0075 3142
968	−0.0052 6524	−0.0052 6276

A careful check of these calculations indicates that his results are apparently incorrect.

[2] E. Meissel, "Beitrag zur Theorie der allgemeinen Bessel'schen Function," Astronomische Nachrichten, vol. 128, 1891, cols. 145–154.

[3] E. Meissel, "Einige Entwickelungen, die Bessel'schen I-Functionen betreffend," Astronomische Nachrichten, vol. 127, 1891, cols. 359–362.

[4] E. Meissel, "Abgekürzte Tafel der Bessel'schen Functionen $I_x^{(h)}$," Astronomische Nachrichten, vol. 128, 1891, cols. 153–156.

TABLE OF BESSEL FUNCTIONS $J_n(1000)$

n	$J_n(1000)$	n	$J_n(1000)$
935	−0.0288 2562	985	+0.0368 6213
936	−0.0160 5401	986	+0.0452 3671
937	−0.0012 2749	987	+0.0523 4465
938	+0.0137 5369	988	+0.0580 9164
939	+0.0270 2942	989	+0.0624 4443
940	+0.0370 0756	990	+0.0654 2344
941	+0.0425 4479	991	+0.0670 9398
942	+0.0430 6174	992	+0.0675 5683
943	+0.0385 8352	993	+0.0669 3877
944	+0.0297 0678	994	+0.0653 8357
945	+0.0175 0289	995	+0.0630 4376
946	+0.0033 7367	996	+0.0600 7352
947	−0.0111 1990	997	+0.0566 2269
948	−0.0244 3476	998	+0.0528 3212
949	−0.0352 0841	999	+0.0488 3023
950	−0.0423 9080	1000	+0.0447 3067
951	−0.0453 3411	1001	+0.0406 3112
952	−0.0438 3467	1002	+0.0366 1282
953	−0.0381 2711	1003	+0.0327 4098
954	−0.0288 3560	1004	+0.0290 6558
955	−0.0168 9122	1005	+0.0256 2271
956	−0.0034 2662	1006	+0.0224 3607
957	+0.0103 3952	1007	+0.0195 1866
958	+0.0232 1646	1008	+0.0168 7451
959	+0.0341 4321	1009	+0.0145 0035
960	+0.0422 7023	1010	+0.0123 8720
961	+0.0470 1562	1011	+0.0105 2179
962	+0.0480 9380	1012	+0.0088 8786
963	+0.0455 1685	1013	+0.0074 6724
964	+0.0395 7165	1014	+0.0062 4077
965	+0.0307 7729	1015	+0.0051 8903
966	+0.0198 2852	1016	+0.0042 9297
967	+0.0075 3142	1017	+0.0035 3429
968	−0.0052 6276	1018	+0.0028 9577
969	−0.0177 2013	1019	+0.0023 6150

TABLE OF BESSEL FUNCTIONS $J_n(1000)$—*Continued*

n	$J_n(1000)$	n	$J_n(1000)$
970	−0.0290 7884	1020	+0.0019 1697
971	−0.0386 9283	1021	+0.0015 4911
972	−0.0460 6263	1022	+0.0012 4632
973	−0.0508 5292	1023	+0.0009 9836
974	−0.0528 9716	1024	+0.0007 9633
975	−0.0521 9074	1025	+0.0006 3253
976	−0.0488 7479	1026	+0.0005 0035
977	−0.0432 1285	1027	+0.0003 9419
978	−0.0355 6311	1028	+0.0003 0931
979	−0.0263 4860	1029	+0.0002 4176
980	−0.0160 2745	1030	+0.0001 8823
981	−0.0050 6520	1031	+0.0001 4599
982	+0.0060 8953	1032	+0.0001 1280
983	+0.0170 2504	1033	+0.0000 8683
984	+0.0273 8169	1034	+0.0000 6660
		1035	+0.0000 5089